UNIVERSITAT POLITÈCNICA DE VALÈNCIA

DEPARTAMENTO DE INGENIERÍA HIDRÁULICA Y MEDIO AMBIENTE

PROGRAMA DE DOCTORADO EN INGENIERÍA DEL AGUA Y MEDIO AMBIENTE

Ph. D. TESIS

METODOLOGÍA BASADA EN EL DESARROLLO DE ESTRATEGIAS DE REGULACIÓN PARA LA MEJORA DE INDICADORES DE SOSTENIBILIDAD A TRAVÉS DE LA INSTALACIÓN DE MICROGENERACIÓN ELÉCTRICA EN SISTEMAS DE DISTRIBUCIÓN PRESURIZADOS

AUTOR

CARLOS ANDRÉS MACÍAS ÁVILA

DIRECTORES DE TESIS

Dra. PETRA AMPARO LÓPEZ JIMÉNEZ
Dr. MODESTO PÉREZ SÁNCHEZ

Valencia, España
Octubre de 2022

Esta página se dejó intencionalmente en blanco

Agradecimientos

A Dios, por protegerme ante toda situación, mantenerme con salud y darme fuerzas cada día para ser constante y permitirme luchar por lo que anhelo.

A mi familia: Venus, Juan Carlos, Junior, Diana, Guido y Matías por ser apoyo en cada momento difícil y darme las palabras de ánimos correctas en los días difíciles. A mi ángel Violetita, por ser una de mis mayores motivaciones, por aquella última conversación donde me pediste que tome el doctorado, esto va para ti.

Agradezco inmensamente a mis tutores: Modesto, Amparo y Paco. Como siempre se los he dicho "sin ustedes esto no sería posible". Gracias Modesto por tu paciencia, por estar siempre predispuesto en apoyarme, guiarme, aconsejarme y decirme ¡Ánimos Carlos!; Amparo, porque cuando escribí aquel correo aceptaste ser mi tutora sin dudarlo y me permitiste acceder a este programa de doctorado, por darme ánimos y decirme ¡Ya no queda nada!. ¡Finalmente, Paco! por su apoyo en cada uno de los trabajos publicados, por su paciencia y ánimos en la enseñanza brindada en tutorías. Valoro mucho el aporte que cada de ustedes entregó, su humildad y buen ánimo en la enseñanza. Quedaré eternamente agradecido por permitirme cumplir este sueño.

Por último, pero no menos importante… A ti, por estar, por decirme: ¡envía ese correo! por darme la confianza de asumir este reto, por darme la seguridad de que podía lograrlo, por ser un ejemplo y mi admiración en todo este proceso. Porque los sueños se cumplen, porque siempre hay alguien quien nos quiere…

Resumen

El agua y la energía son uno de los recursos más importantes para el desarrollo de la sociedad. El nexo entre el agua y la energía es de gran interés por su importancia dentro de los objetivos de desarrollo sostenible *(ODS)*. Como respuesta a la búsqueda de la sostenibilidad y la mejora de la calidad de vida, se desarrollan nuevas tecnologías que permiten la recuperación de energía mediante el potencial hidráulico que existe en las redes de distribución de agua urbana o de riego. El exceso de presión, envejecimiento de las tuberías y otros factores externos, incrementan los niveles de fugas, afectando al rendimiento volumétrico en las redes de distribución de agua potable. Esta pérdida del recurso agua es sinónimo de pérdidas económicas, debido a que el caudal inyectado para lograr satisfacer la demanda hídrica deberá ser mayor para compensar el volumen de agua perdido por fugas. Las fugas suponen una pérdida de energía en la red, lo que obligará a incrementar la presión en las estaciones de bombeo para cumplir las presiones mínimas requeridas en las tomas. El aumento de la potencia en estos equipos generará mayores costes energéticos. Actualmente, la creación de energía renovable reemplaza la producción de energía no renovable, permitiendo la reducción de gases de efecto invernadero.

El objetivo principal de esta tesis es desarrollar estrategias hidráulicas para mejorar la recuperación de energía en los sistemas de distribución de agua, considerando la influencia de las fugas en el sistema, mediante la optimización de la ubicación y selección de bombas funcionando como turbinas (*PAT*, por su acrónimo en inglés *pumps working as turbines*).

El cumplimiento de los objetivos de esta tesis requirió de la elaboración de cuatro artículos publicados, que permitieron: (i) la contextualización sobre las fugas, los métodos de cálculo existentes para la estimación de las fugas en las redes de distribución y su influencia en el rendimiento volumétrico de los sistemas. En este punto se han analizado 45 redes de distribución de agua con fugas y 17 redes donde se habían instalado *PAT*, esto permitió definir diferentes indicadores claves de rendimiento *KPI* (por su acrónimo en inglés key performance indicators) y caracterizar el estado de las redes hidráulicas; (ii) la propuesta de diferentes expresiones de regresión que permitan definir las tres curvas de operaciones cuando las *PAT* operan bajo la estrategia de velocidad de giro variable, estas son: curva de altura de mejor eficiencia *(BEH)*, curva de mejor altura de potencia *(BPH)* y

curva de mejor flujo de potencia *(BPF)*; (iii) la propuesta de una metodología que permita definir la ubicación y la selección del sistema de recuperación de energía, a través de un procedimiento "simulated annealing" en una red de riego; y (iv) la aplicación y mejora de la metodología en una red de abastecimiento de agua urbana.

Se exponen diferentes métodos de cálculo de fugas y de calibración de modelos hidráulicos en el Artículo 1. Los estudios publicados de tipo experimental han definido los parámetros que permiten estimar los niveles de fugas existentes en las redes. Estos se basan fundamentalmente en el tamaño del orificio en las tuberías, material, edad, entre otros. La extracción de información de los 62 casos de estudio analizados permitió calcular los rendimientos volumétricos del sistema, los porcentajes de fugas, la energía perdida por fugas y el coste asociado. La revisión bibliográfica permitió estimar que el uso de las *PAT* reduce entre 4 y 63 % el volumen de fugas y se estima que la energía anual recuperada está entre 28470 y 714679 kWh. Este estudio muestra la influencia de las fugas en las redes de distribución.

Para estimar el comportamiento de las *PAT* se requiere conocer sus curvas características (altura, eficiencia y potencia) y cómo varían en función de la modificación de la velocidad de giro. Al existir poca información sobre las curvas, se propone en esta tesis una serie de expresiones de regresión, modificando las leyes de semejanza, a partir de una base de datos de estudios experimentales de 15 *PAT* con velocidades específicas entre 5.67 y 50.71 rpm (m, kW). Estas fueron probadas a 87 velocidades de rotación. Para obtener una mejor aproximación de las expresiones, esta propuesta fue validada a través de un análisis de error en comparación con otros métodos publicados. El desarrollo de las curvas se explica en el Artículo 2.

La primera etapa de la metodología de optimización propuesta para la determinación de la mejor ubicación y selección de *PAT*, parte del desarrollo del modelado de la red, sea urbana o de riego. Esta requiere del conocimiento de: (i) la topología de la red, (ii) los volúmenes inyectados y consumidos en la red, (iii) modos de operación, entre otros. La simulación hidráulica realizada en EPANET permite estimar los valores de caudal en cada línea y la presión en los nudos en periodos de simulación extendida.

A través de un balance hídrico entre el caudal inyectado y el consumo en la red en cada instante de tiempo, se determina el volumen de fugas. Cuando los índices *KEI* (por su acrónimo en inglés, key error index) son aceptables y los errores son

minimizados, la calibración finaliza y se realiza el balance de energía. A partir de los requerimientos hidráulicos mínimos de presión en la red, para no afectar su comportamiento, se implementan una serie de expresiones que permiten estimar el total de energía existente en el sistema, la energía teórica disponible y recuperable. Además de los puntos de operación de altura y caudal.

El primer procedimiento "simulated annealing" es realizado para determinar la ubicación óptima de los dispositivos de recuperación de energía a instalarse, a través de la definición de una serie de parámetros. El segundo procedimiento "simulated annealing" es realizado para determinar la selección de las *PAT*. En esta etapa se define el número y tipo de *PAT* a instalarse, además del modo de regulación y su configuración en serie o paralelo. El desarrollo y aplicación de la metodología se muestra en el Artículo 3 y 4 de esta tesis.

La metodología propuesta ha sido aplicada en dos casos de estudio de redes reales, la primera de riego en Vallada (España) y la segunda de distribución urbana en Manta (Ecuador). El desarrollo de la metodología en la red de riego muestra la influencia en la reducción de fugas cuando se instalan *PAT* en la red. La recuperación anual de energía se estimó con valores de alrededor de 32000 kWh, una reducción anual del volumen fugado de 18000 m^3 y la disminución de las emisiones de CO_2 de 4.38 a 0.24 kg por cada m^3 de agua recuperado por fugas. Para la red urbana ubicada en Manta (Ecuador), en caso de instalarse un sistema de recuperación con 3 máquinas, es posible generar anualmente 23624 kWh de energía, una reducción del volumen fugado de 96000 m^3 de agua y 11.58 t de CO_2. Al instalar 2 sistemas de recuperación con 3 máquinas en paralelo cada uno, se recuperaría anualmente un valor de energía de 34490 kWh, se reducirían 120000 m^3 de agua fugada y 969 t de CO_2 al año.

Resum

L'aigua i l'energia són un dels recursos més importants per al desenvolupament de la societat. El nexe entre l'aigua i l'energia és de gran interés per la seua importància dins dels objectius de desenvolupament sostenible *(ODS)*. Com a resposta a la cerca de la sostenibilitat i la millora de la qualitat de vida, es desenvolupen noves tecnologies que permeten la recuperació d'energia mitjançant el potencial hidràulic que existeix en les xarxes de distribució d'aigua urbana o de reg. L'excés de pressió, envelliment de les canonades i altres factors externs, incrementen els nivells de fugides, afectant el rendiment volumètric en les xarxes de distribució d'aigua potable. Aquesta pèrdua del recurs aigua és sinònim de pèrdues econòmiques, pel fet que el cabal injectat per a aconseguir satisfer la demanda hídrica haurà de ser major per a compensar el volum d'aigua perdut per fugides. Les fugides suposen una pèrdua d'energia en la xarxa, la qual cosa obligarà a incrementar la pressió en les estacions de bombament per a complir les pressions mínimes requerides en les preses. L'augment de la potència en aquests equips generarà majors costes energètics. Actualment, la creació d'energia renovable reemplaça la producció d'energia no renovable permetent la reducció de gasos d'efecte d'hivernacle.

L'objectiu principal d'aquesta tesi és desenvolupar estratègies hidràuliques per a millorar la recuperació d'energia en els sistemes de distribució d'aigua, considerant la influència de les fugides en el sistema, mitjançant l'optimització de la ubicació i selecció de bombes funcionant com a turbines (*PAT*, pel seu acrònim en anglés pumps working as turbines).

El compliment dels objectius d'aquesta tesi va requerir de l'elaboració de quatre articles publicats, que van permetre: (i) la contextualització sobre les fugides, els mètodes de càlcul existents per a l'estimació de les fugides en les xarxes de distribució i la seua influència en el rendiment volumètric dels sistemes. En aquest punt s'han analitzat 45 xarxes de distribució d'aigua amb fugides i 17 xarxes on s'havien instal·lat *PAT*, això va permetre definir diferents indicadors claus de rendiment *KPI* (pel seu acrònim en anglés key performance indicators) i caracteritzar l'estat de les xarxes hidràuliques; (ii) la proposta de diferents expressions de regressió que permeten definir les tres corbes operacions quan les *PAT* operen sota l'estratègia de velocitat de gir variable, aquestes són: corba d'altura de millor eficiència *(BEH)*, corba de millor altura de potència *(BPH)* i corba de millor flux de potència *(BPF)*; (iii) la proposta d'una metodologia que permeta definir la ubicació i

la selecció del sistema de recuperació d'energia, a través d'un procediment "simulated annealing" en una xarxa de reg; i (iv) l'aplicació i millora de la metodologia en una xarxa de proveïment d'aigua urbana.

Diferents mètodes de càlcul de fugides i de calibratge de models hidràulics són exposats en l'Annex I. Estudis publicats de tipus experimental han definit els paràmetres que permeten estimar els nivells de fugides existents en les xarxes. Aquests es basen fonamentalment en la grandària de l'orifici en les canonades, material, edat, etc. L'extracció d'informació dels 62 casos d'estudis analitzats va permetre calcular els rendiments volumètrics del sistema, els percentatges de fugides, l'energia perduda per fugides i els costes associats. La revisió bibliogràfica va permetre estimar que l'ús de les *PAT* redueix entre 4 i 63 % el percentatge de fugides, mentre que s'estima que l'energia anual recuperada està entre 28470 i 714679 kWh. Aquest estudi mostra la influència de les fugides en les xarxes de distribució.

Per a conéixer el comportament de les *PAT* es requereix conéixer les seues corbes característiques (altura, eficiència i potència) i com varien aquestes corbes en funció de la modificació de la velocitat de gir. En existir poca informació sobre les corbes, es proposen en aquesta tesi una seriosa d'expressions de regressió, modificant les lleis d'afinitat, a partir d'una base de dades d'estudis experimentals de 15 *PAT* amb velocitats específiques entre 5.67 i 50.71 rpm (m, kW) provades a 87 velocitats de rotació. Per a obtindre una millor aproximació de les expressions, aquesta proposta va ser validada a través d'una anàlisi d'error en comparació amb altres mètodes publicats. El desenvolupament de les corbes s'explica en l'Annex II.

La primera etapa de la metodologia d'optimització proposada per a la determinació de la millor ubicació i selecció de *PAT*, part del desenvolupament del modelatge de la xarxa, siga urbana o de reg. Aquesta requereix del coneixement de: (i) la topologia de la xarxa, (ii) volums injectats i consumits en la xarxa, (iii) manera d'operació, entre altres. La simulació realitzada en EPANET permet conéixer els valors de cabal en cada línia i la pressió en els nusos en períodes de simulació estés.

A través d'un balanç hídric entre el cabal injectat i el consum en la xarxa en cada instant de temps es determina volum de fugides. Quan els índexs *KEI* (pel seu acrònim en anglés, key error index) són acceptables i els errors són minimitzats, el calibratge finalitza i es realitza el balanç d'energia. A partir dels requeriments hidràulics mínims de pressió en la xarxa per a no afectar el seu comportament, s'estima el total d'energia existent, l'energia teòrica disponible i recuperable. A més dels punts d'operació d'altura i cabal. L'ús d'una sèrie d'expressions permet estimar

el total d'energia existent, les pèrdues per fricció, l'energia requerida en el sistema, l'energia teòrica disponible i recuperable. A més dels punts d'operació d'altura i cabal.

El primer procediment "simulated annealing" és realitzat per a determinar la ubicació òptima dels dispositius de recuperació d'energia a installarse, a través de la definició d'una sèrie de paràmetres. El segon procediment "simulated annealing" és realitzat per a determinar la selecció de les *PAT*, en aquesta etapa es defineix el número i tipus de *PAT* a installarse, a més de la manera de regulació i la seua configuració en parallel. El desenvolupament i aplicació de la metodologia es mostra en l'Annex III i IV d'aquesta tesi.

La metodologia proposada ha sigut aplicada en dos casos d'estudi de xarxes reals, la primera de reg a Vallada (Espanya) i la segona xarxa de distribució urbana en Manta (l'Equador). El desenvolupament de la metodologia en la xarxa de reg mostra la influència en la reducció de fugides quan s'installen *PAT* en la xarxa. La recuperació anual d'energia es va estimar amb valors d'al voltant de 32000 kWh, una reducció anual del volum escapolit de 18000 m^3 i la disminució de les emissions de CO_2 de 4.38 a 0.24 kg per cada m^3 d'aigua recuperat per fugides. Per a la xarxa urbana situada en Manta (l'Equador), en cas d'installarse un sistema de recuperació amb 3 màquines és possible generar anualment 23624 kWh d'energia, una reducció de volum escapolit de 96000 m^3 d'aigua i 11.58 t de CO_2. En installar 2 sistemes de recuperació amb 3 màquines en parallel cadascun, es recuperaria anualment un valor d'energia de 34490 kWh, una reducció de 120000 m^3 d'aigua i 969 t de CO_2 a l'any.

Summary

Water and energy are one of the most important resources for the development of society. The nexus between water and energy is of great interest due to its importance within the sustainable development goals *(SDGs)*. In response to the search for sustainability and improvement of the quality of life, new technologies are developed that allow the recovery of energy through the hydraulic potential that exists in urban water distribution or irrigation networks. Excess pressure, pipe aging and other external factors increase leak levels, affecting volumetric performance in drinking water distribution networks. This loss of water resources is synonymous with economic losses, because the flow injected to satisfy the water demand must be greater to compensate for the volume of water lost due to leaks. Leaks entail a loss of energy in the network, which will make it necessary to increase the pressure at the pumping stations to meet the minimum pressures required at the intakes. The increase in power in this equipment will generate higher energy costs. Currently, the creation of renewable energy replaces the production of non-renewable energy allowing the reduction of greenhouse gases.

The main objective of this thesis is to develop hydraulic strategies to improve energy recovery in water distribution systems, considering the influence of leaks in the system, by optimizing the location and selection of pumps operating as turbines *(PATs* for its acronym in english pumps working as turbines).

The fulfillment of the objectives of this thesis required the elaboration of four published articles, which allowed: (i) the contextualization of leaks, the existing calculation methods for the estimation of leaks in distribution networks and their influence on the volumetric performance of the systems. At this point, 45 water distribution networks with leaks and 17 networks where *PATs* had been installed have been analyzed, this allowed defining different key performance indicators *(KPIs)* and characterizing the state of the networks. hydraulic; (ii) the proposal of different regression expressions that allow defining the three operating curves when the *PATs* operate under the variable rotational speed strategy, these are: best efficiency height curve *(BEH)*, best power height curve *(BPH)* and Best Power Flow *(BPF)* curve; (iii) the proposal of a methodology that allows defining the location and selection of the energy recovery system, through a "simulated annealing" procedure in an irrigation network; and (iv) the application and improvement of the methodology in an urban water supply network.

X

Different methods for calculating leaks and for calibrating hydraulic models are set out in Annex I. Published experimental studies have defined the parameters that make it possible to estimate the levels of leaks in networks. These are mainly based on the size of the hole in the pipes, material, age, etc. The extraction of information from the 62 case studies analyzed made it possible to calculate the volumetric performance of the system, the percentages of leaks, the energy lost due to leaks, and the associated costs. The literature review allowed estimating that the use of *PATs* reduces the percentage of leaks between 4 and 63 %, while it is estimated that the annual energy recovered is between 28470 and 714679 kWh. This study shows the influence of leaks in distribution networks.

In order to know the behavior of the *PATs*, it is necessary to know its characteristic curves (height, efficiency and power) and how these curves vary depending on the modification of the turning speed. As there is little information about the curves, a series of regression expressions are proposed in this thesis, modifying the affinity laws, from a database of experimental studies of 15 *PATs* with specific speeds between 5.67 and 50.71 rpm (m, kW) tested at 87 rotational speeds. To obtain a better approximation of the expressions, this proposal was validated through an error analysis in comparison with other published methods. The development of the curves is explained in Annex II.

The first stage of the proposed optimization methodology for determining the best location and selection of *PATs*, part of the development of network modeling, whether urban or irrigation. This requires knowledge of: (i) network topology, (ii) volumes injected and consumed in the network, (iii) mode of operation, among others. The simulation carried out in EPANET allows knowing the flow values in each line and the pressure in the nodes in extended simulation periods.

Through a water balance between the flow injected and the consumption in the network at each instant of time, the volume of leaks is determined. When the *KEI* indices (for its acronym in english, key error index) are acceptable and the errors are minimized, the calibration is finished, and the energy balance is performed. Based on the minimum hydraulic pressure requirements in the network so as not to affect its behavior, the total existing energy is estimated, as well as the theoretical available and recoverable energy. In addition to the operating points of head and flow. The use of a series of expressions allows estimating the total existing energy, the friction losses, the energy required in the system, the theoretical available and recoverable energy. In addition to the operating points of head and flow.

The first "simulated annealing" procedure is performed to determine the optimal location of the energy recovery devices to be installed, through the definition of a series of parameters. The second "simulated annealing" procedure is performed to determine the selection of the *PATs*. In this stage, the number and type of *PATs* to be installed are defined, as well as the regulation mode and their parallel configuration. The development and application of the methodology is shown in Annexes III and IV of this thesis.

The proposed methodology has been applied in two case studies of real networks, the first irrigation network in Vallada (Spain) and the second urban distribution network in Manta (Ecuador). The development of the methodology in the irrigation network shows the influence on the reduction of leaks when *PATs* are installed in the network. The annual energy recovery was estimated with values of around 32000 kWh, an annual reduction in the leaked volume of 18000 m³ and a decrease in CO_2 emissions from 4.38 to 0.24 kg for each m³ of water recovered from leaks. For the urban network located in Manta (Ecuador), if a recovery system with 3 machines is installed, it is possible to generate 23624 kWh of energy annually, a reduction in leaked volume of 96000 m³ of water and 11.58 t of CO_2. By installing 2 recovery systems with 3 machines in parallel each, an energy value of 34490 kWh would be recovered annually, a reduction of 120000 m³ of water and 969 t of CO_2 per year.

Contenido

Lista de acrónimos

A	Área del orificio	m^2
AL	Leyes de semejanza	*Adimensional*
β, α, N_1	Exponente emisor de fugas	*Adimensional*
BEH	Curva de altura de mejor eficiencia	*Adimensional*
BEP	Punto de mejor eficiencia de la máquina	*Adimensional*
BPH	Curva de mejor altura de potencia	*Adimensional*
BPF	Curva de mejor flujo de potencia	*Adimensional*
α	Velocidad de rotación	rpm
α_c	Radio de enfriamiento	*Adimensional*
C_d	Coeficiente de descarga	*Adimensional*
$CDRPE$	Ratio entre la reducción de emisiones de CO_2 por la producción de cada kWh de energía renovable	t
$CDRBL$	Ratio entre la reducción de emisiones de CO_2 por cada metro cúbico de agua ahorrado por fugas.	$kgCO_2/m^3$
$CWSBRL$	Coste de cada metro cúbico de agua por cada metro cúbico de agua ahorrado.	€
D	Diámetro	mm
ΔV_L	Reducción de fugas en la red de distribución	m^3
EC	Curva de eficiencia	$m/l/s$
E_{FR_J}	Energía disipada por fricción	kWh
ERP	Porcentaje de energía recuperable utilizada sobre el total de energía consumida en el sistema	%

E_{RS_J}	Energía requerida	kWh
E_{TA_J}	Energía teórica disponible	kWh
E_{T_J}	Energía total	kWh
E_{TN_J}	Energía teórica necesaria	kWh
E_{TR_J}	Energía teóricamente recuperable	kWh
$E_{TR_{mj}}$	Energía máxima recuperable	kWh
$FAVAD$	Descarga de área fija y variable	$Adimensional$
g	Aceleración de la gravedad	m/s^2
h	Altura de presión	mca
H_0	Altura recuperada en velocidad de rotación nominal	mca
i	Instante de tiempo	s
IAE	Suma de la energía activa total consumida en la red	kWh
$IAAE$	Suma de la energía activa total consumida en la red restada de la suma de la energía total recuperada en la red	kWh
$IAEFW$	Relación entre el *IAAE* y el volumen total de agua introducida en la red	kWh/m^3
IED	Relación entre la energía de fricción y la energía de entrada	$Adimensional$
$IEFW$	Relación entre la energía activa consumida y el volumen total de agua introducida en el sistema	kWh/m^3
IER	Suma de la energía total recuperada en la red	kWh
$IRLGP$	Relación entre la reducción del volumen de fuga por cada potencia instalada.	m^3/kWh

ILI	Índice de fugas de infraestructura	*Adimensional*
KEI	Indicadores claves de error	
KPI	Indicadores claves de rendimiento	
$LCOE$	Coste nivelado de energía	$€/kWh$
L_{DMA}	Tasa de fugas	%
MAD	Desviación media absoluta	
$MOAL$	Leyes de semejanza modificadas	
MNF	Caudal mínimo nocturno	
MRD	Desviación media relativa	
η_L	Rendimiento de fugas en el sistema de agua	%
η_0	Velocidad de rotación nominal	rpm
η_{st}	Velocidad específica	rpm
η_v	Eficiencia volumétrica	%
p, h, e, q	Parámetros de Suter	rpm
P	Presión en el nudo	mca
P_0	Potencia generada	kWh
PAT	Bombas funcionando como turbinas	
$PBIAS$	Porcentaje *BIAS*	%
P_{min}	Presión mínima en un punto de consumo	mca
VRP	Válvulas reductoras de presión	
REC	Producto del coste de la tarifa eléctrica por cada kWh de energía producida	$€$
RS	Estrategia de regulación	
$RMSE$	Media cuadrática	*Adimensional*

V_I	Volumen inyectado en la red	m^3
V_M	Volumen total medido en el sistema	m^3
VOS	Estrategia de operación variable	
ql_i	Caudal fugado en el nudo	m^3/s
Q_i	Caudal circulante	m^3/s
Q_0	Tasa de flujo	m^3/s
Q_{leak}	Caudal fugado	m^3/s
Q_{LNC}	Consumo nocturno legítimo	m^3/s
Q_{MNF}	Tasa mínima de flujo nocturno	m^3/s
T_i	Temperatura inicial en el procedimiento "simulated annealing"	$ºC$
T_f	Temperatura final en el procedimiento "simulated annealing"	$ºC$
T_t	Temperatura de transición en el procedimiento "simulated annealing"	$ºC$
ϑ	Velocidad teórica	rpm
γ	Peso específico del fluido	N/m^3
z_i	Nivel geométrico sobre un plano de referencia de un punto de consumo	m
z_0	Nivel geométrico sobre un plano de referencia de la lámina libre	m

1. Introducción

1.1. Motivación

El agua es un recurso valioso para la supervivencia humana. En muchos lugares del mundo, el recurso actual no permite cubrir la demanda mínima de consumo de agua [1]. La falta de cobertura del agua en la población no es solamente producto del estrés hídrico, sino que está relacionado también a factores de gestión, políticos, económicos, ambientales, hidráulicos, entre otros. Actualmente, existen grandes volúmenes de agua que son perdidos a causa de fugas en las redes de distribución de agua. Estas pérdidas pueden ser debidas a: (i) excesos de presión en redes, (ii) envejecimiento de tuberías, (iii) falta de gestión y monitorio [2], (iv) fallos en la instalación, defectos del material, entre otras razones [3]. Se estima que entre el 5 y 55 % del agua fugada se infiltra en el suelo y no es contabilizada. En los países desarrollados, donde se aplican planes de gestión, se alcanzan valores de 15 al 24 % en pérdidas del volumen total de agua inyectado en la red [4]. Para llevar a cabo una estimación de los volúmenes fugados, la Asociación Internacional del Agua (*IWA*, por su acrónimo en inglés *International Water Association*) proporciona una serie de indicadores para ser aplicados a los sistemas de abastecimiento de agua, donde se contemplan las pérdidas reales de agua, las pérdidas de agua de las conexiones domiciliarias y la tasa de fugas [5].

A medida que la red de abastecimiento de agua se deteriora estructural y funcionalmente, las roturas aumentan y se disminuye la capacidad hidráulica de la red [6], una red con fallos físicos puede estar expuesta, bajo ciertas condiciones de operación a intrusiones de patógenos que afectan la calidad del agua [7].

19

Las investigaciones consultadas han descrito diferentes métodos internos y externos para la detección de fugas. Entre los métodos de detección externa se encuentran de tipo: acústicos, fibra óptica, inducción magnética, entre otros [8]. Los métodos internos son métodos de equilibrio, monitoreo de flujo de presión, enfoque de procesamiento de señales, análisis estadístico, métodos basados en modelos, entre otros [9]. La reducción de fugas en las redes de distribución de agua es una prioridad absoluta. En la literatura revisada, se han propuesto estrategias de gestión de la presión para abordar este problema, tales como: el índice de rendimiento de fugas *LPI* (por su acrónimo en ingles *Leakage Performance Index*) [10], algoritmos de optimización para la reducción de fugas [11], implementación de válvulas reductoras de presión *(VRP)* en la red [12] y algoritmos genéticos aplicados a redes de agua con turbinas hidráulicas instaladas [13].

Uno de los elementos más utilizados en la gestión de la presión en redes de distribución son las *VRP*. Una *VRP* consta de una válvula principal y un controlador que detecta la presión de salida y ajusta la apertura de la válvula principal para mantener la presión de salida en un punto de ajuste determinado, lo que permite disipar la energía del fluido y reducir las fugas en la red de distribución [14]. En las redes de distribución de agua, las bombas funcionando como turbinas *(PAT)* se pueden usar en lugar de las *VRP*, tanto para la reducción de presión como para la producción de energía [15].

Las *PAT* son bombas de agua estándar que se utilizan como turbinas hidráulicas al invertir la dirección del flujo a través de ellas. El uso de las *PAT* fue propuesto como solución sostenible no convencional para reducir la presión y recuperar energía [16]. Esta recuperación energética es un proceso en el que se recupera energía de la presión residual de la red cuando se aplica en sistemas de agua [17]. La poca disponibilidad de coste y la falta de información es probablemente una barrera para la implementación de *PAT* de manera más generalizada [18]. Las *PAT* tienen un coste menor en comparación de las turbinas hidráulicas. El uso de estas nuevas tecnologías es clave para mejorar la eficiencia energética en los sistemas de agua a presión. Otro factor muy importante es el análisis completo de estas mejoras energéticas [19].

El conocimiento de sus curvas características, que son: curva de altura (*HC*, por su acrónimo en ingles *Head Curve*), curva de eficiencia (*EC*, por su acrónimo en ingles *Efficiency Curve*) y la curva de potencia (*PC*, por su acrónimo en ingles *Power Curve*) es difícil de saber de antemano si los gestores del agua consultan el catálogo del fabricante [20]. La falta de esta información ha sido un desafío, en el que los

investigadores intentaron suplir esta escasez proponiendo expresiones empíricas [21]. Estas funciones se basan en el desarrollo de pruebas experimentales. El uso de estas expresiones ayudaron a comprender mejor el funcionamiento de estas máquinas cuando estos sistemas de recuperación funcionan como turbina [22].

Para definir las ecuaciones que permitan estimar el comportamiento de las máquinas se analizaron dos aspectos: (i) el conocimiento del mejor punto de operación de la máquina *(BEP,* por su acrónimo ingles *best efficiency point)* cuando opera como turbina y el gestor de agua solo conoce las curvas características en modo bomba; y (ii) la necesidad de regular la velocidad de rotación de la máquina para maximizar la efectividad la energía recuperada del sistema cuando se aplica una estrategia de operación variable *(VOS,* por su acrónimo del inglés *variable operation strategy)* [23]. El conocimiento de las curvas de operación a través de los aspectos mencionados permitirá estimar la ubicación y selección óptima de las *PAT.*

La determinación de la ubicación y selección óptima de las *PAT* dentro de una red de distribución de agua puede producir energía y reducir las fugas [24]. En un caso de estudio desarrollado en Estados Unidos, los resultados mostraron que es factible reemplazar las *VRP* por *PAT.* La instalación de tres *PAT* generó una potencia total de 47965 kW, que es más del 30 % de la demanda eléctrica diaria de la red de agua [25]. Lima, Luvizotto y Brentan [26], compararon el uso de *PAT* frente a las *VRP,* indicando que con la instalación de *PAT* es posible recuperar un valor anual de energía igual a 169360 kWh y reducir las fugas un 60 %. Un estudio en Polokwane, identificó un potencial de energía recuperable mediante *PAT* de 2.3 GWh, lo que supone una reducción anual del 4.2 % en fugas de agua. Mediante la instalación de *PAT* fue posible disminuir las fugas, aumentando el rendimiento volumétrico del sistema de 0.73 a 0.90 [27].

La gestión eficiente de las pérdidas en los sistemas de distribución de agua es uno de los temas clave de las empresas de agua. En particular, las herramientas y los métodos para gestionar las fugas se desarrollan activamente entre los componentes de las pérdidas [28]. Los *KPI* aplicados a los sistemas de agua, son una herramienta de gestión para conocer el estado de la red y poder caracterizarla, estos indicadores sostenibles están clasificados en tres grupos diferentes: índices energéticos, económicos y ambientales [29].

La instalación de *PAT* permite que las ciudades sean más inclusivas, seguras, resilientes y sostenibles, esto se relaciona de forma directa con varios de los objetivos del desarrollo sostenible *(ODS)* [30].

1.2. Estructura de la tesis

Este documento se encuentra dividido en ocho capítulos.

En el *Capítulo 1*, se presenta la introducción, principal motivación de esta investigación, la estructura de la tesis, los objetivos y herramientas y software empleados en su desarrollo.

El *Capítulo 2*, contiene la introducción, materiales y métodos, resultados y conclusiones de la publicación del Artículo 1, denominada "Leakage Management and Pipe System Efficiency. Its Influence in the Improvement of the Efficiency Indexes". Este artículo describe los principales métodos de cálculo para la estimación de fugas, analiza los datos de casos de estudios de redes existentes para proponer una serie de indicadores de rendimiento. Finalmente, se muestra la influencia de las fugas cuando se instalan PAT en las redes.

El *Capítulo 3*, contiene la introducción, materiales y métodos, resultados y conclusiones de la publicación del Artículo 2, denominada "Definition of the Operational Curves by Modification of the Affinity Laws to Improve the Simulation of PATs". Este artículo propone una serie de expresiones de regresión para definir tres curvas operativas cuando las máquinas operan a velocidad de rotación variable. La propuesta es comparada con las expresiones publicadas por otros autores.

El *Capítulo 4,* contiene la introducción, materiales y métodos, resultados y conclusiones de la publicación del Artículo 3, denomiada "Optimization tool to improve the management of the leakages and recovered energy in irrigation water systems". Este artículo aplica la metodología propuesta en esta tesis a una red de riego, ubicada en Vallada (España).

El *Capítulo 5,* contiene la introducción, materiales y métodos, resultados y conclusiones de la publicación del Artículo 4, denominada "Improve leakage management to reach sustainable water supply networks through by green energy systems. Optimized case study". Este artículo aplica la metodología propuesta en esta tesis a una red urbana de abastecimiento, ubicada en Manta (Ecuador).

En el *Capítulo 6*, se muestran los Resultados y Discusión, enumerando los principales resultados de cada uno de los objetivos.

En el *Capítulo 7,* se muestran las principales conclusiones de la tesis y las futuras líneas de investigación para la mejora de los sistemas de recuperación de energía en redes presurizadas.

El *Capítulo 8,* recoge las referencias utilizadas en los diferentes capítulos de la tesis.

A continuación, se muestra información adicional de cada uno de los artículos publicados dentro del estudio del doctorado.

Artículo 1: <u>Leakage Management and Pipe System Efficiency. Its Influence in the Improvement of the Efficiency Indexes.</u>

a. Co-autores:
>Carlos Andrés Macías Ávila; Francisco-Javier Sánchez-Romero; P. Amparo López-Jiménez; Modesto Pérez-Sánchez.

b. Revista:
>Water ISSN 2073-4441.
>Factor de Impacto 3.103. JCR (Q2; Posición 36/100). Water Resources.

c. Estado:
>Publicado [Water 2021, 7, 9; doi:10.3390/w13141909].

Artículo 2: <u>Definition of the Operational Curves by Modification of the Affinity Laws to Improve the Simulation of *PATs*.</u>

a. Co-autores:
>Carlos Andrés Macías Ávila; Francisco-Javier Sánchez-Romero; P. Amparo López-Jiménez; Modesto Pérez-Sánchez.

b. Revista:
>Water ISSN 2073-4441.
>Factor de Impacto 3.103. JCR (Q2; Posición 36/100 Water Resources).

c. Estado:
>Publicado [Water 2021, 7, 6; doi: 10.3390/w13141880]

Artículo 3: <u>Optimization tool to improve the management of the leakages and recovered energy in irrigation water systems.</u>

a. Co-autores:
>Carlos Andrés Macías Ávila; Francisco-Javier Sánchez-Romero; P. Amparo López-Jiménez; Modesto Pérez-Sánchez.

b. Revista:
>Agricultural Water Management ISSN 0378-3774.
>Factor de Impacto 4.516. JCR (Q1; Posición 5/90 Agronomy; 11/100 Water Resources).

c. Estado:
>Publicado [Elsevier 2021, 10, 1; doi: 10.1016/j.agwat.2021.107223].

Artículo 4: Improve leakage management to reach sustainable water supply networks through by green energy systems. Optimized case study.

a. Co-autores:

Carlos Andrés Macías Ávila; Francisco-Javier Sánchez-Romero; P. Amparo López-Jiménez; Modesto Pérez-Sánchez.

b. Revista:

Sustainable Cities and Society ISSN 2210-6707.

Factor de Impacto 7.587. (JCR Q1; Posición 2/68 Construction and Buildings Tecnology; 16/119 Energy and Fuels).

c. Estado:

Publicado [Elsevier 2022, 3, 15; doi: 10.1016/j.scs.2022.103994].

1.3. Objetivos

La presente tesis está enfocada en el desarrollo de estrategias hidráulicas para mejorar la recuperación de energía en los sistemas de distribución de agua considerando la influencia de las fugas en el sistema, mediante la optimización de la ubicación y selección de *PAT*.

El objetivo principal posee varios objetivos secundarios que son necesarios para desarrollar la tesis, estos objetivos son los siguientes:

1.   Realizar una revisión del estado de arte de las diferentes metodologías de cálculo existentes de fugas en redes de distribución, considerando un análisis de la influencia de la instalación de *PAT* en las fugas.

2.   Implementar expresiones semiempíricas correlacionadas obtenidas dentro del software específico desarrollado que realicen las curvas de operación óptimas.

3.   Definir una matriz de operación que contenga las diferentes estrategias de regulación atendiendo a caudales y alturas, así como la disposición en serie o en paralelo.

4.   Desarrollar una metodología que pueda implementarse en un modelo integrado de análisis de redes presurizadas donde el binomio *"fugas-PAT"* pueda ser analizado.

5.   Estudiar el impacto de las fugas en la variación de caudales y alturas turbinadas, así como la repercusión en la selección de máquinas.

6.   Definir indicadores ligados a los Objetivos de Desarrollo Sostenible que muestren la evolución temporal de la red en función de las fugas existentes y los sistemas de recuperación instalados.

7.   Aplicar la metodología propuesta a redes existentes de riego y de abastecimiento.

1.4. Herramientas y software empleado

La presente tesis busca desarrollar una metodología que permita a través de un procedimiento de optimización energético, volumétrico y económico, la estimación de la energía teóricamente recuperable (E_{TR}), el volumen recuperado por reducción de fugas (ΔV_L), la disminución de emisiones de gases de efecto invernadero, el valor actual neto *(VAN)* y el coste nivelado de energía *(LCOE)* en las redes de distribución de abastecimiento urbano y de riego. El procedimiento de optimización de energía permite estimar el potencial energético recuperable que existe en la red, considerando la energía perdida por fricción y la mínima que requiere la red hidráulica para su funcionamiento.

Esta metodología permite maximizar la recuperación energética y minimizar el volumen fugado. Además, esta metodología emplea parámetros económicos relacionados con el agua y la energía. La metodología incluye un procedimiento de calibración de fugas, que separa las fugas reales de las aparentes, a partir de la diferencia volumétrica entre el registro de los datos del caudal inyectado en la red respecto a los consumos de los usuarios. Los coeficientes utilizados en las expresiones para la estimación de las fugas han sido definidos a través de la búsqueda bibliográfica que recopila diferentes casos de estudio. El procedimiento de calibración se realiza utilizando el software EPANET y es validado a través de índices de error *(KEI,* por su acrónimo en inglés *Key Error Index)*. Los errores utilizados son: error medio cuadrático *(RMSE)*, desviación media absoluta *(MAD)*, desviación media relativa *(MRD)*, porcentaje *(BIAS)*.

Esta investigación está fundamentada en métodos, metodologías y materiales, en los que los resultados obtenidos y su conexión entre ellos, constituyen la metodología para optimizar la recuperación energética, reducir el volumen de fugas y de gases de efecto invernadero en los sistemas de distribución de agua. Los métodos y metodologías se incluyen en cada uno de los objetivos definidos. Estos son mostrados como resultados intermedios de esta investigación, logrando el fin propuesto en cada fase de la estrategia de optimización.

Los métodos utilizados se implementan para alcanzar el objetivo principal de esta investigación. Estos métodos son: (i) definición del modelo analítico de cálculo hidráulico para estimar los caudales y presiones en el tiempo; (ii) calibración del modelo de cálculo hidráulico en función de las variables observadas; (iii) la optimización de la energía recuperada mediante una estrategia analítica; y (iv) el estudio de modelos analíticos para estimar la eficiencia de las *PAT* cuando operan a velocidad variable y se introducen fugas en la red.

La definición del modelo analítico determina los caudales en el tiempo que circulan en la red hidráulica. En las redes de riego, esta definición se centra en la determinación de la apertura o cierre en cada punto de riego en función del balance entre la necesidad de riego y el volumen de riego acumulado. En las redes urbanas de abastecimiento se centra en la apertura o cierre de cada punto de consumo urbano. Estos pueden abastecer a un grupo de viviendas o sectores en función de la curva de consumo y el volumen total de agua inyectado en la red. La apertura en ambos tipos de red se establece en función de diferentes patrones, estos mostraran las tendencias de consumo a lo largo del día, semana y año.

Esta metodología es desarrollada en la presente investigación en el artículo 3 para una red de riego y en el artículo 4 para una red urbana.

La estrategia de calibración es realizada en los modelos hidráulicos mediante un balance hídrico entre el caudal inyectado y consumido. La bondad del ajuste del modelo entre los caudales estimados y registrados se realiza a través de indicadores de error *(KEI)* [31]. Esta estrategia de calibración es definida y aplicada en redes hidráulicas en el artículo 3 y 4.

La optimización de la energía recuperada mediante una estrategia analítica se divide en dos fases. La primera fase es a través de un balance de energía en un volumen de control. Los términos energéticos son expresados a través de ecuaciones que permiten estimar el total de energía existente en la red, la energía recuperable y no recuperable en el sistema, entre otras. La aplicación del balance energético y el algoritmo heurístico se desarrolla y aplica en los artículos 3 y 4.

La optimización de la recuperación energética, así como la selección de las máquinas está sustentada en el conocimiento de las curvas características. La eficiencia de las *PAT* es un parámetro importante para conocer el mejor punto de operación de la máquina. Las leyes de semejanza modificadas y los parámetros de Suter fueron considerados para estimar la energía recuperable cuando las máquinas

operan bajo la condición de velocidad variable. La aplicación de este método es descrita en el artículo 2.

El desarrollo de esta tesis se basa en el uso de las herramientas de software EPANET (de uso libre) y WaterPAT, software desarrollado por los tutores de esta tesis, así como coautores de los artículos publicados en la misma. Para determinar los parámetros hidráulicos de las redes de distribución de agua se utilizó el software EPANET. Este permite el análisis en simulaciones hidráulicas de periodo extendido, puede representar diferentes elementos, como: tuberías, nudos, bombas, válvulas, reservorios, patrones de consumo, reglas de operación, entre otros. El software WaterPAT plantea una metodología que optimiza bajo criterios energéticos, ambientales y económicos, tanto la ubicación de los sistemas de recuperación, como la selección y definición de la máquina o máquinas a utilizar, las curvas de operación y los modos de regulación, obteniendo las soluciones óptimas según los criterios escogidos. A dicho software, se le fue implementado los diferentes métodos y propuestas desarrollados en esta tesis.

Los materiales empleados en el desarrollo de la tesis son: (i) entrevista a gestores de la red para conocer el modo de operación de la red, que sirvieron como datos de entrada en el modelo analítico desarrollado para la estimación del caudal en el tiempo; (ii) registro histórico de datos del caudal registrado en el tiempo de la red de riego y urbana, los cuales se analizan en cada caso de estudio desarrollado; (iii) base de datos experimentales de las curvas características de las bombas como turbinas.

Las entrevistas realizadas a los agricultores y a los gestores de la red urbana de agua permitirán estimar los caudales y presiones en las redes. Estos resultados son mostrados en los artículos 3 y 4.

Los datos de la topología de la red y caudales registrados por contadores son utilizados al realizar la estrategia de calibración en el artículo 3, para red de riego en Vallada (España) y en el artículo 4 para la red urbana de abastecimiento en Manta (Ecuador).

La tesis recopila una amplia base de datos desarrollada a partir de publicaciones de diferentes investigadores que analizaron experimentalmente las *PAT*, tanto a velocidad fija como velocidad variable. El artículo 2 considera los resultados de otras publicaciones de 15 diferentes máquinas que fueron probadas a 87 diferentes velocidades de rotación. En el artículo 3 y 4 la metodología utiliza una base de datos que contiene 110 máquinas probadas.

Los materiales y métodos mostrados son aplicados en las distintas fases para optimizar en función del criterio escogido, implementando los resultados de salida como entrada de otros pasos tal como se describe en el siguiente capítulo.

2. Artículo 1

"Leakage Management and Pipe System Efficiency. Its Influence in the Improvement of the Efficiency Indexes"

2.1. Description

Coautores: Carlos Andrés Macías Ávila; Francisco-Javier Sánchez-Romero; P. Amparo López-Jiménez; Modesto Pérez-Sánchez.

Revista: Water ISSN 2073-4441.

Factor de impacto: 3.103. JCR (Q2; Posición 36/100). Water Resources.

Estado: Publicado [Water 2021, 7, 9; doi:10.3390/w13141909].

Abstract

Water is one of the most valuable resources for humans. Worldwide, leakage levels in water distribution systems oscillate between 10 % and 55 %. This causes the need for constant repairs, economic losses, and risk to the health of users due to possible pathogenic intrusion. There are different methods for estimating the level of leakage in a network, depending on parameters such as service pressure, orifice size, age and pipe material. Sixty-two water distribution networks were analyzed to determine the leakage method used, the calibration method, and the percentage of existing leaks. Different efficiency indicators were proposed and evaluated using this database. Several cases of installation of pumps working as turbines *(PATs)* in water distribution networks were analyzed in which the use of these recovery systems caused a pressure drop, reducing the level of leaks and recovering energy.

Keywords: leakage; PATs; efficiency indexes; water networks; energy recovery.

2.2. Introduction

Water is probably the world's most precious natural resource. It is sad then to think that so many people already live with less than their daily needs and that this situation is predicted to get even worse [32].

In a survey carried out by the International Water Services Association *(IWSA),* water losses vary between 8 % and 24 % in developed countries, 15–24 % in newly industrialized countries, and 25–45 % in developing countries [4]. Current statistical surveys indicated that 50% of the treated drinking water in city centers is lost and unaccounted for in big countries like Turkey [33]. According to other surveys [34], water leakages in a water distribution system may vary from 5 % to 55 % of the total supply and generally increase with pressure and it can therefore have an important effect on the operation of the system. When a network is simulated by a model considering the relationship between pressure and leakage flows, it can provide more realistic results compared to if no leakage is assumed [35].

Detecting and locating leaks in pipes has become an important aspect of water management systems. Since monitoring leakage in large-scale water distribution networks *(WDNs)* is a challenging task, the need to develop a reliable and robust leak detection and localization technique is essential for loss reduction in potable WDNs [9].

The literature describes different methods for detecting leaks in the water supply [9] classified leak detection methods as internal and external. The external detection methods are acoustics, fibre optics, gas injection, magnetic induction, ground penetration radar, among others. The internal methods are balancing methods, pressure/flow monitoring, signal processing approach, statistical analysis, model-based methods. Currently, the use of Transient Test-Based Techniques *(TTBTs)* is a good technique to improve the water management of the systems [36]. The merit of the TTBTs results from the simplicity and the limited cost of the equipment [37]. There is extensive literature which shows the development and progress of the current transitional theory, including transient flow models, models of unstable friction and turbulence and numerical simulation methods.

The contribution described in [38] presented a literature review of some major standpoints in hydraulic transient-based leak detection of pipe systems from 1992 to 2018. Reference [39] proposed a technique for leakage detection based on the well-known properties of transient pressure waves. A method for the analysis of inverse transients through a numerical model is proposed in [40].

This research focuses on model-based leakage detection methods. Reference [35] showed the formulation of a rupture prediction model that relates the rupture of a pipe with the exponent of its age, the optimal moment to replace a pipe, and the economic analysis with water losses for leaks.

Managing losses in water distribution systems efficiently is one of the key issues of water utilities. In particular, tools and methods for managing leakage are actively developed among components of losses [28]. There are many causes of such leakages, including natural process of wear, corrosion of the inner and outer surface of pipes, mechanical damage of pipes caused by excessive loads, assembling errors, seasonal temperature changes, movements of a subsoil, and material defects of pipes. The failure of pipelines is usually attributed to the ageing infrastructure and/or severe environmental conditions [3].

As water mains deteriorate both structurally and functionally, their breakage rates increase, network hydraulic capacity decreases and the water quality in the distribution system may decline [6]. A network with physical failures may be exposed, under certain operating conditions, to pathogen intrusions that affect the quality of water [7]. The leaky pipes increase pumping energy to guaranties the service levels. In addition, the energy wasted in leaks involves an environmental burden related to the many impacts associated with energy production and

consumption, including greenhouse gas emissions, acid rain, and resource depletion [9].

The general objectives of pressure management for leakage minimization are three-fold [41]: (i) reduce background leakage which refers to acoustically undetectable seeps at pipe joints and small cracks; (ii) decrease the rate of new leaks and breaks which occur on mains and service connections, due to diminished stress on the pipes; and (iii) minimize the flow rate from any leaks and breaks. To reduce leakage in the distribution network, it is necessary to apply models to know their efficiency volumetric. Different methods were found in the literature review discussed below.

Related to pressure management, one of the most used elements are pressure reduction valves *(PRVs)*. A *PRV* consists of the main valve and a *PRV* controller which senses the output pressure and adjusts the opening of the main valve to maintain the outlet pressure at a given set-point, thereby reducing leakage and mitigating the stress on the downstream water distribution network. A research topic is how to understand and explain the instability phenomena in pressure control schemes for low flow rates (small valve openings) [14]. The results of a mathematical model representing the static and dynamic properties of a hydraulic controller and a PRV show good agreement with experimental data [42]. Optimization models through genetic algorithms are used to minimize leaks in water distribution sites through the most effective location and adjustment of control valves [43].

A hybrid multi-objective algorithm was established, which has as decisive variables the pipe diameter and the positions and settings of the valves. Analysis of the results shows that the new algorithm is more efficient than a multiobjective genetic algorithm widely adopted in the scientific literature [44]. The analysis of the tests demonstrates the versatility of *PRVs* as a powerful tool for pressure management, and also when the flow condition changes according to the users' demand pattern. Notwithstanding the crucial importance of *PRVs*, few experimental data are available in the literature [45]. The pressure control strategy through *PRVs* has been thoroughly researched as a management strategy. In contrast, little experimental data is available in the literature, regarding the transient behavior of *PRV* in terms of its response to incoming pressure waves, as well as the time required to reach the pressure set point [46].

The use of pumps working as turbines *(PATs)* was proposed by [16] as an unconventional solution to reduce pressure and recovery energy. PATs are standard water pumps utilized as hydraulic turbines by reversing the flow direction across them. Electric power generation through *PATs* has a lower cost compared to

hydraulic turbines. However, in the literature, the few available cost figures relative to *PAT* purchase price are discordant and often outdated, and such a lack of information is likely a severe barrier to a more widespread *PAT* implementation [18].

The application of *PATs* appears as an alternative and sustainable solution to either control network pressure as well as to produce energy [47]. Different pumps suitable to run in turbine mode for low-capacity power generation in micro- hydropower plants as well as in water supply piping systems are discussed. The research work on *PAT* including criteria for selection of pump running as turbine, cavitation analysis, force analysis, loss distribution, various methods of performance enhancement, cost analysis of hydropower plant with conventional hydro turbine and *PAT*, applications of *PAT* in water supply pipelines, among others [48].

Performance data in pump and turbine mode were published in [15]. An energy evaluation is shown considering a test case of a water distribution network. Due to some problems such as limited resources and environmental pollution that they cause in recent years, researchers and engineers have focused on various types of renewable energies. Benefiting renewable resources improves air quality and prevents further greenhouse gas emissions [15]. Being the implementation of *PATs* a sustainable alternative for the reduction of leaks and energy production.

The objective of this research is to show the different methodologies to determine the leakage flow in distribution networks as well as the implications of leaks in volumetric performance, energy losses, and the costs associated with the loss of water and energy in forty-five case studies. The comparison between different case studies enables to show the range of the different key performance indicators *(KPIs)* applied to them.

2.3. Materials and Methods

2.3.1. Leakages Evaluation and KPIs

Different methods were used to estimate the leakages in the water systems. The most used are Torricelli theorem [41], *MNF* [49], Fixed and Variable Area Discharges *(FAVAD)* [9], N1 Power Law and leakages model [50], and Background and Bursts Estimates *(BABE)* [51].

Figure 1 shows the process and analysis carried out in this research. Forty-five different distribution networks were selected and analyzed for leaks. The leak calculation method implemented in the model was identified and relevant information was subsequently extracted from each case to calculate the efficiency

indicators. The water distribution systems were different in terms of topology and pressure. However, to consider the general indicators and get the normalization of the different indicators, the research work with the value of average pressure to establish the correlation between indicator values. However, the different cases studies were analyzed in the different published studies considering the pressure value in the different leakage methods.
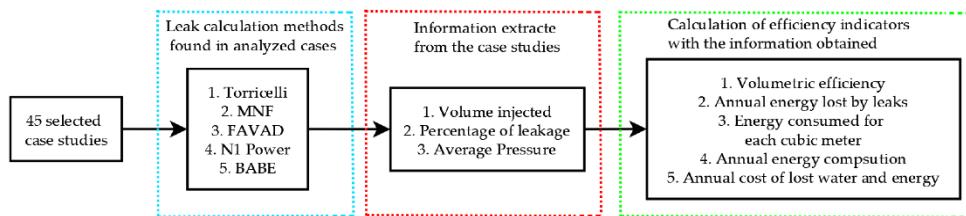
Figure 1. Analysis and calculations made to case studies

2.3.1. Torricelli Teorem

The hydraulics of orifices is well understood, and a fair amount of research has been conducted on different orifice shapes and conditions. In Torricelli's equation, the velocity through an orifice is expressed as [52]:

$$v = \sqrt{2gh} \qquad (1)$$

where v is the theoretical velocity (m/s); g is the acceleration due to gravity (m/s^2) and h is the pressure head (m w.c.).

The starting point is that water leakages in *WDN* are directly related to pressure as well as to the age and material of *WDN* elements (joints, valves, pipes, etc.). Many numerical models were developed starting from experimental observations and assuming the validity of the Torricelli law in the following form, which is valid for a single leak orifice [51].

One of the major factors that influence leakage rate is the pressure in the distribution system. A conventional physical model that relates the pressure and the leakage rate is the well-known Torricelli orifice equation, described as [53]:

$$Q_{leak} = C_d A \sqrt{2gh} \qquad (1)$$

where Qleak represents the leakage flow rate, Cd is the leakage discharge coefficient, h denotes the pressure head, and A the area of the leak opening in m^2. However, from several studies on real *WDNs*, it has been shown that the Torricelli

34

law does not provide a satisfactory model for the relationship between leakages with pressure within a WDN [51].

2.3.2. Minimum Night Flow (MNF) Analysis

Minimum Night Flow *(MNF)* analysis is the most common method for leakage assessment at the scale of the *DMA*. The *MNF* is the lowest inflow in the *DMA* over 24 h along the day, which occurs depending on consumption patterns but reportedly, between 02:00 and 04:00 AM when most of the customers are probably inactive and the flow at this time is predominantly leakage [54]:

$$L_{DMA} = Q_{MNF} - Q_{LNC} \tag{2}$$

Where L_{DMA} is the leakage rate in the *DMA* (m^3/h) at the time hour of *MNF*, Q_{MNF} is the minimum flow rate *(MNF)* and Q_{LNC} is the legitimate nighttime consumption in the *DMA* at the *MNF* time.

The leakage in the *MNF* time cannot be generalized for all the hours of the day because of the pressure leakage relationship, where higher pressure at night leads to higher night leakage and lower pressures during the day lower the day leakage. For this reason, the *MNF* leakage should be modelled according to the leakage-pressure relationship [49]. Lambert [55] in his research shows three basic steps that must be performed to determine the *MNF*.

Once the leakage flow has been obtained in the hour of the night minimum, its value can be extrapolated to the rest of the hours using a multiplying factor known as the hour-day factor *(HDF)*. The *HDF* represents the change throughout the day of the leakage flow and it is proportional to the pressure variation in the network for the pressure of the hour of minimum night flow. This pressure variation is calculated in the Average Zone Pressure *(AZP)*, which is assumed to be the most representative point of pressure in the network, therefore [56]:

$$Q_{leak(t)} = Q_L(t_{MNF}) \cdot \left[\frac{P_{AZP(t)}}{P_{AZP}(t_{MNF})} \right]^\alpha \tag{3}$$

where $Q_{leak(t)}$ is the leakage flow at a different time from that considered for the night minimum, (t_{MNF}) is the time at which the night minimum flow is measured, $P_{AZP(t)}$ is the pressure in the *AZP* (selected as point average of the pressures in the network), $P_{AZP}(t_{MNF})$ is the pressure in the *AZP* at the hour (t_{MNF}) and finally, α is the exponent of the emitter. This equation is based on the *FAVAD* theory. Stenberg

[54] has found that night leakage flow rates should then be multiplied by 20 h. This assumption does not consider that pressure is not constant over a period.

2.3.3. FAVAD Concept

A variety of different concepts have been proposed to explain the diversity of pressure: leakage rate relationships including the widely used fixed and variable area discharge *(FAVAD)* model. This model offers a means to demonstrate the sensitivity to the pressure of different leaks and to quantify the change of the area of elastically deforming leaks subject to hydraulic pressure loading [41].

The *FAVAD* concept, as realistic modelling of leakage and intrusion, flows through leak openings in pipes in water supply systems, allows for variations in leaks resulting from changes in pressure [55]. The *FAVAD* concept as the principle of conservation of energy provides a logical hydraulic basis to explain, analyze and predict diverse relationships between Average Zone Pressure *(AZP)* and leak flow rates [57].

Emitters are devices associated with junctions that model the flow through a nozzle or orifice that discharges to the atmosphere [58]. The technique for a more consistent description of demands is to allocate part of the total metered inflow to the leakage component, and account for this as a pressure-dependent demand [39].

When the leakage flow at each pipe is known, this value can be assigned to each node according to Equation (5) [59]:

$$ql_i = c_i \cdot P_i^{\beta} \tag{4}$$

where ql_i is the leakage flow at node (ls^{-1}), β is the emitter exponent which takes into account the pipe material and the shape of the orifice, and P_i is the pressure at node i. [60] defined the leakage exponent as α, which is sometimes called N1. The coefficient C_i was determined by equation:

$$C_i = \alpha \cdot 0.5 \cdot \sum_{j=1}^{K_{ji}} L_{ji} \tag{5}$$

α is a coefficient $(ls^{-1}m^{-1-\beta})$, j is an index related to pipe, K_{ji} is the number of pipes connected to node i and L_{ji} is the length of pipe j connected to node i (m). The leakage volume was obtained by applying the equation:

$$Vl = \frac{1}{1000} \cdot \sum_{h=1}^{24} Ql_h \cdot \Delta h \qquad (6)$$

where the term 1/1000 is used to convert units from ls^{-1} to m^3s^{-1}, Ql_h is the total leakage flow at time h and Δh (s) is the time in which Ql_h ls^{-1} is applied.

α and β variables are two leakage model parameters, representing the influence of some factors on the relationship leakage/pressure. Parameter β can represent the pipe deterioration over time, thus it depends on both pipe characteristics (pipe age, diameter, and material) and various external factors (mainly the average pressure, but also other environmental conditions, traffic loading, external stress, and corrosion, etc.). In contrast, α is a function of pipe characteristics only (material and elasticity) [40,50].

In general, β is more closely related to the number of leaks (or leakage area) per unit of pipe length while α is more strongly related to the type of leakage (therefore to the hydraulics of leakage) as governed by the pipe material. For this reason, changes in β need to be determined for the specific system, i.e., by model calibration, while most experimental studies have focused mainly on leakage parameter α [34,50]. Table 1 shows the range of α and β coefficients for different pipe materials.

Table 1. Coefficients for different materials

Material	α	β
Cement	$10^{-7} \leq \beta \leq 10^{-5}$	$0.75 \leq \alpha \leq 1.10$
Steel	$10^{-6} \leq \beta \leq 10^{-4}$	$1 \leq \alpha \leq 1.3$
PVC	$10^{-5} \leq \beta \leq 10^{-4}$	$1.1 \leq \alpha \leq 1.5$

The value of the leakage parameter, α, can be described using the fixed and variable area discharge (*FAVAD*) approach. The range of exponents observed reflects substantial differences in the impact of pressure on the rate of leakage. For example, when the pressure halved in a pipe it caused a decrease of the flow rate of 29%, 50% and 82% respectively, when the exponents were 0.5, 1.0 and 2.5 [60]. Reference [61] showed the coefficient is a function of the length of the pipe and the type of material in the network. Table 2 shows the leakage emitter exponent used in different study cases. It is observed that the most used emitter exponent in the analyzed case studies is 0.5, however, in some cases, they use different coefficients to observe the sensitivity of the parameter to the model.

Table 2. Case study emitter exponent

Reference	ID	Emitter Exponent	Material
[50][62][63][64]	7, 9, 12, 13, 27, 33	0.5	PVC, HDPE, steel, asbestos cement and cast iron
[65]	-	0.61	PVC, asbestos cement, galvanized steel
[66]	8	0.5–1	PVC, Polyethylene (PE), iron, steel.
[67]	1	0.91–1.13–1.41	PVC, metal, ambient.
[68],[69]	2, 10	1.1	PVC, iron.
[70]	5	0.5–1.18	-
[71]	3	1.1–1.18	Ductile iron, Steel, High-Density Polyethylene (HDPE)
[72],[73],[10]	11, 14, 15, 18	1.18	PVC, asbestos cement, galvanized steel
[57][60][74][75][76]	-	0.5–2.5	PVC, iron, galvanised iron, asbestos cement.
[41][52]	16	0.5–2.79	PVC, asbestos cement.
[74][76]	-	0.5–2.95	-

The research described in [77] confirmed that the leak exponents can be significantly higher than the theoretical value of 0.5. While leakage exponents for round holes were near 0.5, the values for corrosion holes varied between 0.67 and 2.30, for longitudinal cracks between 0.79 and 1.85, and circumferential cracks between 0.41 and 0.52. A variety of different concepts have been proposed to explain the diversity of pressure: leakage rate relationships including the widely used fixed and variable area discharge *(FAVAD)* model [78].

2.3.4. FAVAD and the N1 Power Law

The *N1* Power Law an approximate version of the *FAVAD* concept—has been increasingly used internationally since 1994 for practical assessment of pressure-dependent leakage in water distribution systems. The estimation of system leakage and average zone pressure head *(AZP)* before and after pressure management can be used to estimate the leakage coefficient C and leakage exponent *N1* [79]. When modelling the pressure-leakage rate relationship in individual water distribution

systems, a more general form expression was proposed instead of the orifice equation [57]:

$$Q_{leak} = Ch_{AZP}^{N_1} \tag{7}$$

Where Q_{leak} is the leakage flow rate and h_{AZP} the *AZP* Equation (8) is also called the *N1* power-law or the *N1* equation. The N1 Power Law approximation simplifies *FAVAD* by assuming that the leak flow rate varies with average pressure *N1*, where *N1* lies between 0.5 (less sensitive) and 1.5 (more sensitive). *FAVAD* and *N1* are both widely used internationally in distribution systems and laboratory tests [55].

Different investigations [77], [80], [81] experiment with the materials of the pipes to calibrate the parameters of *C* and *N1*, according to the orifice in the pipe, it is transverse, longitudinal or circular (Table 3).

Table 3. Summary of leakage exponents N_1

Failure Type	uPVC	Asbestos Cement	Mild Steel
Round hole	0.52	-	0.52
Longitudinal crack	1.38–1.85	0.79–1.04	-
Circumferential crack	0.41–0.53	-	-
Corrosion cluster	-	-	0.67–2.30

The median used is 1.15 depending on the mixture of leaks and the dominant type of leaks (fixed area leaks: *N1* = 0.5; longitudinal split which opens in one dimension: *N1* = 1.5; linear-radial opening: *N1* = 2.0–2.5). Typically found in the literature an exponent value of 0.5 [41]. Ref. [7] presented a methodology for evaluating water losses where a sensitivity analysis of the coefficients is carried out to determine the influence of various leakage exponents on the results of the study.

2.3.5. Background Leakage and Emitter Coefficient (*BABE*)

It is assumed that leakage continuously increases with pressure and can be expressed as the sum of the background leakage and the burst leakage. So, the pressure-leakage relationship for a pipe k can be stated as follows:

$$q_k^{leak}(P_k) = \begin{cases} \beta_k l_k(P_k)^{\alpha_k} + C_k(P_k)^{\delta_k} & P_k > 0 \\ 0 & P_k \leq 0 \end{cases} \tag{8}$$

Where q_k^{leak} is the total leakage along pipe k; lk is the length of pipe k; α_k and β are parameters of the background leakage model; C_k and δ_k are parameters of the

bursts leakage model; and P_k is the average pressure in pipe k computed as the mean of the pressure values of its end nodes. The leakage model assumes a uniform distribution along the pipe [34], which is the most common experimental relationship between leakage and pressure [35]. Several studies model leaks along the pipe [41],[75], [82] .For each pipe, the total leakage is assigned to its end nodes, half to each node. So, the nodal leakage flow q_i^{leak} for a node i can be computed as follows:

$$q_i^{leak} = \frac{1}{2} \sum_k q_k^{leak}$$

(9)

2.3.6. Summary of Leak Calculation Methodologies

As mentioned above, there are different methodologies to calculate water leaks in distribution networks. These methods are used in designs to know the leakage percentage of a network. Table 4 shows the calculation equations, parameter calibration methods, advantages and disadvantages of the leakage methodologies described in this research.

Table 4. Methodologies for calculating leaks (Continue in next table)

Technique	Reference	Equation	Calib.
Torricelli	[43][83][84] [85][86]	$Q_{leak} = C_d A \sqrt{2gh}$	-
MNF	[49][50][56][87][88][84] [87][89][90]	$L_{DMA} = Q_{MNF} - Q_{LNC}$ $Q = Q(t_{MNF}) \cdot \left[\frac{P_{AZP(t)}}{P_{AZP}(t_{MNF})} \right]^\alpha$	-
FAVAD Fixed and Variable Area Discharges	[9][41][50][51][52][55] [54][57][61][65][63][65] [66][69][71][74][76][78] [79][83][84][86][91][92] [93][94][95][96][97][98]	•The equation can be written in different ways: $Q_{i,l}(t) = K_i[P_i(t)]^\alpha$ $ql_i = c_i \cdot P_i^\beta$ $Q_{leak} = \beta P^\alpha$	K_i, C, β [80][74][99]
The N1 Power Law	[50][52][55][57][62][77] [93][80][81][90] [98]	$Q = C_d h_{AZP}^{N_1}$	N_1[80][74]
Background leakages model	[35][100][57] [62] [101][82][102][103][90] [97][98][104][105][106] [107] [108]	$Q = \beta_k l_k (P_k)^{\alpha_k} + C_k (P_k)^{0.5}$	β and α [109] β[106][102]

Table 4. (Cont). Methodologies for calculating leaks

Advantage	Disadvantages
•Pressure dependent • The scale is to system-wide • No need lots of network data • No need for a mathematical model • Consider that the area of the orifice varies with pressure • Analyse field data and volumes of bursts and the rates of small background leaks	• Only applicable for rigid pipe orifices • Does not consider the flexibility of the pipes • It does not provide a satisfactory model of the relationship between leakage and pressure • Need to data loggers and mechanical flow meter •Needs measurements • Intensive fieldwork, zoning • Many assumptions • Further calibrations are useful
•Pressure dependent • The scale is to system-wide	• It is an empirical equation and therefore not founded on fundamental principles of fluid mechanics • The values of C and N1 are not constant for a given system but depending on the pressures at which they are being estimated • The equation is dimensionally awkward since the units of C include the variable N1
• Consider leaks along the pipe • Pressure dependent • The scale is to system-wide	• Further calibrations are useful

2.3.7. Leakages Modelling and Calibration

In a distribution network under *MNF* conditions, using leakage and pressure data, the leakage exponent of the system was determined by the following expression. From the two data sets, system leakage exponent *N1* was calculated using the equation below [90]:

$$N_1 = \frac{log\left(\frac{Q_1}{Q_2}\right)}{log\left(\frac{AZP_1}{AZP_2}\right)} \tag{10}$$

Where Q_1 and Q_2 are system leakages and $AZNP_1$ and $AZNP_2$ are average zone night pressures before and after pressure reduction, respectively. Van Zyl, Lambert,

and Collins [91] suggested a modified version of the orifice equation where fixed orifice area and flexible orifice area are considered as shown in equation (11).

$$Q_{leak} = sgn(h)C_d A\sqrt{2g}(A_0|h|^{0.5} + m|h|^{1.5})$$ (11)

where Q_{leak} is leakage flow, sgn(h) is the sign function, Cd is the discharge coefficient, h is the pressure head, g is the acceleration of gravity and A_0 is the initial area of the orifice.

Calibration methods can leverage steady-state hydraulic models and optimization tool technology, such as Genetic Algorithms (*GAs*) to improve the detection of a leak [76][110]. Reference [111] proposed a methodology for the estimation of C and γ, based on the solution of an inverse modelling problem where demand and leakage pattern are assumed as unknowns, is solved using *GAs*. Reference .[109] proposed a genetic algorithm using Epanet to calibrate the alpha and beta coefficients in a network and shows the variation of the coefficients in the case of new and old pipes.

Reference [83] showed a table of calibrated coefficients, which were determined through experimental tests on *PVC* and Steel materials from 1″ to 3″ with holes from 1.5 to 10 mm. References [28] and [112] proposed a method of estimating area leakages in virtual areas of a water network to prioritize leak surveys for the areas.

To calibrate both emitter *C* and exponent *N1* coefficients, the leakage flow rate was calculated as the difference between the upstream and downstream measured flow rates, this methodology is described in [80]. This research used a *CFD* model with experimental results to different geometric configurations of the orifice, to assess the dependence of the orifice geometry and orientation on the calibration of leakage law parameters.

Reference [110] showed a GA. This is used to solve optimization problems of searching for calibration parameters values while minimizing the differences between observations and model predictions. A Matlab optimization code was developed for model calibration and was linked to the Epanet toolkit. The optimization process uses a non-dominated sorting genetic algorithm II (*NSGA II*) [13]. A multi-objective procedure based on non-dominated sorting GAs has been developed to calibrate a water supply system characterized by elevated pressure and a high amount of background leakages [106].

Reference [102] used a method of optimization in the network through a differential evolution algorithm (DE). It is a simple power and population-based stochastic

optimization algorithm that outperforms many meta-heuristic algorithms on numerical single-objective optimization problems.

Reference [113] proposed a method of optimization using is the BOBYQA algorithm, this model is an iterative algorithm for finding a minimum of a function. Table 5 shows a summarize of the used algorithms.

Table 5. Summary of optimization algorithms (Continue in next page)

Reference	Algorithm	Parameters	Objective Function	Error
[109][114] [115][70] [111][76][95] [97][106] [110][116] [117][118]	Genetic algorithm.	Operation conditions, flows, demands, pressures, total leakage.	Minimize network pressure and producing a new generation of solutions α and β.	0.5 to 23%, with an average value of 11%.
[9][50][108]	Algorithm for detecting and estimating background leakage.	Operation conditions flow, pressure and fluid temperature.	Detect critical causes and their location for possible pressure control.	-
[105]	Pseudogenetic algorithm.	Basic network	Operational costs, capital costs (pipe and pump replacement, tank expansion, and PRVs), and constraints.	-
[90]	Global Gradient Algorithm.	Flow, pressure.	Reduce excess pressure.	-
[32]	Neural networks.	Flow, pressure.	Detection of water leaks.	-
[119]	Differential evolution with temporal analysis.	Water distribution network.	Estimation and location to leakage.	Root mean squared error: 0.05

Table 5. (Cont.) Summary of optimization algorithms

Reference	Algorithm	Parameters	Objective Function	Error
[102]	Differential evolution.	Flow, pressure, network data.	Estimation of leakage.	-
[101]	Algorithm with convergence analysis.	Operation conditions, flows, demands, pressures.	Estimation to leakage	-
[70]	Sequential Quadratic programming.	Water distribution network.	Leakage minimization	-

2.3.8. Leakages Key Performance Indicators *(LKPIs)*

Performance indicators are a powerful management tool, they can provide measures of how many resources are being used relative to those available, they can be used to assess the extent to which management objectives are being met, and even to assess the overall impact of strategies management [120]. Some proposed key performance indicators leakages are pressure-dependent demand, volumetric efficiency, performance indicators for water supply services:

1. Pressure-dependent demand concept; Two types of pressure-dependent demands are considered: consumptions and leakage (background and bursts). For pressure-dependent consumption, it is assumed that the available demand (q_i^{avl}) is computed with the pressure-demand relationship [103][108]:

$$q_i^{avl}(P_i) = q_i^{req} \cdot \begin{cases} 1 & P_i \geq P_i^{ref} \\ \left(\dfrac{P_i - P_i^{min}}{P_i^{ref} - P_i^{min}} \right)^{\alpha} & P_i^{min} P_i < P_i^{ref} \\ 0 & P_i \leq P_i^{ref} \end{cases} \tag{12}$$

where P_i^{ref} is the reference pressure necessary to satisfy the required demand q_i^{req}, P_i^{min} is the pressure below which no water can be supplied, α (typically 0.5) is the exponent of the pressure-demand relationship, P_i is the current pressure at node i.

2. Volumetric efficiency (η_v); One of the most important ratios among the system's efficiency indicators is volumetric performance. The volumetric performance η_v of a

network or an isolated sector of the same is defined as the relationship between the registered volume V_{Reg} and the total volume V_{Tot} contributed in the same reference period [121].

$$\eta_v = \frac{V_{Reg}}{V_{Tot}} \tag{13}$$

3. Performance Indicators for Water Supply Services; International water association (IWA) provides performance indicators of water supply systems to compare the management of water losses, these are (i) Water losses and real losses as a % of system input volume; (ii) Water losses per house connection and km of mains per day(density of connections $<$ 20 per km of mains), and (iii) Infrastructure Leakage Index (*ILI*) [122].

4. Infrastructure Leakage Index (*ILI*); The *ILI* is a measure of how well a distribution network is managed (maintained, repaired, rehabilitated, etc.) for the control of real losses, at the current operating pressure. It is the ratio of the Current Annual volume of Real Losses (*CARL*) to Unavoidable Annual Real Losses (*UARL*) [123].

$$ILI = \frac{CARL}{UARL} \tag{14}$$

5. Unavoidable Annual Real Losses (*UARL*); *UARL* is a useful concept as it can be used to predict the lowest technically annual real losses for any combination of mains length (18 liters/km mains/day/meter of pressure), number of connections (0.8 liters/service connection/day/meter of pressure), customer meter location and average operating pressure (25 liters/km/day/m of pressure) assuming that the system is in good condition with high standards for the management of Real Losses [124].

6. Absolute annual consumed energy (*IAAE*); this index is sum of the total active consumed energy in the network subtracted by the sum of the total energy recovered in the network, the units are $kWh/year$ [125].

7. Absolute consumed energy per unit volume (*IAEFW*); Ratio between *IAAE* and the total volume of water introduced in the network, the units are kWh/m^3 [126].

2.4. Results

2.4.1. Case Studies

To observe the different methodologies applied to real cases of water distribution networks in different parts of the world, this research analyzed 45 case studies, as shown in Table 6.

Table 6. Information of the studied cases

ID	Case Study	Year	Ref	ID	Case Study	Year	Ref
1	Skiathos, Greece	2020	[67]	24	Zarqa, Jordan	2020	[84]
2	Leicester, United Kingdom	2012	[12]	25	Zarqa, Sana'a, Yemen	2020	[84]
3	Benevento, Italy	2017	[127]	26	Mwanza, Tanzania	2020	[84]
4	Pretoria, South Africa	2017	[50]	27	Mutarea, Zimbabwe	2006	[88]
5	Polokwane, South Africa	2019	[70]	28	Skopje, Macedonia	2011	[128]
6	Villarreal, Spain	2014	[129]	29	Pittsburgh, Pensilvania	2005	[130]
7	Guayaquil, Ecuador	2015	[63]	30	Azogues, Ecuador	2019	[39]
8	Antalya, Turkey	2017	[66]	31	Mankessim, Ghana	2014	[131]
9	Konyaalti, Turkey	2012	[87]	32	Rzesów, Poland	2019	[32]
10	Valencia, Spain	2015	[69]	33	Gorino Ferrarese, Italy	2021	[64]
11	Palermo, Italy	1999	[72]	34	Salzburg, Austria	2011	[132]
12	Nagpur, India	2016	[133]	35	Belgium	2014	[134]
13	Nagpur, India	2016	[133]	36	Dryanovo, Bulgaria	2014	[134]
14	London, United Kingdom	1989	[73]	37	Pula, Croatia	2014	[134]
15	London, United Kingdom	1989	[73]	38	Lemesos, Cyprus	2013	[134]
16	Nourhan Samir, Egypt	2017	[100]	39	Odense, Denmark	2013	[134]
17	C-Town	2015	[135]	40	England	2013	[134]
18	Verona, Italy	2019	[136]	41	Bordeaux, France	2012	[134]
19	Udine, Italy	2014	[118]	42	Munich, Germany	2014	[134]
20	Patras, Greece	2016	[137]	43	Italy	2010	[134]
21	Case I.- San Gregorio, México	2014	[84]	44	Lisbon, Portugal	2014	[134]
22	Case II.-San Gregorio, México	2014	[84]	45	Scottish, United Kingdom	2014	[134]
23	Drama, Greece	2016	[84]		-	-	-

Relevant information from the distribution networks was extracted from each case (Table 7) such as location, annual injected volume, mean operating pressure, leakage percentage, leak calculation method, calibration method.

Table 7. Information from case studies (Continue in next page)

ID Case	Leakage (%)	Average pressure (m)	Annual volume consumed (m³)	Energy consumed per m³ injected (kWh/m³)	Annual consumption (kWh)	Annual energy lost by leaks (kWh)
1	57.56	54	33016	0.15	115093	66252
2	51.00	93	629552	0.25	325600	166056
3	12.03	50	807.216	0.14	1250363	150387
4	25.00	63	12772080	0.17	2923529	730882
5	27.16	70	27899748	0.19	7306457	1984580
6	3.05	60	2332019	0.16	393260	11975
7	23.00	55	320397	0.15	62363	14343
8	34.94	45	1436640	0.12	268653	93873
9	34.38	47	513336	0.13	101834	35010
10	31.37	40	1277500	0.11	202904	63656
11	45.60	41	3190939	0.11	659074	300538
12	15.00	40	5361120	0.11	687485	103123
13	15.00	40	7505568	0.11	962479	144372
14	14.90	59	11003226	0.16	2068799	308251
15	17.20	34	4047330	0.09	452881	77895
16	54.00	30	169243	0.08	30077	16242
17	26.05	40	5370085	0.11	791534	206194
18	23.92	65	1577530	0.18	367280	87860
19	28.31	31	8842478	0.09	1052511	297966
20	55.00	30	9855000	0.08	1790325	984679
21	28.45	40	251605	0.11	38328	10903
22	34.41	40	308260	0.11	51230	17630
23	19.80	30	9358600	0.08	953945	188879
24	63.27	50	24588597	0.14	9122084	5771888
25	38.24	50	13766774	0.14	3037055	1161332
26	46.06	50	16231357	0.14	4100160	1888637
27	57.00	77	18049250	0.21	8750213	4987622
28	52.50	40	426919	0.11	97967	51432
29	40.00	114	862194	0.31	446401	178560

Table 7. (Cont.) Information from case studies

ID Case	Leakage (%)	Average pressure (m)	Annual volume consumed (m³)	Energy consumed per m³ injected (kWh/m³)	Annual consumption (kWh)	Annual energy lost by leaks (kWh)
30	46.86	75	157946	0.20	60746	28465
31	12.00	56	430151	0.15	74592	8951
32	30.00	40	2571680	0.11	400623	120187
33	13.33	30	81994	0.08	7734	1031
34	5.57	46	12210000	0.13	1620776	90252
35	20.70	38	130180000	0.10	16998768	3518629
36	74.96	42	1780000	0.11	813740	610019
37	22.55	40	6630000	0.11	933040	210370
38	23.22	40	10120000	0.11	1436620	333540
39	47.00	30	530009	0.08	81751	38423
40	17.54	44	330660000	0.12	48079900	8433766
41	15.87	37	40010000	0.10	4795237	761229
42	13.33	60	91000000	0.16	17167500	2289000
43	24.71	44	33830000	0.12	5387107	1330890
44	12.99	51	26524047	0.14	4236514	550334
45	58.69	45	147752776	0.12	43854719	25736535

The *FAVAD* method is the most used in research analyzed, there is an extensive literature of its application in real case studies where the calibration methods applied in the networks are shown. With the information extracted from each case study, key performance indicators (*KPIs*) such as volumetric efficiency of the system, the volume of water lost annually and its associated cost, the energy lost in kWh for each m^3 injected and its cost was calculated.

2.4.2. Influence of the Leakages in the *KPI* of the Water Systems

Water leaks in distribution networks condition the quality and quantity of water for users. The existence of leaks increases the loss of water and the operating costs of the networks management because more energy is required in the flow to guarantee the minimum operating pressure.

For each of the case studies shown in Table 7, the following information was extracted: annual volume injected into the network, percentage of leaks, and mean

pressure. The analysed data enabled the calculation of the following parameters: volumetric efficiency of the network, energy consumed for each cubic meter of water injected into the network, annual energy consumption, energy lost due to leaks, and the associated costs due to loss of water and energy.

As mentioned above, volumetric efficiency is the ratio of recorded volume to total volume over a period. For the 45 case studies, the distribution corresponding to the volumetric efficiency is shown in Figure 2a resulting in a mean of η=0.73 and quartiles of η=0.53 and η=0.83. Figure 2b shows the leakage percentage in the distribution networks with an average leakage value of 27 % and quartiles of 17 % and 46 %.
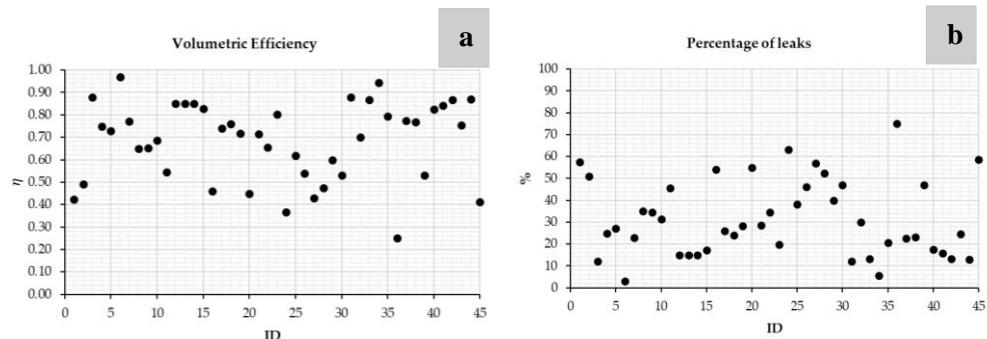

Figure 2. Volumetric efficiency (a) and percentage of leaks (b)

Each of the distribution networks has different physical characteristics, such as diameters, lengths, valves, pressures, and flow rates. The configuration of each network will depend on the design conditions, this will make each of them operate differently, some of the networks transport the flow by gravity and others under pressure using pumps.

The average pressure of each distribution network was obtained as shown in Figure 3a. Its average value was 44 m.w.c. and the quartiles were 40 and 45 m.w.c. Two atypical values are observed that correspond to networks where their topography had high slopes. Figure 3b shows the annual volume injected into the network. The average value was $7.26 \, Hm^3$ and the quartiles were 1.21 and $24.24 \, Hm^3$. There were 5 cases above $50 \, Hm^3$. These reached annual values of up to $400 \, Hm^3$.
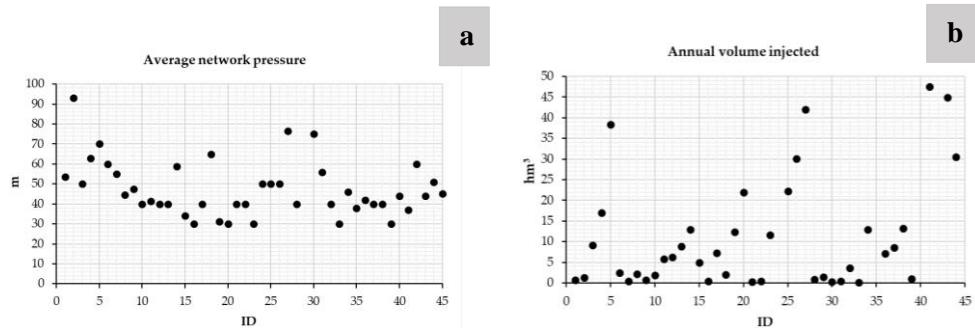
Figure 3. Average pressure (a) and annual flow injected into the network (b)

The average pressure of each case study was related to the percentage of leaks and the volumetric efficiency of the system. The ratio between the average pressure and the leakage percentage is shown in Figure 4a. The values are between 50 and 500, being the average equal to 243. Figure 4b shows the relationship between the average pressure of the network and the volumetric performance. This ratio shows values between 40 and 200, being the average value equal to 78 m.
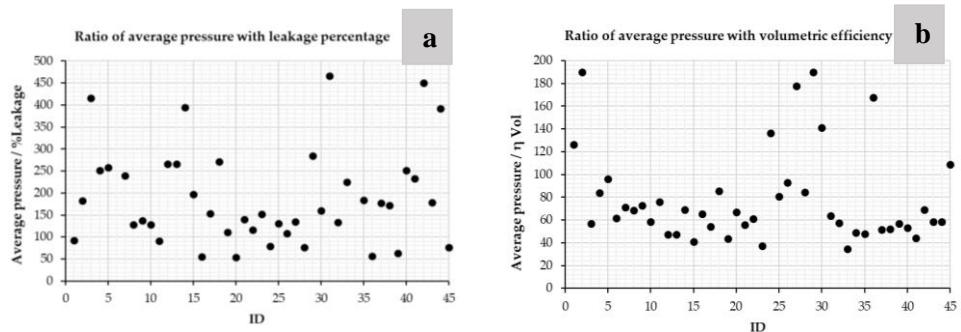
Figure 4. Ratio between average pressure with leakage percentage (a) and volumetric efficiency (b)

In energy terms, the value of average pressure and flow injected into the network enabled to estimate average energy consumption of the network per unit volume ($kWh \cdot m^{-3}$). Subsequently, when the percentage of leaks associated with each network was known, the annual unit energy lost was determined [138]. Figure 5a shows the average value of the energy lost for the case studies is $178600\ kWh$ with quartiles $60600\ kWh$ and $817100\ kWh$. Above $1000000\ kWh$ there were 10 cases that reached values of up to $10\ GWh$.
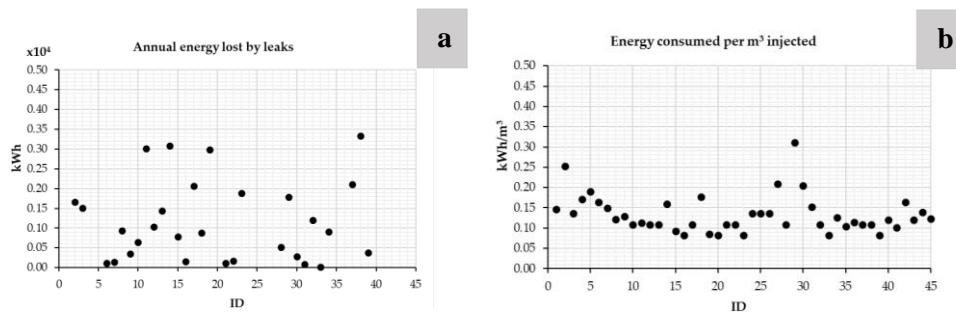
Figure 5. Annual energy lost by leaks (a) and energy consumed per m³ injected (b)

Once the percentage of leakage from the network was known, the water lost in the network was calculated. The average value of the annual volume leaked was $1325000\ Hm^3$, being the quartiles between $470400\ Hm^3$ and $7793000\ Hm^3$. Figure 5b shows the energy lost for each m^3 of water injected into the distribution networks. The average value was $0.12\ kWh/\ m^3$, being the quartiles between 0.11 and $0.15\ kWh/m^3$ To estimate the lost economic value of energy and water, the following rates were established: for water $1.9\ €/m^3$ and energy $0.11\ €/kWh$. Once the value of the volume of water lost in leaks had been calculated, its average annual cost corresponding to a value of €2097000 with quartiles €885,600 and €11180000 as shown in Figure 6a.
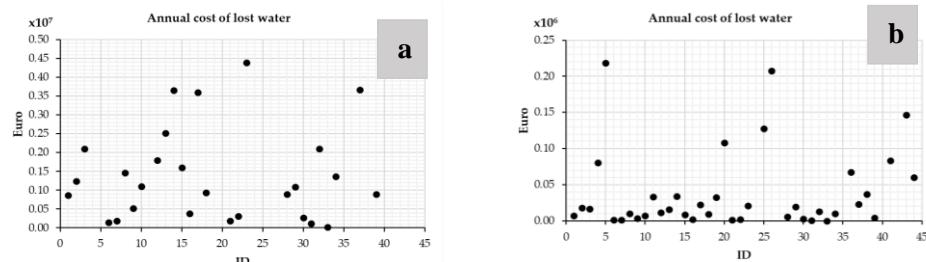
Figure 6. The annual cost of lost water (a) and the annual cost of lost water (b)

Above €10000000 13 cases reached values of up to €100000000 Similarly, the average annual energy cost lost is €121400 with quartiles €51270 and €647400 as shown in Figure 6b. The leak calculation methods such as *BABE, MNF,* and water balance were applied and compared in different case studies, which were defined by [[139]and [140]. The analysis was established to determine the real water loss in million $m^3/year$ as shown in Table 8.

Table 8. Leak method comparison

Method	Zarqa, Jordan	Sana'a, Yemen	Mwanza, Tanzania	Gavankola, Iran
Water Balance	40	7.1	12.2	-
MNF	16.2	-	12.2	34.9
BABE	4.2	0.4	5.8	39.4

Using the *MNF* and *BABE* methods, the average of real water loss in the studied region was calculated at 28 % and 37 %, respectively. According to the results of the *BABE* method, the highest leakage values were related to the reported bursts and the background leaks from connections [140]. The water balance method is the difference between the volume of water injected into the network concerning the volume of water consumed. The result of the difference corresponds to leaks, where it is observed that the results obtained are greater than those obtained with the methods calculation of *BABE* and *MNF* leaks.

Applying each method requires verification for the factors and as sumptions in each method and their sensitivities and uncertainties. Conducting *MNF* analysis in one or several small areas in the network (*DMAs*) and extrapolating it to the entire network might be justifiable in some cases, but it is not very rational because every *DMA* differs in terms of the mains length, service connections, pressure, and burst frequencies. The component analysis of the leakage method (*BABE*) remains the only way to break down the leakage into subcomponents, enabling the water utilities to understand the nature and behavior of the leakage in their systems. However, the component analysis of the leakage analyses only a small portion of the total leakages [139].

2.4.3. Pump Working as Turbine Using Leakages Models

Micro and mini-hydropower generators can be installed in water distribution systems to ensure both pressure control for leakage reduction and energy production [141]. Jain [48] in his research, shows a wide state of the art on pumps working as turbines, from their selection, methods, and cases of application. In water distribution networks *(WDNs)*, the *PATs* can be used instead of pressure-reducing valves *(PRVs)* for both pressure reduction and energy production [15].

Reference [125]showed a table with the advantages and disadvantages of installing *PATs* in the distribution system compared to other methods that reduce pressure and leakage. Ref. [142] implemented a model through Simulink in Matlab to reduce

the pressure in the distribution networks through the installation of *PATs*. This model was implemented in a real case study by [143].Reference [24]mentioned the importance of the implementation of *PATs* for pressure management, benefiting the reduction of leaks in the distribution network. In the applied case, this research shows that the proposed optimization model allows a leakage reduction of 26.6% and an energy recovery of 182.15 kWh/day.

Reference [24] showed a methodology for the optimal location of *PAT* within a water distribution network to produce energy and reduce leakage. The total amount of saved water has been accounted as 275870 $m^3/year$ while the net present value *(NPV)* resulted as € 75936. Reference [66] estimated a reduction in pressure of approximately 1 bar and a flow reduction of the order of 50 m^3/h were achieved just after the operation of the *PAT* system in Antalya, Turkey. Reference [144] showed the possibility of optimally managing a water distribution system by reducing leaks and recovering energy. The study considered the installation of between 10 to 15 *PATs* in the network of the Sorrento Peninsula (Italy) that distributes water in a network of 90000 users.

Reference [145] estimated that the installation of *PATs* represents a 45 % reduction in water savings equivalent to 7000 $m^3/year$. An optimization method is proposed that uses an objective function for the reduction of leaks and energy production by implementing *PATs* in a distribution system [146]. This study proposed a new preliminary model to optimize the location of *PATs* in a water distribution network. The optimization aims to determine the best number and location of turbines to reduce pressure, thus water leakage, and produce energy. The implementation of 6 *PATs* in the case study would mean a water-saving of 929 m^3/day and an average power of 14.53 kW. Reference [147] proposed a method for the optimal location of *PAT* through a mixed integer non-linear program *(MINLP)*. Using the model in the case study, it achieves an average water reduction of 7.88 l/s and an energy recovery of 1958 kWh/day.

The Leakage Control and Energy Recovery Using Variable Speed Pumps as Turbines in two water distribution networks are proposed by [148]. It demonstrated a methodology through flow diagrams for the selection of *PATs* and different combinations of *PATs* applications operating constantly and variably, obtaining as results leakage reductions and energy recovery.

Table 9 shows the influence of the installation of *PATs* in various case studies, where relevant information such as flow, pressure, leakage percentage, annual energy and water recovered per installation were extracted. It is observed that for all the case

studies the implementation of *PATs* supposes a reduction of leaks in the distribution network Because not all the case studies show the percentage of total network leakage, 27 % leakage is adopted as the average value since this was the value obtained in the leakage study cases previously analyzed.

Table 9. Information extracted from case studies

Ref.	ID	Flow (l/s)	H (m)	Annual Energy recovered by installing PATs (kWh/year)	Annual volume recovered by use of PATs (m³)	Leakage reduction by use of PATs (%)	η_v before installing PATs	η_v after installing PATs
[121]	46	29	59	43800	-	-	-	-
[121]	47	74	54	87600	-	-	-	-
[121]	48	19	67	39420	-	-	-	-
[121]	49	33	55	43800	-	-	-	-
[121]	50	19	63	35040	-	-	-	-
[121]	51	14	71	26280	-	-	-	-
[121]	52	31	65	52560	-	-	-	-
[26]	53	29	21	28470	22813	63	0.73	0.90
[26]	54	183	33	169360	1634590	52	0.73	0.87
[26]	55	72	36	130305	98185	63	0.73	0.90
[15]	56	302	61	55626	2475059	26	0.73	0.80
[15]	57	212	39	71876	667554	10	0.73	0.76
[15]	58	314	50	66485	1829359	19	0.73	0.78
[142]	59	187	70	54985	-	-	-	-
[24]	60	110	45	125213	339085	10	0.73	0.76
[146]	61	110	45	113880	328865	9	0.73	0.75
[147]	62	350	45	714670	248504	3	0.73	0.74

Pressure Management *(PM)*, which is usually the best way to reduce the Non-Revenue Water *(NRW)* level in a water distribution network, is achieved mainly by forming (dividing the network into several) District Metered Areas *(DMAs)*. In the city of Kozani (Greece), [121] analyzed the possibility of implementing P*ATs* in the water distribution system. The implementation of *PATs* in the case study would suppose a reduction of leaks between 20 % and 40 % approximately. The reduction of leakages

decreased 325500 kWh of lost energy. The investigation shows the possible combinations of *PATs* with different installed power values from 5 to 12 kW.

Figure 7a shows the influence of the installation of *PATs* in a *WDN*. Figure 7a shows the reduction of the leakage flow after the installation of *PATs* varies from 18 to 65 %, while Figure 7b shows the pressure reduction with values from 29 to 55 %.
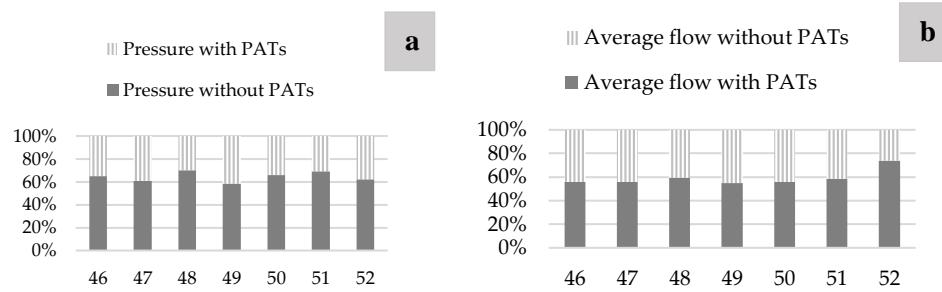
Figure 7. Influence of the installation of PATs. Comparison of network pressure by the installation of PATs (a); Comparison of flow injected into the network by the installation of PATs (b)

Once the leakage value was known, the volumetric efficiency was calculated, which was 0.73 before the consideration of the *PATs* systems. For all the case studies, the reduction of leaks significantly increases the volumetric performance after installing *PATs* in the distribution network. Figure 8 shows the efficiency indicators calculated in water distribution networks with the installation of *PATs* for the selected case studies. Figure 8a shows the annual energy consumption, the average value of the cases is 93000 $kWh/year$. Figure 8b shows the energy consumed for each m³ injected into the network with an average value of 0.10 kWh/m^3.
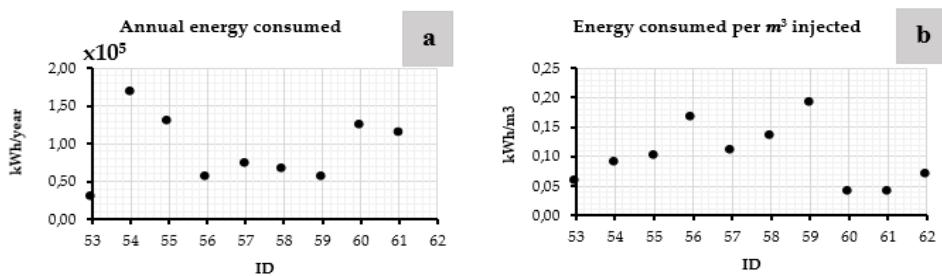
Figure 8. Efficiency indicators in networks with PATs installed. Annual Energy consumed (a); Energy consumed per m³ injected (b)

2.4.4. Energy Index Calculation Case Study

For each of the study cases, the energy indices were calculated. The energy indices determined in Table 10 are: absolute energy consumed annually (*IAAE*) in kWh/year, recovered energy (*IER*) in kWh/year, percentage of recoverable energy (*ERP*) in %, absolute energy consumed per unit volume *(IAEFW)* in kWh/m^3. Besides, a new index was proposed to consider the influence of the *PATs* system in the reduction of leakage. This index, called index reduction leakage flow as a function of generating power *(IRLGP)*, shows the ratio between reduction of the leakage volume for each installed power. The units of this index are m^3/kW.

Table 10. Calculable energy indices with available data

Reference	ID	*IAAE* (kWh/year)	*IER* (kWh/year)	*ERP* (%)	*IEFW* (kWh/m³)	*IRLGP* (m³/ kW)
[26]	53	52335	28470	54	0.06	8
[26]	54	518965	169360	3	0.09	-
[26]	55	222745	130305	58	0.10	4
[15]	56	1583106	55626	4	0.17	2
[15]	57	710516	71876	10	0.11	16
[15]	58	1349189	66485	5	0.14	13
[142]	59	1124897	54985	5	0.19	-
[24]	60	141794	125213	29	0.12	5
[146]	61	141794	113880	27	0.12	5
[147]	62	751937	714670	53	0.12	4

Annual energy consumption in the analyzed distribution networks ranges from 141794 to 1583106 kWh. By installing *PATs* in the distribution networks, annual energy recovery values are obtained from 28470 to 714670 kWh. Using the *IAAE* and *IER* values, the *ERP* index was determined, resulting in recovery values from 3 to 58 %. The relationship of the annual volume of water injected into the network concerning *IAAE* allowed the calculation of the *IEFW* index. This shows values between 0.06 and 0.19 kWh/m^3. The difference between the total leaked volume in the network compared to the volume recovered by using *PATs* is used to calculate the reduction of the volume leaked by the installation of *PATs*. Considering the relationship between the reduced volume and the annual energy recovery, the *IRLGP* index was calculated, which shows values between 2 and 16 m^3/kW.

2.5. Conclusions

Several leakage methods have been implemented in distribution networks, and for each formulation it was possible to extract its main characteristics, advantages, and disadvantages. The *FAVAD* method is the most widely used in the case of studies for estimating leaks in water distribution networks. It was evidenced that through experimentation and estimates different values of leakage exponents have been determined for each type of formulation depending on the type of leak, age and pipe material.

Different methods for calibrating leak models are proposed by various authors, with genetic algorithms being the most widely implemented in the models. The analysis carried out on sixty-two case studies allowed the extraction of relevant information from the network to calculate and compare various efficiency indices such as volumetric performance, percentage of leaks, energy lost due to leaks, annual energy consumption for each cubic meter injected into the network and costs for loss of water and energy.

The analyzed case studies, which had installed *PATs* systems showed the implementation of micro-hydropower systems causes a considerable reduction in the pressure of the network, reducing the level of leaks between 4 % and 63 %, while the recovered energy was estimated between 28470 and 714670 kWh/year.

To improve the sustainable development goals, the use of efficiency indicators are an important tool for the analysis and management of water distribution networks. In this line, the researchers analyzed the variation of the different indicators in 62 cases studies in energy, economic and environmental terms deeply. The proposal of sustainable measurements should start, knowing the state of the water system. The installation of *PATs* in the distribution networks is a solution to reduce the volume of leakage and an opportunity to recover clean energy. The analysis of the *PATs* systems should be considered when leakages are considered. The influence of the leakages can cause differences in the selection, operation and regulation of the recovery machines and it should be considered by water managers in energy optimization procedures as well as the energy analyses. Besides, the installation of *PATs* systems in real case studies should consider the significance of the leakages in the operation of these recovery machines. This research shows the need to apply the analysis of indicators for the improvement of the energy analysis. Future works should develop around this topic. This new research should develop optimization procedures in which the leakages will be considered as a decision variable. The analysis of the leakages will include the influence of these water losses in the

selection and regulation of the *PATs* systems, and therefore, its impact in the recovered energy.

Author Contributions

Conceptualization, P.A.L.-J. and M.P.-S.; methodology, C.A.M.Á. and F.-J.S.-R.; software, writing—original draft preparation, C.A.M.Á. and M.P.-S.; writing—review and editing, M.P.-S. and P.A.L.-J.; visualization M.P.-S.; supervision, P.A.L.-J. All authors have read and agreed to the published version of the manuscript.

3. Artículo 2

"Definition of the Operational Curves by Modification of the Affinity Laws to Improve the Simulation of PATs"

3.1. Description

Coautores: Carlos Andrés Macías Ávila; Francisco-Javier Sánchez-Romero; P. Amparo López-Jiménez; Modesto Pérez-Sánchez.

Revista: Water ISSN 2073-4441.

Factor de impacto: 3.103. JCR (Q2; Posición 36/100). Water Resources.

Estado: Publicado [Water 2021, 7, 6; doi: 10.3390/w13141880].

Abstract

New technologies for water pressurized systems try to implement the introduction of strategies for the improvement of the sustainable indicators. One of these technologies is the implementation of pumps working as turbines. The use of these recovery machines was proposed some years ago, and the interest in this technology has increased over the last years. The simulation of these machines is necessary when analyzing pressurized water systems, or when optimization procedures are proposed for their management, great care must be taken. In these cases, the knowledge of the operation curves is crucial to reach accurate results. This study proposes different regression expressions to define three operational curves when the machines operate under variable rotational speed. These curves are the best efficiency head, the best power-head and the best power flow. The here proposed methods were compared with other five published methods. The comparison shows the proposed method was the best when it is compared with the rest of the published procedures, reducing the error values between 8 and 20 %.

Keywords: variable rotational speed; affinity laws; *PATs*; water networks; energy recovery.

3.2. Introduction

The use of micro-hydropower systems is key to improve the energy efficiency in water pressurized systems. The accuracy of the energy analyses is also very important in the complete analysis of these energy improvements [19]. Pump working as turbines (*PATs*) are hydraulic machines, which are commonly recommended to be used as recovery machines in water pressurized systems [149]. These favorable aspects were defined by different published researches in which the feasibility, simple operation, availability in the market and great range of applications are some of the most important characteristics of these systems, when they are compared with classical machines such as Francis or Pelton turbine. However, the use of these recovery machines has the main disadvantage joined to low efficiency compared to classical machines [150]. The knowledge of their characteristic curves (i.e., head, efficiency and power) is difficult to know in advance if water managers look in the manufacturer catalogue.

The lack of this information has been a challenge, in which researchers tried to fill this shortage by proposing empirical expressions [21]. These functions are based on

the development of the experimental tests. These helped to understand better the operating of these machines when these recovery systems operate as turbine [22]. The need to establish these equations are focused on two main aspects: (i) the knowledge of the best operation point of the machine (*BEP*) when it operates as turbine and the water manager only knows the characteristic curves in pump mode; and (ii) the need to regulate the rotational speed of the machine to maximize the recovered energy of the system when variable operation strategy is applied.

The first challenge was studied by different researchers. Ref. [151] established a common empirical equation to estimate the best efficiency point of the machine when it operates as a turbine from a pump. These expressions and the empirical equations proposed by [152] are the most used last years. However, other published researches focused on their effort to improve these expressions. Ref. [153] proposed computational fluid dynamics analysis to characterize and improve the accuracy of these methods, which tried to predict the operational point. Different methods were reviewed by [154], who proposed empirical expressions using the greater database, particularly 181 different *PATs*. The proposed expressions estimated the *BEP* operation as a turbine with errors lower than the rest of the methods reviewed by [150]. In this line, Ref. [155] defined regression expression to estimate the curve of head and efficiency when the rotational speed changes by modification of the affinity laws, improving the results obtained in others researches [156].

The use of these empirical equations focuses on improving the simulation of PAT systems operating under variable rotational speed. Ref. [149] showed the need to know these curves in the energy estimation strategies in the water systems. The analysis of the hydropower potential contributes to incorporate sustainable measurements in which the water-energy nexus acquires relevance in the water management of the systems [157]. When micro-hydropower systems are analyzed, the effectiveness increases when the variable operation strategy (*VOS*) is applied [23]. Therefore, the improvement in the estimation of the operational curves makes sense to search for the best strategy to maximize the recovered energy by the recovery system [15].

The knowledge of expressions, which allow water managers to use with software and optimization procedure will improve the decision making in the water systems [15]. The future strategies should be focused on improving sustainability as well as the alignment of the operation indicators with the sustainable development goals [158]. The research is focused on the development of regression expressions. These equations define the generated power as a function of the flow under variable

rotational speed. These curves are: (i) the best efficiency head, proposed by [159] and (ii) the best power curve proposed in this research, which is key in the maximization of energy. Besides, the research compiles the great database used by researchers to analyze the *PATs* systems operating under variable rotational speed. This research considers 15 different machines, which were tested on 87 different rotational speeds. The proposed regression equations, which are based on non-dimensional parameters is validated by the error analysis compared to other published methods, obtaining better approaches.

3.3. Material and Methods

3.3.1. Hydraulic Mathematical Development

The modification of the affinity laws is recommendable when the characteristic curves must be estimated by water managers, n accordance with the aforementioned references. The characteristics curves are head curve (*HC*), efficiency curve (*EC*) and power curve (*PC*). These curves are defined by the following expression:

$$H_0 = A + BQ_0 + CQ_0^2 \tag{16}$$

$$\eta_0 = E_4 Q_0^4 + E_3 Q_0^3 + E_2 Q_0^2 + E_1 Q_0 + E_0 \tag{17}$$

$$P_0 = P_4 Q_0^4 + P_3 Q_0^3 + P_2 Q_0^2 + P_1 Q_0 + P_5 \tag{18}$$

where: H_0 is the recovered head in nominal rotational speed in m w.c. (water column); Q_0 is the flow rate in m^3/s; η_0 is the efficiency of the machine; P_0 is the generated power in kW. The rest of the coefficients (*A, B, C,* $E_4, E_3, E_2, E_1, E_0, P_4, P_3, P_2, P_1$ and P_5) are the coefficients, which define the *HC, EC* and *PC* of the pump working as the turbine.

The variation of the rotational speed is defined by affinity laws when classical concepts are considered. The definition of the affinity laws is based on the analysis of the congruence parabola (H_{CP}), which was defined and applied by [160]. This parabola is defined by the following expression:

$$H_{CP} = \frac{H_0}{Q_0^2} Q^2 = k_{H,AL} Q^2 \tag{19}$$

Considering an operation point (Q_0, H_0), when the congruence parabola concept is applied, the affinity laws are defined by the following expressions [160]:

$$\frac{Q_1}{Q_0} = \frac{n_1}{n_0} = \alpha \tag{20}$$

$$\frac{H_1}{H_0} = \left(\frac{n_1}{n_0}\right)^2 = \alpha^2 \tag{21}$$

$$\frac{\eta_1}{\eta_0} = 1 \tag{22}$$

$$\frac{P_1}{P_0} = \left(\frac{n_1}{n_0}\right)^3 = \alpha^3 \tag{23}$$

Where n_1 is the new rotational speed in rpm, n_0 is the nominal rotational speed in rpm; Q_1 is the circulating flow when the rotational speed is n_1; H_1 is the recovered head when the machine operates for a flow equal to Q_1 in m w.c.; η_1 is the new efficiency of the machine when it operates in Q_1.

Different published researches established the need to modify these affinity laws to approach better the estimation of the characteristics curves of the machine. These affinity laws can define using non-dimensional numbers of the machines (*q, h, e* and *p*), which enable the establishment of the operation function for determining any rotational speed.

$$q = \frac{Q}{Q_0} \tag{24}$$

$$h = \frac{H}{H_0} \tag{25}$$

$$e = \frac{\eta}{\eta_0} \tag{26}$$

$$p = \frac{P}{P_0} = qhe \tag{27}$$

where $q, h, e \; and \; p$ are operation functions for different rotational speed (α), Q is any flow value of *PAT* in m^3/s. This value is inside of the *VOS*; H is the recovered head for this flow in m w.c. when the machine operates at the ratio of rotational speed equal to α; η is the efficiency for values of Q, H and α; P is the shaft power in this operation point in kW; Q_0, H_0, P_0 and η_0 are referred to any point of the characteristic curve of the machine when it is operating at nominal rotational speed (i.e., *α=1*).

The curves for any rotational speed inside of the *VOS* were defined by [155], who established the following expressions:

$$H = h(A + B\frac{Q}{q} + C\left(\frac{Q}{q}\right)^2)$$ (28)

$$\eta = e\ (E_4\left(\frac{Q}{q}\right)^4 + E_3\left(\frac{Q}{q}\right)^3 + E_2\left(\frac{Q}{q}\right)^2 + E_1\left(\frac{Q}{q}\right) + E_0)$$ (29)

$$P = p\ (P_4\left(\frac{Q}{q}\right)^4 + P_3\left(\frac{Q}{q}\right)^3 + P_2\left(\frac{Q}{q}\right)^2 + P_1\left(\frac{Q}{q}\right) + P_5)$$ (30)

This relationship between *q* and *Q* is linear and it is determined by the slope *m*. The *m* value will adopt a constant value according to the curve analyzed (Best efficiency head, *BEH*; Best power head, *BPH* or Best Power Flow, *BPF*) [19], [20]. Any value of Q_0 has an associated line, which has a slope equal to *m* (Figure 9a).
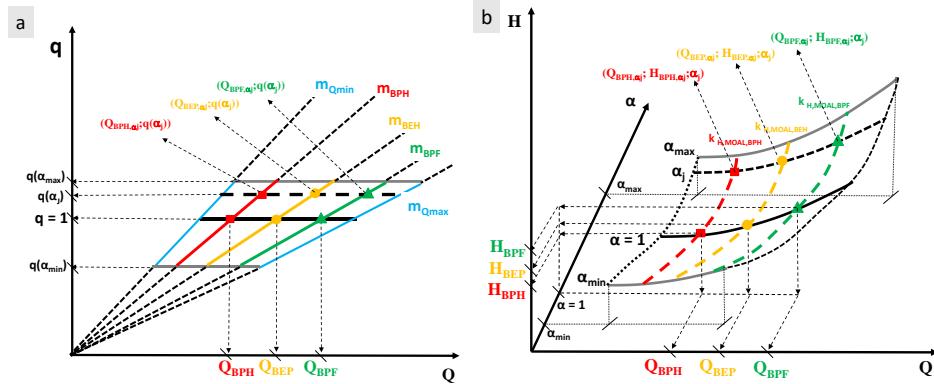
Figure 9. (a) m coefficient (b) *VOS* zone

The *m* value remains constant either in affinity laws or modified affinity laws, changing the *q* expression. When the *VOS* is defined by affinity laws, *q* is equal to α. If the modified affinity laws (*MOAL*) is used, *q* is a function both α and Q/Q_{BEP} [155]. The *m* value is defined by the following expression:

$$m = \frac{1}{Q_0}$$ (31)

$$q = mQ_0$$ (32)

The m parameter enables to simplify the development of expressions, which are used to develop the expression when a machine operates under variable rotational speed.

The variation of the rotational speed inside of the *VOS* is defined by the previously cited congruence parabola (*CP*). This *CP* enables to define the change the rotational speed. Besides, when these *CPs* are used, they help to define the analytical curves of the characteristic curves (head, efficiency, and power) both the application of the affinity laws and modified affinity laws (Figure 9b). These new curves were called the modified affinity laws (*MOAL*) [161][162][163]. When coefficients of the congruence parabola (k_i) are operated comparing between affinity laws (*AL*) and modified affinity laws, the following expressions are obtained. The modification of these expressions is defined in Table 11.

Table 11. Definition of the curves as a function of k_i parameter

Curve Type	AL	MOAL
Head $H = k_H Q^2$	$k_{H,AL} = \dfrac{H_0}{Q_0^2} = (Am^2 + Bm + C)$	$k_{H,MOAL} = \dfrac{h}{q^2}\, k_{H,AL}$
Efficiency $\eta = e\eta_0$	$\eta_{AL} = \eta_0$	$\eta_{MOAL} = e \cdot \eta_{AL}$
Power $P = k_P Q^3$	Using head and efficiency curves $k_{P,AL} = 9.81 \cdot k_{H,AL} \cdot \eta_{AL}$ Using power expression $k_{P,AL} = \dfrac{P_0}{Q_0^3}$ $k_{P,AL} = \left(\dfrac{P_4}{m} + P_3 + P_2 m + P_1 m^2 + P_5 m^3\right)$	$k_{P,MOAL} = \dfrac{he}{q^2} k_{P,AL}$ $k_{P,MOAL} = \dfrac{p}{q^3} k_{P,AL} = \dfrac{he}{q^2} k_{P,AL}$

Each congruence parabola has one *m* parameter, which is associated to α value. The *m* parameter enables the estimation of the curves *H-Q*, *η-Q* and *P-Q*, directly. *m* is the unknown value and it should be solved for the different operational curves inside of the *VOS* zone. Once, *m* or Q_0 are known, the estimation of the characteristic curves is possible and therefore, the definition of the following curves is possible.

Best Efficiency Head (BEH), defined by [159], this curve is the line, which establishes the α value in which the efficiency is maximum for a defined flow. The analysis of this equation is defined in the following

$$\frac{d\eta}{d\alpha} = 0 \tag{33}$$

Considering the equation (17), (20) and (24):

$$\frac{d\eta}{d\alpha} = \frac{d\left(E_4\left(\frac{Q}{\alpha}\right)^4 + E_3\left(\frac{Q}{\alpha}\right)^3 + E_2\left(\frac{Q}{\alpha}\right)^2 + E_1\left(\frac{Q}{\alpha}\right) + E_0\right)}{d\alpha} = 0 \tag{34}$$

As the relationship between α and Q is $\alpha = m\,Q$, considering equation (31) and (32), the expression enables to calculate the m parameter is:

$$E_1 m^3 + 2E_2 m^2 + 3E_3 m + 4E_4 = 0 \tag{35}$$

Best Power Head (BPH), this curve is the line, which establishes the α value in which the power is maximum for a defined flow [161], [162]. The analysis of this equation is defined in the following

$$\frac{dP}{d\alpha} = 0 \tag{36}$$

Considering the equation (16), (17), (20) and (24):

$$\frac{dP}{d\alpha} = \frac{d\left(9.81Q\alpha^2\left(A + B\frac{Q}{\alpha} + C\left(\frac{Q}{\alpha}\right)^2\right)\left(E_4\left(\frac{Q}{\alpha}\right)^4 + E_3\left(\frac{Q}{\alpha}\right)^3 + E_2\left(\frac{Q}{\alpha}\right)^2 + E_1\left(\frac{Q}{\alpha}\right) + E_0\right)\right)}{d\alpha} = 0 \tag{37}$$

As the relationship between α and Q is $\alpha = m\,Q$, considering equation (31) and (32), the expression enables to calculate the m parameter is:

$$\begin{aligned} (2E_0 A)m^6 + (E_0 B + E_1 A)m^5 + (-E_1 C - E_2 B - E_3 A)m^3 + (-2E_2 C - 2E_3 B - 2E_4 A)m^2 \\ + (-3E_3 C - 3E_4 B)m + (-4E_4 C) = 0 \end{aligned} \tag{38}$$

Best Power Flow (BPF), this curve is the line, which establishes the Q value in which the power is maximum for a defined α. The analysis of this equation is defined in the following

$$\frac{dP}{dQ} = 0 \tag{39}$$

Considering the equation (16), (17), (20) and (24):

$$\frac{dP}{dQ} = \frac{d(9.81Q\alpha^2(A + B\frac{Q}{\alpha} + C(\frac{Q}{\alpha})^2)(E_4\left(\frac{Q}{\alpha}\right)^4 + E_3\left(\frac{Q}{\alpha}\right)^3 + E_2\left(\frac{Q}{\alpha}\right)^2 + E_1(\frac{Q}{\alpha}) + E_0))}{dQ} = 0 \tag{40}$$

As the relationship between α and Q is $\alpha = m\,Q$, considering equation (31) and (32), the expression enables to calculate the m parameter is:

$$\begin{aligned} (E_0 A)m^6 + 2(E_0 B + E_1 A)m^5 + 3(E_0 C + E_1 B + E_2 A)m^4 + 4(E_1 C + E_2 B + E_3 A)m^3 \\ + 5(E_2 C + E_3 B + E_4 A)m + 6(E_3 C + E_4 B)m + 7E_4 C = 0 \end{aligned} \tag{41}$$

Once, the three curves (*BEH*, *BPH* and *BPF*) are known, the knowledge of the *m* parameter is demonstrated it can be solved by a polynomial equation, which has the next typology.

$$\gamma_6 m^6 + \gamma_5 m^5 + \gamma_4 m^4 + \gamma_3 m^3 + \gamma_2 m^2 + \gamma_1 m + \gamma_0 = 0 \qquad (42)$$

Table 12 summarizes the value of the different coefficients for *BEH*, *BPH* and *BPF* as a function of the characteristic curve when they operate in nominal conditions. The introduction of the 'm' parameter simplifies the analysis of the mathematical expressions that allow to study of the behaviour of the machines along the *VOS* zone, facilitating the analysis in situations different from the nominal regime.

Table 12. Coefficients for the knowledge of the m parameters

Curve	BEH	BPH	BPF
Restriction	$\dfrac{d\eta}{d\alpha} = 0$	$\dfrac{dP}{d\alpha} = 0$	$\dfrac{dP}{dQ} = 0$
γ_6	0	$2E_0 A$	$E_0 A$
γ_5	0	$E_0 B + E_1 A$	$2(E_0 B + E_1 A)$
γ_4	0	0	$3(E_0 C + E_1 B + E_2 A)$
γ_3	E_1	$-E_1 C - E_2 B - E_3 A$	$4(E_1 C + E_2 B + E_3 A)$
γ_2	$2E_2$	$-2E_2 C - 2E_3 B - 2E_4 A$	$5(E_2 C + E_3 B + E_4 A)$
γ_1	$3E_3$	$-3E_3 C - 3E_4 B$	$6(E_3 C + E_4 B)$
γ_0	$4E_4$	$-4E_4 C$	$7E_4 C$
Solution	m_{BEH}	m_{BPH}	m_{BPF}

3.3.2. Methodology

The proposed methodology is based on ten different steps (Figure 10). This figure contains two different phases. The first phase analyses the experimental database from step A to D. The second phase considers the analytical procedure to define the best equation to establish the operation curves of the machine from step E to J.

<u>Step A.</u> Using the different experimental database, the characteristic curves are obtained for each machine as well as considering different rotational speeds.

<u>Step B.</u> When the curves are known, the procedure determines the flow for the different curves when the machine operates on nominal rotational speed. The flow values are: (i) Best Efficiency Head (Q_{BEH}), (ii) Best Power Head (Q_{BPH}), and (iii) Best Power Flow (Q_{BPF}).

Step C. Defined the three flow values in step B, the procedure defines these flow values for the different values of the rotational speed (α_j), which were tested experimentally. Therefore, Q_{BEH,α_j}, Q_{BPH,α_j} and Q_{BPF,α_j} are determined.

Step D. The non-dimensional parameters, $(h/q^2)_{Exp}$ and $(he/q^2)_{Exp}$, are defined using the experimental database for different values of the rotational speed.

Step E. It is the first step of the second phase, where the best regression expression will be defined. In this step, different functions are proposed and analysed using the database. Table 13 shows the regression expression, which is used in the procedure.

Table 13. Proposed functions to be analysed (Continue in next page)

Function Model (FM)	Polynomial function (From F_1 to F_6): $$NP = \beta_1\left(\alpha\frac{Q}{Q_{BEP}}\right) + \beta_2(\frac{Q}{Q_{BEP}})^2 + \beta_3\left(\frac{Q}{Q_{BEP}}\right) + \beta_4\alpha^2 + \beta_5\alpha + \beta_6$$ Potential function (From F_7 to F_{10}): $$NP = (\frac{Q}{Q_{BEP}})^{\beta_3}\alpha^{\beta_5} \cdot exp^{\beta_6}$$
F_1	$$NP = \beta_4\alpha^2 + \beta_5\alpha$$
F_2	$$NP = \beta_4\alpha^2 + \beta_5\alpha + \beta_6$$
F_3	$$NP = \beta_2(\frac{Q}{Q_{BEP}})^2 + \beta_4\alpha^2 + \beta_5\alpha$$
F_4	$$NP = \beta_2(\frac{Q}{Q_{BEP}})^2 + \beta_4\alpha^2 + \beta_5\alpha + \beta_6$$
F_5	$$NP = \beta_1\left(\alpha\frac{Q}{Q_{BEP}}\right) + \beta_2(\frac{Q}{Q_{BEP}})^2 + \beta_3\left(\frac{Q}{Q_{BEP}}\right) + \beta_4\alpha^2 + \beta_5\alpha$$
F_6	$$NP = \beta_1\left(\alpha\frac{Q}{Q_{BEP}}\right) + \beta_2(\frac{Q}{Q_{BEP}})^2 + \beta_3\left(\frac{Q}{Q_{BEP}}\right) + \beta_4\alpha^2 + \beta_5\alpha + \beta_6$$
F_7	$$NP = \alpha^{\beta_5}$$
F_8	$$NP = \alpha^{\beta_5} \cdot exp^{\beta_6}$$
F_9	$$NP = (\frac{Q}{Q_{BEP}})^{\beta_3}\alpha^{\beta_5}$$
F_{10}	$$NP = (\frac{Q}{Q_{BEP}})^{\beta_3}\alpha^{\beta_5} \cdot exp^{\beta_6}$$

*NP is the non-dimensional parameter. It can be $\frac{h}{q^2}$ or $\frac{he}{q^2}$

Step F. Once the proposed regression expression is defined in the previous step, the values of $(h/q^2)_{Form}$ and $(he/q^2)_{Form}$ are estimated for each F_i, defining the error indexes, which enable to choose of the best regression expression to define the proposed functions (*BEH*, *BPH* and *BPF*).
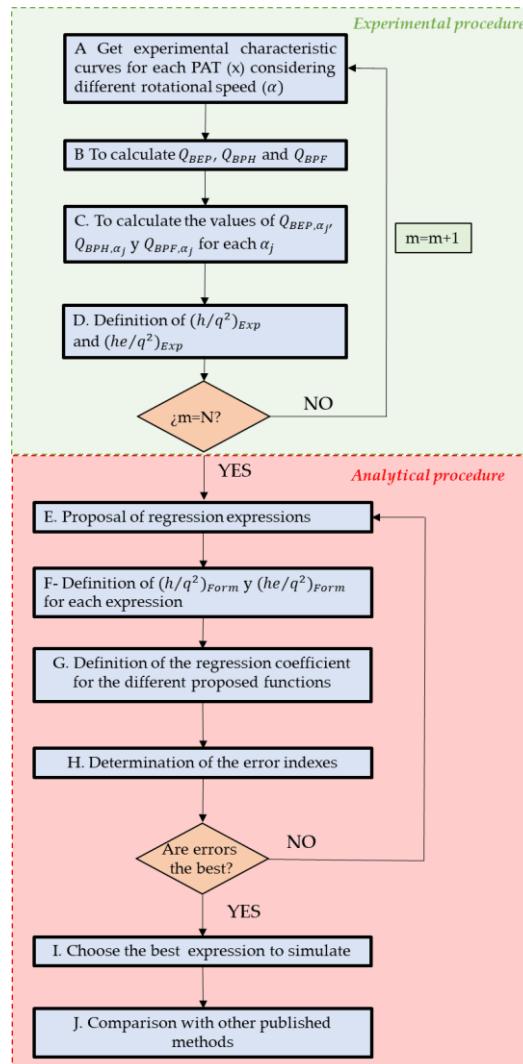

Figure 10. The methodology proposed to reach the expressions

<u>Step G.</u> Definition of the regression expression for $\frac{h}{q^2}$ and $\frac{he}{q^2}$.

<u>Step H.</u> The error indexes were estimated for each function when the dimensionless parameters ($\frac{h}{q^2}$ and $\frac{he}{q^2}$) were applied to *BEH*, *BPH* and *BPF*. The error indexed are defined in Table 4.

<u>Step I.</u> The function, which minimizes the errors is defined to establish the *BEH*, *BPH* and *BPF*.

<u>Step J.</u> The chosen function is compared with other published methods, comparing the error indexes, which were defined in Step H to show the accuracy between this study, other published methods and experimental tests when *BEH*, *BPH* and *BPQ* are defined both analytical and experimental.

Table 14. Error indexed used in the analysis

Error Index	Equation	Variable	Accuracy
Root Mean Square Error (*RMSE*)	$RMSE = \sqrt{\dfrac{\sum_{i=1}^{s}[O_i - P_i]^2}{s}}$	O_i are the estimated values; P_i the experimental values and s the number of observations	Perfect fit when *RMSE* is zero
Mean Absolute Deviation (*MAD*)	$MAD = \sum_{1}^{s} \dfrac{1}{s}|O_i - P_i|$	O_i are the estimated values; P_i the experimental values and s the number of observations	Perfect fit when *MAD* is zero
Mean Relative Deviation (*MRD*)	$MRD = \sum_{1}^{s} \dfrac{|O_i - P_i|/P_i}{s}$	O_i are the estimated values; P_i the experimental values and s the number of observations	-
BIAS	$BIAS = \dfrac{\sum_{i=1}^{s}[O_i - P_i]}{s}$	O_i are the estimated values; P_i the experimental values and s the number of observations	Perfect fit is zero

3.3.3. Materials

The here described analytical development was applied to different machines, which were tested in different published experimental tests. In this case, the used machines were fifteen *PATs*, which have a specific speed between 5.67 and 50,71

rpm (m, kW). The nominal rotational speed was between 800 and 3000 rpm. The non-dimensional curves of the machines are shown in Figure 11. The number of experimental curves (*RS*) was 87. These curves were tested for different rotational speed. The use of the experimental data enabled to interpolation of more than 10000 parabolas. All curves were used to define the regression expressions except ID11, which was used to compare the empirical equations with the experimental data.
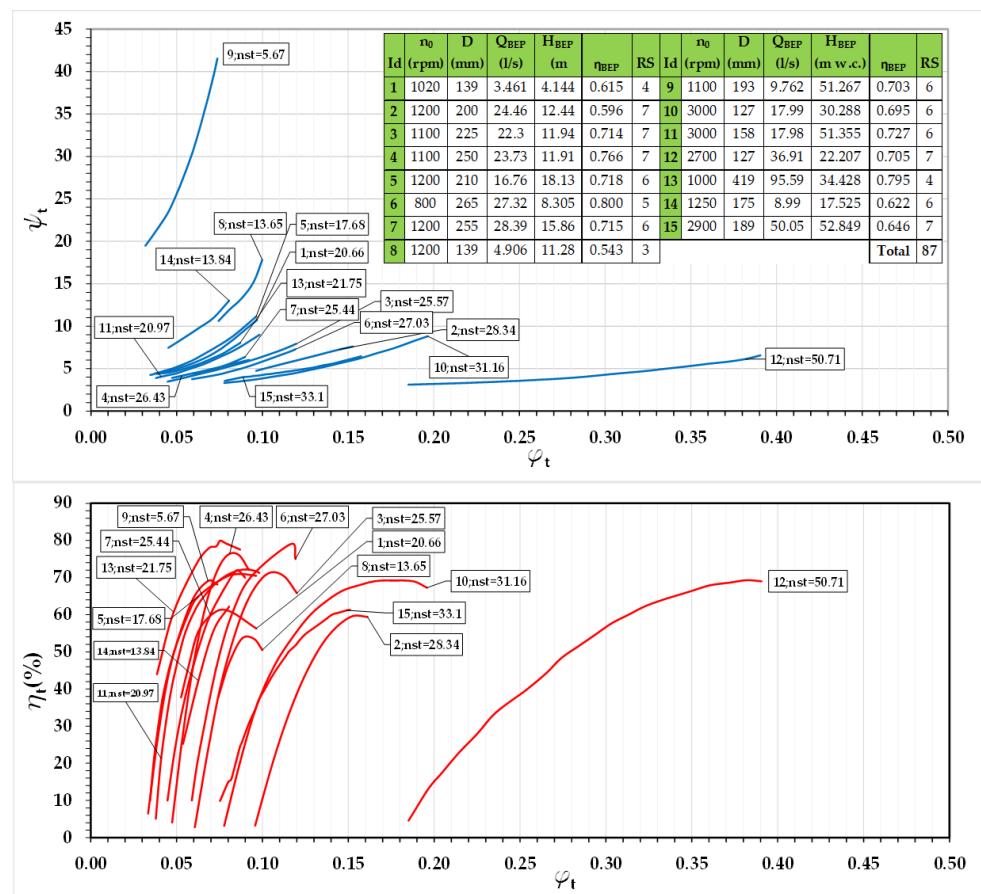

Figure 11. Experimental database. ID1 [164]; ID2-ID4 [165]; ID5-ID7 [162]; ID8 [166]; ID9 [167]; ID10-ID12 [168]; ID13 [169]; ID14 [170]; ID15 [150]

3.4. Results

3.4.1. Definition of the regression expression to define F_i

The regression expressions propose for $\frac{h}{q^2}$ and $\frac{he}{q^2}$ are shown in Table 15. It shows the different values of the β_i for each function F_i. These ten functions are used to estimate the *BEH, BPH* and *BPF* curves using the $\frac{h}{q^2}$ and $\frac{he}{q^2}$ the dimensionless coefficient for each machine.

Table 15. Proposed expression for the dimensionless numbers. (Continue in next page)

Function Model (FM)	Expressions
F_1	$$\frac{h}{q^2} = -0.512\alpha^2 + 1.63\alpha \ (R^2 = 0.978)$$ $$\frac{he}{q^2} = -0.826\alpha^2 + 1.843\alpha \ (R^2 = 0.979)$$
F_2	$$\frac{h}{q^2} = 1.048\alpha^2 - 1.487\alpha + 1.469 \ (R^2 = 0.738)$$ $$\frac{he}{q^2} = -0.1706\alpha^2 + 0.5336\alpha + 0.617 \ (R^2 = 0.151)$$
F_3	$$\frac{h}{q^2} = -0.235\left(\frac{Q}{Q_{BEP}}\right)^2 - 0.5196\alpha^2 + 1.789\alpha \ (R^2 = 0.981)$$ $$\frac{he}{q^2} = -0.024\left(\frac{Q}{Q_{BEP}}\right)^2 - 0.826\alpha^2 + 1.858\alpha \ (R^2 = 0.979)$$
F_4	$$\frac{h}{q^2} = -0.1139\left(\frac{Q}{Q_{BEP}}\right)^2 + 0.965\alpha^2 - 1.254\alpha + 1.395 \ (R^2 = 0.764)$$ $$\frac{he}{q^2} = 0.032\left(\frac{Q}{Q_{BEP}}\right)^2 - 0.148\alpha^2 + 0.469\alpha + 0.637 \ (R^2 = 0.154)$$
F_5	$$\frac{h}{q^2} = -1.508\left(\alpha\frac{Q}{Q_{BEP}}\right) - 0.471\left(\frac{Q}{Q_{BEP}}\right)^2 + 1.93\left(\frac{Q}{Q_{BEP}}\right) + 0.714\alpha^2 + 0.342\alpha (R^2 = 0.986)$$ $$\frac{he}{q^2} = 0.532\left(\alpha\frac{Q}{Q_{BEP}}\right) - 0.828\left(\frac{Q}{Q_{BEP}}\right)^2 + 0.757\left(\frac{Q}{Q_{BEP}}\right) - 0.757\alpha^2 + 1.287\alpha (R^2 = 0.98)$$
F_6	$$\frac{h}{q^2} = -0.69\left(\alpha\frac{Q}{Q_{BEP}}\right) + 0.122\left(\frac{Q}{Q_{BEP}}\right)^2 + 0.313\left(\frac{Q}{Q_{BEP}}\right) + 1.222\alpha^2 - 1.267\alpha + 1.294 \ (R^2 = 0.778)$$ $$\frac{he}{q^2} = 0.993\left(\alpha\frac{Q}{Q_{BEP}}\right) - 0.494\left(\frac{Q}{Q_{BEP}}\right)^2 - 0.156\left(\frac{Q}{Q_{BEP}}\right) - 0.471\alpha^2 + 0.38\alpha + 0.73 \ (R^2 = 0.191)$$

Table 15. (Cont.) Proposed expression for the dimensionless numbers

Function Model (FM)	Expressions
F_7	$\dfrac{h}{q^2} = \alpha^{0.214} (R^2 = 0.207)$ $\dfrac{he}{q^2} = \alpha^{0.245} (R^2 = 0.175)$
F_8	$\dfrac{h}{q^2} = \alpha^{0.305} \cdot exp^{0.077} (R^2 = 0.402)$ $\dfrac{he}{q^2} = \alpha^{0.202} \cdot exp^{-0.036} (R^2 = 0.116)$
F_9	$\dfrac{h}{q^2} = (\dfrac{Q}{Q_{BEP}})^{-0.23} \alpha^{0.451} (R^2 = 0.506)$ $\dfrac{he}{q^2} = (\dfrac{Q}{Q_{BEP}})^{0.11} \alpha^{0.132} (R^2 = 0.22)$
F_{10}	$\dfrac{h}{q^2} = (\dfrac{Q}{Q_{BEP}})^{-0.166} \alpha^{0.422} \cdot exp^{0.032} (R^2 = 0.478)$ $\dfrac{he}{q^2} = (\dfrac{Q}{Q_{BEP}})^{0.083} \alpha^{0.143} \cdot exp^{-0.013} (R^2 = 0.129)$

The estimation considered all experimental rotational speed of the *PATs*, considering their characteristic curves. When these curves are defined, the error indexed were calculated compared with each experimental value and calculating the average value (Tables 16 and 17). Table 16 shows the average error indexed when the non-dimensional parameter, h/q^2, was calculated for the different 10 proposed functions. When *BEH* curve is analysed, the function which showed the minimum average error was F_2. *RMSE*, *MAD* and *MRD* were 0.1035, 0.0735 and 0.0628, respectively. However, the second function was F_6, which the error difference was 2.4 % and 4.7 % for *RMSE* and *MAD* respectively, while the *MRD* was better for F_2, reducing a -0.94 % compared to F_2.

Table 16. Average error indexed for h/q^2 applied (Continue in next page)

	BEH			
FM	RMSE	MAD	MRD	BIAS
F_1	0,1515 (9)	0,1144 (9)	0,1023 (10)	-0,04 (3)
F_2	0,1035 (1)	0,0735 (1)	0,0628 (2)	-0,0172 (1)
F_3	0,1636 (10)	0,1154 (10)	0,0999 (9)	-0,0966 (10)

*(x) indicated the position when the error is considered and compared between functions

Table 16. Average error indexed for h/q^2 applied (Continue in next page)

		BEH		
FM	RMSE	MAD	MRD	BIAS
F_4	0,1134 (3)	0,0819 (3)	0,0695 (3)	-0,0441 (5)
F_5	0,1398 (7)	0,0974 (7)	0,0778 (7)	-0,0755 (7)
F_6	0,1077 (2)	0,0755 (2)	0,0622 (1)	-0,0408 (4)
F_7	0,1341 (6)	0,0927 (6)	0,074 (6)	-0,0865 (8)
F_8	0,1194 (4)	0,0865 (4)	0,0727 (5)	-0,0308 (2)
F_9	0,1418 (8)	0,0998 (8)	0,0819 (8)	-0,0929 (9)
F_{10}	0,1289 (5)	0,0885 (5)	0,0724 (4)	-0,0673 (6)
		BPH		
FM	RMSE	MAD	MRD	BIAS
F_1	0,1863 (8)	0,1354 (10)	0,1136 (10)	-0,0356 (5)
F_2	0,1537 (3)	0,1107 (3)	0,0917 (7)	-0,0128 (1)
F_3	0,1882 (9)	0,1321 (9)	0,1055 (9)	-0,0585 (8)
F_4	0,1531 (2)	0,1106 (2)	0,0898 (6)	-0,0249 (2)
F_5	0,1924 (10)	0,1275 (8)	0,0954 (8)	-0,0754 (9)
F_6	0,1479 (1)	0,1043 (1)	0,0819 (2)	-0,0313 (4)
F_7	0,1641 (5)	0,1116 (4)	0,0813 (1)	-0,082 (10)
F_8	0,1596 (4)	0,1127 (5)	0,0887 (4)	-0,0263 (3)
F_9	0,1719 (7)	0,1171 (7)	0,0895 (5)	-0,0543 (7)
F_{10}	0,1654 (6)	0,1138 (6)	0,088 (3)	-0,0386 (6)
		BPF		
FM	RMSE	MAD	MRD	BIAS
F_1	0,1393 (7)	0,1059 (7)	0,0964 (8)	-0,0238 (3)
F_2	0,0959 (1)	0,0708 (1)	0,0629 (1)	-0,001 (1)

Table 16. (Cont.) Average error indexed for h/q^2 applied

FM	RMSE	MAD	MRD	BIAS
F_3	0,2115 (9)	0,1709 (9)	0,1515 (9)	-0,1634 (9)
F_4	0,119 (4)	0,0957 (6)	0,0838 (6)	-0,0635 (5)
F_5	0,3517 (10)	0,257 (10)	0,2114 (10)	-0,2302 (10)
F_6	0,1056 (2)	0,079 (2)	0,0664 (2)	-0,0432 (4)
F_7	0,1213 (5)	0,0844 (4)	0,0676 (3)	-0,0703 (6)
F_8	0,1146 (3)	0,0828 (3)	0,0712 (4)	-0,0146 (2)
F_9	0,149 (8)	0,1128 (8)	0,0951 (7)	-0,1052 (8)
F_{10}	0,1265 (6)	0,0879 (5)	0,0725 (5)	-0,0721 (7)

*(x) indicated the position when the error is considered and compared between functions

Table 17. Average error indexed for he/q^2 (Continue in next page)

BEH				
FM	RMSE	MAD	MRD	BIAS
F_1	0,1 (9)	0,0741 (9)	0,0766 (9)	-0,0269 (8)
F_2	0,073 (6)	0,056 (6)	0,0582 (6)	-0,0173 (6)
F_3	0,1017 (10)	0,075 (10)	0,0771 (10)	-0,0326 (10)
F_4	0,0702 (5)	0,054 (5)	0,0568 (5)	-0,0099 (4)
F_5	0,0972 (8)	0,0723 (8)	0,0737 (8)	-0,0307 (9)
F_6	0,0677 (3)	0,0513 (1)	0,0539 (1)	-0,0138 (5)
F_7	0,0669 (2)	0,0517 (3)	0,0552 (4)	-0,0002 (1)
F_8	0,0744 (7)	0,0572 (7)	0,0589 (7)	-0,0248 (7)
F_9	0,0659 (1)	0,0515 (2)	0,0551 (3)	0,003 (2)
F_{10}	0,0679 (4)	0,0522 (4)	0,055 (2)	-0,0076 (3)

Table 17. (Cont.) Average error indexed for he/q^2

BPH				
FM	RMSE	MAD	MRD	BIAS
F_1	0,0754 (8)	0,0529 (8)	0,0549 (8)	-0,0241 (8)
F_2	0,0523 (3)	0,0386 (3)	0,0398 (2)	-0,0145 (5)
F_3	0,0763 (9)	0,0536 (9)	0,0553 (9)	-0,0264 (9)
F_4	0,0534 (4)	0,0407 (4)	0,0424 (4)	-0,0111 (4)
F_5	0,0849 (10)	0,0631 (10)	0,0649 (10)	-0,0301 (10)
F_6	0,0467 (1)	0,0356 (1)	0,0371 (1)	-0,0054 (2)
F_7	0,0504 (2)	0,038 (2)	0,0399 (3)	0,0026 (1)
F_8	0,0554 (5)	0,0414 (5)	0,0424 (5)	-0,022 (7)
F_9	0,0584 (7)	0,0451 (7)	0,0473 (7)	-0,0098 (3)
F_{10}	0,0581 (6)	0,0441 (6)	0,0459 (6)	-0,0162 (6)
BPF				
FM	RMSE	MAD	MRD	BIAS
F_1	0,1502 (8)	0,1162 (7)	0,1206 (6)	-0,0139 (5)
F_2	0,1438 (6)	0,1111 (4)	0,1183 (3)	-0,0043 (1)
F_3	0,1529 (9)	0,1171 (9)	0,1193 (5)	-0,0279 (7)
F_4	0,1415 (2)	0,1111 (3)	0,1213 (7)	0,013 (4)
F_5	0,2814 (10)	0,2218 (10)	0,2061 (10)	-0,1608 (10)
F_6	0,1433 (4)	0,1129 (5)	0,1164 (2)	-0,0407 (9)
F_7	0,1388 (1)	0,1089 (2)	0,1192 (4)	0,0128 (3)
F_8	0,1422 (3)	0,1087 (1)	0,1147 (1)	-0,0118 (2)
F_9	0,1451 (7)	0,1168 (8)	0,1307 (9)	0,0302 (8)
F_{10}	0,1437 (5)	0,1135 (6)	0,1247 (8)	0,0157 (6)

When *BPH* are analyzed, the best fitting function was F_6. When considering *BPF*, F_2 was the expression with less error but the F_6 is near such as *BEH* case. However, considering the analysis developed by [155], F_6 was chosen to define the characteristic curve of the machine when other methods were compared to define the *BEH, BPH* and *BPF*. This comparison will show in Section 3.2. Therefore, when the head curve is defined the function will be the following expression:

$$H = \left[-0.69 \left(\alpha \frac{Q}{Q_{BEP}} \right) + 0.122 \left(\frac{Q}{Q_{BEP}} \right)^2 + 0.313 \left(\frac{Q}{Q_{BEP}} \right) + 1.222\alpha^2 - 1.267\alpha + 1.294 \right] (Am^2 + Bm + C)Q^2 \tag{43}$$

Besides, F_6 has the advantage the expression considers both ratio of the rotational speed and the ratio between Q/Q_{BEP}, therefore, it considers the closeness to the best efficiency point when it is compared concerning operation flow.

Table 17 shows the average errors for *RMSE, MAD, MRD* and *BIAS* when the non-dimensional value of he/q² is calculated. In this case, F_6 was the expression, in which the errors were low when *BEH* and *BPH* are observed.

In all cases, *BIAS* values were low, and this index was between 0 and $\pm 3\%$. These values are no significant because they show average errors, which are less than 3 % when the head curve and power curve are estimated.

To develop the comparison of methods, F_6 was chosen to define the power curve of the machine according to the expression shown in Table 11. The following expression enables to estimate the power when the head curve and efficiency curve in nominal conditions are known.

$$P = \left[0.993 \left(\alpha \frac{Q}{Q_{BEP}} \right) - 0.494 \left(\frac{Q}{Q_{BEP}} \right)^2 - 0.156 \left(\frac{Q}{Q_{BEP}} \right) - 0.471\alpha^2 + 0.38\alpha + 0.73 \right] 9.81 \cdot \eta_0 (Am^2 + Bm + C)Q^3 \tag{44}$$

3.4.2. Comparison of the proposal study vs other published methods applied to *BEH, BPH* and *BPF*

The proposed methodology was compared with five different published methods. These were: (i) Classical Affinity Laws [160]; (ii) Carravetta et al. [163]; (iii) Fecarotta et al. [171]; (iv) Pérez-Sánchez et al. [159]; and (v) Tahani et al. [156].

$$Affinity\ Laws \begin{cases} h = \alpha^2 \\ q = \alpha \\ p = \alpha^3 \\ e = 1 \end{cases}$$

$$Carraveta\ et\ al., (2014) \begin{cases} h = 1.0253\alpha^{1.5615} \\ q = 1.0323\alpha^{0.7977} \\ p = 0.9741\alpha^{2.3207} \\ e = -0.4013\alpha^2 + 0.845\alpha + 0.5606 \end{cases}$$

$$Fecarotta\ et\ al., (2016) \begin{cases} h = 0.972\alpha^{1.603} \\ q = 1.004\alpha^{0.825} \\ p = -- \\ e = -0.317\alpha^2 + 0.587\alpha + 0.707 \end{cases}$$

$$Pérez - Sánchez\ et\ al., (2018) \begin{cases} h = 1.89\alpha^2 - 1.54\alpha + 0.74 \\ q = 1.08\alpha^{0.7} \\ p = 4.59\alpha^2 - 6.33\alpha + 2.50 \\ e = -0.36\alpha^2 - 0.69\alpha + 0.66 \end{cases}$$

$$Tahani\ et\ al., (2020) \begin{cases} h = 0.9962\alpha^{1.0851} \\ q = 0.9974\alpha^{0.3651} \\ p = 0.9767\alpha^{1.4888} \\ e = -4.3506\alpha^2 + 8.8879\alpha - 3.544 \end{cases}$$

The last cited methods were operated to get the best efficiency head, best power head and best power flow. The *BEH, BPH* and *BPF* for each method were compared with the experimental database for each machine. In all cases, when the average error indexes were calculated, the proposal of non-dimensional parameters (i.e., h/q^2 and he/q^2) showed the minor error values of both *BEH, BPH* and *BPF*.

Figure 12a table (a) — Error indexes for h/q^2:

	BEH				BPH				BPF			
	RMSE	MAD	MRD	BIAS	RMSE	MAD	MRD	BIAS	RMSE	MAD	MRD	BIAS
This study	0.1077	0.0755	0.0622	-0.0408	0.1479	0.1043	0.0819	-0.0313	0.1056	0.079	0.0664	-0.0432
Affinity Laws	0.1304	0.0899	0.0697	-0.0668	0.1748	0.1206	0.0896	-0.0624	0.1322	0.0958	0.078	-0.0506
Carravetta et al.	0.147	0.1039	0.081	-0.0944	0.1863	0.128	0.0935	-0.09	0.1436	0.104	0.0832	-0.0783
Fecarotta et al.	0.1464	0.1025	0.0796	-0.0914	0.1872	0.1282	0.094	-0.0869	0.1444	0.1045	0.0839	-0.0752
Pérez-Sánchez et al.	0.1544	0.123	0.1065	-0.1066	0.194	0.1468	0.1204	-0.1022	0.1394	0.1109	0.0968	-0.0904
Tahani et al.	0.1478	0.1054	0.088	-0.0964	0.1759	0.1218	0.0933	-0.092	0.1292	0.0916	0.0763	-0.0802

Figure 12b table (b) — Error indexes for he/q^2:

	BEH				BPH				BPF			
	RMSE	MAD	MRD	BIAS	RMSE	MAD	MRD	BIAS	RMSE	MAD	MRD	BIAS
This study	0.0677	0.0513	0.0539	-0.0138	0.0467	0.0356	0.0371	-0.0054	0.1433	0.1129	0.1164	-0.0407
Affinity Laws	0.0921	0.0731	0.078	0.022	0.07	0.0543	0.0579	0.0248	0.1813	0.1473	0.1647	0.035
Carravetta et al.	0.0944	0.0718	0.0723	-0.0288	0.0687	0.0492	0.0495	-0.026	0.1673	0.1289	0.1345	-0.0158
Fecarotta et al.	0.1057	0.0808	0.0803	-0.0367	0.0826	0.0598	0.0599	-0.0339	0.1824	0.1401	0.1455	-0.0237
Pérez-Sánchez et al.	1.2201	1.065	1.0709	-1.065	1.2152	1.0622	1.0795	-1.0622	1.2172	1.052	1.06	-1.052
Tahani et al.	0.4051	0.2838	0.2898	-0.2701	0.3814	0.269	0.2819	-0.2673	0.3974	0.2891	0.3035	-0.2571

Figure 12. (a) Error indexes for the different methods applied to h/q^2; (b) Error indexes for the different methods applied to he/q^2

Figures 12a and 12b shows error indexes classified in the different methods. When the non-dimensional parameter, (he/q^2), is observed similar results were obtained. The proposed functions were the best compared to the other five methods. *RMSE, MAD* and *MRD* were 0.067, 0.051 and 0.054, respectively. When these error indexes were compared with the second-best value (affinity laws or Carravetta method), the error values decreased between 26.5, 28.8 and 25.4 %. For *BPH*, the trend of the results was similar. The proposed method was the most accurate, decreasing the errors between 25 and 32 % compared with the second-best functions (Carravetta). When *BPF* was analyzed, *RMSE, MAD* and *MRD* decreased 14.3, 12.4 and 13.4 %, respectively. The use of *MOALs* demonstrated better accuracy in the operational curves when these results are compared with the affinity laws, which are simpler, but they showed higher errors [156][159][171][163]. Figure 12 shows the decrease of the error in the different curves. Therefore, although the expressions use high

degree equations, they improve the simulation of the *PATs* when they operate under variable rotational speeds.

If h/q^2 (Figure 12a) is considered for *BEH*, the *RMSE, MAD* and *MRS* errors were 0.1077, 0.0755 and 0.622, respectively. These errors decreased between 17.4, 16 and 0.7 % respectively, compared to the second-best method (affinity laws). If the *BPH* is analyzed similar results were obtained. The proposed functions were the best and the error indexed were reduced between 9 and 16 % compared to the second-best method. When the error indexes were calculated for the *BPF*, the proposed study was the best, and the error values decreased 20.1, 17.5 and 14.9 % for *RMSE, MAD* and *MRD* respectively.

When h/q^2 is analysed in Figure 12a. The proposed regression expression showed errors between 8.6 % and 49.8 % less than the obtained errors by application of the affinity laws, which was the second-best method for *BEH* and *BPH*, being the third when *BPF* was calculated. RMSE value was 0.1 for *BEH* and *BPF*, while it was 0.148 when *BPH* was estimated. If the *MAD* and *MRD* were analysed in this table, these values were around 0.07 and 0.06 respectively when *BEH* was compared. If *BPH* is compared, the *MAD* and *MRD* errors 0.1 and 0.08 respectively when they were 0.12 and 0.09 when the second-best method (affinity laws) is compared.

A similar analysis can be developed if Figure 12b is observed. The proposed expression regressions were the best when *BEH, BPH* and *BPF* were defined using all previous cited methods and the errors calculated. If *BEH* is analyzed, the proposed expressions in this research reduced the error indexes (*RMSE, MAD* and *MRD*) by around 30 % compared to Affinity laws and Carravetta's method, which were the second and third best methods for this *BEH* curve. In this curve, the *BIAS* was near -1 %. If *BPH* is analyzed, a similar analysis was done. The error indexes reduced between 33 and 36 % the error of the second-best method, while the *BIAS* value was 0.5 % for *BPH*. Finally, if *BPF* is observed, the proposed expressions decreased the error indexed. Particularly, *RMSE, MAD* and *MRD* decreased 21, 23 and 30 % respectively between the proposed method and Carravetta's method.

If *BPF* is analyzed, *RMSE* error was 0.14. It decreased 14 % compared with the second-best method (Carravetta method). *MAD* and *MRD* got similar values, which were reduced by 12.4 and 14.1 %, respectively.

Both parameters, h/q^2 and he/q^2 showed the regression proposed using F_6 enabled to estimate the best efficiency head, best power head and best power flow.

Three lines are strategic considerations when water managers define operations rules to maximize the energy recovery using micro hydropower systems.

3.4.3. Application of the Proposed Curves to Experimental Machine

The proposed empirical regressions were applied to a tested experimental machine to show the accuracy of the expressions applied in real case studies. In this case, the tested machine was NK–140 125/127 [169], being a specific speed in turbine mode of 31.16 rpm (m, kW). Its *BEP* operating as the turbine was 17.99 l/s, 30.31 m w.c. with an efficiency of 0.695. The machine was tested on six different rotational speed, being 3000 rpm its nominal rotational speed. Figure 13a shows the head as a function of the flow of the BEH. The m value for this machine is 0.056. If this curve is analyzed, Figure 13b shows the curve, which defines the power as a function of the flow. Both figures show good accuracy when making visual comparison. When the error was measured, *RMSE* and *MRD* were 0.077 and 0.059 respectively, being *BIAS* equal to 0.0585. If the head curve is analyzed using the proposed expressions in NK–140 125/127, the average error values of *RMSE* and *MRD* were 0.2195 and 0.0096, respectively. The error values decreased around 65.6% in both errors when they were compared to affinity laws. When the power curve is analyzed, *RMSE* and *MRD* were 0.0123 and 0.005 respectively. These errors decreased and *MRD* errors decreased around 82.6% compared to affinity laws. The expressions indicate the good fit for the whole range of nst when Figure 12 and Figure 13 are considered, and the errors are evaluated.

Figure 13c shows the operation curve (*H–Q*), representing the best power head. This is the most important curve since the operation based on this curve is the best to maximize the recovered energy, when variable operation strategy is applied in a water pressurized systems. Comparison of the power curve between the estimated and experimental *BPH* values (Figure 13d) also shows a good fit.

Figure 13e,f show the difference between trend parabolas and tested curves when *BEH, BPH* and *BPF* were considered both the curves (i.e., head and power curve). These three curves (i.e., *BEH, BPH* and *BPF*) are the curves, which should be considered when regulation strategies want to be considered to maximize the recovered energy.
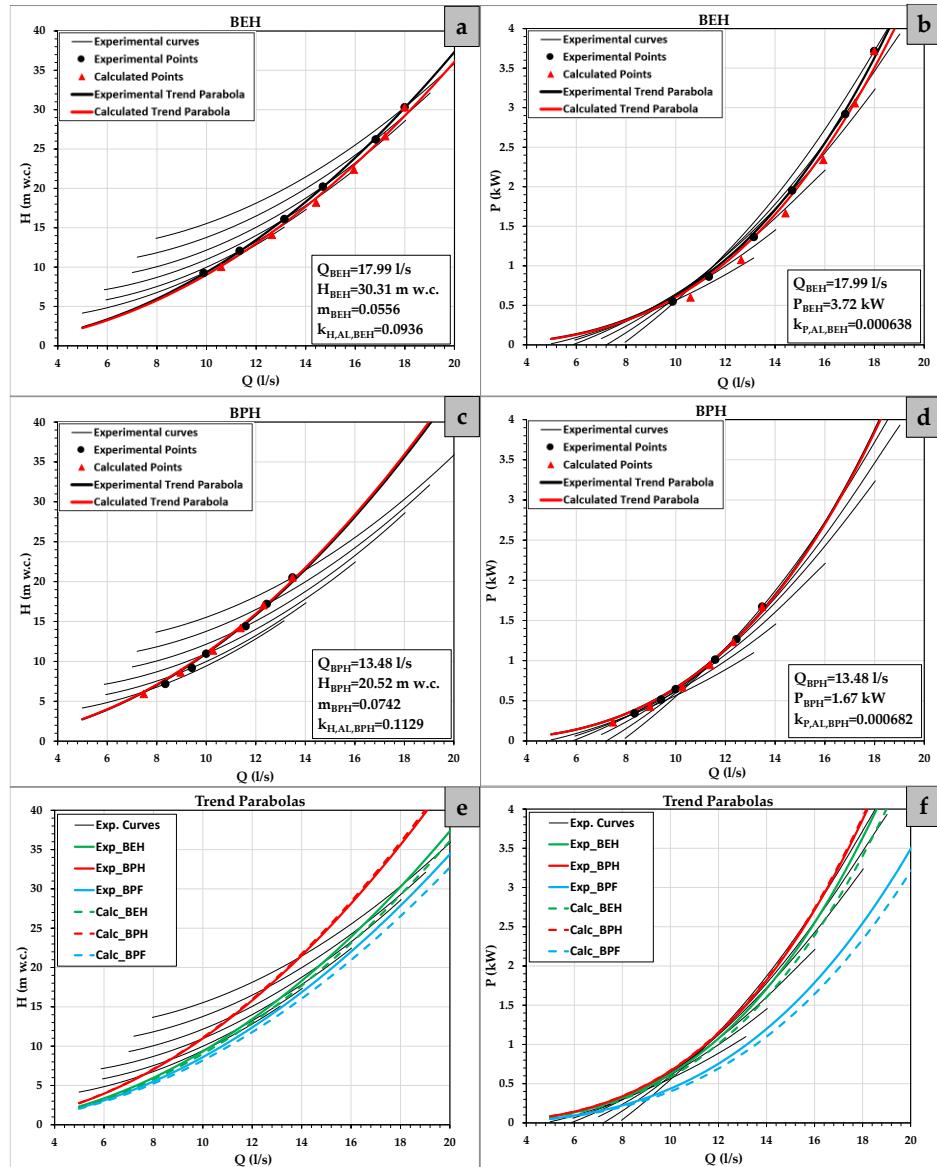
Figure 13. (a) *H-Q* for *BEH*; (b) *P-Q* for *BEH*; (c) *H-Q* for *BPH*; (d) *P-Q* for *BPH*; (e) *H-Q* for *BEH, BPH* and *BPF*; (f) *P-Q* for *BEH, BPH* and *BPF*

3.5. Conclusions

The present research proposed a new modification of the affinity laws (*MOAL*) when applied to pumps working as turbines. These new expressions were compared to the rest of the published methods and affinity laws, showing the best results in the estimation of the best efficiency head, best power head and best power flow. Analyses of these curves in other published research showed that they are key in the operation of the recovery systems to maximize recovered energy. Therefore, the modified affinity laws proposed in this study were found to decrease the error indexes by 8 to 30 % compared with existing methods and can help water system managers to improve the accuracy of energy predictions.

The analysis of the different tested curves as well as the consideration of the analytical expressions showed the importance of the Q_{BPH} value. This value should be considered when the machine is chosen, and it is always greater than Q_0, min. Therefore, the *PATs* system could operate under the best power head conditions when the constrain '$Q_{0,min} \leq Q_{BPH}$' is satisfied.

Incorporating these curves (i.e., *BEH*, *BPH* and *BPF*) when the potential recovery is analyzed by water managers is crucial to get the best results, when the *BPH* achieves the best results in terms of recovered energy. However, the analysis of *BEH* and/or *BPF* is recommended because it can be useful when the recovered energy is not the main goal to be achieved and other factors such as valves regulation or sustainable measures are considered.

These *MOAL* were validated when the specific speeds of the *PATs* systems were between 5 and 50 rpm using 15 different machines and 87 different rotational speed. The analysis showed the need to increase the tests applied on axial machines to increase the operating range by the research community. Future research should focus on developing axial machines analyses. These machines are significant in the water pressurized systems because there are many potential recovery points in which the flow is high, but the recoverable head is low, and therefore, the recovery systems should be established by axial machines.

Author Contributions

4. Artículo 3

"Optimization tool to improve the management of the leakages and recovered energy in irrigation water systems"

4. Artículo 3. "Optimization tool to improve the management of the leakages and recovered energy in irrigation water systems"

4.1. Description

Coautores: Carlos Andrés Macías Ávila; Francisco-Javier Sánchez-Romero; P. Amparo López-Jiménez; Modesto Pérez-Sánchez.

Revista: Agricultural Water Management ISSN 0378-3774.

Factor de Impacto: 4.516. JCR (Q1; Posición 5/90 Agronomy; 11/100 Water Resources).

Estado: Publicado [Elsevier 2021, 10, 1; doi: 10.1016/j.agwat.2021.107223].

Abstract

The use of pumps working as turbines is a new solution, which has been recently analysed to improve the water management in the different water systems. The improvement of sustainability involved with this use should be considered in these networks, and it focuses on the reduction of the consumption energy as well as the reduction of leakages. Both variables have a great influence on the rest of economical, technical and environmental indicators of network behavior, becoming key in their improvement. In this line, the research develops a methodology, which includes the estimation of the leakages in the different junctions and pipes as a function of the injected and registered volume data in the water. The present methodology proposes different operation scenarios according to leakages and it develops a double optimization procedure to locate and select the best recovery machines considering different objective functions. The methodology is applied to a real case study, which has serial data of water registered volume since 2001. The research shows the leakages influence in the operation points as well as the recovered energy. Different sustainable indicators are analysed for the different scenarios according to optimized procedures: The *IRLGP* index was defined as the ratio between reduction of the leakage volume for each installed power and it reached the annual value of 11280.8 m^3/kW; The optimized procedure establishes the significance to consider the leakages when the hydraulic machines are selected. Their best efficiency points increase to 195 % and 205 % compared to the ideal scenario without leakages.

Keywords: Leakages; Water irrigation networks, system sustainability; Micro-hydropower; Energy recovery.

4.2. Introduction

Hydroelectric micro-energy can be a valuable answer to the need for low-cost and long-life electrical energy, using natural or artificial waterfalls, which do not harm environmental damage. Unconventional solutions are at the forefront of many developing countries to achieve energy self-sufficiency [16]. The need for research ideas on the field of reducing wastage of water can save a great amount of water, money, time or energy. Water leakages is an essential problem in the field of supply systems [101]. Water distribution networks are low-energy efficiency systems since they need high energy levels to satisfy consumption in terms of pressure. These

high values cause a high leakages level increasing the energy consumption and decreasing the performance and sustainability indexes of the system [172].

The growth of the energy demand, the increase of its price as well as the limitation of access to exploitation sites due to environmental limitations caused new challenges to appear, addresing new technologies to improve the management of the water systems. These technologies are focused on hydraulic recovery and they try to reduce the investment and exploitation costs compared to traditional machines [15]. In such a scenario, microhydraulic solutions for energy recovery can play a key role in exploiting small water resources [173]. This energy recovery, which is defined as a process in which energy is recovered from the residual supply pressure [17] when it is applied in water systems, the use of micro-hydropower technology can enhance the sustainability of the water industry [174].

The new strategies of water management are focused on the improvement of sustainable indexes. In this line, the leakages reduction in water distribution networks is an absolute priority and many pressure management strategies have been proposed in the literature to tackle this issue [10]. These new trends join the pressure management with the use of micro-hydropower systems, mainly pump working as turbines *(PATs)* [97] in which they play a key role to increase the self-consumption of the energies communities [143]. *PATs* are standard water pumps, which operate in reverse mode. Although these machines show low-efficiency values compared to traditional machines, their low-cost technology could help to expand hydropower exploitation in water resources worldwide, helping to reduce climate change greenhouse gas emissions [18].

The efficiency analysis was analyzed for different researches over time. The main published researches were: [175] developed a comparative study between efficiencies the machines operate as pump or turbine. [176] proposed linear equations to estimate the best efficiency point of the machine operate as a turbine. [177] presented a study on the comparison of different calculation methods for turbine performance prediction [152] using the best efficiency value [178]. [179] tried to estimate hydraulic parameters (i.e., head, flow and efficiency) in turbine mode using pump data by CFD techniques. [180] proposed a new approach for the *PAT* power plant, which is a design based on a constant head, instead of a traditional operation, in constant flow rate. [181] evaluated both best efficiency points *(BEP)* and performance of *PATs* in an accurate way using the artificial neuronal networks. [182] defined new approach equations to estimate the *BEP* of the *PATs* and the characteristic curves using an experimental database of 181

different *PATs*. Previously studies considering the machine operate under fixed rotational speed. [163] studied the efficiency when the affinity laws are modified, considering variable rotational speed and improving the energy estimation. [183] defined new analytical expressions, which enable the estimation of the best efficiency head, best power head and best power flow when the machine operated under rotational speed, showing the need to incorporate these expressions in the energy analyses, improving the predictions [171][184].

presented an investigation focused on the optimal location of *PATs* within a water distribution network to produce energy and reduce leakage. Avoiding using pressure reducing valves (*PRV*) where only energy is lost and not recovered [15]. [48] showed extensive information on the historical development, methods, selection criteria and the results of the installation of *PATs* in water distribution networks as an energy recovery system. [97] developed an efficient optimization process for energy recovery and reduction of water leaks. The procedure proved to be more cost-effective and realistic compared to others proposed in the literature. A nonlinear programming (*NLP*) algorithm for the optimal setting of *PATs* within *WDNs* was extended to the case of leakage reduction [146]. A multi-objective optimization methodology is presented to minimize leakage and minimize the difference between pumping operating costs and revenues generated through energy recovery by strategically locating *PATs* in the network, which can act analogously to conventional *PRVs* [144]. [172] established a study to define the optimal location of a *PAT* within a distribution network, in order to minimize installation costs and maximize the production of energy and water savings. [185] developed two mixed integer nonlinear programming models to find the optimal number and location of *PATs* and to minimize the cost of power generation in water and power systems. The results showed that it is feasible to replace *PRV* by *PATs*, the installation of three *PATs* generates a total power of 479.65 kW, which is more than 30 % of the daily electricity demand of the water network.

Traditionally, pressure management was developed by using pressure reduction valves, which allow the reduction of leaks but dissipate excess energy. [26] compared the use of *PATs* versus *PRVs*, indicating that it is possible by installing *PATs* to recover up to 169360 $kWh/year$ as well as reducing leaks. These leakages decrease, increasing the volumetric performance of the system from 0.73 to 0.9. [26] proposed a method that replaces a *PRV* with a *PAT* to produce electrical energy and reduce pressure. This method was improved by adding variable speed pumps to control the dynamic operation of networks, in order to improve energy recovery and reduce leakage [148]. This solution enables the recovery above 40 % of the gross

power potential of an existing *PRV* could be converted to electrical energy using a *PAT* while also controlling pressure [186].

To increase this recovery, other researchers developed Particle Swarm Optimization (*PSO*) selection algorithm, incorporating the model into a network that allows a total daily energy of 182 kWh [15]. In this line, [187] defined the economic feasibility of installing a *PAT* in an aqueduct in the city of Merano. The results show a nominal power of 19.18 kW and a daily electrical energy production of 338 kWh. [27] conducted an analysis within the Polokwane Central District Metered Area in which it identified a recoverable energy potential of 2.3 GWh, resulting in a 3.3 % and 4.2 % annual reduction in water leakage. Patelis et al. [188] studied the energy recovery in Kozani (Greece). The possibility of installing 7 *PATs* in different districts of the city with flow rates ranging between 14 l/s and 79 l/s and pressures between 55 and 71 m w.c. was evaluated. Using this hypothesis, annual energy recovery of 328500 kWh possible, decreasing the leakages between 18 % and 65 %. [147] evaluated a water system that operates with a flow rate of 350 l/s and a pressure of 45 m w.c. The installation of *PATs* under these operating conditions enables the annual generation of 714670 kWh and the leakages decrease of 3 %. This reduction saved 248504 m^3.

These contributions improved the different sustainability indicators. They can help to analyze the management of the water systems. Sustainability indicators are necessary to determine the efficiency of a system concerning criteria such as (i) annual energy consumption and cost for each cubic meter of water injected into the network, (ii) the percentage of energy recoverable in the network by energy excesses and (iii) the reduction of energy consumption for each cubic meter of water leaked. The recommended indicators that are analyzed in the water distribution networks are shown in Table 18.

Table 18. Sustainability indicators in *PATs* systems (Continue in next page)

Indexes	Abbreviation	Units	Indicator	Definition
Energy [189], [125]	IED	Dimensionless	Energy dissipation	Ratio between friction energy and input energy
	IAE	kWh/year	Annual consumed energy	Sum of the total active energy consumed in the network
	IEFW	kWh/m³	Consumed energy per unit volume	Ratio between the active energy consumed and the total volume of water introduced in the system
	IER	kWh/year	Energy recovered	Sum of total energy recovered in the network
	ERP	%	Recoverable energy percentage	Recoverable energy percentage used of the total energy consumed in the system
	IAAE	kWh/year	Absolute annual consumed energy	Sum of the total active energy consumed in the network subtracted by the sum of the total energy recovered in the network
	IAEFW	kWh/m³	Absolute consumed energy per unit volume	Ratio between *IAAE* and the total volume of water introduced in the network
	IRLGP	m³/kW	Water recovery per unit volume per installed energy.	Ratio between reduction of the leakage volume for each installed power.

Table 18. (Cont.) Sustainability indicators in PATs systems

Indexes	Abbreviation	Units	Indicator	Definition
Economic [190], [125]	REC	€	Cost of recoverable electrical energy per installation of PATs	Product of the cost of the electricity tariff per kWh of energy produced
	IEC	€/m³	Energy cost per unit volume introduced	Ratio between energy cost and the total volume of water introduced in the system
	CWSBRL	€/m³	Cost of water saved by reducing leaks when installing PATs	Product of the cost of each cubic meter of water for each covered meter of water saved.
Environmental [116]	CDRPE	CO_2/kWh	Carbon Dioxide reduced by produced energy	Ratio between the reduction of CO_2 emission by the production of each kWh of renewable energy
	CDRBL	CO_2/m³	Carbon dioxide reduced by each cubic meter of water saved by leaks	Ratio between the reduction of CO_2 emission for each cubic meter of water saved by leaks.

Several sustainability indicators for pressurized water systems were proposed by [189]. [125] developed a proposal for a recovery system based on the installation of PATs in different points. It enables the annual theoretical generation of 847301 kWh. In this case study, some results of the sustainability indicators mentioned in Table 19 are shown. [190] defined some results of the sustainability indicators. IAAE,

IER, ERP, IEFW and *IRLGP* are shown for 10 water distribution networks in which there are installed *PATs* recovery systems. In these studies, the annual energy consumption in the analyzed distribution networks ranges from 141794 to 1583106 kWh, the annual energy recovery varies from 28470 to 714670 kWh and the energy recovery values were found between 3 % and 58 %. [116] demonstrated the economic and environmental impacts when energy recovery systems are installed in water distribution networks in which the savings can support the electricity use of more than 20 average American households, corresponding to an annual reduction of 177 tons of CO_2 emissions. The indicators depend on the network topology and therefore, there are different between them. It implies one indicator cannot be adapted exclusively.

Table 19. Equations to calculate the energy balance

Type	Equation	ID
Total Energy (E_{T_j})	$\gamma Q_j(z_o - z_i)\,\Delta t/3600$	(13)
Friction Energy (E_{FR_j})	$\gamma Q_j(z_o - (z_j + P_j))\,\Delta t/3600$	(14)
Theoretical Energy Necessary (E_{TN_j})	$\gamma Q_j P_{minj}\,\Delta t/3600$	(15)
Energy Required (E_{RS_j})	$\gamma Q_j P_{minSj}\,\Delta t/3600$	(16)
Theoretical Available Energy (E_{TA_j})	$\gamma Q_j(P_j - P_{minj})\,\Delta t/3600$	(17)
Theorical Recoverable Energy (E_{TR_j})	$\gamma Q_j(P_j - \max(P_{minj}; P_{minSj}))\,\Delta t/3600$	(18)
Theorical Recoverable Energy ($E_{TR_{mj}}$)	$\gamma Q_j \eta_i H_i\,\Delta t/3600$	(19)

Sustainable Development Goals (*SDGs*) acknowledge the inter-linkages between human wellbeing, economic prosperity, and a healthy environment and, hence, they are associated with a wide range of topical issues that include the securities of water, energy and food resources, poverty eradication, economic development, climate change, health, among others [30].

The implementation of *PATs* in water distribution systems is related to objective 9 [191] of the sustainable development objectives called "Industry, innovation and infrastructure" due to the introduction of promotion of new technologies that allow the efficient use of water resources as indicated by objective 6 [192] called "Clean water and sanitation". The installation of *PATs* makes cities more inclusive, safe, resilient and sustainable [193] allowing the generation of electricity in a renewable, affordable, reliable and modern way as indicated by goal 7 [192] "Affordable and clean energy" and reducing environmental indices emissions, contributing to the objective 13 [194] of the *SDG*.

This research aims to establish a methodology, which optimizes the location and selection of the machine considering the influence of the leakages in the selection of the machine as well as its influence on the location when leaks are considered. The novelty focuses on the characterization of the operation points for different leakages values as well as the double application of the simulated annealing to optimize the location as well as the selection of the recovery systems. To develop the study, the methodology proposes an internal iterative procedure, which allows the estimation of the leakages in each line and consumption point according to measured volume data (i.e., injected and registered) by the water managers. The methodology was applied to the real irrigation network. It is located on the township called Vallada in the province of Valencia (Spain).

4.2.1. Methodology

The proposed optimization procedure is divided into six different phases in which each one contains different steps (Fig. 14). The model needs different inputs to develop the optimization procedure and there are two simulated annealing procedures includes in this methodology. These optimization procedures are applied on localization of the recovery systems in the different ones and define the best machine and its regulation control.

4.2.1.1. Optimization stages

Fig. 14 shows the proposed methodology, which is divided into five different stages: Network model (I), Leakages calibration (II), Energy Balance (III), Location Optimization (IV), Selection Optimization (V) and Definition of the best solution (VI).

- **Network model**

The first stage is a preliminary phase in which the network model is developed according to the available information. This should define both the topology of the water systems as well as the demand base and the consumption patterns. The model is simulated to check the flow and pressure in all lines and nodes. When the model is correct, the model is ready to be calibrated, considering leaks. The model uses the calibrated methodology, which estimates the flow over time considering the consumed volume in the irrigation points as well as the irrigation needs and consumption trends of the farmers [31], [195].
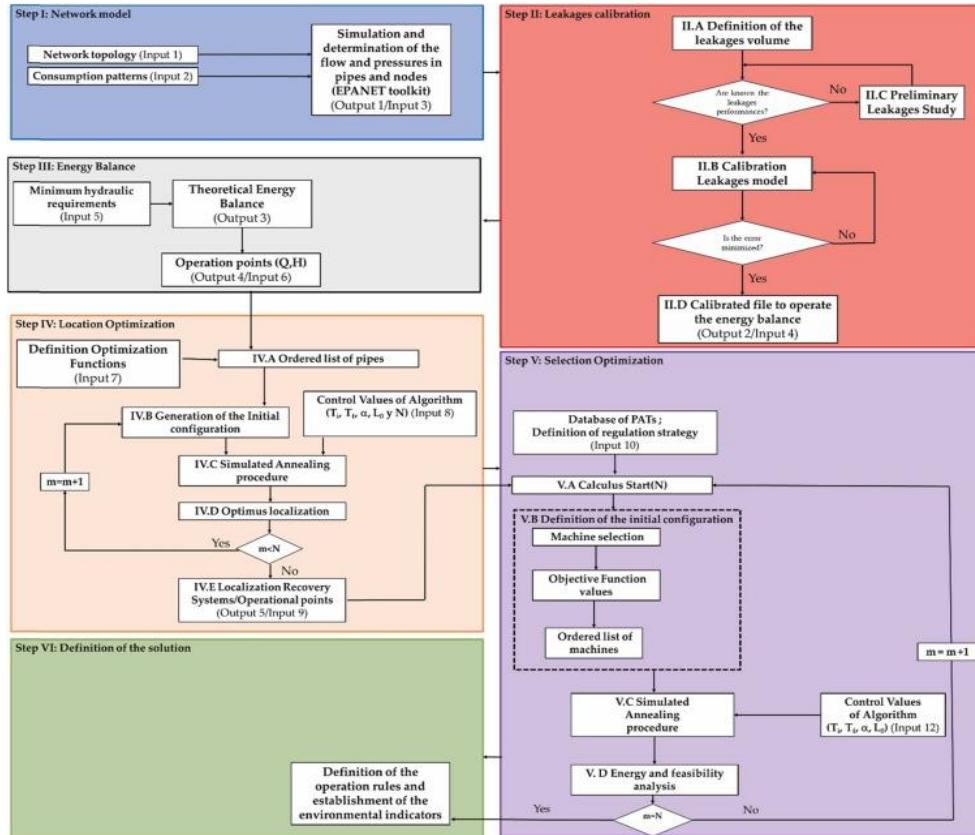
Figure 14. Optimization procedure

- **Leakages calibration**

The second step proposes a calibration strategy to consider the leakages in the water systems. The method is applied when the water managers have information on the water meters of the consumption. Therefore, the proposed method establishes a balance of the water volumes. The first step is the development of the implemented volume analysis, establishing the following continuity balance (Step II.A):

$$V_I = V_M V_L \qquad (45)$$

where V_I is the injected volume in the network in m^3; V_M is the total measured volume by water meters in the consumption nodes in m^3; and V_L is the total leakages volume in the water system in m^3.

If this data volume is known, the different volume performance of the network can be defined according to the following equations:

$$\eta_L = \frac{V_L}{V_M} \tag{46}$$

$$\eta_M = \frac{V_M}{V_I} \tag{47}$$

Where η_L is the leakage performance of the water system and η_M is the measured volume performance of the water system.

The leaks can be divided into two types, which are called apparent and real losses [196] in which the real leakages are assigned in the distribution lines while the apparent losses are assigned to the irrigation consumption points. These leakages enable the definition of the following ratio:

$$\eta_{AL} = \frac{V_{AL}}{V_L} \tag{48}$$

$$\eta_{RL} = \frac{V_{RL}}{V_L} \tag{49}$$

where η_{AL} is the ratio between apparent leakages and total leakages; V_{AL} is the total volume of the apparent losses in m^3; η_{RL} is the ratio between real leakages and total leakages; V_{RL} is the total volume of the real losses in m^3. The apparent losses are the uncontrolled leakeages in the water systems, which cannot be measured [197].

The calibration model distributes the leakages once the performances (i.e., η_{AL}, η_{RL}, and η_L) are known. This distribution establishes the different criteria as a function of the leakage type (Step II.B). The model determines the different emitter coefficients assigned to the lines and consumption points in different iterations, minimizing the error between simulated leakage volume and leakage volume of the water system. The model considers the following equation to evaluate the leakage in each element (i.e., line or tap).

$$q_{L,ij} = K_j (P_{ij})^N \tag{50}$$

where $q_{L,ij}$ is the leakage flow for the element j (i.e., line or consumption point) at the time i; P_{ij} is the pressure in the element j at the time i (if the element is a line, the chosen pressure is the average pressure value of the line $-P_{ij} = \bar{P}_{ij} -$); N is the leakage exponent; and K_j is the global emitter coefficient.

Using Eq. (50), the leakage volume is estimated by the following expression:

$$V_{L,j} = \sum_{i=1}^{i=T} (q_{L,ij} \Delta t) \sum_{i=1}^{i=T} (K_j (P_{ij})^N \Delta t) \tag{51}$$

where Δt is the interval time in s, $V_{L,j}$ is the leakage volume for the element in m^3, assuming the K_j is constant in all annual simulations. It is defined by the following expression through iterative procedure:

$$K_j = \frac{V_{L,j}}{\sum_{i=1}^{i=T} ((P_{ij})^N \Delta t)} \tag{52}$$

The definition of the calibration of the leakages is based on the estimation of the parameter, K_j, assuming that the total leakage volume is distributed between all elements of the network. It assumed the leakage volume of each element (i.e., line or tap) will be proportional to some variables, which are related to network characteristics. In this case, the leakage volume of each element $V_{L,j}$ can be determined by the following expression:

$$V_{L,j} = \delta_j \qquad V_L = \delta_j \quad \eta_L \ V_I \tag{53}$$

Where δ_j is the distributed coefficient assigned to each element of the network. The addition of all distributed coefficients is equal to 1.

δ_j is estimated by the following expressions, which difference if δ_j is for a line (Eq. (53)) or consumption point (Eq. (54)).

$$\delta_j = \frac{L_j \cdot \tau j}{\sum_{j=1}^{i=k} (L_j \cdot \tau j)} \tag{54}$$

where L_j is the length of the line j in m; τj is the weighted coefficient, which is novel concerning other published researches; k is the number of lines of the model. It depends on the material of the line.; k is the number of pipes.

Eq. (54) establishes the proposed expression to estimate the distributed coefficient, which weighs the apparent losses in the consumption points. In this case, the distribution coefficient is based on the ratio between consumed volume in the consumption point and total consumed volume.

$$\delta_j = \frac{V_{T,j}}{\sum_{j=1}^{j=m} (V_{T,j})} \tag{55}$$

where $V_{T,j}$ is the total consumed volume of the irrigation points (j), including both measured (invoiced) for irrigation as well as the leakage volume (no invoiced); m is the number of consumption points of the model.

The iterations to assign the different distributed coefficients finalizes when the error is minimized in this distribution. When this error is minimum, compared between simulated and measured volume, the model is ready to be used in the optimization procedure (Step II.D).

When the water managers do not know the leakage performance, the proposed methodology develops a preliminary analysis of leaks (Step II.C). Step II.B develops a series of simulations to obtain ranges of values and define the scenarios correctly. The model supposes the calculus of the real leakages in the lines. It enables the estimation of the real leakage performance (η_{Rl}) and establish the N exponent. In this hypothesis, the leaked volume is not known and the methodology assigned different leakage parameters to the lines, following the alignment of the other published researches [101], [198]. The following expression is used:

$$q_{L,ij} = \beta_j \cdot L_j \cdot (\bar{P}_{ij})^N \tag{56}$$

where β_j is the leakage coefficient, which characterizes the pipe in terms of age, diameter, material, thickness, among others. In this case, the model does not need to iterate since the used emitter coefficient in EPANET is:

$$K_j = \beta_j L_j \tag{57}$$

β_j varied between 10^{-4} and 10^{-7} as a function of the material (cement, steel or PVC) [2]. It grows over time and this increase depends on the material. Different scenarios are defined in this case, which weighted the β_j value. Besides, N exponent is defined in the calibration model, estimating the value through of normalized valued, which oscillates between 0.5 and 1.5 according to published researches [2]. Step II.B enables the estimation of the η_{RL} and N exponent.

- **Energy Balance**

Once phases I and II occour, the energy balance can be established to know the energy audit and therefore, the available operational points in each line and consumption point. This energy balance is crucial since it should consider the minimum hydraulic requirements. Table 19 shows the equations used to establish

the energy balance and define the operation points (i.e., flow and theoretical head), which are the main input to develop the first optimization procedure (Step IV).

The different variables of Table 18 are: γ is the specific weight of the fluid in kN/m^3, which is equal to the ratio $9.81/3600$; E_{T_j} is the total energy supplied in the system in kWh; E_{FR_j} is the friction energy, which is lost in the water system in kWh; E_{TN_j} is the minimum energy required in a hydrant or line to ensure the minimum pressure of irrigation in the more unfavorable point in kWh; E_{TA_j} it is the available energy for recovery in a tap or line in kWh; E_{RS_j} is the minimum energy required in a point to ensure the quality in the service in kWh; E_{TR_j} it is the maximum theoretical recoverable energy in an irrigation point, hydrant or line of the network in kWh; $E_{TR_{mj}}$ is the recovered energy by a recovery system considering the efficiency of the PATs systems; Q_j is the circulating flow in an element (i.e., line or consumption point) over time in m^3/s; z_0 is the head level of the reservoir in m w.c.; z_j is the geometry level in m; $P_{min\,j}$ is the pressure in the element j (line or node); is the minimum pressure in the element to guarantee the pressure in the more unfavorable point in m w.c.; $P_{min\,Sj}$ is the minimum service pressure in any consumption point in m w.c.; H_i is the recovered head by the recovery system (i) in m w.c.; η_i is the efficiency of the recovery system for this flow Q_j; Δt is the considered interval time in s.

- **Location optimization**

Once the available operation points are known when the energy balance is developed (Input 6), the objectives functions (Input 7) are defined to develop the first optimization procedure. The proposed objective functions are: (i) Theoretical Recovered energy ($\psi_1 = E_{TR}$), which establishes the maximization of the theoretical recovered energy in the system; (ii) Reduction of the leakages in the network ($\psi_2 = \Delta V_L$); and (iii) Net Present Value (*NPV*) represents the cumulative sum of all revenues minus all costs, expected over the life of the project.

Input 6 and Input 7 enable the development of Step IV.A. This step establishes an ordered list of the elements according to each objective function. Once the ordered list is established, the procedure is ahead to Step IV.B. The optimization procedure is based on simulated annealing defined by [199]. The installation of different recovery systems provides a significant number of possible combinations. In this situation, the simulated annealing method is particularly suitable, since it satisfies the basic requirements for its application [200]. These requirements are (i) clear configuration

of the decision variables, (ii) definition of the target variables, (iii) procedure for generating new system configurations, (iv) control parameters and analogous cooling scheme, and (v) algorithm completion criteria. In this case, the algorithm searches for the best locations for the recovery systems based on the defined objective functions, as well as the number of established recovery systems.

The optimization process maximizes the established objective functions; this process is shown in Steps IV.B and IV.C. Once, the objective function to be considered is selected, generating a list in descending order of the elements that enter the optimization according to the energy balances performed and the chosen objective function. The control parameters of the algorithm are defined and they are: the initial temperature (T_i); the final temperature (T_f); cooling ratio (α) and number of transitions for each temperature step (L_0). These parameters can be set by a previous sensitivity analysis. The transition temperature (T_t) is calculated according to a geometrical relation according to:

$$T_t = \alpha \quad T_{t-1} \tag{58}$$

When the control parameters are defined, the maximum number of recovery systems (N) should be determined. The range of this parameter is between 2 and the maximum number of elements (i.e., lines and nodes) of the water system. In the initial step of the procedure (Step IV.B), the initial configuration should be considered. This configuration begins by considering two recovery systems (m) in the two first elements of the list. Hereafter, the simulated procedure (Steps IV.C) develops a new combination between different elements for each value of the m recovery system. When the optimization process finishes, the methodology establishes the best location for this value of m (Step IV.D). If the m value is lower than N, then the procedure comes back from Step IV.B in which the new configuration for the m+1 recovery system is developed. The final result of this stage (Step IV.E) is the knowledge of the optimum configuration for the N recovery system (Output 5). This output is input 9, which is used in Step V.

- ## Selection optimization of the machines

The main goal of this stage is the definition of the most suitable machine or machines. It implies the selection of the machine, the definition of the maximum number of machines in each recovery system (if needed) and the best strategy to regulate according to the chosen objective variables. These inputs are previously defined, and the methodology used a database that used 110 different *PATs*. The machines are defined according to specific speed η_{st}, head number and discharge

number. These values allow the definition of the dimensionless parameters of the machines included in the database. To define the machine the dimensionless best efficiency point (*BEP*) is used, through the 110 tested machines. It considers different values of impeller diameter and rotational speed. Both values enable the definition of the generated best efficiency point of the theoretical machine. When the *BEP* is known, the characteristic curves are defined by the methodology proposed by [201]. Once, the characteristic curve is estimated, the variable operation strategy zone is defined. The machine operates under variable rotational speed and the best efficiency head (*BEH*), best power head (*BPH*) and best power flow (*BPF*) is estimated. This prediction of the variation of the rotational speed is developed according to the proposed methodology by [183]. Considering these curves, the algorithm developed the optimization by iterations using different regulation strategies (*RS*). These strategies can be (i) nominal rotational speed (*NR*); (ii) *BEH*; (iii) *BPH*; (iv) *BPF*; and (v) operational area considering the maximum and minimum recoverable head.

The use of an optimization procedure is necessary because there are different variables: (i) the possibility to use a different number of machines, which can be installed in serial or parallel in the same recovery system; (ii) different regulation strategies; (iii) and different possible number of recovery systems installed in the network. It implies a high number of combinations. In this case, the methodology proposes the use of the simulated annealing again. The initial step of this stage (V.A) includes the definition of the problem, which indicates the number of recovery systems and their location in the water network as a function of the objective function (Input 9, which is the result of the previous optimization procedure, Step IV). Besides, the water managers should be defined the different regulation strategies.

Defined the inputs, the procedure continues to Step V.B in which the definition of the initial configuration is established. In each recovery system, an ordered list of the possible machines is developed, according to the objective function, establishing the initial operation rules. When the machine is chosen, an iterative procedure analyses whether there are other operation rules, which will be better to improve the objective function. Finally, Step V.B the best machine and operation rules, getting the initial configuration, which is used in the following Step V.C. Step V.B repeated the procedure for each recovery system.

Step V.C includes the definition of the control parameters, which are defined similarly to stage IV. A new configuration of the operation is developed in each

iteration in which a recovery system is chosen randomly and another machine is checked in that recovery system. The beginning probability of the machine is proportional to the value of the objective function, keeping the ordered list. The beginning probability of the upstream recovery systems is greater than downstream systems in the first iterations. This probability decreases when the calculus procedure advances. Once, the machine and strategy are optimized the procedure continues to Step V.D, in which the energy and feasibility analysis is developed, developing iterations to reach the best solution in the combination of the N located recovery machines, the used database and the regulation strategy as well as considering the chosen scenario. The feasibility analysis is developed considering the recovered energy (E_{TR}), reduction of the leakages in the network (ΔV_L) and the Net Present Value *(NPV)* and the Internal Ratio Return *(IRR)*

$$NVP = -IC_0 + \sum_{i=1}^{i=n} \frac{AI_i - AC_i}{(1+k)^i} + RI_n \qquad (59)$$

where: IC_0 is the initial investment in year 0; AI_i is the annual income in the year i; RV_n is the annual costs in the year i; AC_i is the recovered residual value in the year n; AI_0 is the annual income by the sale of energy and reduction of leakages; k is the discount rate. The internal return ratio (*IRR*) is the discount rate that makes *NPV* equal to zero.

The initial investment cost (IC_0) includes the initial investment for the implementation, installation and operation of the recovery systems [202], [203]. The annual costs (AC) refer to the annual operating costs of the recovery systems over the life of the system [11]. The annual incomes (AI) refer to the annual incomes generated by the facility through the sale of energy or self-consumption benefits. The incomes also consider the reduction of leakages and therefore, the benefit for the water saving. In addition, they may include other types of benefits due to reduced leakage and reduced CO_2 emissions. The residual income (RI) is a concept that takes into account the possible income from the sale of the different elements once their function in the facility has ended.

- **Best solution**

The final step is the development of the best solution through an iterative procedure in which the different sustainable indicators are analysed to consider the best recovery system. These indicators are shown in Table 18 and the optimization procedure calculates them in each iterative procedure of the selection of the machine.

4.3. Materials and Methods

The proposed methodology was applied using a database of a total number of 110 pumps working as turbines. The dimensionless best efficiency point, characteristic of the machine and rotational speed is shown in [125]. Using this database, which classifies the recovery systems considering their specific speed, 7826 synthetic machines are generated through turbine generators published by [199]. When the simulated annealing is applied, a previous selection is developed considering the available operational points in this line. This first selection enables the decrease of computational times and an improvement of the final selected machine.

The research applies the proposed methodology to a real water system. The case study is located on Vallada (Spain) and it is an irrigation pressurized system, which was built in 2001.
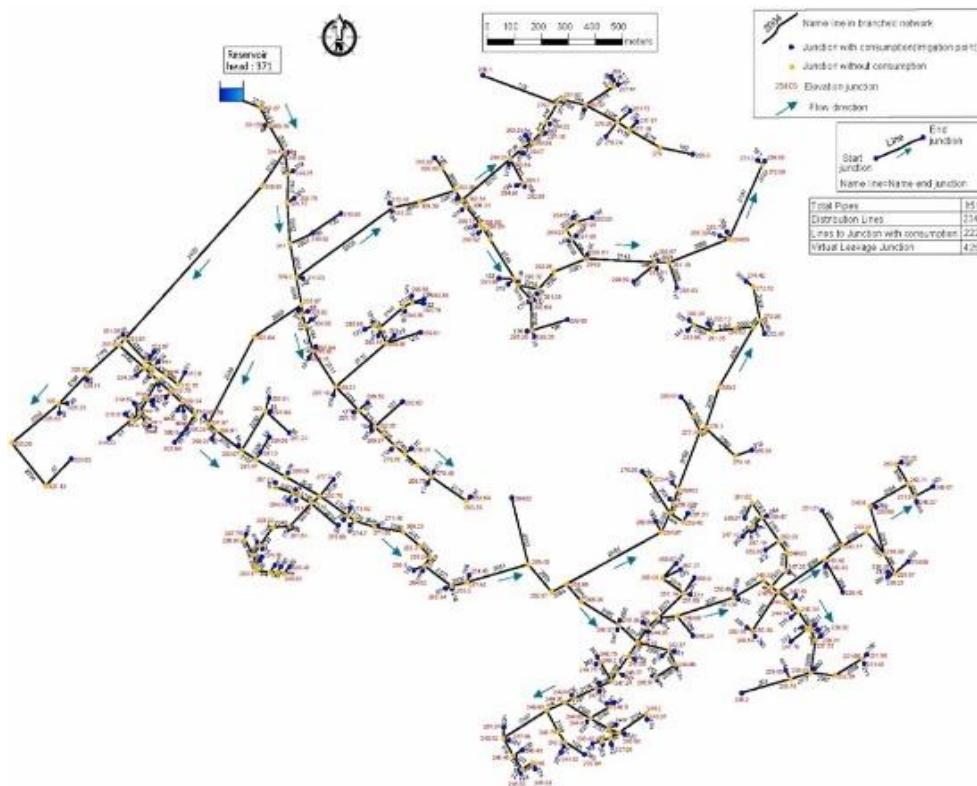

Figure 15. Case study located on Vallada (Spain)

The network supplies around 230 ha. The crop is citric tree mainly and the water resources are got from a well, which is pumped to a reservoir. The pipelines of the network are built on asbestos cement pipes (10780 m) and polyvinyl chloride (11015 m). The diameter oscillated between 90 and 450 mm and the total length of the main pipes and branches is around 22 km. There are 222 irrigation consumption points. The base demand was assigned considering the different farms facilities. The adopted plantation frame was 4×6 squared meter plantation frame and the flow rate of the dripper used was 4 l/h, applying the irrigation needs of the citric tree for each (Fig. 15).

Table 20 shows the recorded data of the water consumption (injected to the grid and measured) as well as the leakages of the system from 2001 to 2020. The present research proposes the establishment of four different scenarios to group the years in similar ranges of leakages. These scenarios are S0 from 2001 to 2005; S1 from 2006 to 2010; S2 from 2011 to 2015; S3 from 2016 to 2020. S0 is considered the ideal situation, which has no leakages. S1 considers an average of leakages of 4.98%, therefore, it considers a total leakage performance equal to 5 %. S2 has an average of leakages of the 13.75 %. This scenario was approached to 15 %. Finally, S3 approaches the leakages at 25% since the real data operated between 2016 and 2020 the average leakages was 22.61 %. The serial data shows the lack of maintenance in the network, and therefore, the increase of the potential leaks in the system.

EPANET-Toolkit [204] was used fot the modeling, with consumption patterns, which were applied in each irrigation point were defined considering both consumed volume as well as the irrigation area of each tap and defining the base demand of the irrigation point according to irrigation needs of the crop. The model calibration was developed establishing different leakages scenarios. These scenarios were considering the previous scenario in Table 20.

They consider leakages equal to 0 % (S0), 5 % (S1), 15 % (S2), 25 % (S3), 35 % (S4) and 50 % (S5). S4 and S5 are future scenarios considering the water managers will not be maintained and the leakages increase according to the observed trend between 2001 and 2020. S4 and S5 are hypothetical and they showed the trend of the systems if the water managers will not apply corrective actions to improve the water systems and reduce the leakages. S4 and S5 are included to analyse the influence of the leakages in the recovery energy and the selection of the hydraulic systems.

Table 20. Data volume registered between 2001 and 2020

Scenario	Year	VI (m³)	VM (m³)	VL (m³)	ηL (%)
S0	2001	77114249	76853961	260287	33
	2002	69616969	69363139	25383	36
	2003	75297467	75050416	247051	33
	2004	92287716	92051431	236285	26
S1	2005	92229183	91986551	1950115	211
	2006	96151176	95914583	3021309	314
	2007	86352055	86123869	2178934	252
	2008	81090129	8086801	6348139	783
	2009	90265586	90024385	3754017	416
	2010	88087919	8786381	6185612	702
S2	2011	107016052	106796152	10733013	1003
	2012	100537864	100297067	9608459	956
	2013	123268842	123033922	17938346	1455
	2014	145182495	144949097	26743108	1842
	2015	138992112	138760313	22326534	1606
	2016	15341545	153184367	20802437	1356
S3	2017	142340357	142104906	28634139	2011
	2018	15940298	159173633	42181013	2646
	2019	170797114	170566859	47724607	2794
	2020	166359731	166135824	41317979	2483

4.4. Results

Once the model is developed used EPANET Toolkit (Step I), the methodology established a preliminary leakages model (Step II. C). It defines the real and apparent leakages performance since there is not this information registered by the water managers. This analysis enabled the estimation of the real and apparent losses. It enables the assignment of the exponent N both lines and irrigation consumption points considering the scenario (Step II.B) as a function of the registered volume data and total leakages performances (Step II.A, Table 20). The η_r and η_A values are defined through an iterative procedure in which the methodology analyse different values of N and compare with the real losses in Step II.C. These N values were obtained to adjust the leakages volume in each scenario by an iterative procedure in which the N and β are calibrated to minimize the error between registered data and

simulated values. Table 21 shows the calibration values, which were obtained for this case study.

Table 21. Calibration results for each scenario

Scenario	η_L (%)	η_R (%)	η_A (%)	N	$B_{PVC}/\beta_{asbestos}$
S1	5	65	35	5	100
S2	15	75	25	55	59
S3	25	75	25	55	36
S4	35	75	25	55	14
S5	50	80	20	6	10

Fig. 16a shows the different values of the energies balance in taps as a function of the analysed scenario, previously to analyse the optimization procedure. The figure shows the annual total energy values for friction, theoretical recoverable and required energy. All energy values were considered and there is no direct relationship between different values, since the theoretical recoverable energy, required energy, as well as friction energy, depending on topology and characteristic of the network (i.e., length, the diameter of pipes, level of the consumption points, level of nodes and head of the reservoir, among others). The annual friction energy oscillates between 10255 and 13426 kWh.

This increase is trivial since when the flow increases, the friction losses increase on squared growth. In this case, the annual friction energy increased 4.1% in the most unfavorable scenario (S5) compared to the ideal situation (S0). The annual required energy, which is necessary to satisfy the minimum pressure requirements, is also increased to compensate for the flow and friction losses. It oscillated between 78968 and 94716 kWh for the S0 and S5 respectively. This increase represented around 20% compared to S0 (ideal scenario without leakages).

Finally, the annual theoretical recoverable energy, which is available to be recovered partially when the recovery system is installed and their efficiency is considered was between 152906 and 182264 kWh for S0 and S5 respectively. The annual energy recoverable alsoincreased 26.2% when S5 is analysed.

104
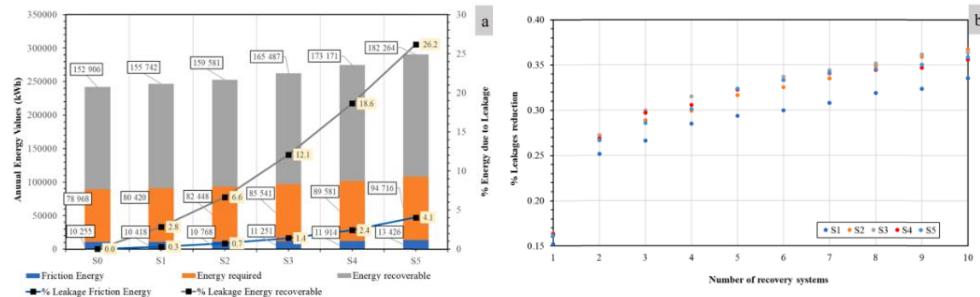
Figure 16. (a) Annual Energy Values for the different scenarios. (b) Reduction of the leakages as a function of the number of recovery systems

Fig. 16b shows the analysis of the percentage of leakages reduction as a function of the number of recovery machines installed. These results were obtained when the objective function was the reduction of the leakages. It is observed the reduction oscillated between 0.15 and 0.37 when the number of recovery machines changed between 1 and 10 respectively. The figure shows not much difference in the reduction of the leakages when the different scenarios are considered. When simulations are extended increasing the number of recovery machines, the maximum decrease of leakages was 0.41 for S1, 0.44 for S2 and S3, and 0.43 for S4 and S5. The hypothetical number of recovery systems was 204 for these results.

The optimization procedure was developed for the three objective functions (i.e., theoretical recoverable, reduction of leakages and net present values). Table 22 shows the different results when these functions were optimized. The optimization procedure considered the following combinations: 204 when N was 1; 20706 for N equal to 2; 1394204 when N was 3; 70058751 when N was 5, the possible combinations were 2802350040; $9.2945 \ 10^{10}$ for N equal to 6; 2.62910^{12} when N was 7; $6.4739 \ 10^{13}$ for N equal to 8; 1.409910^{15} for N equal to 9; and $2.7493 \ 10^{16}$.

The iterations oscillated between 140 and 2640 depending of the combinations and the simulated parameters for the optimization of the locations were: Initial temperature was 10; final temperature was 0.001, the cooling rate was 0.9 and the transition change was 10. These parameters were defined previously through sensitive analysis. The simulated parameters were changed when the optimization of the selection was applied. The following parameters were used: Initial temperature was 10; final temperature was 0.001, the cooling rate was 0.5 and the transition change was 10.

Table 22 shows that the use of three number of recovery systems (N) allows the potential recovery of around 0.8 of the available energy in all scenarios, in which the theoretical recoverable energy increases proportionally with the leakages values. If the objective function is the reduction of the leakages, the reduction range oscillates between 0.37 and 0.66 when the N varies between 1 and 3.

The leakages decrease is around 0.8 when the procedure is optimized using ten recovery systems. Although this solution is not feasible if the *NPV* values are analysed. Finally, when the *NPV* function is analysed it shows feasibility between S1 and S5, although this feasibility reduces according to N and it increases when there is a high percentage de leakages in the network since the circulating flow is higher. Besides, the *NPV* function considers both recovered energy as well as the reduction of the leakages for the decrease of the pressure when *PATs* operate in the network. The installations of *PAT* systems enable the reduction of the leakages and therefore, there is a benefit by the cost of the water that does not leak due to recovery systems. Therefore, the third function considers economic, energy and technical indicators to locate the recovery systems in the network.

Table 22. Location results for the optimization procedure for each leakages scenario. (Continue in next page)

N	S0		S1		S2	
	E_{TR} (kWh)	$\dfrac{E_{TRn}}{E_{TRmax}}$	E_{TR} (kWh)	$\dfrac{E_{TRn}}{E_{TRmax}}$	E_{TR} (kWh)	$\dfrac{E_{TRn}}{E_{TRmax}}$
1	36957	0.46	38924	0.45	43539	0.45
2	57963	0.72	61287	0.72	69206	0.71
3	64799	0.80	68326	0.80	76643	0.79
4	67054	0.83	70753	0.83	79501	0.82
5	68696	0.85	72455	0.85	81330	0.84
6	70017	0.87	73856	0.86	82917	0.85
7	71007	0.88	74910	0.87	84125	0.87
8	71933	0.89	75952	0.89	85475	0.88
9	72345	0.89	76452	0.89	86213	0.89
10	73544	0.91	77644	0.91	87350	0.90
204	80848	1.00	85626	1.00	97020	1.00

Table 22. Location results for the optimization procedure for each leakages scenario. (Continue in next page)

N	S0		S1		S2	
	ΔV_L (m³)	$\dfrac{\Delta VL}{\Delta VL_{max}}$	ΔV_L (m³)	$\dfrac{\Delta VL}{\Delta VL_{max}}$	ΔV_L (m³)	$\dfrac{\Delta VL}{\Delta VL_{max}}$
1	0	–	7777	0.37	28206	0.38
2	0	–	12838	0.62	40607	0.54
3	0	–	13592	0.65	49253	0.66
4	0	–	14557	0.70	52569	0.70
5	0	–	14999	0.72	54135	0.72
6	0	–	15290	0.74	55246	0.74
7	0	–	15711	0.76	56870	0.76
8	0	–	16277	0.78	58929	0.78
9	0	–	16533	0.80	59824	0.80
10	0	–	17128	0.82	62005	0.83
204	0	–	20762	1.00	75084	1.00
N	S0		S1		S2	
	NPV (€)	IRR (years)	NPV (€)	IRR (years)	NPV (€)	IRR (years)
1	-25038	–	15163	21.83	118934	6.68
2	-20636	–	19870	19.97	124172	6.65
3	-22607	–	17217	21.05	123054	7.01
4	-29361	–	16908	24.27	119446	7.65
5	-30333	–	10545	25.05	115689	7.60
6	-38067	–	5369	29.24	111073	8.38
7	-39309	–	3139	30.00	102916	8.03
8	-45724	–	-6494	–	96663	8.68
9	-51069	–	-11817	–	91423	9.18
10	-57484	–	-18180	–	85170	9.91
204	-4183255	–	-3796038	–	-3490233	–

Table 22. Location results for the optimization procedure for each leakages scenario. (Continue in next page)

N	S3		S4		S5	
	E$_{TR}$ (kWh)	$\dfrac{E_{TRn}}{E_{TRmax}}$	E$_{TR}$ (kWh)	$\dfrac{E_{TRn}}{E_{TRmax}}$	E$_{TR}$ (kWh)	$\dfrac{E_{TRn}}{E_{TRmax}}$
1	49347	0.44	56817	0.44	73449	0.43
2	79099	0.71	91664	0.71	119992	0.70
3	87079	0.78	100417	0.78	130235	0.76
4	90475	0.81	104550	0.81	136069	0.80
5	92467	0.83	106743	0.82	138663	0.81
6	94289	0.85	108869	0.84	141470	0.83
7	95689	0.86	110503	0.85	143648	0.84
8	97410	0.88	112679	0.87	146935	0.86
9	98431	0.88	114038	0.88	149141	0.87
10	99513	0.89	115063	0.89	149923	0.88
204	111273	1.00	129474	1.00	170558	1.00
N	S3		S4		S5	
	ΔV$_L$ (m³)	$\dfrac{\Delta VL}{\Delta VL_{max}}$	ΔV$_L$ (m³)	$\dfrac{\Delta VL}{\Delta VL_{max}}$	ΔV$_L$ (m³)	$\dfrac{\Delta VL}{\Delta VL_{max}}$
1	53173	0.38	85440	0.38	157130	0.37
2	76560	0.54	123092	0.54	227658	0.54
3	92748	0.66	148429	0.65	273333	0.65
4	98998	0.70	158500	0.70	291536	0.70
5	101964	0.72	163345	0.72	300565	0.72
6	104081	0.74	166878	0.74	307444	0.73
7	107082	0.76	171316	0.76	315413	0.75
8	110995	0.78	177795	0.78	327867	0.78
9	112684	0.80	180522	0.80	332856	0.79
10	116778	0.83	186964	0.82	344855	0.82
204	141468	1.00	226777	1.00	419160	1.00

Table 22. *(Cont.)* Location results for the optimization procedure for each leakages scenario

N	S3		S4		S5	
	NPV (€)	IRR (years)	NPV (€)	IRR (years)	NPV (€)	IRR (years)
1	246326	3.64	410875	2.31	776680	1.28
2	252298	3.69	417773	2.35	785112	1.31
3	251924	3.89	418319	2.49	787494	1.39
4	250980	4.21	420584	2.68	797616	1.49
5	244875	4.15	411647	2.63	781774	1.46
6	242899	4.53	412872	2.85	790596	1.58
7	227765	4.26	383620	2.70	742135	1.48
8	221655	4.53	377690	2.85	736575	1.55
9	216501	4.71	372627	2.94	731783	1.60
10	210391	4.99	366697	3.10	726222	1.67
204	-3202062	–	-2829678	–	-1994308	–

The optimization procedure enables the preselection of the machine according to theoretical operational points to develop the second procedure of the optimization (Step V). In this case, the machine is chosen to optimize its operating in terms of flow, head and efficiency. The procedure chooses the best machine for each scenario in one of the defined lines, which were established by the location optimization procedure. The model develops an iterative procedure to define the best regulation strategy (*RS*) to evaluate the recovered energy, reduction of leakages and *NPV* values. The recovery never reaches 100% of the theoretical recoverable energy because the efficiency of the recovery systems is less than 1 since this study did not consider ideal machines.

Fig. 17 shows the influence map in which the selection optimization operates to locate the best machine. The color gradient shows the ratio between the variable value and the maximum value. Therefore, the red areas are the best to improve the variable objective. Fig. 17a and b show the results for line 2004 of the network when the recovered energy is maximized in both S1 and S5. All figures show a black cross, which indicates the selected machine. In each case, the selected machines are different, showing the regulation strategy, specific speed, rotational speed of the machine as well as the best efficiency point of the machine. This variability of the machine shows the importance of considering the leakages when the recovery

systems want to be chosen. For example, when the S1 is analysed, the best efficiency point of the machine is 24.4 l/s and 14.21 m w.c. If S5 is analysed, the best efficiency point of the machine increases 195% and 205% particularly, 47.7 l/s and 30.64 m w.c., respectively.
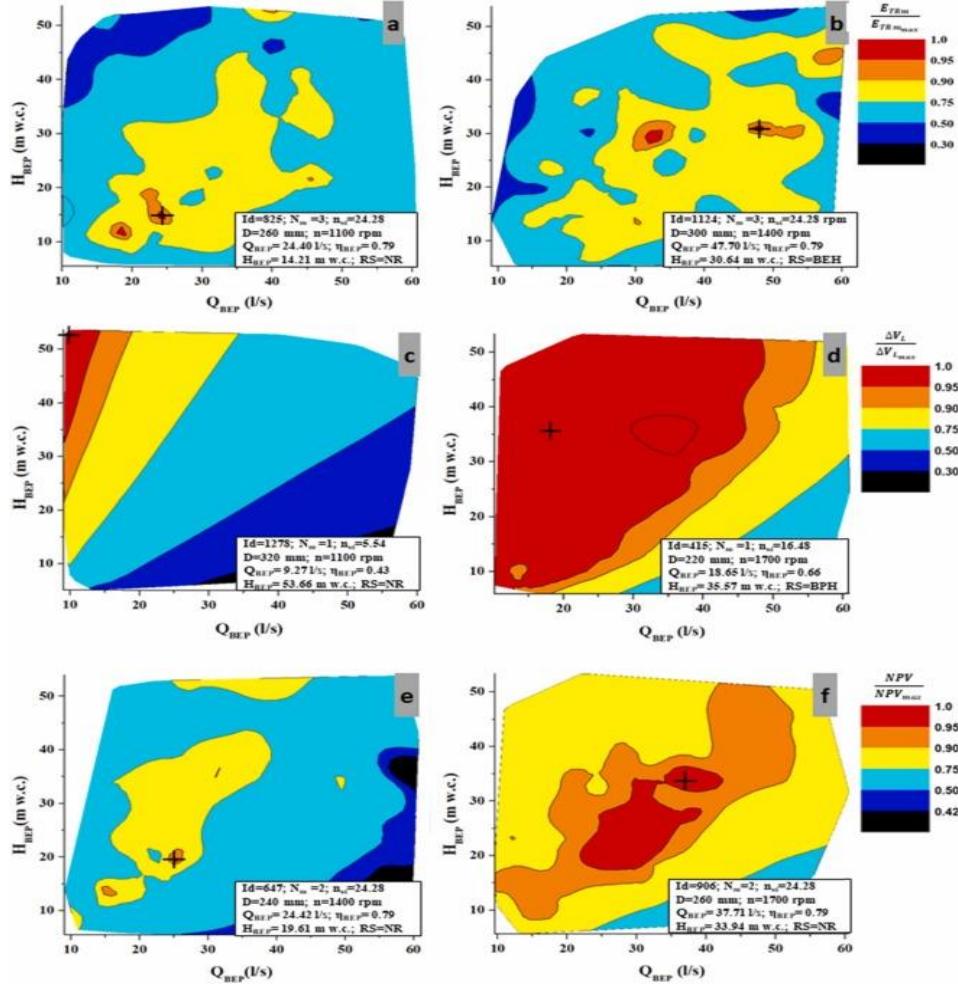

Figure 17. Recovery system installed in line 2004. (a) Recovered energy for S1; (b) Recovered energy for S5; (c) Reduction leakages for S1; (d) Reduction leakages for S5; (e) NPV for S1; (f) NPV for S5

Fig. 17c and d show the optimized solution to select the best machine both S1 and S5 when the optimized variable is the leakages reduction. Similar results were obtained in the selection, where the *BEP* of the machine varied from 9.27 to

18.65 l/s. The head in the *BEP* changed from 53 to 35 m w.c. The regulation strategy (RS) established on S1 it was *NR*, while the S2 operated under *BPH*. Fig. 17e and f defined the best machine when the *NPV* value was optimized. In both scenarios shown (S1 and S5), the best regulation strategy was *NR*. In S1, the best efficiency point was 24.42 l/s and 19.61 m w.c., while it increases for S5. In this case, the *BEP* was 37.71 l/s and 33.94 m w.c.

In addition, the analysis of each scenario, as well as of each combination of installed recovery systems (*N*), allows to know the recovered energy, the reduction of leaks as well as the *NPV* analysis as a function of the number of machines installed in each recovery system (*Nm*) and their characterization of them using specific speed (nst), impeller diameter (D), rotational speed (n) and best efficiency point. Table 23 shows an example of the information selection obtained in the optimized procedure when the S2 was analysed under the hypothesis of the *NPV* function. The table 23 shows annual recoverable energy values above 32000 kWh and annual leakages decrease above 18000 m³ in some configurations with different recovery systems (N).

Table 23. Example of optimized selection of PAT for S2 when the chosen objective function is *NPV*

N	1	2		3		
ID Location	2004	2004	2092	2004	2092	2138
n_s (rpm)	24.28	18.59	9.3	18.59	9.3	5.54
N_m	2	2	2	2	2	1
D (mm)	240	220	134	220	134	260
n (rpm)	2000	1400	3100	1400	3100	800
Q_{BEP} (l/s)	34.89	17.45	3.85	17.45	3.85	3.62
H_{BEP} (l/s)	40.02	22.38	59.38	22.38	59.38	18.74
RS	BEH	NR	BEH	RN	BEH	NR
Annual E_{TR} (kWh)	32456	28570	1932	28570	1932	1179
P (kW)	11.55	7.14	1.41	7.14	1.41	0.55
Leakage Reduction (m³)	13947	17004	206	17004	206	708
NPV (€)	44421	51421	1531	51421	1531	48896
IRR (years)	11.83	10.36	12.27	10.36	12.27	11.4

The inclusion of the *PATs* in water systems is developed to improve the sustainability indicators. Fig. 18 shows the influence of the *PATs* in the improvement of these indicators defined in Table 18 depending on the scenario analysed. Fig. 18a shows four indexes. *IED* showed values between 0.042 and 0.046, increasing in the S5 mainly. *IEC* decreased 40 % between S0 and S5. It shows the decrease of unit cost

when *PATs* are used in the irrigation system. *IEFW* and *IAEFW* showed similar trends with decreases equal to 40.1 % and 45.4 %.
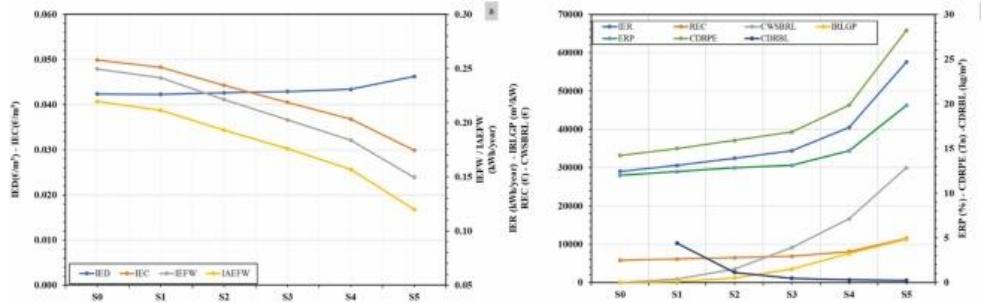

Figure 18. (a) IED, IEC, IEFW and IAEFW indexes according to analysed scenario; (b) IER, IRLGP, REC, CWSBRL, ERP, CDRPE and CDRBL indexes in each analysed scenario

IER showed annual values between 29,010 and 57,543 kWh (Fig. 18b). Another index, which is related to *IER* is the *IRLGP*. This index shows the reduction of leaks in the system considered the installed recovery power. If *IRLGP* is observed in Fig. 18b, the zero value is defined for the ideal situation (S0). The rest values for the different scenarios were 265.3 (S1), 1207.6 (S2), 7584.5 (S3), 7584.6 (S4) and 11280.8 (S5) m^3/kW. This index is too significant since it shows the influence of leakage reduction when recovery systems are installed and therefore, it demonstrates the advantage of incorporating micro hydropower systems in the network. Related to environmental indexes, *CDRPE* and *CDRBL* were applied considering the conversion parameter from kWh to $kgCO_2$ reduction. In this case, the research considered the value 0.49 kg/kWh defined by [47]. *CDRPE* showed the same trend of *ERP* and *CDRBL* decreased from 4.38 to 0.24 $kgCO_2$ emissions for each cubic meter of water saved by leakages.

4.5. Conclusions

The present research represents a new step forward in improving the sustainability of irrigation systems. The new optimized procedure was developed in which three novelties were introduced. A double simulated annealing procedure was introduced to determine the location of the recovery system, considering three different objective functions and the selection of the best machine, as well as the best regulation strategy. The regulation strategy considered the operation of the machines in different work modes between them, the recovery systems can operate under *BEH, BPF* and *BPH* using the modified affinity laws. The methodology uses a

database in which there are 7826 *PATs* which were defined using the dimensionless numbers generated by 110 tested machines.

The second novelty shown in this research is the need to consider, evaluate and estimate the leaks in the network to carry out a correct selection of the machines in the different recovery systems. Leaks can cause significant variations of the best efficiency point to choose the machine, mainly in terms of flow. The particular case study in which the methodology was applied showed a variation around 200% in terms of flow and head related to the best efficiency point of the machine. These values show the significance of the leakages consideration in the new future energy balances. There are no published studies that consider the variation of the operating points of the machines. Besides, tool is presented that combines all aspects of analysis within the water distribution systems that affect the efficiency of the system, developing a novel methodology applicable to any type of network.

As a third novelty, the research allows the characterization of the sustainability indicators in the selection of the machines and therefore, includes the analysis of the sustainability indicators in each iteration. Besides, the methodology operates with different scenarios in which different leakages values could be considered as a function of the serial data and future scenarios. The methodology enables the fit of the calibrated leakages model. The applicability enables the use of this tool by water managers, improving the efficiency of the water systems. The leakages management as well as the use of renewable energies system will open new research trends, which are focused on reach new targets of the sustainable development goals inside of the water systems.

Finally, the proposal was applied to a real irrigation system. The calibration model was developed considering serial data of twenty years in which five different scenarios were developed defining different leakages levels in one of them. The application of the methodology shows the great influence of the leakages reduction when the recovery systems were installed in the water networks. The annual recoverable energy values above 32000 *kWh* and annual leakages decrease above 18000 m^3 in the best configurations, using three recovery systems, which are configurated with three *PAT* each one. The *IRLGP* index was defined as the ratio between reduction of the leakage volume for each installed power and it reached the annual value of 11280.8 m^3/kW and *CDRBL* decreased from 4.38 to 0.24 $kgCO_2$ emissions for each cubic meter of water saved by leakages. Future works should be focused on apply the measurement of sustainable indicators to the different supply

systems and develop new optimization procedures, which support to the sustainable management of the hydraulic systems.

Funding

Credit authorship contribution statement

Modesto Pérez-Sánchez, Francisco-Javier Sánchez-Romero: Conceptualization, Methodology, Software. Carlos Andrés Macías Ávila, Modesto Pérez-Sánchez, Francisco-Javier Sánchez-Romero: Validation, Formal analysis. P. Amparo López-Jiménez, Modesto Pérez-Sánchez, Carlos Andrés Macías Ávila: Writing – original draft preparation, Writing – review & editing. P. Amparo López-Jiménez: Supervision. Modesto Pérez-Sánchez, P. Amparo López-Jiménez: Final review. All authors have read and agreed to the published version of the manuscript.

5. Artículo 4

"Improve leakage management to reach sustainable water supply networks through by green energy systems"

5.1. Description

Coautores: Carlos Andrés Macías Ávila; Francisco-Javier Sánchez-Romero; P. Amparo López-Jiménez; Modesto Pérez-Sánchez.

Revista: Sustainable Cities and Society ISSN 2210-6707.

Factor de Impacto: 7.587. (JCR Q1; Posición 2/68 Construction and Buildings Tecnology; 16/119 Energy and Fuels).

Estado: Publicado [Elsevier 2022, 3, 15; doi: 10.1016/j.scs.2022.103994].

Abstract

The cities and townships should increase their sustainability to achieve the different targets, which are included in the sustainable development goals. The water distribution networks are present in urban areas. It implies the improvement of their management is key to reaching this sustainability. The water managers use different strategies to reach sustainable values in their facilities, searching for the reduction of the leakage volume. The proposed research develops a new methodology, which enables the self-calibration of leaks in water supply, knowing the injected flow and the consumed volume in the water networks. Besides, the proposed tool enabled the incorporation of the recovery systems to improve the energy efficiency of the network, increasing the use of renewable energies and reducing the leakages volume. These improvements affect positively the hydraulic efficiency of the system, and therefore, it improves the use of the water resources of the cities and reduces the cost for the citizens. The methodology was applied to a real case study located in Manta (Ecuador). The proposed procedure, which is optimized by two simulated annealing procedures inserted in an iterative procedure enables the decreased volume of the leakages above 120000 m^3 and increased the annual generated renewable energy by 34490 kWh, decreasing the emission of 969 tCO_2 each year.

Keywords: leakages; sustainable water supply system; green water management.

5.2. Introduction

Sustainability is key in the development of the improvement of the cities management, guaranteeing the supply and reducing the non-renewable resources [205]. The use of new technologies to reduce the leakages volume is crucial since this lost volume is considerably high around the world. Its control is essential to meet the increasing water demand caused by rapid population growth and urbanization [206] towards smart water management cities [207]. Currently, water leaks in water networks are a worldwide problem. Water losses vary between 8 and 24 % in developed countries. These values oscillate between 15 and 24% in recently industrialized countries and they are between 25 and 45 % in developed ones [4]. In the United States and the United Kingdom, the leakages range is between 10 % and 30 % [208]. As another example, the lost volume by leakages is 37 % in South Africa

[209], estimating the cost/value of water lost amounts to USD 39 billion per year [210].

The leakages estimations could be developed by different methods applied in water distribution networks by operation strategies for their detection [211]. One of them is Torricelli's theorem [100], which is dependent on pressure, orifice area and a discharge coefficient. Another commonly used method to determine leaked volume is *FAVAD* (Fixed and Variable Area Discharges) equation, this indicates that the cross-sectional area of some types of leaks (holes, breaks in tubes, joints or fittings) can also vary with pressure, while the flow velocity continues to vary with the square root of pressure [79]. This method was applied to a real case in a water distribution network in Kwadabeka, South Africa [98]. Another strategy was based on the *FAVAD* concept. It is the N1 Power Law [55]. It increased its use since 1994 for practical assessment of pressure-dependent leakage in water distribution systems. Explains a study on the relationship between pressure and leakage, and guides equations for data analysis and prediction in individual situations [57]. This method contains in its equation a leak coefficient C and the leak exponent N1 that has been evaluated in different investigations and can vary from 0.5 to 2.3 depending on the material and type of failure [80].

The estimation of the leakage is not enough and the modelling is necessary to carry out the different simulations in the water distribution system. In this line, two different modellings were used by different authors. The minimum night flow was proposed by [212]. This method is the most popular for estimating real leaks, under the assumption that during the last hours of the night and the first hours of the morning consumption is minimal and pressure is high. [49] established a minimum night flow analysis, which was carried out on a district metered area (*DMA*) in an intermittent supply system in Zarqa, Jordan.

The other modelling concept was proposed by [84] that showed the equations of the *BABE* (Burst and background estimates) method. This method enables the determination of the background losses and leaks, considering that the leaks occur along the pipe. Whatever method is used, most of the leaks can be avoided. However, there was an unavoidable part, even in new or well-managed water distribution networks [213]. In water distribution networks, leakage types have evolved into three categories namely reported, unreported, and background leakage. Reported and unreported leakage are defined as burst or mains leakages and are caused by structural pipe failure [214]. In this line, the researchers tried to reduce the leakages volume by management of the water distribution networks

using pressure reduction valves [215]. For example, the reduction from 39 to 31 m w.c. the daily water loss was reduced by 20.52 %, respectively, and the average critical point pressure is reduced by 21.13 % [216].

The leakages reduction can develop using pressure reduction valves, which cause a positive impact on the hydraulic efficiency of the system but the behaviour is negative when the energy efficiency is evaluated [217]. [218] investigated the possibility to use green valve systems as a new smart and self-powered control device. This study was an ahead step to improving sustainability. It was aligned with other different studies that considered the use of pumps working as a turbine (*PATs*) in the water distribution network, replacing pressure reduction valves to reduce the reliance on non-renewable energy. In Kozani (Greece) [121], the implementation of *PATs* enabled the reduction of leaks in values between 20 and 40 %. The location and selection of *PATs* were proposed by [26], replacing the pressure reduction valves. The optimization was based on maximizing recovered energy. The volumetric efficiency increased from 0.7 to 0.9 and the annual recovered energy could be 169360 kWh. PSO algorithm was proposed to select the different *PATs* when the location is defined [15] reaching daily values of recovered energy equal to 182 kWh.

A methodology was proposed to define scenarios and configurations for the improvement of hydraulic efficiency in water distribution systems. It was programmed on MATLAB Simulink [142]. [24] focused on the optimal location of *PATs* to produce energy and reduce the leakages in water distribution networks. [146] developed the optimal configuration of a chosen number of *PATs*, taking into account energy costs and volumes of water saved. [147] achieved a daily energy recovery of 1958 kWh, reducing almost half of the average excess pressure using an MINLP model. [11] proposed an adaptive management framework for water distribution systems by reconfiguring the original network layout into dynamic district metered areas, improving the efficiency of the systems and showing an annual recovered energy potential of 19 MWh and leakage reduction of up to 16%.

In this sustainable line, different layouts for the installation of pumps used as turbines were analyzed and compared to a couple of pressure reduction and hydropower generation in water distribution networks, showing the environmental and technical implications [219], as well as social implications in which some authors developed a proposed mathematical algorithm [220]. It included a simulation model and optimization model based on different decision variables such as operational cost, customer satisfaction and reliability. The use of these new technologies

enables the improvement of the leakage key performance indicators. It enables the evaluation of the theoretical state of the supply network through a series of criteria. [120]. The *IWA* provides a series of indicators of water supply systems such as real water losses, water losses from household connections and the rate of leaks [5]. [29] enumerated these sustainable indicators into three different groups: energy, economic and environmental indexes.

Although different studies analyzed the improvement of the water management by *PATs*, this research proposes a new methodology. It is based on programming on Epanet Toolkit and the proposal enables the automatic calibration of the supply system when the consumed volume by users and the injected flow in the system are known. The methodology includes the development of the calibrated model, which is implemented by the methodology. It incorporates two simulated annealing procedures, which operate inserted in an iterative process working with discretized flows over time.

This procedure allows water managers to locate the best position, choose the best machine and define the best strategy of the regulation based on different objective functions considering the leakages in the operation of the recovery system as well as its influence on the selection of the machines. As a novelty, the proposed research not only makes the model self-calibrate, but it is also able to discretize the leakage volume in the different types. The method can be applied to meshed networks considering hourly values along year.

5.2.1. Methodology

The proposed optimization methodology is divided into four phases. Each one is operated by different steps, inputs and conditions that the model requires to be executed are observed. As a novelty, the proposed methodology includes a self-calibration of the model to define the fit pattern consumption as well as the leakages distribution. Besides, the programming algorithm includes the operation in a meshed network.

5.2.1.1. Optimization stages

Figure 19 shows the steps to carry out the optimization process, these are Network model (A), Leakages calibration (B), Energy Balance (C), and Recovery Analysis (D).
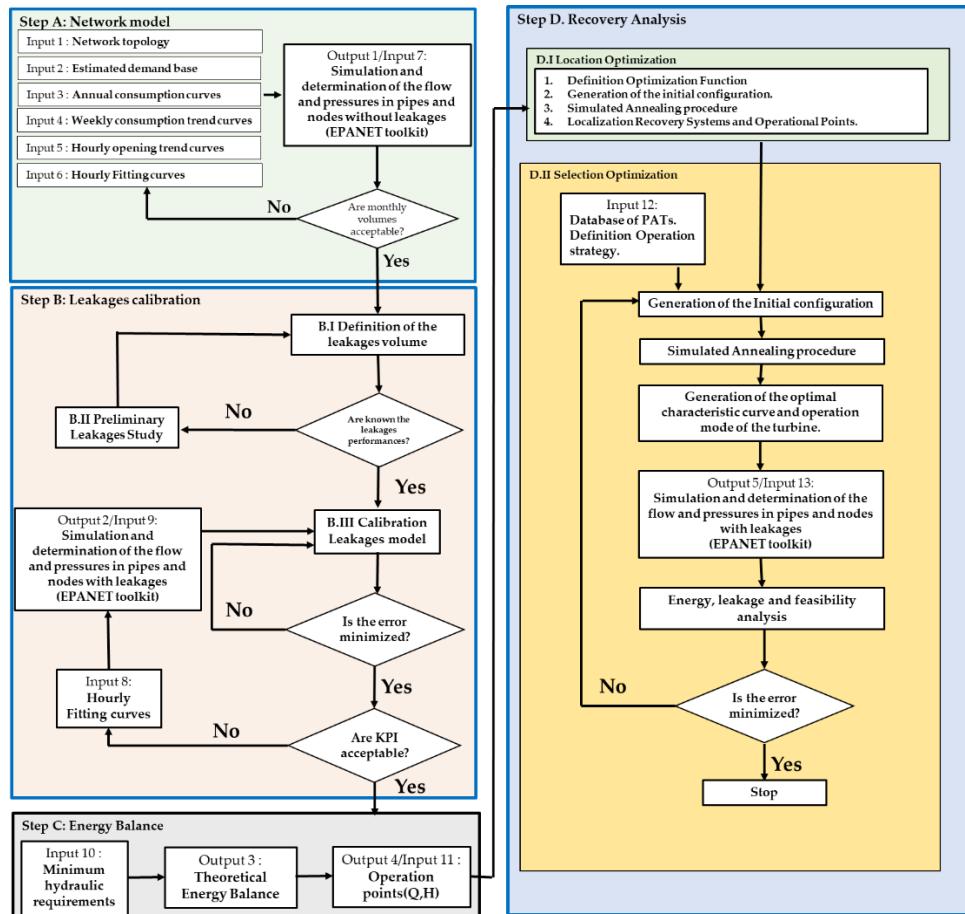
Figure 19. Proposal of the optimization procedure

A.- Network model

The network model will be simulated using EPANET. The model requires six different inputs, which are: (i) Network topology (Input 1), which was obtained by the company management according to joints and pipes; (ii) Estimated demand base (Input 2). This demand was defined by the daily average flow considering the month of the maximum consumption; (iii) Annual consumption curves (Input 3) define the consumption curves, which are related to the weekly consumption trend curves (Input 4).

Input parameters are modified to define the network model. Input 2 estimated the demand base guarantying positive pressure in the system and there are no hydraulic scenarios, which were incoherent. Input 5 (hourly opening trend curves) and Input 6 (hourly fitting curves) were defined using the different registered volumes and flowmeters. Input 5 considers uniform average leakage flow and seeks similarity to demand-only flow estimation. Input 6 develops iterations, which adjust the fitted coefficients to the hourly fitting values. Once the model is defined, it is verified if the monthly volumes are acceptable, and it will be ready to be calibrated in the next Block B. The proposal of the model estimated the roughness according to the material and lifetime of the pipes since the case study does not install pressure sensors in the water system. The proposed methodology could incorporate a preview calibration in Step A when these data are available and it will develop an iterative procedure to minimize the error between simulated and measured pressure similar to the procedure developed in leakages calibration.

B.- Leakages calibration

The second step proposed for the calibration strategy considers the water leaks in the system. It is defined by considering information from the network such as the injected flow rate and consumption to establish a volume balance through the continuity equation (Step B.I). Once the leaked volume is known, the estimation of the volumetric efficiency is possible, using the following equations:

$$\eta_L = \frac{V_L}{V_I} \tag{60}$$

$$\eta_M = \frac{V_M}{V_I} \tag{61}$$

where η_L is the leakage performance of the water system and η_M is the measured volume performance of the water system; V_I is the injected volume in the network in m³; V_M is the total measured volume by water meters in the consumption nodes in m³; and V_L is the total leakage volume in the water system in m³.

If there is a lack of information to know the volume of the leak, the methodology proposes a preliminary leak analysis (Step B.II). If the leakage and volumetric ratio are known, the proposal methodology goes to Step B.III. It developed the calibration model, which distributes the leaks in different ratios.

These ratios are established according to apparent and real losses [221]. Apparent leakages are considered in the consumption joins while the real losses are defined in

the pipes. Some inherent losses, such as cleaning discharges, and hydrants, are considered apparent losses according to [221]. The discretization of these leakages enables the definition of the following ratios:

$$\eta_{AL} = \frac{V_{AL}}{V_L} \tag{62}$$

$$\eta_{RL} = \frac{V_{RL}}{V_L} \tag{63}$$

where η_{AL} is the ratio between apparent and total leakages; V_{AL} is the total volume of the apparent losses in m³; η_{RL} is the ratio between real leakages and total leakages; V_{RL} is the total volume of the real losses in m³. The apparent losses are the uncontrolled leakages in the water systems, which cannot be measured [221].

Step B.II develops a series of simulations to obtain ranges of values and to define the different scenarios correctly. As the leak volume is unknown, the methodology assigned different leak parameters in the lines. The knowledge of these ratios enables the distribution of leakages in the model. It defines the different emitter coefficients in the different iterations. To establish the criteria as a function of the leakage type, the error is analysed between simulated and measured volume. The evaluation of the leakage in lines is developed by the following expression:

$$q_{L,ij} = \beta_j \, L_j (\bar{P}_{ij})^N \tag{64}$$

where $q_{L,ij}$ is the leakage flow for the line at the time i; where β_j is the leakage coefficient, which characterizes the pipe in terms of age, diameter, material, thickness, among others. In Step B.II, the model does not need to iterate since the used emitter coefficient in EPANET is:

$$K_j = \beta_j \, L_j \tag{65}$$

$\bar{P}_{ij}$ is the average pressure in the line j at the time i; L_j is the length of the line j in meters; N is the leakage exponent; and K_j is the global emitter coefficient used.

N and β variables are two leakage model parameters that represent the influence of some factors on the relationship between leakage and pressure. Parameter β represents the pipe deterioration over time, thus it depends on both pipe characteristics and various external factors like mainly the average pressure, but there are also others such as environmental conditions or corrosion. In contrast, N is a function of pipe characteristics only [50][51]. The value of β can be varied between

10^{-4} and 10^{-5} and N oscillates between 0.5 and 1.5. The model calibration enables the estimation of the ratio between real leaks and total leaks and N exponent [29].

Step B.III develops the calibration leakages model. The calibration model distributes the leakages once the perfomances (i.e., η_{AL}, η_{RL}, and η_L) are known. The model considers the following equation to evaluate the leakage in each element (i.e., line or tap):

$$q_{L,ij} = K_j(P_{ij})^N \tag{66}$$

where $q_{L,ij}$ is the leakage flow for the element j (i.e., line or consumption point) at the time i; P_{ij} is the pressure in the element j at the time i (if the element is a line, the chosen pressure is the average pressure value of the line - $P_{ij} = \bar{P}_{ij}$-); N is the leakage exponent; and K_j is the global emitter coefficient. In this step the model determines the value of the global emitter coefficients assigned to lines and consumption points in different iterations, minimizing the error between simulated leakage volume and leakage volume of the water system.

The leakage volume is defined using the following expression:

$$V_{L,j} = \sum_{i=1}^{i=T}(q_{L,ij}\Delta t) = \sum_{i=1}^{i=T}(K_j(P_{ij})^N\Delta t) \tag{67}$$

where Δt is the interval time in s, $V_{L,j}$ is the leakage volume for the element in m^3, assuming the K_j is constant in all annual simulations. It is defined by the following expression through an iterative procedure:

$$K_j = \frac{V_{L,j}}{\sum_{i=1}^{i=T}((P_{ij})^N \cdot \Delta t)} \tag{68}$$

The model calibrates the system by estimating K_j. It considers all elements of the water systems have leakages, therefore, the total leakage volume is distributed in the system. The leakage volume of each element ($V_{L,j}$) can be determined by the following expression:

$$V_{L,j} = \delta_j V_L = \delta_j \eta_L V_I \tag{69}$$

where δ_j is the distributed coefficient assigned to each element of the network. The addition of all distributed coefficients is equal to 1. δ_j is estimated by equation 70 when it is applied to lines and equation 71 when it is used in tap :

$$\delta_j = \frac{L_j}{\Sigma_{j=1}^{j=k}(L_j)} \tag{70}$$

$$\delta_j = \frac{V_{T,j}}{\Sigma_{j=1}^{j=m}(V_{T,j})} \tag{71}$$

where L_j is the length of the line j in m; k is the number of lines of the model. It depends on the material of the line.; k is the number of pipes; $V_{T,j}$ is the total consumed volume of the consumption points (j), including both measured (invoiced) for consumption as well as the leakage volume (no invoiced); m is the number of consumption points of the model.

Once the error is minimized, it should be verified if the *KPI* values are acceptable. If they are not acceptable, the hourly fitting curves (Input 8) should be used and the simulation and determination of the flow and pressures in pipes should be carried out again. The new fitting coefficient applied to all consumption nodes is defined by the following equation:

$$k_i = k_{i,0} \frac{Q_{i,observed} - Q_{i,leakage}}{Q_{i,simulated} - Q_{i,leakage}} \qquad K_j = \frac{V_{L,j}}{\Sigma_{i=1}^{i=T}((P_{ij})^N \cdot \Delta t)} \tag{72}$$

where k_i is the new fitting parameter at time i, $k_{i,0}$ is the ratio between $Q_{i,consumed,0}$ and $Q_{i,simulated,0}$. It is used as a fitting coefficient in all consumption nodes; $Q_{i,consumed,0}$ is the estimated flow, which is consumed at the time i and it is defined by the difference between observed flow ($Q_{i,observed}$) and average leakages flow ($\overline{Q_{leakage,0}}$); $Q_{i,simulated,0}$ is the simulated flow when the leakages are not considered in the simulated model.

This calibration is developed using the EPANET toolkit [58] to calibrate the leakage model (Step B.III). When the key performance indicators (*KPIs*) show acceptable values, the leak calibration ends, and the model is ready for energy balance. The used *KPIs* were bias percentage (*PBIAS*), Mean Relative Deviation (*MRD*), Root Mean Square Error (*RMSE*) and Mean Absolute Deviation (*MAD*).

1. *PBIAS* measures the tendency of the simulated values and establishes if the obtained values in the model are smaller or larger than the registered values. If *PBIAS* is less than zero, the proposed model overestimates the

considered variable; if it shows positive values, it indicates the variable is underestimated, and finally, if the *PBIAS* value is zero, it indicates the model is optimal. *PBIAS* is defined by the following expression:

$$PBIAS(\%) = \frac{\sum_{i=1}^{N}(O_i - P_i)}{\sum_{i=1}^{N} O_i} \cdot 100 \tag{73}$$

where O_i are the registered values; P_i the experimental values and N the number of observations.

When *PBIAS* is lower than +/-10 % the fitness is considered very good. If the *PBIAS* values are between +/-10 and +/-15 %, the fitness is good. When the *PBIAS* value is between +/-15 % and +/-25 % the fitness is satisfactory and if it is higher than +/-25 % it is considered unsatisfactory [222].

2. *MRD* considers the weight of the error to the variable value. If *MRD* is zero, this value indicates a perfect fit. It is defined by the following expression:

$$MRD = \sum_{i=1}^{N} \frac{|O_i - P_i|/P_i}{N} \tag{74}$$

3. *RMSE* is the index, which measures the error between the simulated values and recorded values. When RMSE is zero, this value indicates a perfect fit. It is defined by the following expression:

$$RMSE = \sqrt{\frac{\sum_{i=1}^{N}[O_i - P_i]^2}{N}} \tag{75}$$

4. *MAD* shows the absolute differences between simulated and recorded values. The perfect fit is defined when *MAD* is zero, and it is defined by the following expression:

$$MAD = \sum_{i=1}^{N} \frac{|O_i - P_i|}{N} \tag{76}$$

C.- Energy Balance

Energy balance is crucial to estimate the distribution of the supplied energy in the different energy terms (i.e., required energy, losses, among others) [223]. When the energy balance is developed, the discretization of the different energy terms related to the pressure excess is possible. In this step the water managers can difference the terms for the available energy between the theoretically recoverable energy and the

theoretically non-recoverable energy, considering the pressure and the minimum consumption at each point of consumption (Input 10) [224].

The energy balance will allow us to estimate the recovered height of each flow over time, this would be the data pair (*Q, H*), managing to select the most appropriate machine at each study point (Input 11). Table 24 summarizes the different expressions to consider the energy balance.

Table 24. Equations to define the annual energy balance in kWh

Type	Equation	ID
Total Energy (E_{T_j})	$\gamma Q_j(z_o - z_i)$	(18)
Friction Energy (E_{FR_j})	$\gamma Q_j(z_o - (z_j + P_j))$	(19)
Theoretical Energy Necessary (E_{TN_j})	$\gamma Q_j P_{minj}$	(20)
Energy Required (E_{RS_j})	$\gamma Q_j P_{minSj}$	(21)
Theoretical Available Energy (E_{TA_j})	$\gamma Q_j(P_j - P_{minj})$	(22)
Theorical Recoverable Energy (E_{TR_j})	$\gamma Q_j(P_j - \max(P_{minj}; P_{minSj}))$	(23)
Theorical Recoverable Energy ($E_{TR_{mj}}$)	$\gamma Q_j \eta_i H_i$	(24)

(E_{T_j}) It is the total potential energy supplied to the system when it is not being consumed from the network.; (E_{FR_j}) energy that is dissipated in the network from the point of departure to the point of consumption; (E_{TN_j}) minimum energy required in the system to ensure that the minimum pressure established at the most unfavourable point of the network is met; (E_{RS_j}) it is the energy, for a time interval, necessary for the minimum pressure restriction to be fulfilled at a point; (E_{TA_j}) for a time interval, it is the energy that is theoretically available to be recovered in a line; (E_{TR_j}) is the maximum amount of theoretically recoverable energy at a point of consumption; ($E_{TR_{mj}}$) energy that cannot be recovered in the network; Z_i is the geometric height above the reference plane of the point of consumption; Z_o is the geometric height above the reference plane of the free surface of the water in the tank that supplies the system in m; γ is the specific weight of the fluid in kN/m^3; Q_j is the circulating flow; P_j is the pressure at a point; P_{min} is the minimum pressure that can exist at the point of consumption; H_i is the head level of the reservoir in m w.c.; η_i the efficiency of the recovery system for this flow Q_j [125].

D.- Recovery Analysis

The final block is defined by the recovery analysis. The objective of this phase is to determine the optimal location of the energy recovery points and the optimal definition of regulation strategies from a *PATs* database. In this section, a double annealing simulation procedure is carried out. The energy recovery analysis has two phases, called D.I Location Optimization and D.II Selection Optimization.

The location optimization process begins with the definition of the optimization functions, these objective functions are defined under (i) energy, (ii) hydraulic and (iii) economic criteria. These objective functions were the maximization of the theoretical recoverable energy ($OF1 = E_{TR}$), the reduction of leaks in the distribution network ($OF2 = \Delta V_L$); and the Levelized Cost of Energy ($OF3 = LCOE$). This function only takes into account expenses (initial investment and annual costs) and it does not depend on energy prices.

$$OF3 = \frac{IC_0^T + \sum_{i=1}^{i=T} \dfrac{AC_i^T}{(1+k)^i}}{\sum_{i=1}^{i=t} \dfrac{E_i^T}{(1+k)^i}} \tag{77}$$

where IC_0^T is the initial investment in € in the year 0, considering the electric line to reach the supply points; AC_i^T is the operation and maintenance costs in € for the year i; E_i^T is the annual recovered energy in kWh for the year i; T is the lifecycle in years, considering 25 years; k is the discount rate using a sensitivity analysis between 0.01 and 0.1.

The research presented in [225] proposed a methodology for maximizing energy recovery, assigning *PATs* in water networks through simulated annealing techniques for different objective functions and some machines. This heuristic search algorithm is based on the analogy with the physical process of annealing metals. The algorithm searches for the best locations for the recovery systems based on the defined objective functions as well as the number of recovery systems established. *PATs* were simulated on EPANET as a general-purpose valve in which the *BEH, BPH* or operational curve was defined in each iteration by EPANET Toolkit. The analyzis was develoed considering an simulation, which a demand dependent analysis [58], therefore the demand is not dependent on the pressure but the leakages is influenced by pressure values.

The procedure requires defining the number of iterations and assigning control parameters to characterize the simulated annealing process. These parameters are

the initial temperature (T_i); the final temperature (T_f); the cooling rate (α_c); and the number of transitions (L_0) in each temperature step. These parameters are fixed according to a sensitivity analysis previously performed and they are changed depending on the objective maximized function [29]. Once the control parameters have been defined, the maximum number of recovery systems (N) is determined. The procedure must consider the generation of the initial configuration. The methodology considers two recovery systems (m) in the first two elements of the list initially. A new combination between different elements for each value of the recovery system (m) is developed by the annealing procedure. Subsequently, the optimization process establishes the best location and operating points for this value m. Finally, the result of this stage is to know the optimal configuration of the recovery system to start the last stage of this methodology, the selection optimization.

When step D.I is run and the location is chosen, the second phase (D.II) starts developing an optimized selection of the hydraulic machine. It consists of searching for the selection of the number of machines to be installed and the best regulation strategy according to the defined variables. These are defined based on the specific speed (η_{st}), head and discharge number. These values enable the calculation of dimensionless parameters. To select the machine, the best efficiency point (BEP) from the database of 110 *PATs* is used. The definition of the operational curves is established according to the proposed methodology by [154]. The knowledge of the characteristic curves implies the possibility to define the best regulation strategy considering the rotational variation speed and therefore, the methodology optimizes the key operation according to best efficiency head (BEH), best power head (BPH), Nominal Rotation (NR) or best power flow (BPF) according to the proposed method by [20].

The success of the methodology requires an additional internal annealing simulation procedure, since the optimization process evaluates many combinations, such as (i) the possibility of using a different number of machines that could be installed in series or parallel; (ii) regulation strategies; (iii) and different numbers of possible recovery systems to be installed on the network. As a novelty, the methodology was modified to work in a meshed network. It involved the development of an internal iterative procedure to define the best machine and its regulation, once the located line was established. This iterative procedure is delimited as a function of the error value between iterations, considering both leakage reduction and recovered energy.

5.3. Materials and Methods

5.3.1. Case Study. Manta (Ecuador) water distribution system

The proposed methodology was applied to the case study of the city of Manta, Ecuador. The model of the water supply network is shown in Figure 20a. The drinking water network that supplies 110 neighbourhoods in the city of Manta, provides the flow from a reservoir, which its level is 65 m. There is a flowmeter and it is installed in the main pipe and its main function is the measure the flow supplied to the system. Figure 20b shows the red dots, which represent different consumption nodes. The topology of the network, the height and consumption of the different junctions, the consumption patterns, the recorded values of the flowmeter and the recording of the meters, which are recorded each month. All data are referred to as 2021. The model was developed using EPANET software, using 832 nodes, 875 lines and 1707 virtual leakages nodes. It was established an hourly consumption pattern to develop an hourly energy analysis and water volume evaluation in terms of leakages.
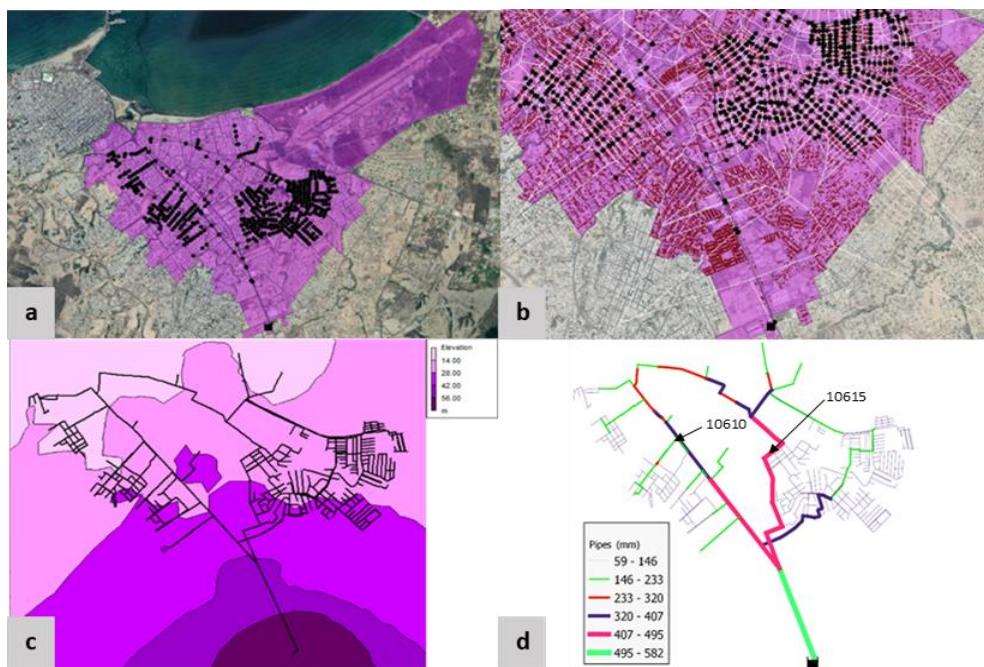
Figure 20. Characteristics of the hydraulic network of Manta. (a) Hydraulic network; (b) Network junctions and users; (c) Height difference in the network; (d) Pipe diameters and locations of two recovery systems

Figure 20c shows the orography of the study area using a contour map of the heights of the network. The highest point is in the reservoir, while the lowest is in the branches of the network. The material of the pipes is polyvinyl chloride (PVC). The pipe diameters of the network are shown in Figure 20d. These diameters vary from 581mm in the main branches to 59 mm in the secondary ones. Table 25 shows the main data of the case study as well as the characteristics of the hydraulic network.

Table 25. Network study data

Network data and study area	Value
Area coverage	1991 ha
Population served (estimated)	100000
Number of metered properties	23885
Total pipe length	65 km
Average daily pressure (2021), estimated by [226]	35.14 m
Nonrevenue water (January and February)	43 %
Junctions	832
Pipes	875
Maximum level difference	59 m
Diameter range	59 – 581mm
Pipe materials	PVC

The network is supplied through a tank, this contains a flow meter in its discharge with flow data every fifteen minutes. This study used recorded values for January and February 2021. Both months showed a similar flow trend since the climatic conditions are similar over time and the city is not touristic, being constant the number of citizens. The maximum registered flow supplied to the network was 543 l/s, the minimum flow was 92 l/s and the average flow was 231 l/s when January was analyzed. When February is analyzed, the maximum flow was 632 l/s, the minimum flow was 91 l/s and the average flow was 246 l/s.

Figure 21 shows the consumption data provided by the management company for the year 2021. The average daily consumption for each of the months of the year varies from 10011 to 12005 m^3. The consumed volume is the highest in January and it is the lowest in November.

Figure 21a shows the daily variation of the water pattern consumption. The highest value was located between 5 and 7 am. Besides, there was a peak between 8 and 10 pm. The lowest value was located between 12 am and 3 am. The monthly recorded

volume in the network varied between 303782 and 372168 m³ (Figure 21b). If the injected volume in the network is analyzed, this annual volume was 6925926 m³, and the recorded volume was 3947778 m³. In this case, the leak percentage was equal to 43 % and the average leakage flow was 92.61 l/s.
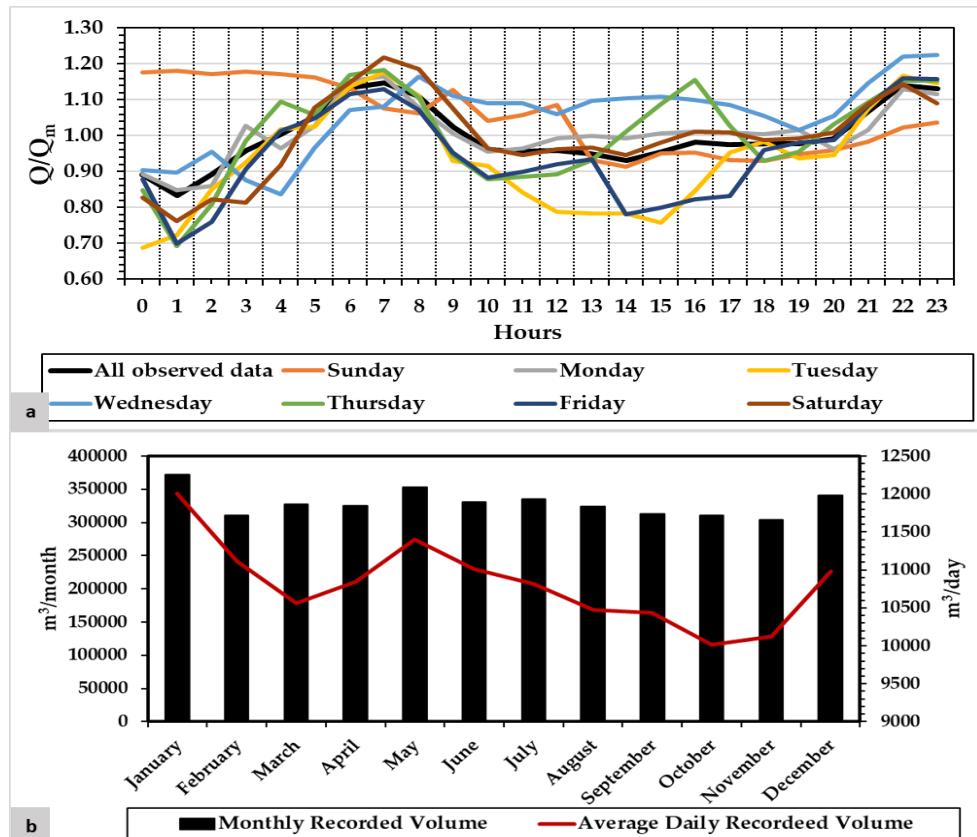

Figure 21. (a) Daily consumption pattern (Qm is the average flow) (m³); (b) Data of the recorded volume of the network in the year 2021

5.4. Results

The analysis to discretize leakages between apparent and real losses was developed as a first step, once the model was established. The discretization of the leaks was necessary to calibrate the model. Knowing the registered volume by counters and the registered volume by the installed flowmeter in the mainline, seven hypotheses were developed in the sensitivity analysis establishing differences between real and apparent losses. Each hypothesis is defined in Figures from 22a to 22d.

It is identified by Hx (y;z) in which "x" is the number of the hypothesis, "y" is the weight of the apparent losses and "z" is the weight of the real losses. This analysis was considered for the different error indexes defined in the methodology. Previously in Step B.II, a first calibration of the α coefficient was established considering the leakages (43 %). This value was 0.65 since all values of β coefficient, which oscillate between 10^{-5} and 10^{-4} are lower than the limit of leaks percentage.
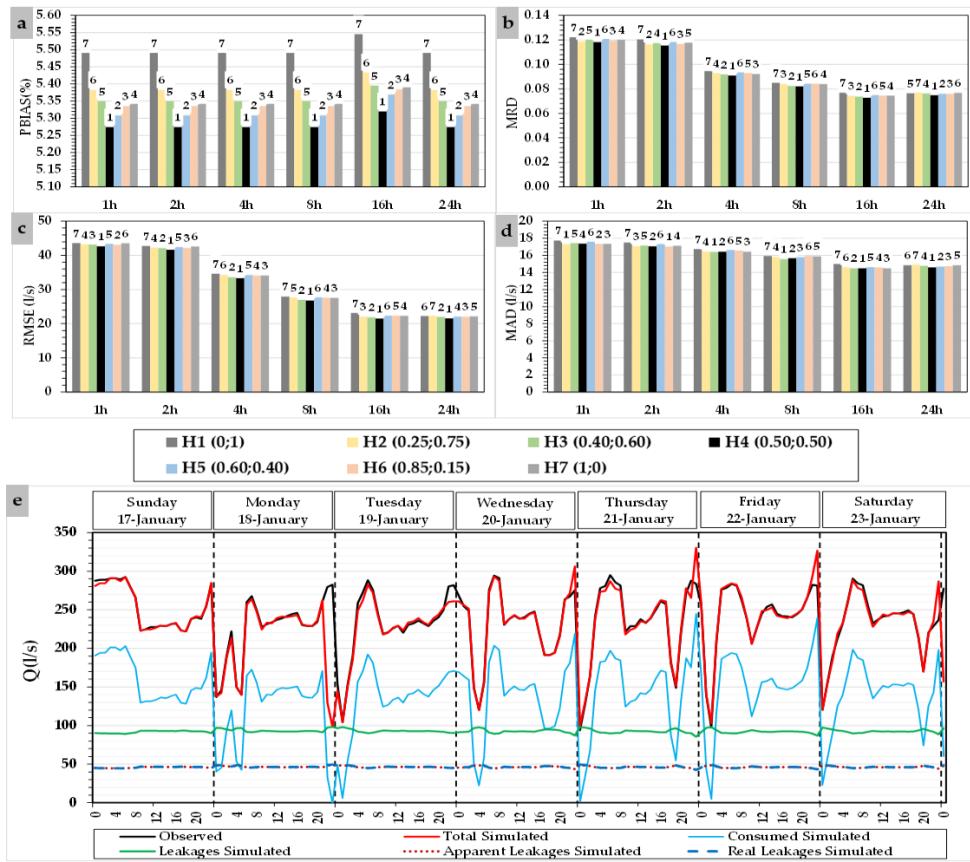
Figure 22. (a) Calibration leakages considering *PBIAS* value; (b) Calibration leakages considering *MRD* values; (c) Calibration leakages considering *RMSE*; (d) Calibration leakages considering *MAD*; (e) Comparison between observed flow and simulated values when the model was calibrated. Example of one week.

Figure 22a shows the results when *PBIAS* was analysed for the different seven hypotheses, considering six different time intervals. The *PBIAS* value was between 5.274 and 5.554 for the different 42 scenarios. All cases showed excellent fit

according to [222]. To simulate the definitive model, H4 was chosen since it showed the lowest *PBIAS* value. H4 also showed the best values for the rest of *KPIs*. Finally, an hourly interval was chosen to develop the simulation. *RMSE, MAD* and *MRD* were also established for the different scenarios. If the hourly interval is analysed, *RMSE* was 42.6 (Figure 22c), *MAD* was 17.36 (Figure 22d) and the *MRD* was 0.118 (Figure 22b). This calibrated model showed the following error between simulated and registered volume (Table 26). The error was defined by the following expression:

$$\varepsilon_V = \frac{(V_{simulated} - V_{registered})}{V_{registered}} \cdot 100 \qquad (78)$$

Table 26. The error between registered and simulated volume, considering H4 in the mainline of the water system

Month	Registered Volume (m³)	Simulated Volume (m³)	Error (%)
January	372168	369734.02	-0.65%
February	311329	309521.17	-0.58%
March	327354	324714.44	-0.81%
April	325230	321086.32	-1.27%
May	353607	352251.86	-0.38%
June	330395	329607.30	-0.24%
July	335415	333407.18	-0.60%
Agost	324746	323471.30	-0.39%
September	312938	311696.57	-0.40%
Octuber	310334	309808.83	-0.17%
November	303782	300630.52	-1.04%
December	340479.5	340115.43	-0.11%
Annual	3947777.5	3926044.94	-0.55%

Figure 22e shows the example of the visual trend between registered and simulated flow in the calibrated model, which used H4 to establish the apparent and real losses and was used to develop the energy balance and the optimization procedure. Table 26 shows the monthly error between the registered and simulated volume. These errors were below 1.5% in all months, considering an average annual error equal to 0.55%. A double calibration is performed. The first calibration takes place in Step A and consists of comparing the monthly and annual volumes observed in the user meters with a hydraulic model that only takes into account the demand (without leaks). The second calibration is performed in Step B. It consists of

comparing the observed values of the main flowmeter for January and February with the hydraulic model that takes into account leakage. For each calibration, the different inputs are modified minimizing the errors and finally determining the hypothesis of weight distribution for real and apparent leakage that minimizes the values for the *KPIs*.

The first optimization procedure established the best lines to install recovery systems as a function of the objective function. The optimization worked using minimum pressure, which must be guaranteed in any scenario.

Table 27 shows the chosen lines according to the three different objective functions. This first optimization procedure enabled the definition of the best location, the energy and leakages volume are further compared with the final values when the machines will be selected. When the case study was analysed using the OF1, the theoretical annual recovered energy oscillated between 47507 and 104123 kWh depending on the used recovery systems (Figure 23a).

The leak reduction varied from 206792 to 379652 m³ (Figure 23b) and *LCOE* value from 0.186 to 0.264 €/kWh (Figure 23c). In all cases, the incorporation of the new lines to install the recovery system influenced the variation of the variable by around 30 % when the second recovery system was added. A similar trend showed the incorporation of the fifth unit, which increased or reduced the variable by around 10%. When OF2 and OF3 were analysed in this D.I step, the results were similar but the lines were different.

Table 27. Preliminary results when D.I step is defined to locate the best line. (Continue in next page)

O F	Line 1	Line 2	Line 3	Line 4	Line 5	E (kWh)	Leakages Reduction (m³)	LCOE (€/kWh)	P (kW)
1	10615					47507	206792	0.186	8.18
1	10615	10610				66163	282333	0.216	12.15
1	10026	10222	10610			83355	313553	0.206	14.88
1	10026	10610	10615	10618		94069	350492	0.244	19.58
1	10026	10208	10222	10610	10618	104123	379652	0.264	24.42
2	10620					46250	210204	0.190	8.05
2	10620	10591				62789	289398	0.228	12.19
2	10227	10591	10615			70839	339118	0.307	16.94

Table 27. (Cont.) Preliminary results when D.I step is defined to locate the best line

O F	Line 1	Line 2	Line 3	Line 4	Line 5	E (kWh)	Leakages Reduction (m³)	*LCOE* (€/kWh)	P (kW)
2	10013	10266	10591	10620		86843	375039	0.262	20.14
2	10013	10266	10591	10620	10663	96533	409669	0.294	24.62
3	10942					18173	36206	0.163	2.88
3	10222	10794				43432	119888	0.207	8.28
3	10013	10266	10971			57209	199560	0.204	11.51
3	10013	10266	10620	10942		83387	341547	0.227	17.79
3	10224	10237	10708	10794	10971	89506	325469	0.242	21.23
2	10013	10266	10591	10620		86843	375039	0.262	20.14

Finally, the chosen OF was the OF1 because it shows similar leakage reduction values and the LCOE values were acceptable to focus the selection of the machine in those lines where the recovered energy will be higher. However, any OF could be chosen to develop the D.II step, comparing the results. Figure 23 shows the information shown in Table 27 in terms of energy (Figure 23a), Leakage reduction (Figure 23b), LCOE values (Figure 23c) and generated power (Figure 23d). These figures show the results obtained in the optimization grouped by OF according to the number of lines installed and the pumps operating as turbines.
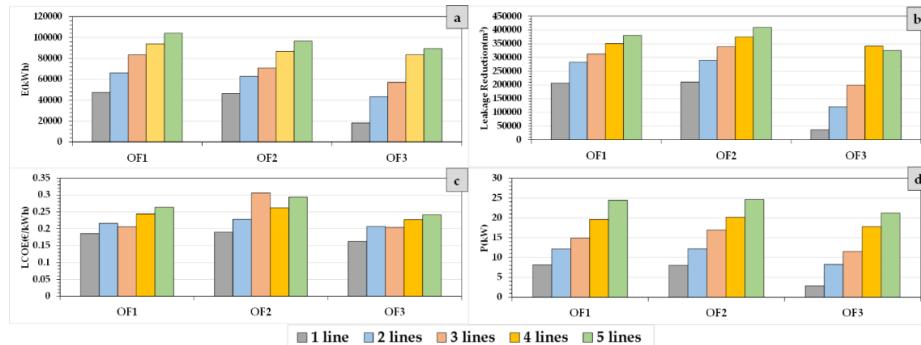

Figure 23. (a) Annual recovered energy; (b) Leakages reduction; (c) *LCOE* values; (d) Generated power

Figure 23a shows the increase of recovered energy when the number of recovery systems increases for any objective function (*OF*). The increase is linear for any OF.

Figure 23b shows the increase of the leakages reduction, which is directly proportional as a function of the number of installed recovery systems from 1 line to 5 lines. Besides, it shows the high increase in the reduction when the number of recovery lines was four considering OF3. Figure 23c shows the LCOE values oscillated between 0.16 and 0.3 €/kWh in the three OFs while the generated power oscillated between 7 and 25 kW as a function of the recovery systems considered in the optimization when OF1 and OF2 were considered. This generated power was lower when OF3 was analyzed in which it varied between 3 and 22 kW. For example, Tables 28 and 29 show the results when the iterative procedure was applied by simulated annealing methodology to choose the best machine.

Table 28. Optimized results when the methodology is considered using a recovery system alone

Iteration	1	2	3	4	5
Configuration	1	1	1	1	1
Line	10615	10615	10615	10615	10615
ID	128	128	128	128	128
n_{st} (rpm) [m, kW]	23.51	23.51	23.51	23.51	23.51
N_m	3	3	3	3	3
D (mm)	400	400	400	400	400
N (rpm)	750	750	750	750	750
Q_{BEP}(l/s)	62.64	62.64	62.64	62.64	62.64
H_{BEP} (m w.c.)	15.95	15.95	15.95	15.95	15.95
SR (Strategy Regulation)	NR	NR	NR	NR	NR
Annual E_{TR} (kWh)	52491	23746	23565	23572	23624
Leakage reduction (m³)	96102	96567	96722	96358	96725
LCOE (€/m³)	0.233	0.1605	0.1659	0.1678	0.1574
P (kW)	14.83	14.98	15.95	16.42	14.04
Energy difference (%)		54.76%	0.76%	-0.03%	-0.22%
Leakage reduction difference (%)		-0.48%	-0.16%	0.38%	-0.38%

Table 28 shows the results when a recovery system was only used. In this case, the line, called 10615 was used. The procedure needed five iterations applying the simulated annealing procedure to reach the best solution in terms of the type of machine to select (specific velocity, n_{st}; the number of machines operating in parallel, N_m; impeller diameter, D; and rotational speed). In this case, the used machine was radial, using three different machines connected in parallel, its best efficiency point (*BEP*) was 62.64 l/s and 15.95 m w.c. The recovery system was

regulated operating in nominal rotational speed (*NR*) and the annual recovered energy was 23625 kWh approximately. This configuration showed an annual leakage reduction of 96726 m³. If the difference between the last iterations is analyzed the energy and leakage reduction was 0.22 a 0.38%, respectively, therefore, the recovery system was established when the methodology stopped. The final energy and leakages values decreased by 50% compared with the preliminary simulated annealing (Table 27), which is considered the ideal machine to operate in the system. Table 29 shows the results when two recovery system was analyzed. In this case, lines 10615 and 10610 were optimized as a function of the results shown in Table 27 when the OF1 was analyzed.

Table 29. Optimized results when methodology is considered using two recovery systems
(Continue in next page)

Iteration	1		2		3	
Configuration	2		2		2	
Line	10615	10610	10615	10610	10615	10610
ID	49	30	128	30	83	54
n_{st} (rpm) [m, kW]	26.68	18.58	23.51	18.58	23.51	31.63
N_m	3	3	3	3	3	3
D(mm)	300	300	400	300	300	300
N (rpm)	750	750	750	750	1200	750
Q_{BEP}(l/s)	53.612	23.31	62.64	23.31	42.28	37.12
H_{BEP}(m w.c.)	12.154	11.3	15.95	11.3	22.98	7.58
SR (Strategy Regulation)	*BEH*	*NR*	*NR*	*NR*	*BEH*	*BEH*
Annual E_{TR}(kWh)	62317.2		41832.661		41279.3	
Leakage reduction (m³)	131251.72		115013.23		128828.66	
LCOE (€/m³)	0.271		0.201		0.22	
P (kW)	19.25		28.62		22.63	
Energy difference (%)	-	-	32.87%		1.32%	
Leakage reduction difference (%)	-	-	12.37%		-12.01%	

Table 29. (Cont.) Optimized results when methodology is considered using two recovery systems

Iteration	4		5		6	
Configuration	2		2		2	
Line	10615	10610	10615	10615	10610	10615
ID	83	54	83	83	54	83
n_{st}(rpm) [m, kW]	23.51	31.63	23.51	23.51	31.63	23.51
N_m	3	3	3	3	3	3
D(mm)	300	300	300	300	300	300
N (rpm)	1200	750	1200	1200	750	1200
Q_{BEP}(l/s)	42.28	37.12	42.28	42.28	37.12	42.28
H_{BEP}(m w.c.)	22.98	7.58	22.98	22.98	7.58	22.98
SR (Strategy Regulation)	BEH	BEH	BEH	BEH	BEH	BEH
Annual E_{TR}(kWh)	29911.87		35483.76		34490.44	
Leakage reduction (m³)	124425.54		122949.00		120245.8	
LCOE (€/m³)	0.337		0.286		0.189	
P (kW)	62.11		63.87		26.66	
Energy difference (%)	27.54%	-18.63%	2.80%		27.54%	
Leakage reduction difference (%)	3.42%	1.19%	2.20%		3.42%	

The use of two recovery systems showed the variation of the typology of the machine as well as the *BEP* of these machines varied until reached the fifth iteration in the optimized procedure.

The selected machines were defined by a specific value of 23.51 and 31.63 rpm (m, kW) for lines 10615 and 10610 respectively. The *BEP* defined in the database was 42.28 l/s and 22.98 m w.c. for line 10615. When line 10610 was optimized, the *BEP* was 37.12 l/s and 7.58 m w.c. In both cases, the strategy of the regulation was the best efficiency head (*BEH*) and the number of used machines in parallel was three. The final annual recovered energy was 34490 kWh. This value was 52.4% of the estimated energy in the first optimization procedure to choose the best location (Table 27). When the leakage value was observed, its reduction was 120246 m³

(42.58 % compared to the maximum reduction using simulated annealing in ideal conditions in Table 27, Step D.I).

The *LCOE* values were feasible in both cases according to feasible limits defined by [227]. When one recovery machine was analyzed the *LCOE* value was 0.157 €/m³. If two recovery systems are installed, this value was 0.189 €/m³. Figure 24a shows the results related to Table 28 when a recovery system was analyzed in the water network as a function of the specific speed of the machine. The figure shows the best solution compared with the available ratios. These ratios were energy ratio (β_E), which defines the ratio between the recovered energy between maximum recovered energy, the *LCOE* ratio (β_{LCOE}), which defines the ratio between *LCOE* and minimum *LCOE* and Leakages ratio (β_L), which defines the ratio between the reduction leakages and maximum reduction leakages. Figure 24a shows this interaction in the best solution reaching an energy ratio of 0.78, $\beta_L = 0.92$ and $\beta_{LCOE} = 1.5$.
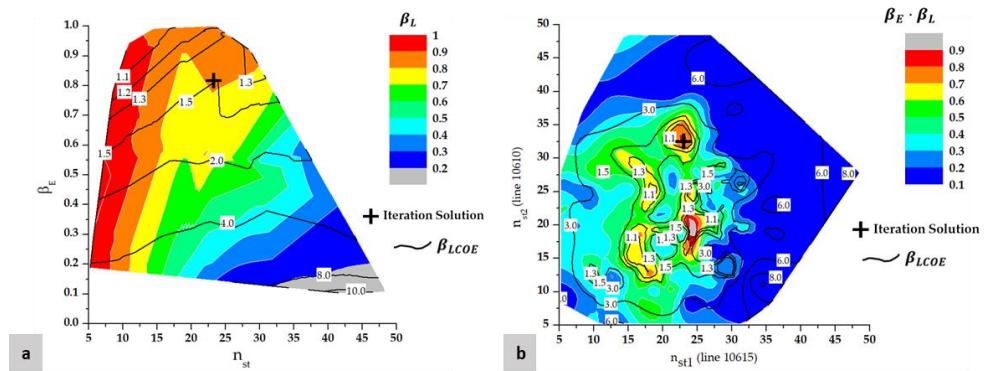
Figure 24. (a) Iteration solution when a recovery system was installed. (b) Iteration solution when two recovery systems were analysed

Figure 25b shows the integration of the best solution when two recovery systems were analysed in which the results are linked to Table 29. The figure shows the best solution is located on the best hill on the contour map. This case shows the interaction between $\beta_E\beta_L$ and the β_{LCOE}, reaching values of 0.8 and 1.1 respectively. Both figures showed the proposed methodology of the optimization established the best solution possible considering the available database of *PATs* and the constraints of the water system. The proposed solution implied a reduction of 96726 and 120246 m³ when one or two recovery systems were analysed respectively. The average pressures were calculated according to [226], using a hydraulic model and weighting according to node elevations. The maximum pressure was 37.98, 37.59

and 38.56 m w.c. for the initial situation, one recovery system and two recovery systems, respectively. The minimum pressure values were 12.99, 10.78 and 11.47 m w.c. for the initial situation, one recovery system and two recovery systems, respectively. The average pressure en in the system when initial situation, one recovery system and two recovery systems were analysed, they were 35.15, 33.86, 33.61 m w.c., respectively.

Figure 25 shows the variation of the pressure over time. It shows a monthly example between 15th January and 15th February for the initial situation of the water system, the scenario of the model considering one recovery system installed in the model and the second scenario, which analysed the installation of the two recovery systems.
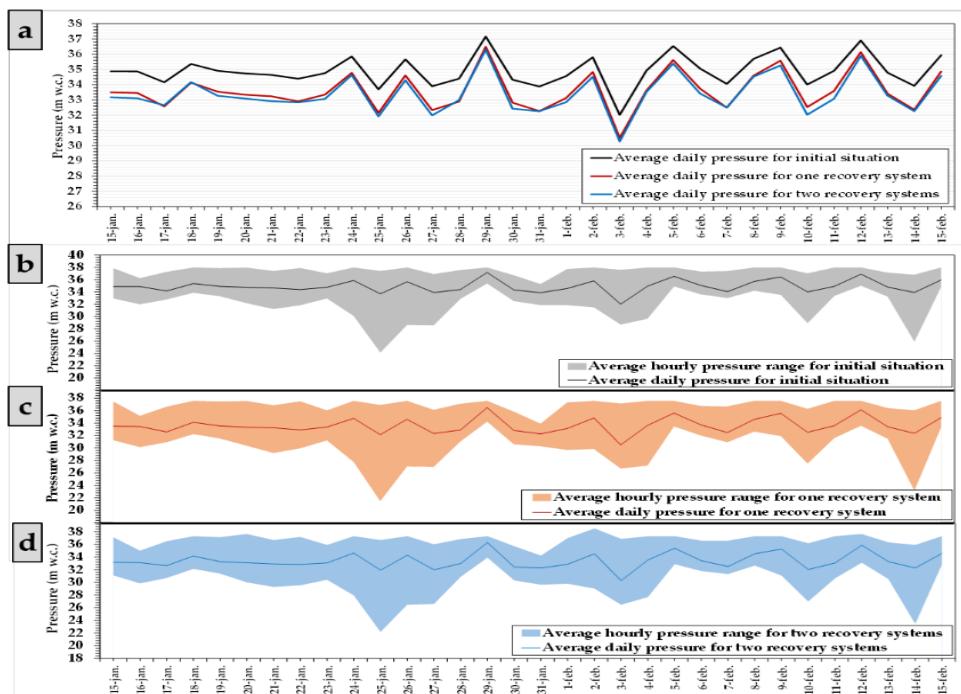
Figure 25. (a) Average daily pressure. (b) Average hourly pressure range for the initial situation; (c) Average hourly pressure range for one recovery system; (d) Average hourly pressure range for one recovery system

The inclusion of these new technologies implied the improvement of the different indicators. In this sense, different indicators were used to show the variation of these

140

indicators in the different iterations and the final decision of the optimization procedure. The results are shown in Table 30.

Table 30. Improvement of the different sustainable indicators. (Continue in next page)

Type	Abbreviation	Definition	Indicator
Energy	IED	Ratio between friction energy and input energy	Energy dissipation
	IAE	Sum of the total active energy consumed in the network	Annual consumed energy
	IEFW	Ratio between the active energy consumed and the total volume of water introduced in the system	Consumed energy per unit volume
	IER	Sum of total energy recovered in the network	Annual Recovered Energy
	ERP	Recoverable energy percentage used of the total energy consumed in the system	Recoverable energy percentage
	IAAE	Sum of the total active energy consumed in the network subtracted by the sum of the total energy recovered in the network	Absolute annual consumed energy
	IAEFW	Ratio between IAAE and the total volume of water introduced in the network	Absolute consumed energy per unit volume
Economic	IRLGP	Ratio between reduction of the leakage volume for each installed power.	Water recovery per unit volume per installed energy.
	REC	Product of the cost of the electricity tariff per kWh of energy produced	Cost of recoverable electrical energy per installation of PATs (1)
Environmental	CWSBRL	Product of the cost of each cubic meter of water for each covered meter of water saved.	Cost of water saved by reducing leaks when installing PATs (2)
	CDRPE	Ratio between the reduction of CO_2 emission by the production of each kWh of renewable energy	Carbon Dioxide reduced by produced energy (3)
	CDRBL	Ratio between the reduction of CO_2 emission for each cubic meter of water saved by leaks.	Carbon dioxide reduced by each cubic meter of water saved by leaks

141

Table 30. (Cont.) Improvement of the different sustainable indicators

Units	Initial Situation	1 Recovery System	2 Recovery Systems
Dimensionless	0.088	0.160	0.178
kWh	600483.38	592677.41	590717.91
kWh/m^3	0.088	0.088	0.088
kWh	0	23624.93	34490.44
%	0	3.99	5.84
kWh	600483.38	569052.48	556227.47
kWh/m^3	0.088	0.084	0.083
m^3/kW	0	6889.31	4510.35
€	0	4724.99	6898.09
€	0	24181.48	30061.45
Tn	0	11.58	16.9
kgr CO$_2$/m^3	0	0.12	0.14

(1) 0.2 €/kWh; (2) 0.25 €/m^3; (3) 0.49 kg/kWh [228]

Both economical, energy and environmental indicators improved. Therefore, the inclusion of the use of green recovery systems improves the management of the supply systems and it contributes to increasing the sustainability of the cities. Interesting results are shown in Table 27 and they are very interesting from the point of view of reducing water losses, although *IRLGP* is lower. It is mainly because the increase in power is greater than the increase in leakage reduction. For example, when two recovery systems were analyzed, the power increases by almost 50 % while the increase in leakage reduction is only 25%, so the *IRLGP* index is lower.

5.5. Conclusions

The improvement of the sustainability of the water distribution networks is key to achieving the different sustainable development goals. This challenge should be confronted by water managers of the cities to increase the efficiency, sustainability and reach of the different targets of the 2030 Agenda.

This research proposes a new strategy to improve the location of green energy recovery systems in the water distribution system. This proposal established an optimization procedure based on discretized hourly analysis along year. The methodology integrated different simulated annealing strategies to locate, select and regulated the best hydraulic machine as a function of the recovered energy, leakages reduction and economical terms (*LCOE* values) in a meshed network. As a novelty, the proposal also included a self-calibration, which enables the definition of

a model characterizing the consumed volume, real leakages and apparent leakages of the network based on injected flow and consumption recorded by the water company.

The methodology was implemented in a real case study located in Manta (Ecuador). The methodology used the recorded data for the year 2021 to analyse the behaviour of the system when green energy recovery systems are implemented in the system. The analysis showed the real possibility to recover energy by improving the performance indicators of the water system. The analysis showed the annual reduction of leakages could be more than 120000 m³. When the ratio between reduction of the leakage volume for each installed power (*IRLGP* index) was estimated, it was equal to 4510 m³/kW. The proposed methodology is limited in the consideration of the monthly consumed volume to calibrate the leakages. This limitation could be adapted for calibrating the leakages according to flow over time in future developments if the water systems had installed remote meter reading systems to increase the number of recording users (e.g., daily or hourly) and more flow meters in the network that could sectorize and discretize it in the analysis.

The use of similar methodologies enable the development of a database of sustainable indicators, and therefore, the different hydraulic system could be classified and compared with each other. Access to this information will be rewarding for other water managers and it will contribute to the management of the different water resources. It will help to establish tools in the different cities. These tools enable the gradual incorporation of sustainable methodologies in water management. The use of sustainable indicators, which enable the definition of the new goals in the management of the water supply will establish the next challenge for the green cities, mainly in developing countries, which show high ranges of improvement.

Conflicts of Interest: The authors declare no conflict of interest.

6. Resultados y Discusión

En esta sección se presenta la estructura de trabajo del Doctorado, así como se resume la relación entre los objetivos, los métodos utilizados y los resultados obtenidos. Cada paso de la investigación está contenido en cada uno de los cuatro artículos de este documento.

El desarrollo de esta investigación permite definir una metodología como herramienta de aplicación para el desarrollo de estrategias de regulación, que permitan la mejora de indicadores de sostenibilidad a través de la instalación de *PAT* en redes presurizadas.

Como se muestra en la Figura 26, este capítulo se distribuye en las siguientes fases:

6.1 Fase de contextualización *(Objetivo 1 / Artículo 1).*

6.2. Fase del procedimiento analítico.

6.2.1. Cuantificación del potencial de energía recuperado.

6.2.1.1. Determinación de expresiones semiempíricas en condiciones de operación de velocidad variable *(Objetivo 2 / Artículo 2).*

6.2.1.2. Determinación de caudal y presión en cada instante de tiempo.

6.2.1.3. Aplicación de metodología de calibración de fugas.

6.2.1.4. Cálculo del balance de energía.

6.2.2. Metodología de optimización con estrategias en base a diferentes funciones objetivos: energía, valor actual neto *(VAN),* coste nivelado de energía *(LCOE)* y reducción de fugas.

A. Aplicación de metodología de optimización para la selección y ubicación de *PAT* en redes de riego, bajo la influencia de fugas y la definición de indicadores de sostenibilidad, economía y energía *(Objetivo 3, 4, 5, 6 y 7 / Artículo 3).*

B. Aplicación de metodología de optimización para la selección y ubicación de *PAT* en redes de abastecimiento urbanas, bajo la influencia de fugas y evaluación de indicadores de sostenibilidad *(Objetivo 3, 4, 5, 6 y 7 / Artículo 4).*
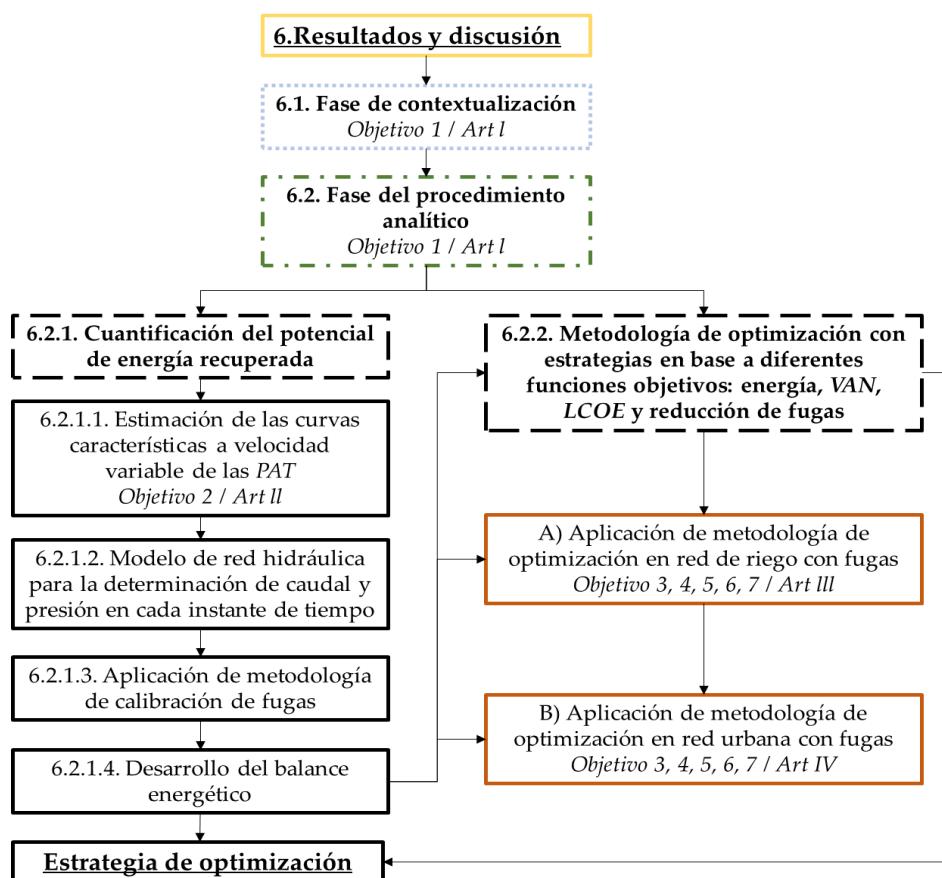

Figura 26. Diagrama de flujo de las etapas para desarrollar los objetivos propuestos

La etapa (6.1) se centra en la contextualización de esta investigación. En este apartado se analizó la importancia del estudio de las fugas de agua en las redes presurizadas. Se analizaron las diferentes expresiones de cálculo existentes para la

145

determinación de las fugas y se seleccionaron 45 casos de estudio de redes reales, de donde se extrajo información como: el volumen inyectado en la red, el porcentaje de fugas y la presión media. Estos datos permitieron calcular los siguientes parámetros: (i) la eficiencia volumétrica del sistema, (ii) la energía anual perdida por fugas, (iii) la energía consumida por cada metro cúbico de agua inyectado en la red, (iv) el consumo anual de energía; y (v) el coste de pérdidas en agua y energía. Adicionalmente, se analizaron 17 casos de estudio de redes presurizadas alrededor del mundo que constaban con *PAT* instaladas. El análisis consistió en la extracción de información tal como: caudal, presión y la energía anualmente recuperada por la instalación de *PAT* en las redes. Esto permitió calcular, el porcentaje de fugas reducido en la red por el uso de *PAT*, el volumen no fugado a consecuencia de instalar *PAT* en la red y la determinación de los rendimientos volumétricos del sistema. A través de los *KPI*, se determinó la influencia de las fugas en el sistema.

La fase del procedimiento analítico (6.2) está compuesta a su vez, por dos fases. De un lado, la cuantificación de energía hidráulica recuperada en las redes presurizadas (6.2.1) y, por otro lado, la metodología de optimización (6.2.2). La cuantificación de la energía está formada a su vez por cuatro subfases:

- **Estimación de la curvas características a velocidad variable de las *PAT* (6.2.1.1).** Propone una metodología que contiene diferentes expresiones de regresión para definir tres curvas operativas cuando las máquinas operan bajo la condición de *VOS*. Estas curvas son la mejor altura de eficiencia *(BEH)*, la mejor altura de potencia *(BPH)* y el mejor caudal de potencia *(BPF)*. El conocimiento de estas curvas permite a los gestores del agua analizar los mejores resultados de recuperación potencial de energía en las *PAT*. La estimación de las curvas se realizó a través de la modificación de las leyes de semejanza cuando las bombas trabajan como turbinas. Los métodos propuestos se compararon con otros cinco métodos publicados, mostrando que el método propuesto reducía los valores de error entre un 8 y un 20 %. Las expresiones propuestas en este método fueron validadas en una máquina experimental. Los datos empleados habían sido publicados en diversas investigaciones, para mostrar la precisión de las expresiones aplicadas en casos reales de estudio. La comparación de los resultados obtenidos mediante las expresiones propuestas y la experimentación presentaron gran similitud.

146
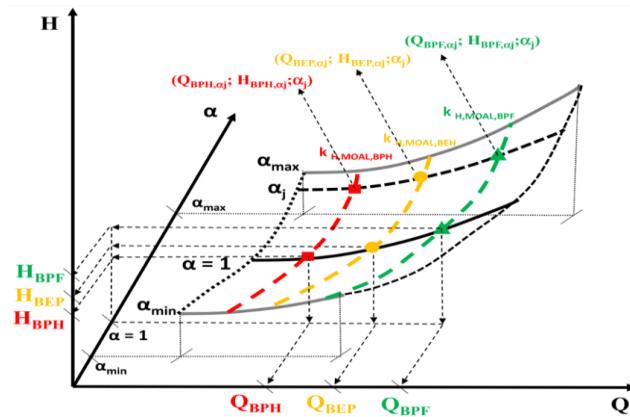
Figura 27. Curvas *BPH*, *BEH* y *BPF* en zona donde se aplica la *VOS*

- **Modelado de la red hidráulica (6.2.1.2).** El modelado es realizado con la finalidad de determinar los caudales y presiones en cada instante de tiempo en la red mediante el uso del software EPANET. Una vez el modelo se encuentre correctamente diseñado, la metodología pasa a la siguiente subfase para la calibración de fugas.
- **Calibración de fugas (6.2.1.3).** Esta etapa se realiza a través de un balance hídrico. Las fugas serán la diferencia entre el caudal inyectado respecto al caudal consumido por los usuarios. Posteriormente, se determinaron los rendimientos volumétricos del sistema donde el modelo distribuye las fugas en reales y aparentes. El modelo determina los diferentes coeficientes emisores asignados a las líneas y puntos de consumo en diferentes iteraciones, minimizando los errores entre el volumen de las fugas simuladas y medidas en el sistema. En esta etapa el objetivo es que el modelo se ajuste lo máximo posible a la situación real.
- **Desarrollo de balance energético (6.2.1.4).** Una vez el modelo está calibrado, se realiza el balance de energía. El objetivo es estimar la energía que el sistema requiere para funcionar correctamente y aquella energía teóricamente recuperable que se puede extraer del sistema. Este procedimiento, es realizado a través de una serie de expresiones propuestas en los artículos 3 y 4.

Una segunda fase, establece la optimización en la ubicación y selección de *PAT* bajo la influencia de fugas (6.2.2). Esta se desarrolla a través de una metodología que contiene un doble procedimiento "simulated annealing", empleando varias

147

funciones objetivo, como: la maximización de (E_{TR}), la maximización (ΔV_L), la minimización del *LCOE* y la maximización del *VAN*. Esta metodología se aplica en una red de riego (A) y de abastecimiento urbano (B).

6.1. Fase de contextualización

La fase de contextualización está basada en un artículo publicado (Artículo 1):

Leakage Management and Pipe System Efficiency. Its Influence in the Improvement of the Efficiency Indexes.
Coautores: Carlos Andrés Macías Ávila; Francisco-Javier Sánchez-Romero; P. Amparo López-Jiménez; Modesto Pérez-Sánchez.
Revista: Water ISSN 2073-4441.
Factor de impacto: 3.103. JCR (Q2; Posición 36/100). Water Resources.
Estado: Publicado [Water 2021, 7, 9; doi:10.3390/w13141909].

El agua es uno de los recursos naturales más preciados en el mundo. Diariamente, grandes volúmenes de agua son perdidos por las fugas existentes en las redes de distribución de agua. Estos niveles son elevados, a pesar de los esfuerzos que realizan las empresas gestoras para mitigar las pérdidas hídricas y energéticas mediante planes de gestión. El presente documento (Artículo 1) se basa inicialmente en la recopilación de los diferentes métodos de estimación de fugas, tales como: el teorema de Torricelli, el método de los caudales mínimos nocturnos *(MNF)*, la descarga de área fija y variable *(FAVAD)*, la ley del exponente *N1* y la estimación de las roturas y fugas de fondo *(BABE)*.

Los métodos propuestos poseen coeficientes que están definidos en función de las características de la red. Por ejemplo, α y β son dos parámetros variables en el modelo de fugas de fondo, estos representan la influencia de algunos factores en relación con la presión/fuga. El parámetro β representa el deterioro del material en el tiempo. Este depende de las características de la tubería (edad de la tubería, diámetro, material) y de factores como la presión en la red, condiciones medio ambientales y cargas de tráfico a las que se expone. El valor de α oscila generalmente entre 0.5 y 2.5 [57], mientras que β oscila entre 10^{-4} y 10^{-5} [29]. Existen diferentes algoritmos de optimización (genéticos, pseudogenéticos, redes neuronales, evolución diferencial, entre otros) para la calibración. Estos algoritmos requieren parámetros de la red como el caudal, consumos, presión y las condiciones de operación de la red. La calibración es utilizada para resolver problemas de optimización de búsqueda de valores de parámetros de calibración, mientras se minimizan las diferencias entre las observaciones reales y las predicciones de los

modelos. La Tabla 31 muestra las expresiones de cálculo de cada uno de los modelos. Se analizó cada uno de los coeficientes que requieren dichas expresiones, considerando diferentes tipos de materiales de las tuberías y de fallos estructurales.

Tabla 31. Métodos y expresiones propuestas para el cálculo de fugas

Técnica	Ecuación de cálculo de fugas	Ecuación
Torricelli	$$Q_{leak} = C_d A \sqrt{2gh}$$	(79)
MNF	$$L_{DMA} = Q_{MNF} - Q_{LNC}$$	(80)
	$$Q = Q(t_{MNF}) \cdot \left[\frac{P_{AZP(t)}}{P_{AZP}(t_{MNF})} \right]^{\alpha}$$	(81)
FAVAD (Descarga de área fija y variable)	$$ql_i = c_i \cdot P_i^{\beta}$$	(82)
Ley de exponent N1	$$Q = C_d h_{AZP}^{N_1}$$	(83)
Roturas y fugas de fondo	$$Q = \beta_k l_k (P_k)^{\alpha_k} + C_k (P_k)^{0.5}$$	(84)

En este estudio, se definieron diferentes *KPI*, estos son una herramienta de gestión que proporcionan medidas de cuánto recurso se utiliza en relación con el disponible. Son utilizados para evaluar hasta qué punto se cumplen los objetivos de gestión e incluso para evaluar el impacto general de las estrategias de gestión. Algunos de los *KPI* propuestos son: la demanda dependiente de la presión, la eficiencia volumétrica, el índice de fugas estructural *(ILI)*, la pérdida anual real inevitable de agua *(UARL)*, entre otros. En la segunda parte, se analizaron los datos extraídos de los 45 casos de estudio de redes con fugas. Estos resultados se muestran en la Tabla 32.

Tabla 32. Información extraída de redes de agua reales con fugas *(Continúa en la siguiente página)*

ID Caso	Fuga (%)	Presión media (mca)	Volumen anual consumido (m³)	Energía consumida por m³ inyectado (kWh/m³)	Consumo anual de energía (kWh)	Pérdida anual de energía por fugas (kWh)
1	57.56	54	33016	0.15	115093	66252
2	51.00	93	629552	0.25	325600	166056
3	12.03	50	807	0.14	1250363	150387
4	25.00	63	12772080	0.17	2923529	730882
5	27.16	70	27899748	0.19	7306457	1984580
6	3.05	60	2332019	0.16	393260	11975

Tabla 32. *(Continuación)*Información extraída de redes de agua reales con fugas

ID Caso	Fuga (%)	Presión media (mca)	Volumen anual consumido (m³)	Energía consumida por m³ inyectado (kWh/m³)	Consumo anual de energía (kWh)	Pérdida anual de energía por fugas (kWh)
7	23.00	55	320397	0.15	62363	14343
8	34.94	45	1436640	0.12	268653	93873
9	34.38	47	513336	0.13	101834	35010
10	31.37	40	1277500	0.11	202904	63656
11	45.60	41	3190939	0.11	659074	300538
12	15.00	40	5361120	0.11	687485	103123
13	15.00	40	7505568	0.11	962479	144372
14	14.90	59	11003226	0.16	2068799	308251
15	17.20	34	4047330	0.09	452881	77895
16	54.00	30	169243	0.08	30077	16242
17	26.05	40	5370085	0.11	791534	206194
18	23.92	65	1577530	0.18	367280	87860
19	28.31	31	8842478	0.09	1052511	297966
20	55.00	30	9855000	0.08	1790325	984679
21	28.45	40	251605	0.11	38328	10903
22	34.41	40	308260	0.11	51230	17630
23	19.80	30	9358600	0.08	953945	188879
24	63.27	50	24588597	0.14	9122084	5771888
25	38.24	50	13766774	0.14	3037055	1161332
26	46.06	50	16231357	0.14	4100160	1888637
27	57.00	77	18049250	0.21	8750213	4987622
28	52.50	40	426919	0.11	97967	51432
29	40.00	114	862194	0.31	446401	178560
30	46.86	75	157946	0.20	60746	28465
31	12.00	56	430151	0.15	74592	8951
32	30.00	40	2571680	0.11	400623	120187
33	13.33	30	81994	0.08	7734	1031
34	5.57	46	12210000	0.13	1620776	90252
35	20.70	38	130180000	0.10	16998768	3518629
36	74.96	42	1780000	0.11	813740	610019
37	22.55	40	6630000	0.11	933040	210370
38	23.22	40	10120000	0.11	1436620	333540
39	47.00	30	530009	0.08	81751	38423
40	17.54	44	330660000	0.12	48079900	8433766
41	15.87	37	40010000	0.10	4795237	761229
42	13.33	60	91000000	0.16	17167500	2289000
43	24.71	44	33830000	0.12	5387107	1330890
44	12.99	51	26524047	0.14	4236514	550334
45	58.69	45	147752776	0.12	43854719	25736535

Cada caso de estudio corresponde a una red presurizada de distribución de agua potable, de donde se extraen datos como la ubicación, consumo anual de agua, la presión media de la red que osciló entre 30 y 95 mca, el caudal inyectado en la red, métodos de cálculo de fugas y de calibración aplicados. Con los datos extraídos se logró determinar: el consumo de energía por cada m^3 de agua inyectado a la red. Este osciló entre 0.08 y 0.31 kWh/m^3. Se determinó el porcentaje de fugas, cuyos valores oscilaron entre 17 a 46 %. El consumo anual de energía, que osciló entre 7.73 y 48079 MWh. El rendimiento volumétrico del sistema entre 0.53 y 0.83. Asimismo, el coste anual del agua perdida que supera valores de 10 M€, el coste anual de la pérdida de energía que osciló entre 51270 y 647400 € y la pérdida anual de energía en la red por la presencia de las fugas que alcanza valores de hasta 3200 €.

En este apartado se analizaron 17 casos de estudio de redes de distribución de agua con fugas con *PAT* instaladas, la información extraída y los resultados obtenidos son mostrados en la tabla 33.

Tabla 33. Información extraída de redes con *PAT* instaladas

ID Caso	Q (l/s)	H (mca)	Energía anual recuperada por instalar *PAT* (kWh)	Volumen anual recuperado por instalar *PAT* (m³)	Reducción de fuga por instalar *PAT* (%)	η_v antes de instalar *PAT*	η_v después de instalar *PAT*
46	29	59	43800	-	20	-	-
47	74	54	87600	-	32	-	-
48	19	67	39420	-	18	-	-
49	33	55	43800	-	21	-	-
50	19	63	35040	-	29	-	-
51	14	71	26280	-	65	-	-
52	31	65	52560	-	21	-	-
53	29	21	28470	22813	63	0.73	0.90
54	183	33	169360	1634590	52	0.73	0.87
55	72	36	130305	98185	63	0.73	0.90
56	302	61	55626	2475059	26	0.73	0.80
57	212	39	71876	667554	10	0.73	0.76
58	314	50	66485	1829359	19	0.73	0.78
59	187	70	54985	-	-	-	-
60	110	45	125213	339085	10	0.73	0.76
61	110	45	113880	328865	9	0.73	0.75
62	350	45	714670	248504	3	0.73	0.74

El Artículo 1 analiza la relación que existe entre las fugas y el exceso de presión en la red, que es comúnmente controlado a través de *VRP* e introduce la importancia de estudiar la micro generación eléctrica a través de las *PAT* en las redes presurizadas de distribución de agua. Diferentes estudios demuestran que, en redes de distribución de agua, las *PAT* se pueden usar en lugar de *VRP* tanto para la reducción de la presión como para la producción de energía [156].

Los resultados mostraron que antes de instalarse las *PAT*, la eficiencia volumétrica del sistema se encontraba en valores aproximados a 0.7 y que posterior a la instalación de *PAT*, los valores fueron próximos a 0.9. La recuperación anual de energía variaría entre 26280 a 71460 kWh dependiendo del caso. Además, las fugas lograron reducirse desde un 3 a un 65 %.

Con la información extraída de los casos de estudio con *PAT* instaladas se determinaron los índices de energía de las redes, como se muestra en la Tabla 34. Estos índices son: la energía absoluta anualmente consumida *(IAAE)* en kWh/año, la energía anual recuperada *(IER)* en kWh/año, el porcentaje de energía recuperable *(ERP)* en %, la energía absoluta consumida por m^3 de agua inyectado a la red y como novedad un nuevo índice propuesto que considera la influencia de las *PAT* en la reducción de fugas. Este es el índice *(IRLGP)*, que determina la reducción del caudal fugado en función de la potencia generada, este se mide en m^3/kW.

Tabla 34. Cálculo de índices energéticos en redes con *PAT* instaladas

ID Caso	IAAE (kWh/año)	IER (kWh/año)	ERP (%)	IEFW (kWh/m^3)	IRLGP (m^3/kW)
53	52335	28470	54	0.06	8
54	518965	169360	3	0.09	-
55	222745	130305	58	0.10	4
56	1583106	55626	4	0.17	2
57	710516	71876	10	0.11	16
58	1349189	66485	5	0.14	13
59	1124897	54985	5	0.19	-
60	141794	125213	29	0.12	5
61	141794	113880	27	0.12	5
62	751937	714670	53	0.12	4

Se observa que la energía anual consumida está entre 141794 y 1583106 kWh. La energía anual recuperada desde 28470 a 714670 kWh. Utilizando los índices *IAAE* e *IER*, se determinó el valor *ERP* que mostró valores entre el 3 y el 58 %. Para poder

evaluar el sistema es necesario conocer su estado actual. Se deberá conocer el caudal que se inyecta a la red, los valores de presión y los modelos hidráulicos para tomas de decisión. La influencia de las fugas en las *PAT* puede provocar diferencias en la selección, operación y regulación de las máquinas.

Esta investigación mostró la necesidad de aplicar el análisis de indicadores de eficiencia en la recopilación de los diferentes casos de estudio reales de redes de abastecimiento. La definición de los indicadores parte de criterios económicos, energéticos y ambientales. La novedad de estos indicadores permitió caracterizar el estado de las redes seleccionadas, en función de los datos que usualmente disponen los gestores de abastecimiento, tales como: la presión, el caudal inyectado, las fugas y el consumo energético de la red.

El conocimiento de la influencia de estos indicadores en las redes podría permitir desarrollar procedimientos de optimización. Estos deberían considerar funciones objetivos relacionadas con la maximización de la reducción de fugas, reducción de costes de operación, recuperación energética por exceso de presión, reducción de emisiones de gases de efecto invernadero, entre otros.

6.2. Fase del procedimiento analítico

La segunda fase de la presente tesis contiene el bloque principal de esta investigación. El desarrollo de esta etapa es analizado y discutido. El análisis de este permite proponer la presente metodología para la mejora de los indicadores de sostenibilidad en la instalación de micro generación eléctrica en redes presurizadas.

6.2.1. Cuantificación del potencial de energía recuperado

La cuantificación del potencial de energía recuperable se basa en diferentes puntos, iniciados a través de la determinación del caudal y presión en el tiempo en redes presurizadas a través del software EPANET y se aplica en los artículos 3 y 4. Para la selección de las *PAT*, es necesario estimar las curvas características del sistema de recuperación de energía cuando se encuentran operando bajo la condición de velocidad variable. La definición de estas curvas se explica en el siguiente apartado.

6.2.1.1. Determinación de expresiones semiempíricas en condiciones de operación de velocidad variable.

La metodología es descrita en uno de los artículos publicados (Artículos 2).

Definition of the Operational Curves by Modification of the Affinity Laws to Improve the Simulation of PATs

El conocimiento de las curvas características (altura, eficiencia y potencia) de las *PAT*, es crucial para estimar la máxima recuperación energética en el sistema. La falta de información de las curvas ha generado que diferentes autores propongan expresiones empíricas que permitan estimar el funcionamiento de las *PAT*. Las ecuaciones se centran en: (i) el conocimiento del mejor punto de operación de las bombas cuando funcionan como turbina; y (ii) la necesidad de regular la velocidad de rotación de las *PAT* para optimizar la variable objetivo cuando se aplica la condición de operación *VOS*.

En búsqueda de estrategias para un desarrollo sostenible, la presente investigación muestra la importancia de estudiar la estrategia de regulación de modificación de las curvas a través de las leyes de semejanza. Esta investigación tiene como objetivo el desarrollo de expresiones de regresión. Estas ecuaciones definen la potencia generada en función del caudal bajo la operación de velocidad de rotación variable.

Este artículo recopila una amplia base de datos de investigaciones experimentales realizadas, considerando 15 *PAT* con velocidad específica entre 5.67 y 50.71 rpm (m, kW) y velocidad nominal entre 800 y 3000 rpm, estas fueron probadas a 87 diferentes velocidades de rotación. El uso de datos experimentales permitió la interpolación de más de 10000 parábolas. Las ecuaciones de regresión propuestas están basadas en parámetros adimensionales y son validadas mediante el análisis de error en comparación con otros métodos publicados, obteniendo así mejores aproximaciones.

La modificación de las leyes de semejanza es recomendable cuando las curvas características son conocidas por los gestores del agua. Estas curvas son: curva de altura, eficiencia y de potencia. La variación de la velocidad de rotación es definida por las leyes de semejanza. La definición de las leyes de semejanza está basada en el análisis de la parábola de congruencia [160].

$$H_{CP} = \frac{H_0}{Q_0^2} Q^2 = k_{H,AL} Q^2 \tag{85}$$

Considerando un punto de operación (Q_0, H_0), cuando el concepto de la parábola de congruencia es aplicado, las leyes de semejanza son definidas por las siguientes expresiones:

$$\frac{Q_1}{Q_0} = \frac{n_1}{n_0} = \alpha \tag{86}$$

$$\frac{H_1}{H_0} = \left(\frac{n_1}{n_0}\right)^2 = \alpha^2 \tag{87}$$

$$\frac{\eta_1}{\eta_0} = 1 \tag{88}$$

$$\frac{P_1}{P_0} = \left(\frac{n_1}{n_0}\right)^3 = \alpha^3 \tag{89}$$

Donde n_1 es la nueva velocidad de rotación en rpm, n_0 es la velocidad de rotación nominal en rpm; Q_1 es el caudal circulante en m^3/s cuando la velocidad de rotación es n_1; H_1 es la altura recuperada cuando la máquina opera para caudales iguales a Q_1 en mca; η_1 es la nueva eficiencia de la máquina cuando opera para Q_1.

Diversas investigaciones muestran la necesidad de modificar las leyes de semejanza para mejorar la estimación de las curvas características de las máquinas. Estas leyes pueden ser definidas usando números adimensionales (q, h, e y p). En el análisis de las máquinas, estos permiten establecer la función de operación para determinar cualquier velocidad de rotación.

$$q = \frac{Q}{Q_0} \tag{90}$$

$$h = \frac{H}{H_0} \tag{91}$$

$$e = \frac{\eta}{\eta_0} \tag{92}$$

$$p = \frac{P}{P_0} = qhe \tag{93}$$

Donde q, h, e y p son funciones de operación para diferentes velocidades de rotación (α), Q es cualquier valor de caudal de la *PAT* en m^3/s. Este valor está dentro de la zona de operación de *VOS*; H es la altura recuperable para este caudal en mca cuando la máquina opera con velocidad rotacional igual a α; η es la eficiencia para los valores de Q, H y α; P_0 y η_0 son referidos para cualquier punto de las curvas características de la máquina cuando esta opera a la velocidad de rotación nominal. Conocidos los valores recuperables por la máquina en modo turbina se define la expresión para determinar los diferentes valores de velocidad específica n_{st}.

$$n_{st} = n \cdot \frac{\sqrt{Q}}{H^{\frac{3}{4}}} \tag{94}$$

De esta forma se logra definir las curvas características para cualquier velocidad de rotación dentro de la zona *VOS*. La relación entre q y Q es lineal y está determinada por la pendiente m, que adoptará un valor constante según la curva analizada. El parámetro m permite la simplificación del desarrollo de las expresiones cuando la máquina opera en la zona de operación de *VOS*.

La segunda parte de este documento explica el desarrollo matemático mediante las expresiones de las curvas características de las bombas; además de las leyes de semejanza *(AL)* introducidas en estas curvas, considerando el trabajo de la máquina en zona de *VOS*.

Estas nuevas curvas, que se proponen son llamadas leyes de semejanza modificadas *(MOAL)* y permiten la estimación de *BEH*, *BPH* y *BPF*. Cuando se operan los coeficientes de la parábola de congruencia (k_i), comparando entre *AL* y *MOAL*, se obtienen las expresiones mostradas en la Tabla 35.

Tabla 35. Definición de las curvas en función de parámetro k$_i$

Curva	AL	MOAL
Altura $H = k_H Q^2$	$k_{H,AL} = \dfrac{H_0}{Q_0^2} = (Am^2 + Bm + C)$	$k_{H,MOAL} = \dfrac{h}{q^2}\, k_{H,AL}$
Eficiencia $\eta = e\eta_0$	$\eta_{AL} = \eta_0$	$\eta_{MOAL} = e \cdot \eta_{AL}$
Potencia $P = k_P Q^3$	Utilizando las curvas de altura y eficiencia. $k_{P,AL} = 9.81 \cdot k_{H,AL} \cdot \eta_{AL}$ Utilizando la expresión de potencia. $k_{P,AL} = \dfrac{P_0}{Q_0^3}$ $k_{P,AL} = \left(\dfrac{P_4}{m} + P_3 + P_2 m + P_1 m^2 + P_5 m^3\right)$	$k_{P,MOAL} = \dfrac{he}{q^2} k_{P,AL}$ $k_{P,MOAL} = \dfrac{p}{q^3} k_{P,AL} = \dfrac{he}{q^2} k_{P,AL}$

En la Figura 28 se muestra la metodología para determinar las expresiones de cálculo. Está dividido en una etapa experimental y una analítica.
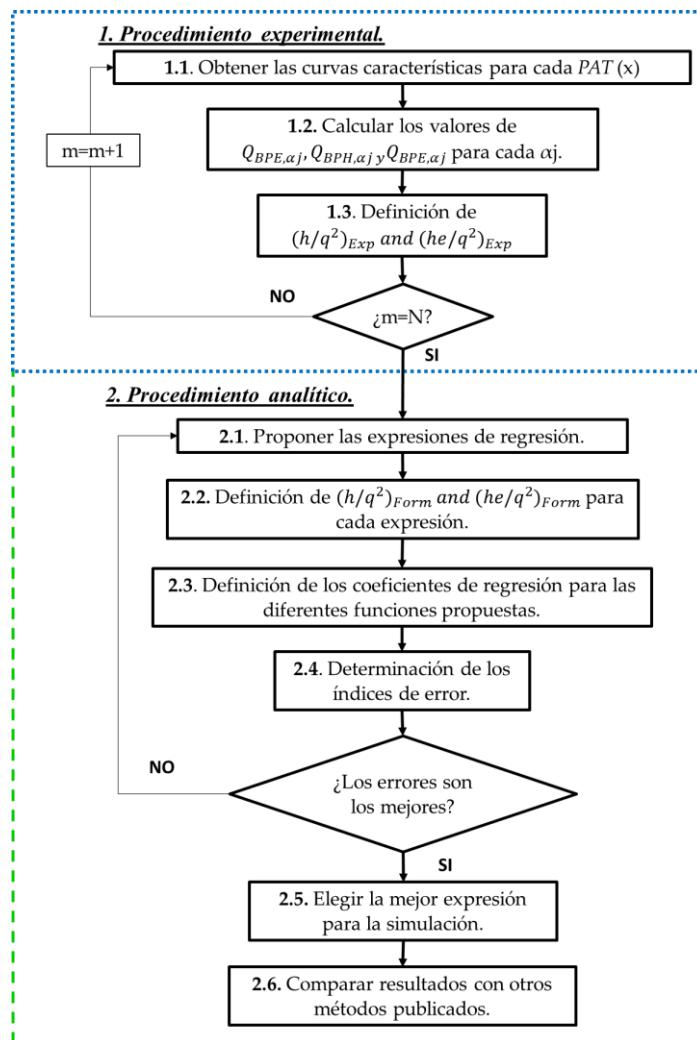
Figura 28. Metodología propuesta para la determinación de expresiones

En la primera etapa del procedimiento experimental (paso 1.1), utilizando la base de datos experimental de las máquinas, se obtienen las curvas características de las *PAT*. Este determina el caudal para las diferentes curvas cuando opera a velocidad de rotación nominal.

En este paso se determinan los valores de caudal para las curvas *BEH, BPH y BPF*. Calculados los tres valores de caudal, el procedimiento define estos valores de caudales para diferentes valores de velocidad de rotación $Q_{BEH_{\alpha j}}$, $Q_{BPH_{\alpha j}}$, $Q_{BPF_{\alpha j}}$

157

(paso 1.2). Posteriormente, se definen los parámetros adimensionales (h/q^2) y (he/q^2) (paso 1.3), utilizando la base de datos experimental de investigaciones publicadas para cada velocidad de rotación (paso 1.4).

En la segunda fase, diferentes funciones son propuestas y analizadas utilizando la base de datos (paso 2.1). En la Tabla 36 se muestran las expresiones de regresión que son utilizadas en este procedimiento.

Tabla 36. Funciones propuestas a ser analizadas

Modelo de la función (FM)	Función polinomial (Desde F_1 hasta F_6): $$NP = \beta_1\left(\alpha\frac{Q}{Q_{BEP}}\right) + \beta_2\left(\frac{Q}{Q_{BEP}}\right)^2 + \beta_3\left(\frac{Q}{Q_{BEP}}\right) + \beta_4\alpha^2 + \beta_5\alpha + \beta_6$$ Función potencial (Desde F_7 hasta F_{10}): $$NP = \left(\frac{Q}{Q_{BEP}}\right)^{\beta_3}\alpha^{\beta_5}\cdot exp^{\beta_6}$$
F_1	$$NP = \beta_4\alpha^2 + \beta_5\alpha$$
F_2	$$NP = \beta_4\alpha^2 + \beta_5\alpha + \beta_6$$
F_3	$$NP = \beta_2\left(\frac{Q}{Q_{BEP}}\right)^2 + \beta_4\alpha^2 + \beta_5\alpha$$
F_4	$$NP = \beta_2\left(\frac{Q}{Q_{BEP}}\right)^2 + \beta_4\alpha^2 + \beta_5\alpha + \beta_6$$
F_5	$$NP = \beta_1\left(\alpha\frac{Q}{Q_{BEP}}\right) + \beta_2\left(\frac{Q}{Q_{BEP}}\right)^2 + \beta_3\left(\frac{Q}{Q_{BEP}}\right) + \beta_4\alpha^2 + \beta_5\alpha$$
F_6	$$NP = \beta_1\left(\alpha\frac{Q}{Q_{BEP}}\right) + \beta_2\left(\frac{Q}{Q_{BEP}}\right)^2 + \beta_3\left(\frac{Q}{Q_{BEP}}\right) + \beta_4\alpha^2 + \beta_5\alpha + \beta_6$$
F_7	$$NP = \alpha^{\beta_5}$$
F_8	$$NP = \alpha^{\beta_5}\cdot exp^{\beta_6}$$
F_9	$$NP = \left(\frac{Q}{Q_{BEP}}\right)^{\beta_3}\alpha^{\beta_5}$$
F_{10}	$$NP = \left(\frac{Q}{Q_{BEP}}\right)^{\beta_3}\alpha^{\beta_5}\cdot exp^{\beta_6}$$

*NP es el parámetro adimensional. Este puede ser h/q^2 ó he/q^2

Una vez son definidas las expresiones de regresión, los valores de $(h/q^2)_{Form}$ y $(he/q^2)_{Form}$ son estimados para cada F_i (paso 2.2). Se definen los coeficientes de regresión para las diferentes funciones propuestas (paso 2.3). Posteriormente, se

definen los índices de error, que permiten elegir la mejor expresión de regresión para definir las funciones propuestas (*BEH, BPH y BPF*). Las expresiones propuestas para estimar los valores de *KEI* son mostradas en la Tabla 37, fueron determinados para cada función cuando los parámetros adimensionales son aplicados a *BEH, BPH* y *BPF* (paso 2.4).

Tabla 37. Índices de error usados en el análisis

KEI	Variable	Precisión	Ecuación
Error medio cuadrático $$RMSE = \sqrt{\frac{\sum_{i=1}^{s}[O_i - P_i]^2}{s}}$$		Ajuste perfecto cuando RMSE es cero	(95)
Desviación media absoluta $$MAD = \sum_{1}^{s}\frac{1}{s}|O_i - P_i|$$	O_i son los valores estimados; P_i son los valores experimentales y "s" el número de observaciones	Ajuste perfecto cuando *MAD* es cero	(96)
Desviación media relativa $$MRD = \sum_{1}^{s}\frac{|O_i - P_i|/P_i}{s}$$		-	(97)
Porcentaje BIAS $$BIAS = \frac{\sum_{i=1}^{s}[O_i - P_i]}{s}$$		El ajuste perfecto es cero	(98)

Se implementaron diez funciones para las expresiones de regresión propuestas h/q^2 y he/q^2 como se muestra en la Tabla 38. Estas funciones se utilizaron para estimar *BEH, BPH* y *BPF*. Los *KEI* se estimaron para cada función, cuando se aplicaron los parámetros adimensionales h/q^2 y he/q^2 a *BEH, BPH* y *BPF*. Los *KEI* utilizados son: error medio cuadrático *(RMSE)*, desviación media absoluta *(MAD)*, desviación media relativa *(MRD)* y el porcentaje *(BIAS)*.

Cuando la curva *BEH* es analizada, la función que muestra el mínimo error medio fue F_2. Los errores *RMSE, MAD* y *MRD fueron* 0.1035, 0.0735 y 0.0628. La segunda función fue F_6, para esta función la diferencia de error fue de 2.4 a 4.7 % para *RMSE* y *MAD* respectivamente, mientras que para *MRD* fue mejor F_2 reduciendo un -0.94 % comparado a F_2. Cuando *BPH* es analizado la mejor función de ajuste fue F_6. Cuando se analiza *BPF*, F_2 fue la expresión con menos error, pero F_6 se aproxima a sus

resultados, como en el caso de *BEH*. Sin embargo, considerando el análisis desarrollado por [155] se eligió F_6, debido a su buena precisión y bajos errores para definir la curva característica de la máquina cuando se compararon otros métodos para definir *BEH*, *BPH* y *BPF*.

Tabla 38. Expresiones propuestas para los números adimensionales *(Continúa en la siguiente página)*

Expresiones de los modelos de función
F_1

$$\frac{h}{q^2} = -0.512\alpha^2 + 1.63\alpha \ (R^2 = 0.978)$$

$$\frac{he}{q^2} = -0.826\alpha^2 + 1.843\alpha \ (R^2 = 0.979)$$

<center>F_2</center>

$$\frac{h}{q^2} = 1.048\alpha^2 - 1.487\alpha + 1.469 \ (R^2 = 0.738)$$

$$\frac{he}{q^2} = -0.1706\alpha^2 + 0.5336\alpha + 0.617 \ (R^2 = 0.151)$$

<center>F_3</center>

$$\frac{h}{q^2} = -0.235\left(\frac{Q}{Q_{BEP}}\right)^2 - 0.5196\alpha^2 + 1.789\alpha \ (R^2 = 0.981)$$

$$\frac{he}{q^2} = -0.024\left(\frac{Q}{Q_{BEP}}\right)^2 - 0.826\alpha^2 + 1.858\alpha \ (R^2 = 0.979)$$

<center>F_4</center>

$$\frac{h}{q^2} = -0.1139\left(\frac{Q}{Q_{BEP}}\right)^2 + 0.965\alpha^2 - 1.254\alpha + 1.395 \ (R^2 = 0.764)$$

$$\frac{he}{q^2} = 0.032\left(\frac{Q}{Q_{BEP}}\right)^2 - 0.148\alpha^2 + 0.469\alpha + 0.637 \ (R^2 = 0.154)$$

<center>F_5</center>

$$\frac{h}{q^2} = -1.508\left(\alpha\frac{Q}{Q_{BEP}}\right) - 0.471\left(\frac{Q}{Q_{BEP}}\right)^2 + 1.93\left(\frac{Q}{Q_{BEP}}\right) + 0.714\alpha^2 + 0.342\alpha$$
$$(R^2 = 0.986)$$

$$\frac{he}{q^2} = 0.532\left(\alpha\frac{Q}{Q_{BEP}}\right) - 0.828\left(\frac{Q}{Q_{BEP}}\right)^2 + 0.757\left(\frac{Q}{Q_{BEP}}\right) - 0.757\alpha^2 + 1.287\alpha$$
$$(R^2 = 0.98)$$

<center>F_6</center>

$$\frac{h}{q^2} = -0.69\left(\alpha\frac{Q}{Q_{BEP}}\right) + 0.122\left(\frac{Q}{Q_{BEP}}\right)^2 + 0.313\left(\frac{Q}{Q_{BEP}}\right) + 1.222\alpha^2 - 1.267\alpha + 1.294$$
$$(R^2 = 0.778)$$

$$\frac{he}{q^2} = 0.993\left(\alpha\frac{Q}{Q_{BEP}}\right) - 0.494\left(\frac{Q}{Q_{BEP}}\right)^2 - 0.156\left(\frac{Q}{Q_{BEP}}\right) - 0.471\alpha^2 + 0.38\alpha + 0.73$$
$$(R^2 = 0.191)$$

La metodología propuesta se comparó con cinco métodos diferentes publicados, estos fueron: (i) leyes de semejanza clásicas; (ii) Carravetta et al. ; (iii) Fecarotta et al.; (iv) Pérez Sánchez et al.; y (v) Tahani et al. Los métodos mencionados se operaron para obtener *BEH*, *BPH* y *BPF*.

Cada método se comparó con la base de datos experimental de cada máquina. En todos los casos, cuando se determinaron los índices de error promedio, la propuesta de parámetros adimensionales mostró los valores de error menor de *BEH*, *BPH* y *BPF*.

La Figura 29a y 29b muestra la clasificación de los errores aplicados en los diferentes métodos en función de los parámetros adimensionales. En la Figura 29a para h/q^2 y en la Figura 29b para he/q^2. Ambos parámetros mostraron que la propuesta de regresión, utilizando F_6, permite estimar *BPF*, *BEH* y *BPH*. Como resultado de las expresiones de este estudio para *BEH* considerando el parámetro h/q^2, los valores de *RMSE*, *MAD* y *MRS*, fueron 0.1077, 0.0755 y 0.622, respectivamente.

Tabla 38. *(Continuación)* Expresiones propuestas para los números adimensionales

Expresiones de los modelos de función
F_7
$\dfrac{h}{q^2} = \alpha^{0.214}(R^2 = 0.207)$
$\dfrac{he}{q^2} = \alpha^{0.245}(R^2 = 0.175)$
F_8
$\dfrac{h}{q^2} = \alpha^{0.305} \cdot exp^{0.077}(R^2 = 0.402)$
$\dfrac{he}{q^2} = \alpha^{0.202} \cdot exp^{-0.036}(R^2 = 0.116)$
F_9
$\dfrac{h}{q^2} = \left(\dfrac{Q}{Q_{BEP}}\right)^{-0.23}\alpha^{0.451}(R^2 = 0.506)$
$\dfrac{he}{q^2} = \left(\dfrac{Q}{Q_{BEP}}\right)^{0.11}\alpha^{0.132}(R^2 = 0.22)$
F_{10}
$\dfrac{h}{q^2} = \left(\dfrac{Q}{Q_{BEP}}\right)^{-0.166}\alpha^{0.422} \cdot exp^{0.032}(R^2 = 0.478)$
$\dfrac{he}{q^2} = \left(\dfrac{Q}{Q_{BEP}}\right)^{0.083}\alpha^{0.143} \cdot exp^{-0.013}(R^2 = 0.129)$

Figura 29. (a) Índices de error de los diferentes métodos aplicados a h/q^2; (b) Índices de error para los diferentes métodos aplicados a he/q^2

Cuando se analizaron los resultados del parámetro he/q^2 para *BEH*, los resultados de *RMSE*, *MAD* Y *MRS* fueron 0.0677, 0.0513 y 0.0539, respectivamente. Ambos parámetros adimensionales mostraron que utilizando la función F_6 se logra obtener las tres curvas antes mencionadas. Se eligió el modelo F_6 para estimar curvas de altura y eficiencia. Esta función mostró los errores más bajos en comparación con el

162

resto de los modelos. Además, este modelo contenía la variación de la velocidad de rotación, así como el uso de la relación Q/Q_{BEP}, con lo que es posible medir la cercanía a *BEP*. Esto permite a los administradores del agua fijar el rango de operación del caudal para que se apliquen las leyes de semejanza.

Haciendo uso de los datos publicados en la bibliografía para una máquina ensayada modelo *NK-140 125/127*, con una velocidad específica modo turbina de 31.16 rpm (m, kW), se validaron los resultados de las expresiones propuestas. Esto permitió analizar el error de los resultados a casos reales.

El punto de operación de la máquina donde existía la mayor eficiencia modo turbina fue de 17.99 l/s y 30.31 mca con una eficiencia de 0.695. La máquina fue ensayada a seis velocidades de rotación diferentes, con una velocidad de rotación nominal de 3000 rpm. La Figura 30a muestra la altura en función del caudal para *BEH*. La Figura 30b muestra la curva que define la potencia en función del caudal. Ambas muestran un buen ajuste. La Figura 30c muestra la curva de operación *(Q vs H)*, representando *BPH*. Esta es la curva más importante, ya que es la mejor para maximizar la energía recuperada cuando se aplica en la zona de operación de la *VOS*.

La Figura 30d muestra la comparación entre la curva *BPH* estimada y experimental. Para estos puntos se observa un buen ajuste. La Figura 30e y la Figura 30f muestran las diferencias entre las parábolas de tendencia y las curvas probadas.

Finalmente, las leyes de semejanza modificadas propuestas en este estudio disminuyen los índices de error entre un 8 y un 30 % en comparación con los métodos existentes y pueden ayudar a los administradores de sistemas de agua a mejorar la precisión de las predicciones de energía.

Las ecuaciones manejadas para definir las diferentes curvas propuestas son aplicadas en el caso de estudio A y B desarrollados en la presente tesis.
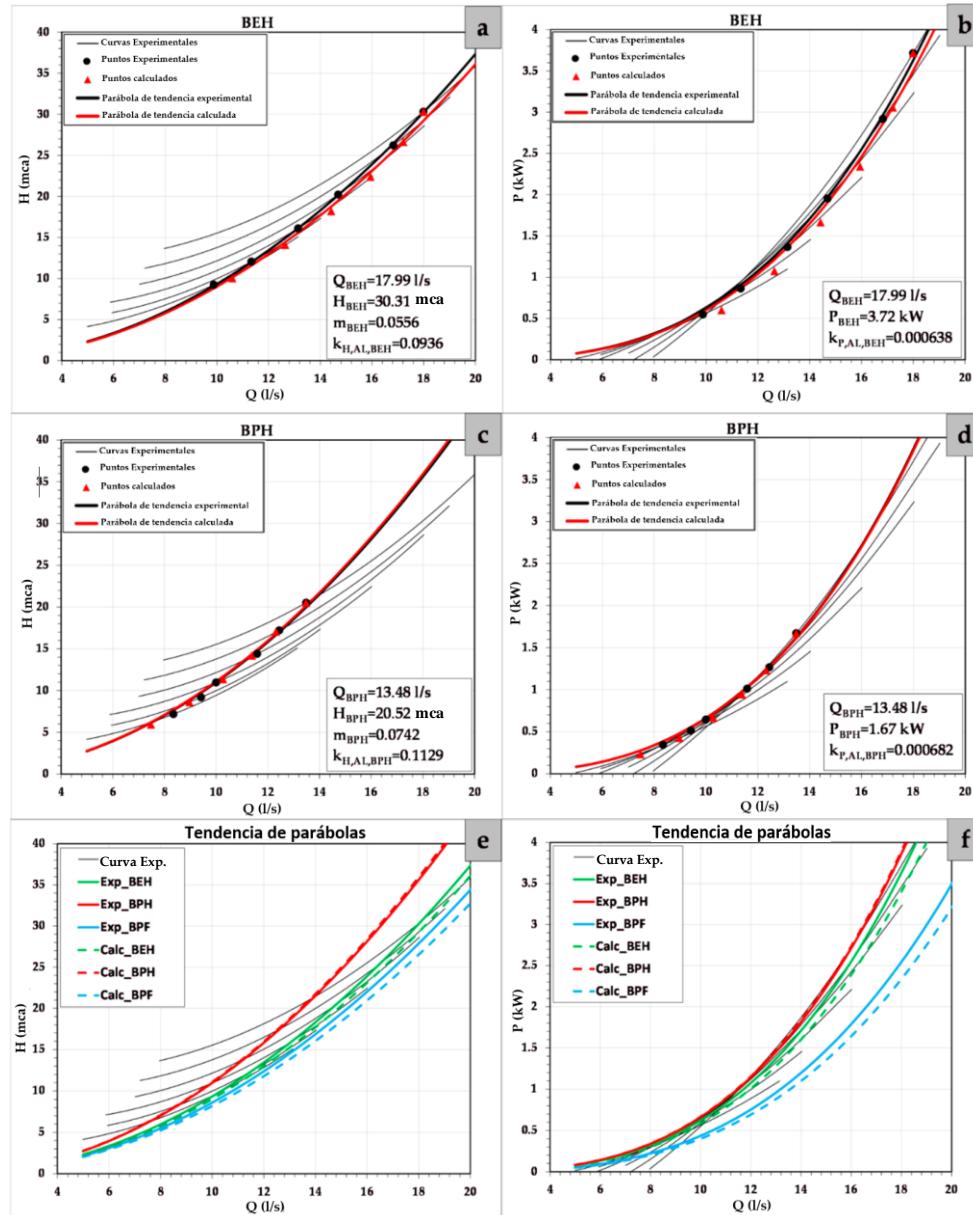
Figura 30. (a) *H-C* para *BEH*; (b) *P-Q* para *BEH*; (c) *H-C* para *BPH*; (d) *P-Q* para *BPH*; (e) *H-C* para *BEH, BPH* para *BPF*; (f) *P-Q* para *BEH, BPH* y *BPF*

6.2.2. Metodología de optimización con estrategias en base a diferentes funciones objetivos: energía, *VAN*, *LCOE* y reducción de fugas

La metodología de optimización se realiza a través de diferentes estrategias en base a diferentes funciones objetivos, como: (i) la maximización de: energía, *VAN* y reducción de fugas y; (ii) la minimización del *LCOE*. La metodología está dividida en 5 fases: modelo de la red (I), calibración de fugas (II), balance de energía (III), ubicación óptima (IV), selección óptima (V) y definición de la mejor solución (VI). El esquema de la metodología se muestra en la Figura 31.

El modelo de la red (I) se desarrolla a través de la información disponible. Esta información fue: (i) la topología de la red, (ii) la demanda base, y (iii) los patrones de consumo. El objetivo es determinar el caudal circulante en las tuberías y la presión en los nudos. El proceso de calibración (II) considera las fugas en el sistema, este método establece un balance del volumen de agua, minimizando el error entre el volumen fugado simulado y el volumen fugado del sistema.

El proceso de calibración (II) considera las fugas en el sistema de agua. Este método es aplicado cuando los gestores de agua tienen información sobre los consumos de los contadores. El método considera un balance hídrico de volúmenes, el volumen fugado será la diferencia entre el volumen inyectado menos el consumido.

Conocidos los volúmenes, se determina el rendimiento de fugas del sistema de agua y el rendimiento del volumen medido del sistema. Las fugas se dividen en dos tipos: reales y aparentes. Las fugas reales son asignadas a las líneas de distribución, mientras las fugas aparentes a los puntos de consumo. La calibración del modelo distribuye las fugas una vez los rendimientos son conocidos. El modelo determina los diferentes coeficientes emisores asignados a las líneas y puntos de consumo en diferentes iteraciones, minimizando los errores entre el volumen de las fugas simuladas y medidas en el sistema.
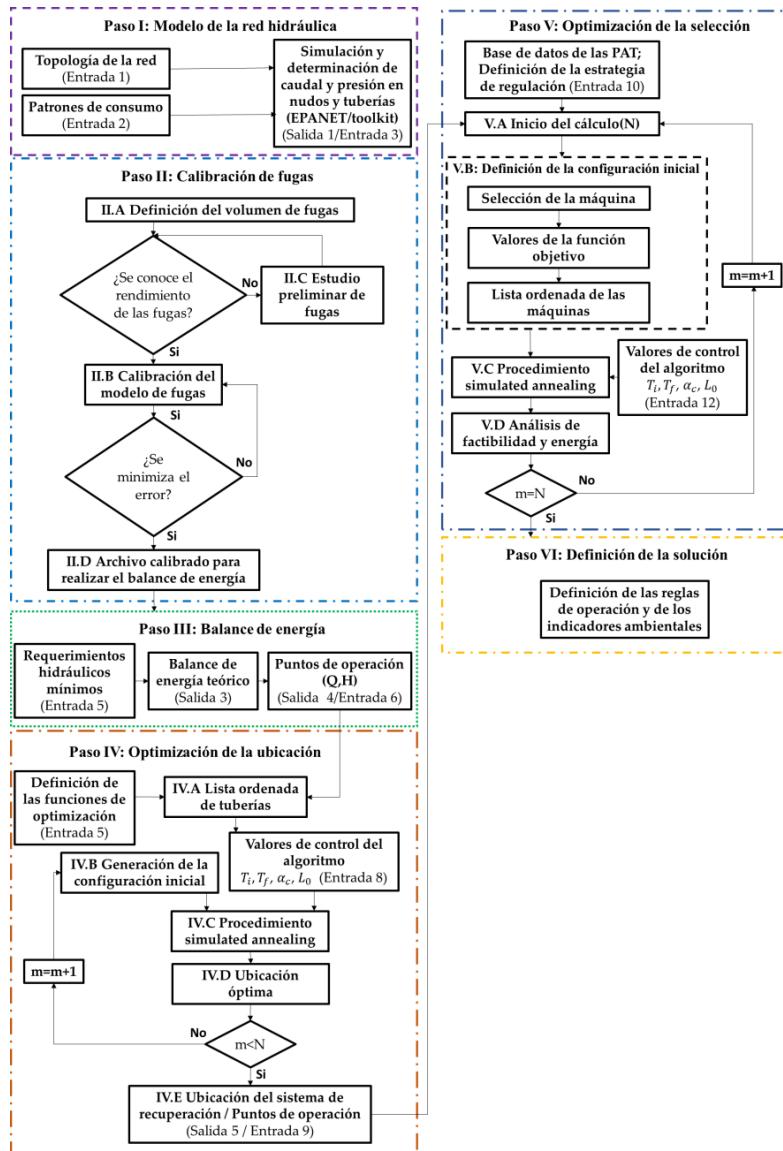
Figura 31. Metodología propuesta del procedimiento de optimización

La calibración de las fugas se basa en la estimación del parámetro K_j, asumiendo que el total del volumen de fugas se distribuye entre todos los elementos de la red. Las iteraciones para asignar los diferentes coeficientes de distribución finalizan cuando el error del escenario simulado y real es minimizado en esta distribución.

Considerando los requerimientos mínimos de presión en la red, se realizó la auditoría energética a través de las expresiones propuestas del balance de energía (III), estas permitirán definir los puntos de operación de caudal y altura teórica.

Las fases de optimización de la ubicación y selección de los sistemas de recuperación son realizadas a través de un doble procedimiento "simulated annealing" mostrado en la Figura 32. Este es un algoritmo heurístico de búsqueda basado en la analogía del proceso físico de recocido de metales. El algoritmo está inspirado en el método de Monte-Carlo, basado en la idea de Metrópolis. Este método busca encontrar la mejor solución en diferentes tipologías de problemas con un alto número de combinaciones, a partir de las funciones objetivos definidas [225]. El procedimiento de optimización se divide en las siguientes etapas:

1. Definición de las funciones objetivo. Bajo criterios energéticos, económicos y volumétricos, estos son: (i) energía teórica recuperada ($\psi_1 = E_{TR}$); (ii) reducción de fugas en la red ($\psi_2 = \Delta V_L$); (iii) el *VAN* y; (iv) el *LCOE*.

2. Elaboración de una lista ordenada de las líneas en orden descendente, según la función objetivo analizada. Se establece el número inicial de sistemas de recuperación $n = 2$.

3. Asignación de los parámetros de control del algoritmo. Se define: el número de iteraciones, la temperatura inicial T_i, temperatura final T_f, la velocidad de enfriamiento α_c y el número de transiciones en cada paso de temperatura L_0. Estos parámetros son fijados según un análisis de sensibilidad realizado previamente y son modificados con base a la función objetivo analizada.

4. Generación de la configuración inicial S_i, donde n es el número de turbinas, cuando $n = 2$, las líneas seleccionadas son las dos primeras. Si n es mayor a 2, el proceso comienza con la solución obtenida para turbinas $n - 1$. A este resultado inicial se añade la línea con mayor valor de la función objetivo que no está contenida en la solución.

5. En el procedimiento simulatead annealing, se genera una nueva combinación S_f, para cada iteración se elimina aleatoriamente una línea o máquina de la combinación y se introduce aleatoriamente otra línea o máquina. Esta suma se realiza considerando las líneas o máquinas con mejor posición en la lista ordenada con mayor probabilidad de ser introducidas en la nueva combinación.
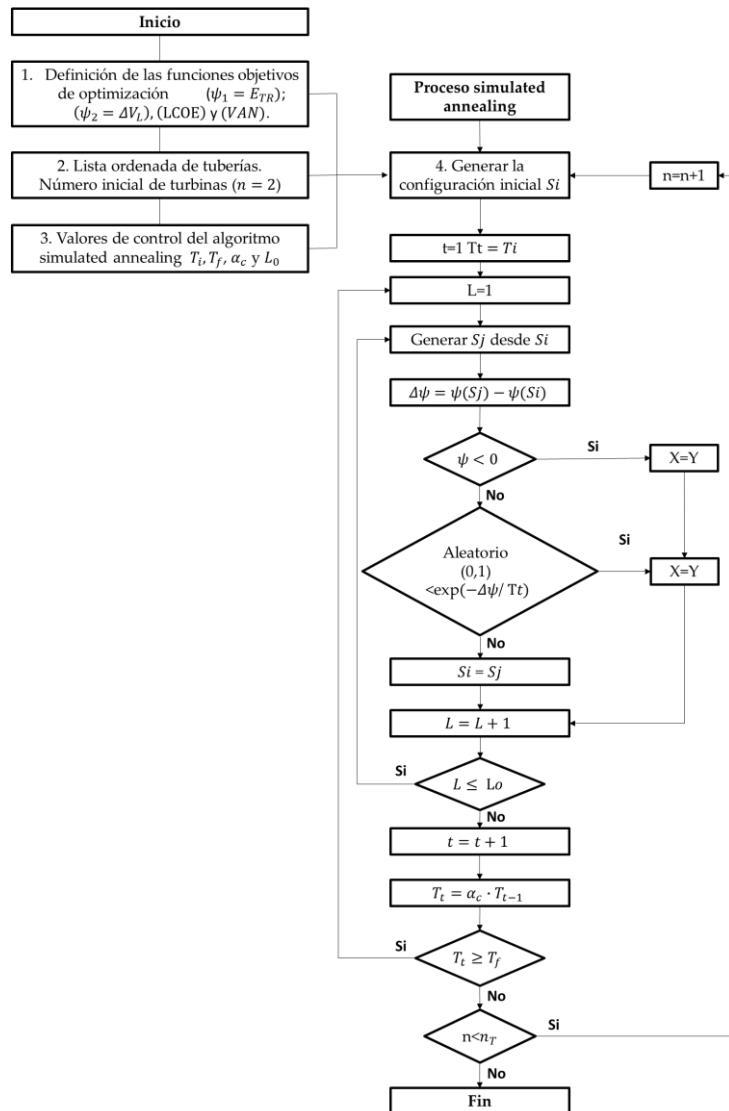
Figura 32. Procedimiento "simulated annealing"

A. Aplicación de metodología de optimización para la selección y ubicación de PAT en redes de riego, bajo la influencia de fugas y la definición de indicadores de sostenibilidad, economía y energía.

La metodología es totalmente descrita en un artículo publicado (Artículo 3).

168

Optimization tool to improve the management of the leakages and recovered energy in irrigation water systems

Coautores: Carlos Andrés Macías Ávila; Francisco-Javier Sánchez-Romero; P. Amparo López-Jiménez; Modesto Pérez-Sánchez.

La presente metodología se aplicó a una red de riego ubicada en el municipio de Vallada en la provincia de Valencia (España), como se muestra en la Figura tiene como objetivo inicial determinar el caudal circulante y la presión en la red. Después se lleva a cabo la calibración del modelo considerando las fugas. Posteriormente, el balance de energía es desarrollado para finalizar con la optimización a través de un doble procedimiento "simulated annealing" de la ubicación y selección de las *PAT*. En este caso, se considera la influencia de las fugas. La red dispone de una base de datos del volumen inyectado en la red desde el año 2001 al 2020.

Datos de la red	
Total de tuberías	851
Líneas de distribución	204
Líneas a nudos de consumo	222
Nudos virtuales de fugas	425
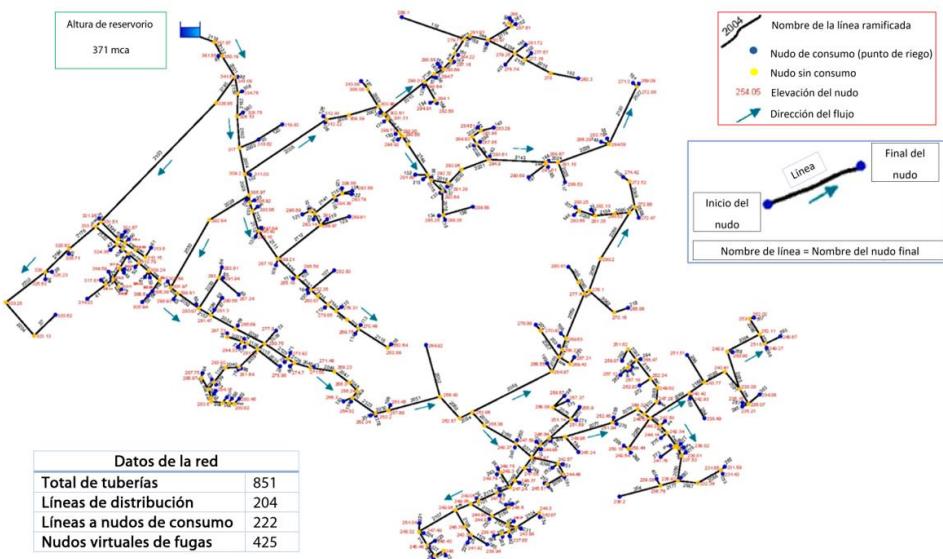
Figura 33. Red de riego en Vallada

La investigación define 4 escenarios discretizados en intervalos de 5 años, denominados S0 hasta S5. El primer intervalo desde 2001 a 2005 se establece como

ideal (S0), debido a que no se consideran fugas, a medida que se incrementan los años en los intervalos, existirán mayores fugas por el deterioro del sistema. Adicionalmente a los 4 escenarios mencionados anteriormente, se proponen dos escenarios futuros, considerando la tendencia de los años anteriores, para analizar la influencia de las fugas en la recuperación de los sistemas.

Con los pasos I y II de la metodología es posible realizar la auditoría energética, a través de una serie de ecuaciones propuestas. En este punto se debe considerar los requerimientos mínimos hidráulicos para el correcto funcionamiento de la red. La Figura 34 muestra los diferentes valores del balance de energía en los nudos de consumo en función del escenario analizado. La energía anual disipada por fricción existente en la red osciló entre 10255 y 13426 kWh. El requerimiento anual de energía osciló entre 78968 y 94716 kWh desde el escenario S0 al S5, respectivamente. Finalmente, la energía anual teóricamente recuperable osciló entre valores de 152906 y 182264 kWh.
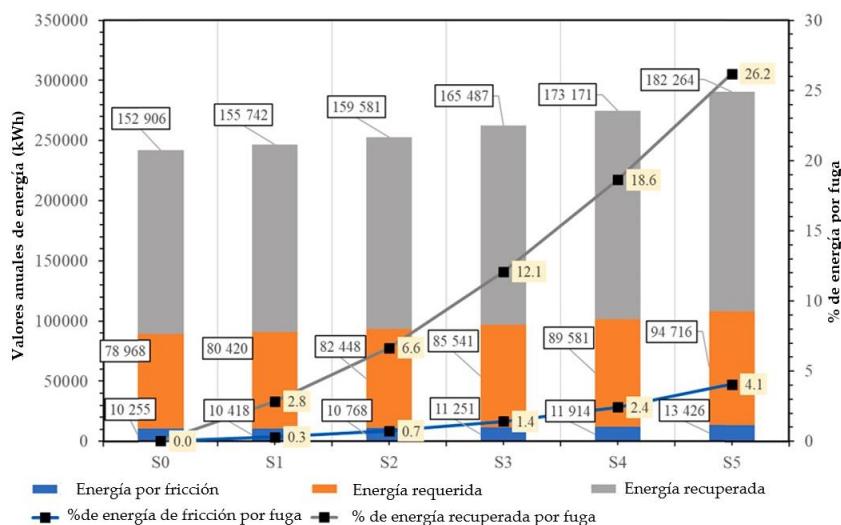

Figura 34. Valores anuales de energía para diferentes escenarios

El primer procedimiento "simulated annealing" tiene como objetivo determinar la ubicación óptima de las *PAT* (IV). En esta etapa se definieron y aplicaron las funciones objetivo en el proceso de optimización, estas funciones son: maximizar (E_{TR}), la reducción del volumen fugado $(\varDelta V_L)$ y el *VAN*. El proceso de optimización realiza entre 140 a 2640 iteraciones, dependiendo de las combinaciones y los parámetros de control de la simulación, estos fueron: temperatura inicial 10;

temperatura final 0.001; radio de enfriamiento 0.9 y la transición de pasos 10. Estos parámetros fueron definidos previamente mediante un análisis de sensibilidad.

Los resultados de la simulación muestran que el uso de tres sistemas de recuperación permite una recuperación potencial de alrededor del 80 % de la energía disponible en todos los escenarios. Adicionalmente, mientras más sistemas de recuperación se instalen las fugas irán reduciéndose. Si la función objetivo es la reducción de fugas el valor osciló entre 0.37 y 0.66. Respecto al *VAN*, la factibilidad reduce a medida que el número de sistemas de recuperación incrementa. Este procedimiento permitió la preselección de las máquinas de acuerdo con los puntos operacionales teóricos, para desarrollar el segundo proceso de optimización.

El desarrollo del segundo procedimiento de optimización "simulated annealing" se realiza para determinar el número de máquinas a implementarse en la red. En esta etapa se utiliza una base de datos de 110 *PAT* que están definidas a partir de su valor de velocidad específica. El procedimiento elige la mejor máquina para cada escenario en una de las líneas definidas. El modelo desarrolla un procedimiento iterativo que selecciona la mejor estrategia de regulación *(RS)* para evaluar cada una de las funciones objetivo: (E_{TR}), (ΔV_L) o el *VAN*.

La aplicación del paso V se muestra en la Figura 35a y 35b, mediante el mapa de influencia en el que opera la optimización de selección de la mejor máquina para la línea 2004 en el escenario S1(a) y S5(b).
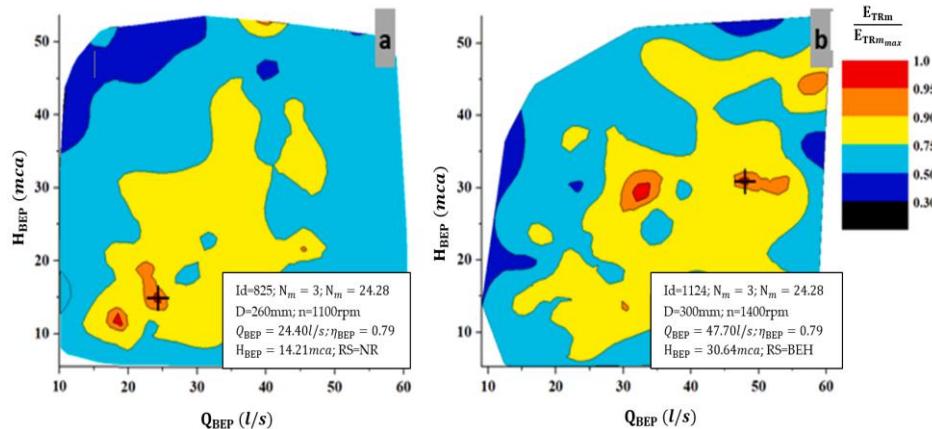

Figura 35. Sistema de recuperación instalado en línea 2004

La cruz negra indica la máquina seleccionada. En cada caso, las máquinas seleccionadas son diferentes, mostrando la estrategia de regulación, velocidad

específica, velocidad de rotación de la máquina, así como el punto de mejor eficiencia de la máquina. El ejemplo de la Figura 35, muestra como la optimización garantiza el mejor ratio de E_{TR}.

La variabilidad de la máquina muestra la importancia de considerar las fugas a la hora de elegir los sistemas de recuperación. Al analizar S1, el punto de mejor eficiencia de la máquina es 24.4 l/s y 14.21 mca. Si se analiza S5, el punto de mejor eficiencia de la máquina aumenta un 195 y un 205 % en particular, 47.7 l/s y 30.64 mca.

La Tabla 3939 muestra un ejemplo de la selección optimizada de *PAT* para el escenario 2 cuando la función objetivo es el *VAN*. Los resultados muestran que la energía anual recuperable está por encima de 32000 kWh y el volumen de las fugas anuales disminuirá por encima de 18000 m³, utilizando tres sistemas de recuperación.

Tabla 39. Ejemplo de selección optimizada de *PAT* para S2 cuando la función objetivo es el *VAN*

N	1	2		3		
ID Ubicación	2004	2004	2092	2004	2092	2138
n_s (rpm)	24.28	18.59	9.3	18.59	9.3	5.54
N_m	2	2	2	2	2	1
D (mm)	240	220	134	220	134	260
n (rpm)	2000	1400	3100	1400	3100	800
Q_{BEP} (l/s)	34.89	17.45	3.85	17.45	3.85	3.62
H_{BEP} (l/s)	40.02	22.38	59.38	22.38	59.38	18.74
RS	*BEH*	*NR*	*BEH*	*RN*	*BEH*	*NR*
Anual E_{TR} (kWh)	32456	28570	1932	28570	1932	1179
P (kW)	11.55	7.14	1.41	7.14	1.41	0.55
Reducción de fugas (m³)	13947	17004	206	17004	206	708
VAN (€)	44421	51421	1531	51421	1531	48896
IRR (años)	11.83	10.36	12.27	10.36	12.27	11.4

Los *KPI* en redes con *PAT* instaladas permiten caracterizar la gestión de los sistemas de agua y son necesarios para determinar la eficiencia de un sistema, atendiendo a criterios ambientales, energéticos y volumétricos.
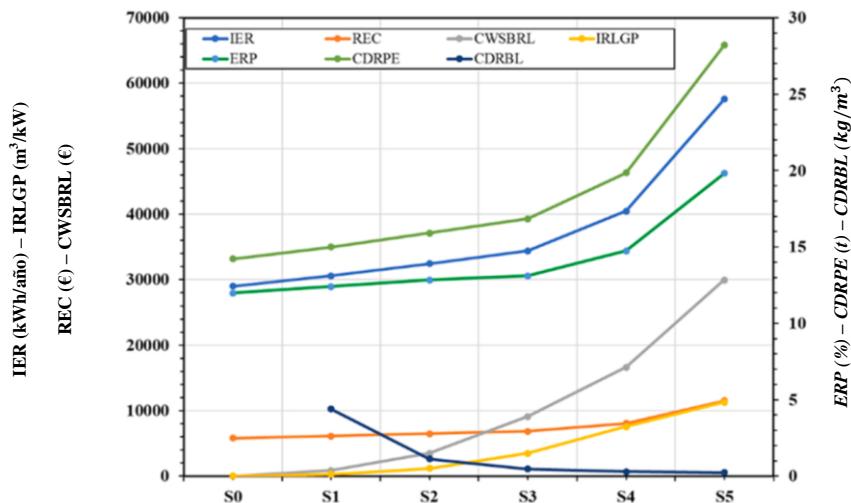
Figura 36. Indicadores de rendimiento para cada escenario

Como se muestra en la Figura 36, la energía anual recuperada *(IER)* osciló entre valores de 29010 y 57543 kWh. Otro índice propuesto en esta tesis es el volumen de agua recuperado por energía instalada *(IRLGP)* que está relacionado con *IER*. Este índice demuestra la ventaja de incorporar *PAT* en la red. La reducción de CO_2 por energía producida *(CDRPE)* mostró la misma tendencia del porcentaje de energía recuperable *(ERP)* y la reducción de CO_2 por cada metro cúbico de agua recuperado por fugas *(CDRBL)* disminuyó de 4.38 a 0.24 kg de emisiones de CO_2.

B. Aplicación de metodología de optimización para la selección y ubicación de PAT en redes de abastecimiento urbanas, bajo la influencia de fugas y evaluación de indicadores de sostenibilidad.

La metodología es totalmente descrita en el (Artículo 4).

Improve leakage management to reach sustainable supply networks through by green energy systems. Optimized case study.

En este estudio se tiene como objetivo la aplicación de una metodología que permite definir la ubicación y selección de *PAT* en una red urbana de abastecimiento de agua ubicada en la ciudad de Manta (Ecuador) que se muestra en la Figura . La empresa local realizó la entrega de información de un tramo de la red que abastece 100000 habitantes, como: (i) la topología de la red, (ii) base de datos del caudalímetro principal y (iii) del consumo mensual de cada vivienda para el año 2021. Se estableció un patrón de consumo horario para desarrollar un análisis energético horario y una evaluación del volumen de agua en función de las fugas. La red es de material *PVC* y sus diámetros varían de 59 a 581 mm. El caudal medio aportado a la red es de 231 l/s y la presión de 35.14 mca. El porcentaje de fugas es de 43 %, de acuerdo con los datos utilizados.

Figura 37. Red de abastecimiento urbano en Manta (Ecuador)

La investigación propuesta desarrolló una nueva metodología que permite la autocalibración de fugas en el suministro de agua, conociendo el caudal inyectado y

el volumen consumido en las redes de agua. El modelo también es capaz de definir el patrón de consumo de ajuste, discretizar el volumen fugado en los diferentes tipos y se puede aplicar en redes malladas considerando valores horarios. El análisis para discretizar fugas entre pérdidas aparentes y reales se desarrolló inicialmente para calibrar el modelo a través del registro de los contadores y el caudalímetro instalado en la línea principal de la red.

La metodología de optimización mostrada en la Figura 38 se divide en 6 pasos.

En cada uno requiere de entradas y condiciones para ser ejecutado. En el primer paso se realiza el modelado de la red, para posteriormente calibrar el modelo de fugas (paso 2) y calcular el balance de energía (paso 3).

El paso 4 de la metodología corresponde a un procedimiento "simulated annealing", donde se determina la ubicación óptima de los sistemas de recuperación en las etapas. El paso 5 determina a través del procedimiento "simulated annealing" la selección óptima de las *PAT*. En este paso se busca la selección del número de máquinas a instalar y la mejor estrategia de regulación. Para seleccionar la máquina, se utiliza el *BEP* de la base de datos de 110 *PAT*. La definición de las curvas de operación implementadas se establece según la metodología propuesta en el Artículo 2.

En los pasos 4 y 5 se definen las funciones de maximización de (E_{TR}); la reducción (ΔV_L); y la minimización de *LCOE*. La función *LCOE* solo tiene en cuenta los gastos (inversión inicial y costes anuales) y no depende de los precios de la energía. Esta función es una medida del coste actual neto promedio de generación de electricidad para un generador durante su vida útil y es utilizado para la planificación de inversiones y para comparar diferentes métodos de generación de electricidad de forma consistente.

Finalmente (paso 6), se definen las reglas de operación y los indicadores claves de rendimiento de las redes.
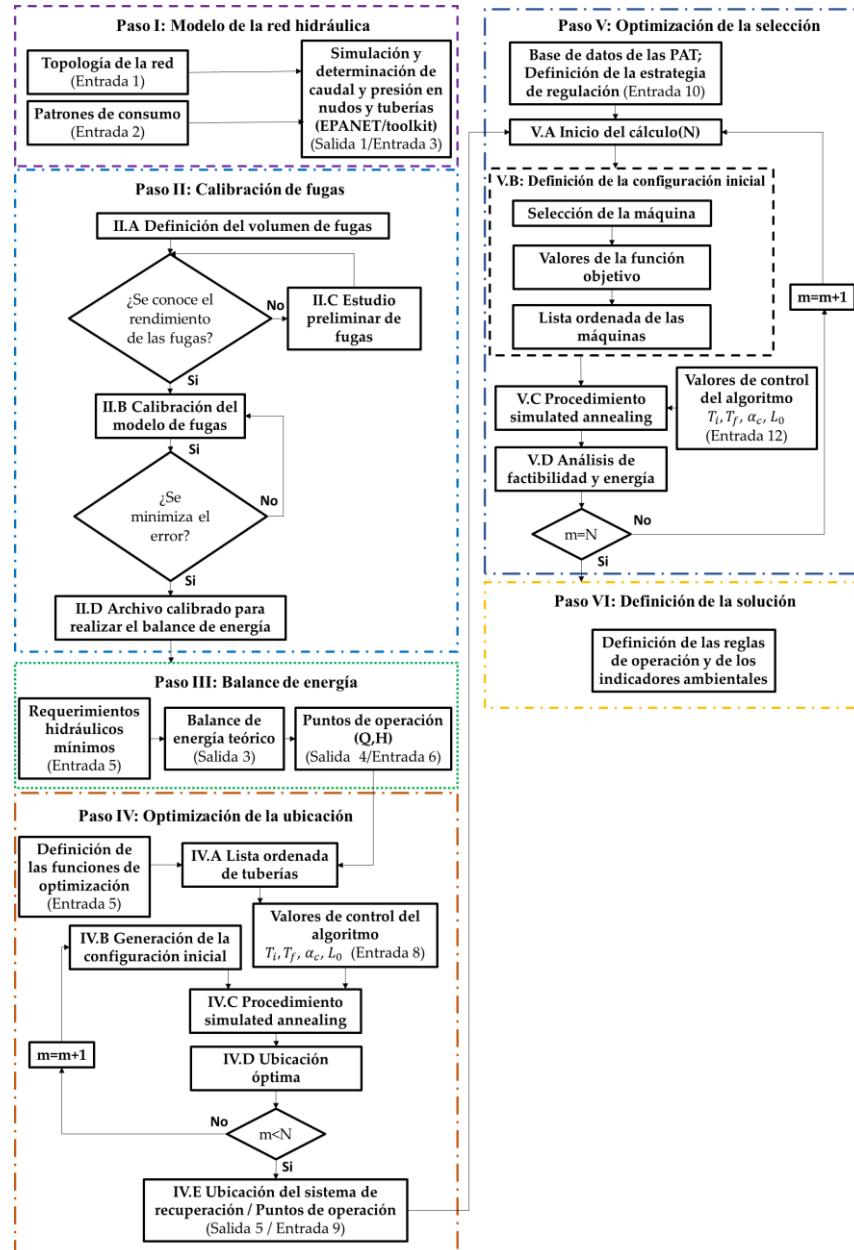
Figura 38. Metodología de optimización propuesta

En el análisis de sensibilidad para la calibración del modelo de fugas se desarrollaron siete hipótesis estableciendo diferencias entre pérdidas reales y aparentes, estas

hipótesis varían su peso de esta entre 0 y 1, como se observa en la Figura 39a. En el procedimiento de calibración se consideró diferentes *KEI*, como: *PBIAS-MRD-RMSE* y *MAD*. Previamente, se estableció una primera calibración del coeficiente α considerando las fugas en un 43 %. Para todos los casos, los *KEI* presentaron excelentes ajustes.

El valor de este coeficiente fue de 0.65 ya que todos los valores del coeficiente β, que oscilan entre 10^{-5} y 10^{-4}, son inferiores al porcentaje límite de fugas. El volumen registrado y simulado permitió establecer el porcentaje de error en la calibración del modelo, los errores estuvieron por debajo del 1.5 % en todos los meses, considerando un error promedio anual igual al 0.55 %.

|	1h	2h	4h	8h	16h	24h
■ H1 (0;1)	5.491	5.491	5.491	5.491	5.546	5.491
■ H2 (0.25;0.75)	5.382	5.382	5.382	5.382	5.433	5.382
■ H3 (0.40;0.60)	5.349	5.349	5.349	5.349	5.395	5.349
■ H4 (0.50;0.50)	5.274	5.274	5.274	5.274	5.320	5.274
■ H5 (0.60;0.40)	5.308	5.308	5.308	5.308	5.369	5.308
■ H6 (0.85;0.15)	5.335	5.335	5.335	5.335	5.385	5.335
■ H7 (1;0)	5.342	5.342	5.342	5.342	5.390	5.342
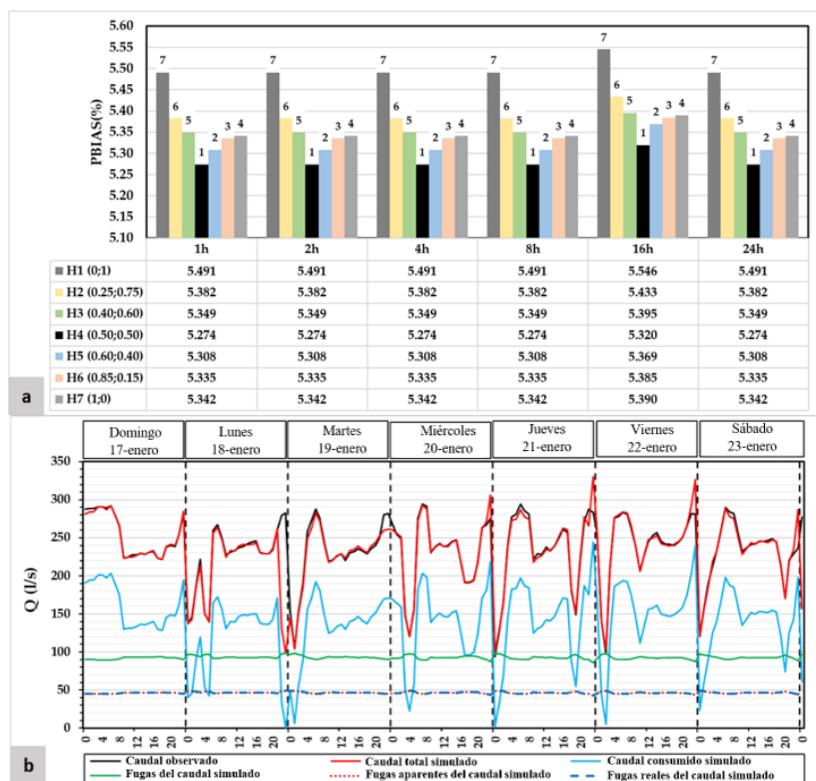
Figura 39. (a) Calibración de pérdidas considerando el valor PBIAS; (b) Comparación entre el caudal observado y los valores simulados cuando se calibró el modelo. Ejemplo de una semana

La Figura 39b muestra el ejemplo de la tendencia entre el caudal registrado y simulado en el modelo calibrado. Este utilizó la hipótesis 4 para establecer las

pérdidas aparentes y reales; y se utilizó para desarrollar el balance de energía y el procedimiento de optimización.

El primer procedimiento de optimización establece las mejores líneas para instalar sistemas de recuperación. Considerando la función objetivo 1 *(OF1)*, la energía anual teórica recuperable (E_{TR}) osciló entre 47507 y 104123 kWh, la reducción de fugas (ΔV_L) de 206792 a 379652 m³ y el *LCOE* de 0.186 a 0.264 €/kWh, como se muestra en la Tabla 40.

Tabla 40. Resultados preliminares cuando se define paso D.I para ubicar la mejor línea

Línea 1	Línea 2	Línea 3	Línea 4	Línea 5	E (kWh)	Reducción de fugas (m³)	*LCOE* (€/kW)	P (kW)
Función objetivo 1								
10615	-	-	-	-	47507	206792	0.186	8.18
10615	10610	-	-	-	66163	282333	0.216	12.15
10026	10222	10610	-	-	83355	313553	0.206	14.88
10026	10610	10615	10618	-	94069	350492	0.244	19.58
10026	10208	10222	10610	10618	104123	379652	0.264	24.42
Función objetivo 2								
10620	-	-	-	-	46250	210204	0.190	8.05
10620	10591	-	-	-	62789	289398	0.228	12.19
10227	10591	10615	-	-	70839	339118	0.307	16.94
10013	10266	10591	10620	-	86843	375039	0.262	20.14
10013	10266	10591	10620	10663	96533	409669	0.294	24.62
Función objetivo 3								
10942	-	-	-	-	18173	36206	0.163	2.88
10222	10794	-	-	-	43432	119888	0.207	8.28
10013	10266	10971	-	-	57209	199560	0.204	11.51
10013	10266	10620	10942	-	83387	341547	0.227	17.79
10224	10237	10708	10794	10971	89506	325469	0.242	21.23

Los resultados de la segunda simulación del procedimiento de "simulated annealing" se muestran en la Tabla 41, se realizó utilizando la línea 10615 cuando solo se utilizó un sistema de recuperación. La máquina utilizada es de tipo radial, utilizando tres máquinas diferentes conectadas en paralelo, el *BEP* fue de 62.64 l/s y 15.95 mca. El sistema de recuperación se reguló operando en velocidad de rotación nominal *(NR)* y la energía recuperada anual fue de 23625 kWh, aproximadamente. Esta configuración mostró una reducción anual de fugas de 96726 m³. Los valores de

energía final y fugas disminuyeron un 50 % en comparación con el "simulated annealing" preliminar. Esto es debido a que el procedimiento preliminar donde se determina la ubicación es teórico, se asume que recupera toda la altura, y por lo tanto las presiones son más pequeñas. Cuando se realiza el procedimiento de selección, solamente se recupera la altura que le da la máquina, siendo esta menor que la teórica.

Tabla 41. Resultados de la optimización cuando la metodología considera un sistema de recuperación

Iteración	1	2	3	4	5
Configuración	1	1	1	1	1
Línea	10615	10615	10615	10615	10615
ID	128	128	128	128	128
n_{st} (rpm) [m, kW]	23.51	23.51	23.51	23.51	23.51
N_m	3	3	3	3	3
D(mm)	400	400	400	400	400
N (rpm)	750	750	750	750	750
Q_{BEP}(l/s)	62.64	62.64	62.64	62.64	62.64
H_{BEP}(mca)	15.95	15.95	15.95	15.95	15.95
SR (Estrategia de regulación)	*NR*	*NR*	*NR*	*NR*	*NR*
E_{TR} anual (kWh)	52491	23746	23565	23572	23624
Reducción de fugas (m³)	96102	96567	96722	96358	96725
LCOE (€/m³)	0.233	0.1605	0.1659	0.1678	0.1574
P (kW)	14.83	14.98	15.95	16.42	14.04
Diferencia de energía (%)	-	54.76	0.76	-0.03	-0.22
Diferencia de reducción de fuga (%)	-	-0.48	-0.16	0.38	-0.38

Se analizó también utilizando dos sistemas de recuperación en las líneas 10615 y 10610. El *BEP* definido de la base de datos fue de 42.28 l/s y 22.98 mca para la línea 10615. Cuando se optimizó la línea 10610, el *BEP* era de 37.12 l/s y 7.58 mca. En ambos casos, la estrategia de la regulación fue *BEH*, el número de máquinas utilizadas en paralelo fue de tres y la energía recuperada anual final fue de 34490 kWh. Cuando se analizó un sistema de recuperación, el valor de *LCOE* fue de 0.157 €/m³. Si se instalan dos sistemas de recuperación, este valor sería de 0.189 €/m³.

La Figura 40 muestra la mejor solución en comparación con las relaciones disponibles. Estos ratios fueron el ratio de energía (β_E), que define la relación de la energía recuperada entre la energía máxima recuperada, el ratio *LCOE* (β_{LCOE}) que

define la relación de *LCOE* y el *LCOE* mínimo; y el ratio de fugas β_L que define la relación entre la reducción de fugas y la reducción de fugas máxima. La Figura 40a muestra esta interacción en la mejor solución alcanzando una relación de energía de 0.78, $\beta_L = 0.92$ y $\beta_{LCOE} = 1.5$.

La Figura 40b muestra la integración de la mejor solución cuando se analizaron dos sistemas de recuperación. Este caso muestra la interacción entre $\beta_E \beta_L$ y el β_{LCOE}, alcanzando valores de 0.8 y 1.1 respectivamente.
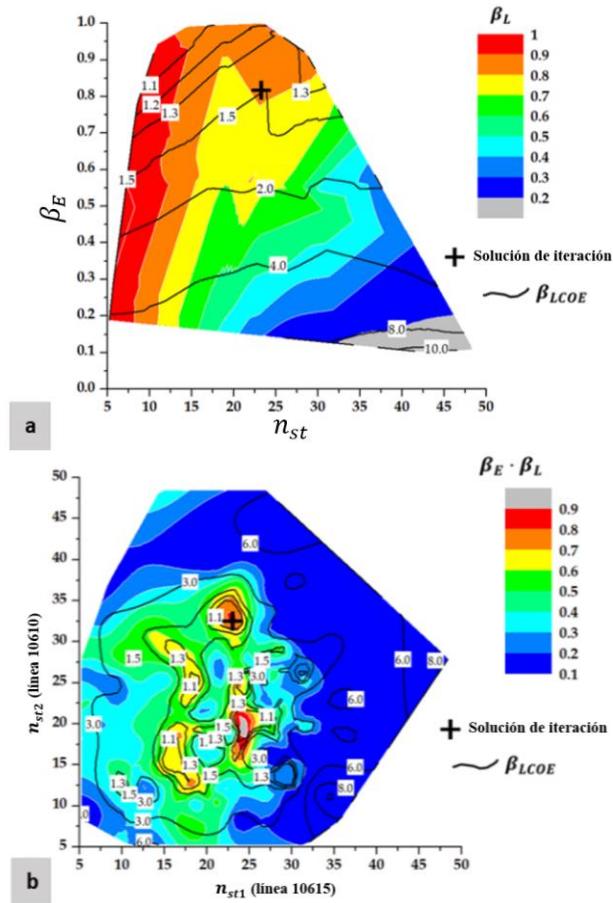
Figura 40. (a) Solución de iteración cuando se instaló un sistema de recuperación. (b) Solución iterativa cuando se instalan dos sistemas de recuperación

La aplicación de 1 o 2 sistemas de recuperación mostraron que la metodología propuesta de optimización estableció la mejor solución posible considerando la

base de datos disponible de *PAT*. La solución propuesta implicó una reducción de 96726 y 120246 m³ de agua, cuando se analizaron uno o dos sistemas de recuperación, respectivamente.

Se utilizaron diferentes indicadores para mostrar la variación de estos indicadores en las diferentes iteraciones y la decisión final del procedimiento de optimización. Los resultados de estos indicadores se muestran en la Tabla 42.

Tabla 42. Indicadores de sostenibilidad cuando se instala 1 y 2 sistemas de recuperación

Tipo	Abreviación	Unidad	Situación Inicial	1 Sistema de recuperación	2 Sistemas de recuperación
Energía	IED	Adimensional	0.088	0.160	0.178
	IAE	kWh	600483	592677	590717
	IEFW	kWh/m^3	0.088	0.088	0.088
	IER	kWh	0	23624	34490
	ERP	%	0	3.99	5.84
Economía	IAAE	kWh	600483	569052	556227
	IAEFW	kWh/m^3	0.088	0.084	0.083
	IRLGP	m^3/kW	0	6889	4510
	REC	€	0	4724	6898
Medio Ambiente	CWSBRL	€	0	24181	30061
	CDRPE	t	0	11.58	16.9
	CDRBL	$kg\ CO_2/m^3$	0	0.12	0.14

Se evaluaron tres escenarios diferentes: (i) la situación inicial de la red donde no existen dispositivos de recuperación, (ii) cuando existe un sistema de recuperación instalado y; (iii) dos sistemas de recuperación instalados. Se observa que para situación inicial no existirá energía recuperada, ahorros económicos o mejoras en los indicadores ambientales. En caso de instalar un sistema de recuperación es posible recuperar 23624 kWh de energía por año, un coste de energía eléctrica recuperable por instalación de *PAT* de 4725 € y una reducción de 11.58 t de CO_2. Si se instalaran dos sistemas de recuperación es posible recuperar 34490 kWh de energía por año, un coste de energía eléctrica recuperable por instalación de *PAT* de 6898 € y una reducción de 16.9 t de CO_2.

7. Conclusiones y Desarrollos Futuros

La presente tesis determinó los rendimientos volumétricos y energéticos en diferentes redes de distribución presurizadas. En busca de la aplicación de nuevas tecnologías para la mejora de la sostenibilidad en sistemas de distribución, se propone una metodología de optimización basada en estrategias de regulación para la mejora de indicadores de sostenibilidad a través de la instalación de micro generación eléctrica en sistemas de distribución presurizados. Las conclusiones y los futuros desarrollos sobre esta temática se discuten en el presente capítulo.

7.1. Conclusiones

La principal conclusión de esta tesis **es la propuesta de una metodología que permite a través de un proceso de optimización, la definición de la ubicación y selección de *PAT* en redes presurizadas de abastecimiento de agua con la influencia de las fugas.** Cada una de las etapas de la tesis fue mostrada en el capítulo 4, donde se estableció la importancia del estudio de esta temática. Las conclusiones se estructuran en cuatro puntos principales:

1. La fase de contextualización **mostró** la necesidad de incorporar el análisis de fugas **en la localización, selección y evaluación energética** de sistemas de micro generación eléctrica. **El estudio de fugas, los métodos de calibración y su aplicación en casos de estudio fueron mostrados en esta etapa de análisis,** dando respuesta al objetivo 1 **de esta tesis.**

1.1. Las redes de distribución de agua con fugas generan pérdidas volumétricas de agua potable, afectando la economía de las empresas gestoras.

I. Las pérdidas de agua representan un 8 a 24 % en países desarrollados, 15 a 24 % en países recién industrializados y 25 a 45 % en países en desarrollo.

II. Se estima un monto de 111264721 € anuales por pérdidas de agua en las redes analizadas de los casos de estudio.

1.2. El análisis realizado a los 45 casos de estudio permitió extraer información relevante del funcionamiento de las redes, con lo que se obtuvo las siguientes conclusiones:

I. La eficiencia media volumétrica en las redes de distribución de agua es del 73 %. La media respecto a las fugas es del 27 %.

II. El coste medio anual por pérdidas económicas en el volumen de agua en las redes de distribución asciende los dos millones de euros.

III. La pérdida media anual de energía perdida por fugas en las redes de distribución es de 178600 kWh.

IV. Los casos de estudio de redes presurizadas con *PAT* instaladas muestran una reducción considerable en la presión de la red, disminuyendo el nivel de fugas entre 4 y 63 %, mientras que la energía recuperada se estimó entre 28470 y 714670 kWh/año.

1.3. La extracción de información de las redes permitió definir diferentes *KPI* que permitieron la caracterización de la red analizada bajo criterios hidráulicos, económicos, energéticos y medio ambientales. Estos indicadores buscan la mejora en los objetivos de desarrollo sostenible.

1.4. Esta nueva investigación muestra la importancia de desarrollar procedimientos de optimización en los que las fugas sean consideradas como una variable de decisión. El análisis de las fugas deberá incluir la influencia de estas pérdidas de agua en la selección y regulación de los sistemas *PAT*, y, por tanto, su impacto en la energía recuperada.

2. Se desarrolló una expresión de modificación de las leyes de semejanza aplicadas a *PAT* operando a velocidad variable, como respuesta al objetivo 2.

2.1. Se propone una nueva función basada en los parámetros de Suter y el *BEP*. Estos parámetros adimensionales permiten analizar y comparar la propia máquina trabajando a diferentes velocidades. Los parámetros fueron considerados para estimar la energía recuperable en las máquinas al operar en la zona *VOS*.

2.2. Se calculó los valores de los *KEI* comparándolos con cada valor experimental y calculando el valor medio para las diez funciones propuestas. Se obtuvo resultados que mejoraban las expresiones previamente publicadas.

I.   Para la curva *BEH*, la función que mostró el mínimo error promedio fue F_2. *RMSE*, *MAD* y *MRD* fueron 0.1035, 0.0735 y 0.0628, respectivamente.

II.   Cuando se analiza la *BPH*, la función de mejor ajuste fue F_6.

III. Al considerar *BPF*, F_2 fue la expresión con menos error, pero F_6 está cerca, como en el caso de *BEH*. Se eligió F_6 para definir la curva característica de la máquina cuando se compararon otros métodos para definir el *BEH*, *BPH* y *BPF*.

2.3. Las regresiones empíricas propuestas se aplicaron a una máquina experimental para mostrar la precisión de las expresiones aplicadas en estudios de casos reales. Se utilizaron los datos experimentales publicados de la máquina NK140 125/127. Como principales resultados se obtuvo:

I.   Cuando se midió el error, *RMSE* y *MRD* fueron 0.077 y 0.059 respectivamente, siendo *BIAS* igual a 0.0585.

II.   Los valores de error disminuyeron alrededor de un 65.6 % en ambos errores cuando se compararon con las leyes de semejanza.

III. Las expresiones indican buen ajuste para todo el rango n_{st}, mostrando su utilidad en la implementación en modelos de optimización para la selección y ubicación de sistemas de micro generación eléctrica.
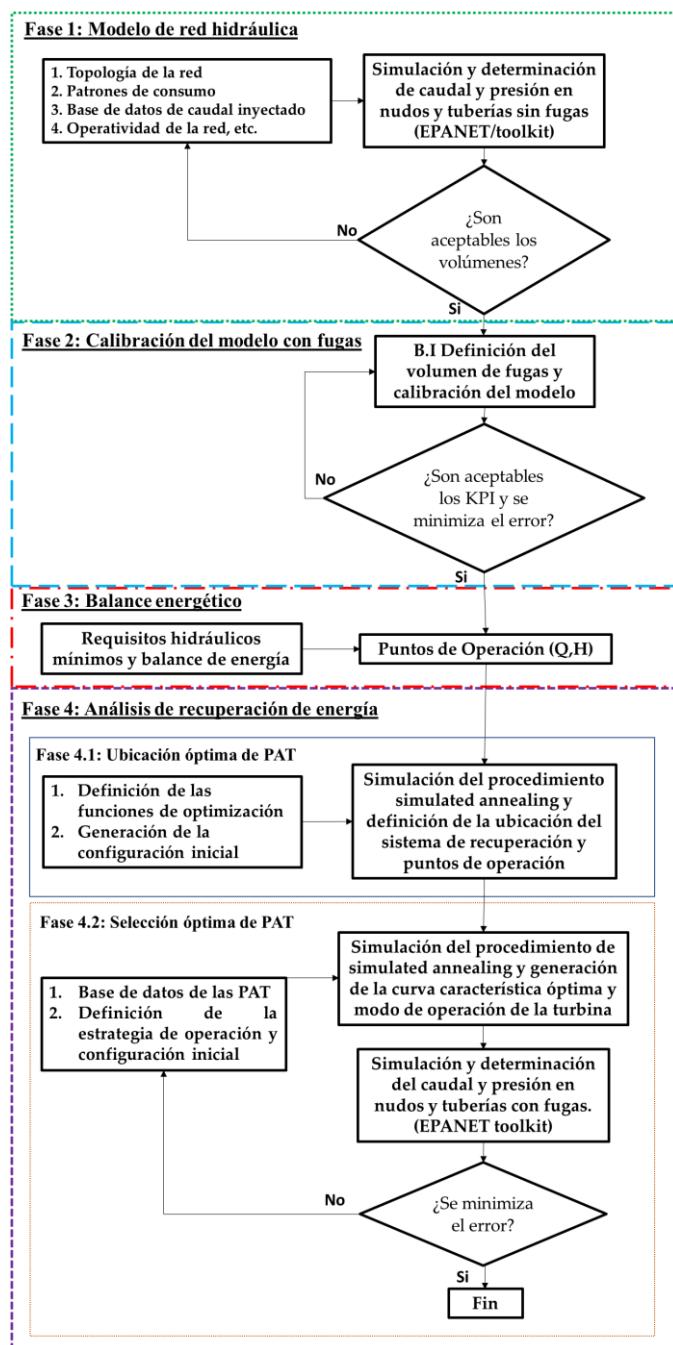
Figura 41. Propuesta de optimización desarrollada en la tesis

2.4. Las leyes de semejanza modificadas propuestas en este estudio reducen los índices de error entre un 8 y un 30 % en comparación con los métodos existentes, y pueden ayudar a los administradores de sistemas de agua a mejorar la precisión de las predicciones de energía.

3. **Se desarrolló** una metodología de optimización para la determinación de la ubicación y selección de *PAT* considerando la influencia de las fugas para la mejora de indicadores de sostenibilidad **en redes presurizadas urbanas y de riego.**

3.1. En la Figura 41 se muestra un diagrama resumen de la metodología en 4 fases, estas son:

(i) Modelo de la red, donde se determinan las presiones y caudales circulantes en la red hidráulica.

(ii) La calibración del modelo con fugas, que permite validar mediante índices de error la diferencia entre los volúmenes del modelo simulado respecto a los reales.

(iii) Balance energético, desarrollado a través de una serie de expresiones que permite estimar la energía teóricamente recuperable.

(iv) El análisis de la recuperación de energía, donde se estima la mejor ubicación de la *PAT* y se selecciona el número de dispositivos a instalar y su estrategia de regulación, desarrollándose así el **objetivo 3.**

Para cumplir el **objetivo 4** se desarrolló en la metodología un modelo que permite analizar la influencia de las fugas en la selección de las *PAT*. El modelo fue simulado a través de EPANET y permite definir un volumen de fugas y estas son calibradas hasta que los índices de error se minimicen.

La fase (4.2) de la metodología mostrada en la Figura 41permitió la selección óptima de las *PAT* y en ella se estudió el impacto de las fugas en la variación de caudales y alturas turbinadas, así como la repercusión en su selección, esto permitió cumplir el **objetivo 5.**

Para dar respuesta al **objetivo 6**, se definieron varios indicadores de eficiencia ligados a los *ODS*, bajo criterios hidráulicos, económicos y ambientales, que permiten caracterizar las condiciones de la red hidráulica en función de las fugas y de los sistema.s de recuperación instalados. Los

dos casos de estudio mostrados en el literal 3.2 y 3.3 respectivamente, dan respuesta a la ejecución del **objetivo 7**, cuando la metodología es aplicada a redes existentes de abastecimiento urbano y de riego.

3.2. El primer caso de estudio se trata de una red de riego ubicada en Vallada (España). La definición de las expresiones de cálculo de fugas permitió incorporar en la metodología el análisis del volumen de agua fugado en las redes de distribución y la influencia que suponían la selección de las *PAT* en ellas, dando respuesta al **objetivo 4** de esta tesis. Así mismo, se analizó la influencia de las fugas en la selección de las máquinas y el impacto que suponen las fugas por la variación de caudales y alturas turbinas, esto dió respuesta al **objetivo 5**. La recuperación anual de energía se estimó con valores alrededor de 32000 kWh y una reducción anual de volumen fugado de 18000 m^3. Las emisiones de CO_2 disminuyeron de en un 95 % por cada m^3 de agua recuperado por fugas.

3.3. La aplicación de la metodología propuesta se realizó también en el segundo caso de estudio, en una red urbana ubicada en Manta (Ecuador). Al instalarse un sistema de recuperación con 3 máquinas es posible generar anualmente 23624 kWh de energía, reducir el volumen fugado de 96000 m^3 de agua y 11.58 t de CO_2. Instalando 2 sistemas de recuperación con 3 máquinas se recuperaría anualmente 34490 kWh de energía y reducirían 120000 m^3 de agua y 16.9 t de CO_2 al año.

3.4. La aplicación de esta metodología está ligada a los indicadores de los objetivos de desarrollo sostenible *(ODS)*, respecto a:

- ✓ Garantizar la disponibilidad de agua y su gestión sostenible *(ODS6)*.
- ✓ Garantizar el acceso a una energía asequible, fiable, sostenible y moderna para todos *(ODS7)*.
- ✓ Promover el crecimiento económico inclusivo y sostenible, el empleo y el trabajo decente para todos *(ODS8)*.
- ✓ Construir infraestructuras resilientes, promover la industrialización sostenible y fomentar la innovación *(ODS9)*.
- ✓ Lograr que las ciudades sean más inclusivas, seguras, resilientes y sostenibles *(ODS11)*.
- ✓ Adoptar medidas urgentes para combatir el cambio climático y sus efectos *(ODS13)*.

Teniendo en cuenta que estos se relacionan con criterios económicos, ambientales y energéticos, en la Tabla 43 se muestra la relación de cada uno de los indicadores propuestos en está tesis con los *ODS*.

Tabla 43. Relación de indicadores de eficiencia con *ODS*

Tipo	Indicadores	ODS relacionados
	IED	7, 9, 11
	IAE	7, 9, 11, 13
	IEFW	7, 9, 11, 13
Energéticos	*IER*	7, 9, 11, 13
	ERP	7, 9, 11, 13
	IAAE	7, 9, 11, 13
	IAEFW	6, 7, 8, 9, 11, 13
Económicos	*IRLGP*	6, 7, 8, 9, 11, 13
	REC	7, 8, 9, 11, 13
	CWSBRL	6, 7, 8, 9, 11, 13
Medio Ambientales	*CDRPE*	6, 7, 8, 9, 11, 13
	CDRBL	6, 7, 8, 9, 11, 13

7.2. Desarrollos futuros

Esta investigación permitió desarrollar una metodología para la la estimación de la energía recuperable en las redes de distribución de agua, la reducción de fugas, la reducción de costes en la operación y de gases de efecto invernadero a través de la instalación de *PAT*. Este estudio permite crear nuevas líneas de investigación, siendo una oportunidad para desarrollar futuros trabajos. Algunas de estas líneas son:

(i) Respecto a la calibración, las investigaciones futuras deberían centrarse en validar la metodología de calibración durante la fase de diseño en los sistemas de distribución, considerando la variabilidad de operación en las estaciones de bombeo.

(ii) Respecto al desarrollo de expresiones para la estimación de curvas características, las investigaciones futuras deberían centrarse en el desarrollo de análisis de máquinas axiales. Estas máquinas son

importantes en los sistemas de agua a presión porque hay puntos de recuperación potenciales en los que el flujo es alto, pero la altura recuperable es baja.

(iii) Respecto a la metodología, los trabajos futuros deben centrarse en aplicar la medición de indicadores sostenibles a los diferentes sistemas de abastecimiento y desarrollar nuevos procedimientos de optimización e indicadores bajo criterios: ambientales, hidráulicos y energéticos, que apoyen la gestión sostenible de los sistemas hidráulicos.

(iv) Respecto a la metodología aplicada en la red de distribución urbana, la metodología propuesta se limitó en la consideración del volumen mensual consumido para calibrar las fugas. Esto podría adaptarse para calibrar las fugas de acuerdo con el flujo a lo largo del tiempo en desarrollos futuros, si los sistemas de agua hubieran instalado sistemas de lectura de medidores remotos para aumentar el número de usuarios de registro y más medidores de flujo en la red que podrían sectorizarlo y discretizarlo en el análisis.

8. Referencias

[1]   R. Moasheri, M. J. Ghazizadeh, and M. Tashayoei, "Leakage detection in water networks by a calibration method," in *Flow Measurement and Instrumentation*, vol. 80, no. June, Tehran, Iran: Elsevier Ltd, 2021, p. 101995.

[2]   M. Maskit and A. Ostfeld, "Leakage Calibration of Water Distribution Networks," *Procedia Eng.*, vol. 89, pp. 664–671, Jan. 2014, doi: 10.1016/J.PROENG.2014.11.492.

[3]   F. García-Ávila, A. Avilés-Añazco, J. Ordoñez-Jara, C. Guanuchi-Quezada, L. Flores del Pino, and L. Ramos-Fernández, "Pressure management for leakage reduction using pressure reducing valves. Case study in an Andean city," *Alexandria Eng. J.*, vol. 58, no. 4, pp. 1313–1326, 2019, doi: 10.1016/j.aej.2019.11.003.

[4]   M. Farley, *Leakage Management and Control. A BEST PRACTICE TRAINING MANUAL.* Geneva, Switzerland, 2001.

[5]   Winarni W., "Infrastructure Leakage Index (ILI) as Water Losses Indicator," *Civ. Eng. Dimens.*, vol. 11, no. 2, pp. 126–134, 2009.

[6]   Y. Rajani, B., and Kleiner, "Comprehensive review of structural deterioration of water mains: physically based models," *Urban Water 3*, vol. 3, no. 3, Ottawa, Canada, pp. 151–164, 2001.

[7]   J. Almandoz, E. Cabrera, F. Arregui, E. Cabrera, and R. Cobacho, "Leakage Assessment through Water Distribution Network Simulation," *Journal of Water Resources Planning and Management*, vol. 131, no. 6, Valencia, Spain, pp. 458–466, 2005.

[8]   H. F. Duan, B. Pan, M. Wang, L. Chen, F. Zheng, and Y. Zhang, "State-of-the-art review on the transient flow modeling and utilization for urban water supply

system (UWSS) management," *J. Water Supply Res. Technol. - AQUA*, vol. 69, no. 8, pp. 858–893, 2020, doi: 10.2166/aqua.2020.048.

[9]   K. B. Adedeji, Y. Hamam, B. T. Abe, and A. M. Abu-Mahfouz, "Towards Achieving a Reliable Leakage Detection and Localization Algorithm for Application in Water Piping Networks: An Overview," *IEEE Access*, vol. 5, Pretoria, South Africa, pp. 20272–20285, 2017.

[10]   G. Cavazzini, G. Pavesi, and G. Ardizzon, "Optimal assets management of a water distribution network for leakage minimization based on an innovative index," *Sustainable Cities and Society*, vol. 54, no. September 2019, Elsevier, Padova, Italy, p. 101890, Mar. 01, 2020.

[11]   C. Giudicianni, M. Herrera, A. di Nardo, A. Carravetta, H. M. Ramos, and K. Adeyeye, "Zero-net energy management for the monitoring and control of dynamically-partitioned smart water systems," *J. Clean. Prod.*, vol. 252, p. 119745, Apr. 2020, doi: 10.1016/J.JCLEPRO.2019.119745.

[12]   H. Abdelmeguid and B. Ulanicki, "Pressure and leakage management in water distribution systems via flow modulation PRVs," *Water Distrib. Syst. Anal. 2010 - Proc. 12th Int. Conf. WDSA 2010*, vol. 41203, no. January, pp. 1124–1139, 2012, doi: 10.1061/41203(425)102.

[13]   K. Deb, A. Pratap, S. Agarwal, and T. Meyarivan, "A fast and elitist multiobjective genetic algorithm: NSGA-II," *IEEE Trans. Evol. Comput.*, vol. 6, no. 2, pp. 182–197, 2002, doi: 10.1109/4235.996017.

[14]   B. Ulanicki and P. Skworcow, "Why PRVs tends to oscillate at low flows," *Procedia Engineering*, vol. 89, Elsevier B.V., Leicester, UK, pp. 378–385, 2014.

[15]   S. Ebrahimi, A. Riasi, and A. Kandi, "Selection optimization of variable speed pump as turbine (PAT) for energy recovery and pressure management," *Energy Conversion and Management*, vol. 227, no. November 2020, Elsevier Ltd, Tehran, Iran, p. 113586, 2021.

[16]   H. Ramos and A. Borga, "Pumps as turbines: An unconventional solution to energy production," *Urban Water*, vol. 1, no. 3, Lisboa, Portugal, pp. 261–263, 1999.

[17]   M. Kramer, K. Terheiden, and S. Wieprecht, "Pumps as turbines for efficient energy recovery in water supply networks," *Renewable Energy*, vol. 122, Elsevier Ltd, Stuttgart, Germany, pp. 17–25, 2018.

[18]   D. Novara, A. Carravetta, A. McNabola, and H. M. Ramos, "Cost Model for Pumps as Turbines in Run-of-River and In-Pipe Microhydropower Applications," *Journal of Water Resources Planning and Management*, vol. 145, no. 5, USA, p. 04019012, 2019.

[19]   A. P. P. Da Silveira and H. Mata-Lima, "Energy audit in water supply systems: A proposal of integrated approach towards energy efficiency," *Water Policy*, vol. 22, no. 6, Lisboa, Portugal, pp. 1126–1141, 2020.

[20]   C. Macías Ávila, F. J. Sánchez-Romero, P. A. López-Jiménez, and M. Pérez-

Sánchez, "Definition of the operational curves by modification of the affinity laws to improve the simulation of pats," *Hydraul. Dyn. Calc. Simul. II. Water,* vol. 13, no. 14, pp. 1–17, 2021, doi: 10.3390/w13141880.

[21] J. W. Kim *et al.,* "Simultaneous efficiency improvement of pump and turbine modes for a counter-rotating type pump-turbine," *Adv. Mech. Eng.,* vol. 8, no. 11, pp. 1–14, 2016, doi: 10.1177/1687814016676680.

[22] M. Binama, W. T. Su, X. Bin Li, F. C. Li, X. Z. Wei, and S. An, "Investigation on pump as turbine (PAT) technical aspects for micro hydropower schemes: A state-of-the-art review," *Renew. Sustain. Energy Rev.,* vol. 79, no. April 2016, pp. 148–179, 2017, doi: 10.1016/j.rser.2017.04.071.

[23] A. Carravetta, G. Del Giudice, O. Fecarotta, and H. M. Ramos, "Pump as turbine (PAT) design in water distribution network by system effectiveness," *Water (Switzerland),* vol. 5, no. 3, pp. 1211–1225, 2013, doi: 10.3390/w5031211.

[24] O. Fecarotta and A. McNabola, "Optimal Location of Pump as Turbines (PATs) in Water Distribution Networks to Recover Energy and Reduce Leakage," *Water Resour. Manag.,* vol. 31, no. 15, pp. 5043–5059, 2017, doi: 10.1007/s11269-017-1795-2.

[25] F. Moazeni and J. Khazaei, "Optimal energy management of water-energy networks via optimal placement of pumps-as-turbines and demand response through water storage tanks," *Appl. Energy,* vol. 283, no. September 2020, p. 116335, 2021, doi: 10.1016/j.apenergy.2020.116335.

[26] G. M. Lima, E. Luvizotto, and B. M. Brentan, "Selection and location of Pumps as Turbines substituting pressure reducing valves," *Renew. Energy,* vol. 109, pp. 392–405, 2017, doi: 10.1016/j.renene.2017.03.056.

[27] G. J. Bonthuys, M. van Dijk, and G. Cavazzini, "Leveraging water infrastructure asset management for energy recovery and leakage reduction," *Sustain. Cities Soc.,* vol. 46, no. October 2018, p. 101434, 2019, doi: 10.1016/j.scs.2019.101434.

[28] S. Adachi, S. Takahashi, X. Zhang, M. Umeki, and H. Tadokoro, "Estimation of area leakage in water distribution networks: A real case study,. 13th Computer Control for Water Industry Conference, CCWI 2015," in *Procedia Engineering,* 2015, vol. 119, no. 1, pp. 4–12, doi: 10.1016/j.proeng.2015.08.846.

[29] C. A. M. Ávila, F. J. Sánchez-Romero, P. A. López-Jiménez, and M. Pérez-Sánchez, "Optimization tool to improve the management of the leakages and recovered energy in irrigation water systems," *Agric. Water Manag.,* vol. 258, p. 107223, Dec. 2021, doi: 10.1016/J.AGWAT.2021.107223.

[30] T. Mabhaudhi *et al.,* "Assessing progress towards sustainable development goals through nexus planning," *Water (Switzerland),* vol. 13, no. 9, pp. 1–13, 2021, doi: 10.3390/w13091321.

[31]   M. Pérez-Sánchez, F. Sánchez-Romero, H. Ramos, and P. López-Jiménez, "Calibrating a flow model in an irrigation network: Case study in Alicante, Spain," *Spanish J. Agric. Res.*, vol. 15, no. 1, p. e1202, 2017, doi: https://doi.org/10.5424/sjar/2017151-10144.

[32]   I. Rojek and J. Studzinski, "Detection and localization of water leaks in water nets supported by an ICT system with artificial intelligence methods as away forward for smart cities," *Sustainability*, vol. 11, no. 2, (Switzerland), 2019.

[33]   L. Öztürk, I., Uyak, V., Çakmakci, M., & Akça, "Dimension of water loss through distribution system and reduction methods in Turkey," *International Congress River Basin Management*, vol. 1, Maslak, Istanbul, pp. 22–24.

[34]   M. Maskit and A. Ostfeld, "Leakage calibration of water distribution networks," *Procedia Engineering*, vol. 89, Israel, pp. 664–671, 2014.

[35]   G. Germanopoulos, "A technical note on the inclusion of pressure dependent demand and leakage terms in water supply network models," in *Civil Engineering Systems*, vol. 2, no. 3, London, UK., 1985, pp. 171–179.

[36]   S. Meniconi, C. Capponi, M. Frisinghelli, and B. Brunone, "Leak Detection in a Real Transmission Main Through Transient Tests: Deeds and Misdeeds," *Water Resources Research*, vol. 57, no. 3, Italy, pp. 1–15, 2021.

[37]   H. F. Duan, B. Pan, M. Wang, L. Chen, F. Zheng, and Y. Zhang, "State-of-the-art review on the transient flow modeling and utilization for urban water supply system (UWSS) management," *Journal of Water Supply: Research and Technology - AQUA*, vol. 69, no. 8, China, pp. 858–893, 2020.

[38]   A. H. Ayati, A. Haghighi, and P. J. Lee, "Statistical Review of Major Standpoints in Hydraulic Transient-Based Leak Detection," *Journal of Hydraulic Structures*, vol. 5, no. 1, Juzestán, Irán, pp. 1–26, 2019.

[39]   F. Garcia, A. Avilés-Añazco, J. Ordoñez-Jara, and C. Guanuchi-Quezada, "Pressure management for leakage reduction using pressure reducing valves. Case study in an Andean City," *Alexandria Eng. J.*, vol. 58, no. 14, pp. 1313–1326, 2019, doi: 10.1016/j.ifacol.2018.09.626.

[40]   C. Capponi, M. Ferrante, A. C. Zecchin, and J. Gong, "Leak Detection in a Branched System by Inverse Transient Analysis with the Admittance Matrix Method," *Water Resour. Manag.*, vol. 31, no. 13, pp. 4075–4089, 2017, doi: 10.1007/s11269-017-1730-6.

[41]   N. Samir, R. Kansoh, W. Elbarki, and A. Fleifle, "Pressure control for minimizing leakage in water distribution systems," *Alexandria Engineering Journal*, vol. 56, no. 4, Faculty of Engineering, Alexandria University, Alexandria, Egypt, pp. 601–612, 2017.

[42]   H. Abdel Meguid, P. Skworcow, and B. Ulanicki, "Mathematical modelling of a hydraulic controller for PRV flow modulation," *Journal of Hydroinformatics*, vol. 13, no. 3, UK, pp. 374–389, 2011.

[43]   M. E. Ali, "Knowledge-Based Optimization Model for Control Valve Locations

in Water Distribution Networks," *Journal of Water Resources Planning and Management,* vol. 141, no. 1, p. 04014048, 2015.

[44]   E. Creaco and G. Pezzinga, "Multiobjective Optimization of Pipe Replacements and Control Valve Installations for Leakage Attenuation in Water Distribution Networks," *J. Water Resour. Plan. Manag.,* vol. 141, no. 3, p. 04014059, 2015, doi: 10.1061/(asce)wr.1943-5452.0000458.

[45]   S. Meniconi, B. Brunone, E. Mazzetti, D. B. Laucelli, and G. Borta, "Hydraulic characterization and transient response of pressure reducing valves: Laboratory experiments," *Journal of Hydroinformatics,* vol. 19, no. 6, Perugia, Italy, pp. 798–810, 2017.

[46]   S. Meniconi, B. Brunone, M. Ferrante, E. Mazzetti, D. B. Laucelli, and G. Bortac, "Transient effects of self-adjustment of pressure reducing valves. 13ht Computer Control fow Water Industry Conference, CCWI 2015," *Procedia Engineering,* vol. 119, no. 1, Elsevier B.V., Perugia, Italy, pp. 1030–1038, 2015.

[47]   M. De Marchis *et al.,* "Energy recovery in water distribution networks. Implementation of pumps as turbine in a dynamic numerical model. 12th International Conference on Computing and Control for the Water Industry, CCWI2013," *Procedia Engineering,* vol. 70, Elsevier B.V., Italy, pp. 439–448, 2014.

[48]   S. V. Jain and R. N. Patel, "Investigations on pump running in turbine mode: A review of the state-of-the-art," *Renewable and Sustainable Energy Reviews,* vol. 30, Elsevier, Ahmedabad, India, pp. 841–868, 2013.

[49]   T. AL-Washali, S. Sharma, F. AL-Nozaily, M. Haidera, and M. Kennedy, "Modelling the leakage rate and reduction using minimum night flow analysis in an intermittent supply system," *Water (Switzerland),* vol. 11, no. 1, 2018, doi: 10.3390/w11010048.

[50]   K. B. Adedeji, Y. Hamam, B. T. Abe, and A. M. Abu-Mahfouz, "Leakage detection and estimation algorithm for loss reduction in water piping networks," *Water (Switzerland),* vol. 9, no. 10, pp. 1–21, 2017, doi: 10.3390/w9100773.

[51]   D. Laucelli and S. Meniconi, "Water distribution network analysis accounting for different background leakage models," *Procedia Engineering,* vol. 119, no. 1, Elsevier B.V., Italy, pp. 680–689, 2015.

[52]   P. Darsana and K. Varija, "Leakage Detection Studies for Water Supply Systems—A Review," *Water Resources Management, Water Science and Technology Library,* Singapore, pp. 141–150, 2018.

[53]   S. Guo, T. Q. Zhang, W. Y. Shao, D. Z. Zhu, and Y. Y. Duan, "Two-dimensional pipe leakage through a line crack in water distribution systems," *J. Zhejiang Univ. Sci. A,* vol. 14, no. 5, pp. 371–376, 2013, doi: 10.1631/jzus.A1200227.

[54]   E. Morales, J. José, E. Cabrera, and R. Cobacho, *Método de los caudales minimos nocturnos: revisión de sus bases científicas, evaluación de errores*

potenciales y propuestas para su mejora, Universida., vol. 146. Valencia, Spain: Universidad Politécnica de Valencia, 2011.

[55]   A. Lambert, M. Fantozzi, and M. Shepherd, "Pressure: Leak flow rates using FAVAD: An improved fast-track practitioner's approach," *CCWI 2017 - 15th Int. Conf. Comput. Control Water Ind.*, no. September, 2017.

[56]   E. G. Sellés, *Caracterización y mejora de la eficiencia energética del transporte de agua a presión*. Valencia, Spain: Universidad Politécnica de Valencia, 2016.

[57]   A. Lambert, "What Do We Know About Pressure: Leakage Relationships in Distribution Systems?," *IWA Conf. Syst. Approach to Leakage Control Water Distrib. Syst.*, pp. 1–8, 2000.

[58]   L. A. Rossman, "The EPANET Programmer's Toolkit for Analysis of Water Distribution Systems," *WRPMD 1999 Prep. 21st Century*, pp. 1–10, 1999, doi: 10.1061/40430(1999)39.

[59]   I. F. García, D. Novara, and A. M. Nabola, "A model for selecting the most cost-effective pressure control device for more sustainable water supply networks," *Water (Switzerland)*, vol. 11, no. 6, 2019, doi: 10.3390/w11061297.

[60]   J. E. Van Zyl and C. R. I. Clayton, "The effect of pressure on leakage in water distribution systems," *Proc. Inst. Civ. Eng. Water Manag.*, vol. 160, no. 2, pp. 109–114, 2007, doi: 10.1680/wama.2007.160.2.109.

[61]   M. Ferrante, B. Brunone, S. Meniconi, C. Capponi, and C. Massari, "The leak law: From local to global scale," *Procedia Eng.*, vol. 70, pp. 651–659, 2014, doi: 10.1016/j.proeng.2014.02.071.

[62]   A. M. Cassa and J. E. Van Zyl, "Predicting the leakage exponents of elastically deforming cracks in pipes. 12th International Conference on Computing and Control for the Water Industry, CCWI2013," *Procedia Eng.*, vol. 70, pp. 302–310, 2013, doi: 10.1016/j.proeng.2014.02.034.

[63]   S. X. Molina, P. L. Iglesias-Rey, and S. Francisco-javier, "Calibración de modelos de redes de distribución de agua mediante la utilización conjunta de demandas y consumos dependientes de la presión," *IV Jornadas Ing. del Agua La precipitación y los procesos erosivos Córdoba*, vol. 10, pp. 2–3, 2015.

[64]   I. Marzola, S. Alvisi, and M. Franchini, "Analysis of MNF and FAVAD models for leakage characterization by exploiting smart-metered data: The case of the gorino ferrarese (fe-Italy) district," *Water (Switzerland)*, vol. 13, no. 5, 2021, doi: 10.3390/w13050643.

[65]   A. Casanova, A. Vigueras-Rodriguez, J. T. García, and C. L. G., "Evaluación y clasificación de efectos de fugas en la red de abastecimiento de Moratalla (Murcia) para la priorización del mantenimiento de tuberías .," *Jornadas Ing. del Agua*, no. año 2014, pp. 1–13, 2017.

[66]   A. Muhammetoglu, I. E. Karadirek, O. Ozen, and H. Muhammetoglu, "Full-Scale PAT Application for Energy Production and Pressure Reduction in a

Water Distribution Network," *J. Water Resour. Plan. Manag.*, vol. 143, no. 8, p. 04017040, 2017, doi: 10.1061/(asce)wr.1943-5452.0000795.

[67]   D. Kofinas, R. Ulanczyk, and C. S. Laspidou, "Simulation of a water distribution network with key performance indicators for spatio-temporal analysis and operation of highly stressedwater infrastructure," *Water (Switzerland)*, vol. 12, no. 4, 2020, doi: 10.3390/W12041149.

[68]   H. Abdelmeguid and B. Ulanicki, "Pressure and Leakage Management in Water Distribution Systems Via Flow Modulation PRVS," in *Water Distribution System Analysis 2010 - WDSA2010*, Tucson, AZ, USA, 2010, pp. 1124–1139.

[69]   R. Cobacho, F. Arregui, J. Soriano, and E. Cabrera, "Including leakage in network models: An application to calibrate leak valves in EPANET," *J. Water Supply Res. Technol. - AQUA*, vol. 64, no. 2, pp. 130–138, 2015, doi: 10.2166/aqua.2014.197.

[70]   J. M. Alonso *et al.*, "Parallel Computing in Water Network Analysis and Leakage Minimization," *J. Water Resour. Plan. Manag.*, vol. 126, no. 4, pp. 251–260, 2000, doi: 10.1061/(asce)0733-9496(2000)126:4(251).

[71]   N. Fontana, M. Giugni, and G. Marini, "Experimental assessment of pressure-leakage relationship in a water distribution network," in *Water Science and Technology: Water Supply*, vol. 17, no. 3, Roma, 2017, pp. 726–732.

[72]   D. T. Tucciarelli, A. Criminisi, "LEAK ANALYSIS IN PIPELINE SYSTEMS BY MEANS OF OPTIMAL VALVE REGULATION," *J. Hydraul. Eng. 125(3)*, vol. 9, no. March, pp. 277–285, 1999.

[73]   G. Germanopoulos and P. W. Jowitt, "Leakage reduction by excess pressure minimization in a water supply network," *Proc. - Inst. Civ. Eng. Part 2. Res. theory*, vol. 87, no. August, pp. 195–214, 1989, doi: 10.1680/iicep.1989.2003.

[74]   M. Pardo and A. Riquelme, "A software for considering leakage in water pressurized networks," in *Computer Applications in Engineering Education*, vol. 27, no. 3, Alicante, Spain, 2019, pp. 708–720.

[75]   H. E. Mutikanga, S. K. Sharma, and K. Vairavamoorthy, "Methods and Tools for Managing Losses in Water Distribution Systems," in *Journal of Water Resources Planning and Management*, vol. 139, no. 2, 2013, pp. 166–174.

[76]   Z. Y. Wu, P. Sage, and D. Turtle, "Pressure-Dependent Leak Detection Model and Its Application to a District Water System," in *Journal of Water Resources Planning and Management*, vol. 136, no. 1, United Kingdom, 2010, pp. 116–128.

[77]   B. Greyvenstein and J. E. Van Zyl, "An experimental investigation into the pressure - Leakage relationship of some failed water pipes," in *Journal of Water Supply: Research and Technology - AQUA*, vol. 56, no. 2, 2007, pp. 117–124.

[78]   S. Fox, R. Collins, and J. Boxall, "Dynamic leakage: Physical study of the leak behaviour of longitudinal slits in MDPE pipe. 16th Conference on Water

Distribution System Analyis, WDSA2014," in *Procedia Engineering*, 2014, vol. 89, pp. 286–289, doi: 10.1016/j.proeng.2014.11.189.

[79] J. Schwaller, J. E. Van Zyl, and A. M. Kabaasha, "Characterising the pressure-leakage response of pipe networks using the FAVAD equation," in *Water Science and Technology: Water Supply*, vol. 15, no. 6, 2015, pp. 1373–1382.

[80] R. Ferraiuolo, F. De Paola, D. Fiorillo, G. Caroppi, and F. Pugliese, "Experimental and numerical assessment of water leakages in a PVC-A pipe," *Water (Switzerland)*, vol. 12, no. 6, 2020, doi: 10.3390/w12061804.

[81] J. Thornton and A. Lambert, "Progress in practical prediction of pressure: leakage, pressure: burst frequency and pressure: consumption relationships," *IWA Spec. Conf. Leakage*, pp. 1–10, 2005, [Online]. Available: http://www.leakssuite.com/Research Papers/2005_ThorntonLambert IWA Halifax.pdf.

[82] O. Giustolisi, L. Berardi, D. Laucelli, D. Savic, T. Walski, and B. Brunone, "Battle of background Leakage Assessment for Water Networks (BBLAWN) at WDSA conference 2014," *Procedia Eng.*, vol. 89, pp. 4–12, 2014, doi: 10.1016/j.proeng.2014.11.153.

[83] A. S. Braga, C. V. S. Fernandes, S. M. Braga, and D. C. Dos Santos, "Leakage modeling through empirical equations: An experimental approach. 1st International WDSA / CWWI Joint Conference," in *1st International WDSA / CCWI 2018 Joint Conference*, Kingston, Ontario, Canada, 2018, p. 7.

[84] J. Canto Ríos, R. U. Santos-Tellez, P. Hansen Rodríguez, E. Antúnez Leyva, and V. Nava Martínez, "Methodology for the identification of apparent losses in water distribution networks," in *Procedia Engineering, 12 the International Conference on Computing and Control for the Water Industry, CCWI2013*, vol. 70, Jiutepec Morelos, Mexico: Elsevier B.V., 2014, pp. 238–247.

[85] F. G. Contreras, "Influencia de la presión en las perdidas de agua en sistemas de distribución," *Int. Symp. Hydraul. Struct. - XXII Congr. Latinoam. Hidraul. Asoc. Ing. Sanit. y Ambient.*, no. 1, 2006.

[86] F. De Paola, A. Cutolo, M. Giugni, and M. Fraldi, "Influence of Hole Geometry and Position in Leaking Pipes under Combined Pressure and Bending Regimes," *J. Hydraul. Eng.*, vol. 145, no. 1, p. 04018081, 2019, doi: 10.1061/(asce)hy.1943-7900.0001556.

[87] I. E. Karadirek, S. Kara, G. Yilmaz, A. Muhammetoglu, and H. Muhammetoglu, "Implementation of Hydraulic Modelling for Water-Loss Reduction Through Pressure Management," *Water Resour. Manag.*, vol. 26, no. 9, pp. 2555–2568, 2012, doi: 10.1007/s11269-012-0032-2.

[88] A. Marunga, Z. Hoko, and E. Kaseke, "Pressure management as a leakage reduction and water demand management tool: The case of the City of Mutare, Zimbabwe," *Phys. Chem. Earth*, vol. 31, no. 15–16, pp. 763–770, 2006, doi: 10.1016/j.pce.2006.08.032.

[89]   J. M. A. Alkasseh, M. N. Adlan, I. Abustan, H. A. Aziz, and A. B. M. Hanif, "Applying Minimum Night Flow to Estimate Water Loss Using Statistical Modeling: A Case Study in Kinta Valley, Malaysia," *Water Resour. Manag.*, vol. 27, no. 5, pp. 1439–1455, 2013, doi: 10.1007/s11269-012-0247-2.

[90]   A. M. Kabaasha *et al.*, "Modelling Pressure : Leakage Response in Water Distribution Systems Considering Leak Area Variation," *CCWI Int. Conf. Comput. Control Water Ind.*, vol. 14th, pp. 1–7, 2017, [Online]. Available: https://hal.archives-ouvertes.fr/hal-01549955.

[91]   J. E. van Zyl, A. O. Lambert, and R. Collins, "Realistic Modeling of Leakage and Intrusion Flows through Leak Openings in Pipes," *J. Hydraul. Eng.*, vol. 143, no. 9, p. 04017030, 2017, doi: 10.1061/(asce)hy.1943-7900.0001346.

[92]   E. Rondán Galán, "Estado del arte de la calibración de modelos hidráulicos. Modelado de fugas con Epanet.," Dep. Inteniería Energética. Escuela Técnica Superior de Ingeniería. Universidad de Sevilla, 2016.

[93]   R. Puust, Z. Kapelan, D. A. Savic, and T. Koppel, *A review of methods for leakage management in pipe networks*, vol. 7, no. 1. UK, 2010.

[94]   D. J. V. González, "Diseño de maniobras de gestión de presiones en sectores de distribución de agua y análisis de su impacto.," Universidad Politécnica de Madrid, Valencia, Spain, 2017.

[95]   J. Roma, R. Pérez, G. Sanz, and S. Grau, "Model calibration and leakage assessment applied to a real Water Distribution Network. 13ht Computer Control for Water Industry Conference, CCWI 2015," *Procedia Engineering*, vol. 119, no. 1, Catalunya, pp. 603–612, 2015.

[96]   G. J. Bonthuys, M. van Dijk, and G. Cavazzini, "Leveraging water infrastructure asset management for energy recovery and leakage reduction," *Sustain. Cities Soc.*, vol. 46, p. 101434, 2019, doi: 10.1016/j.scs.2019.101434.

[97]   G. J. Bonthuys, M. van Dijk, and G. Cavazzini, "The optimization of energy recovery device sizes and locations in municipal water distribution systems during extended-period simulation," *Water (Switzerland)*, vol. 12, no. 9, 2020, doi: 10.3390/w12092447.

[98]   M. Deyi, J. Van Zyl, and M. Shepherd, "Applying the FAVAD concept and leakage number to real networks: A case study in Kwadabeka, South Africa," *Procedia Eng.*, vol. 89, pp. 1537–1544, 2014, doi: 10.1016/j.proeng.2014.11.450.

[99]   E. Rondán, "Estado del arte de la calibración de modelos hidráulicos. Modelado de fugas con Epanet.," p. 80, 2016.

[100]   N. Samir, R. Kansoh, W. Elbarki, and A. Fleifle, "Pressure control for minimizing leakage in water distribution systems," *Alexandria Eng. J.*, vol. 56, no. 4, pp. 601–612, 2017, doi: 10.1016/j.aej.2017.07.008.

[101]   O. Giustolisi, D. Savic, and Z. Kapelan, "Pressure-Driven Demand and Leakage Simulation for Water Distribution Networks," *J. Hydraul. Eng.*, vol. 134, no. 5,

pp. 626–635, 2008, doi: 10.1061/(asce)0733-9429(2008)134:5(626).

[102] N. Moosavian and M. R. Jaefarzadeh, "Pressure-Driven Demand and Leakage Simulation for Pipe Networks Using Differential Evolution," *World Journal of Engineering and Technology*, vol. 01, no. 03, Mashhd, Iran, pp. 49–58, 2013.

[103] J. Muranho, A. Ferreira, J. Sousa, A. Gomes, and A. Sá Marques, "Pressure-dependent demand and leakage modelling with an EPANET extension - WaterNetGen. 16th Conference on Water Distribution System Analysis, WDSA 2014," *Procedia Engineering*, vol. 89, Portugal, pp. 632–639, 2014.

[104] O. Giustolisi and T. M. Walski, "Demand Components in Water Distribution Network Analysis," in *Journal of Water Resources Planning and Management*, vol. 138, no. 4, 2012, pp. 356–367.

[105] P. L. Iglesias-Rey, F. J. Martínez-Solano, D. Mora Meliá, and P. D. Martínez-Solano, "Combining Engineering Judgment and an Optimization Model to Increase Hydraulic and Energy Efficiency in Water Distribution Networks," *J. Water Resour. Plan. Manag.*, vol. 142, no. 5, pp. 1–5, 2016, doi: 10.1061/(asce)wr.1943-5452.0000605.

[106] A. Zanfei, A. Menapace, G. R. Pisaturo, and M. Righetti, "Calibration of Water Leakages and Valve Setting in a Real Water Supply System," *Environ. Sci. Proc.*, vol. 2, no. 1, p. 41, 2020, doi: 10.3390/environsciproc2020002041.

[107] J. Mora-Rodríguez, X. Delgado-Galván, J. Ortiz-Medel, H. M. Ramos, V. S. Fuertes-Miquel, and P. A. López-Jiménez, "Pathogen intrusion flows in water distribution systems: According to orifice equations," *J. Water Supply Res. Technol. - AQUA*, vol. 64, no. 8, pp. 857–869, 2015, doi: 10.2166/aqua.2015.121.

[108] K. B. Adedeji, Y. Hamam, and A. M. Abu-Mahfouz, "Impact of pressure-driven demand on background leakage estimation inwater supply networks," *Water (Switzerland)*, vol. 11, no. 8, pp. 1–12, 2019, doi: 10.3390/w11081600.

[109] M. Maskit and A. Ostfeld, "Leakage calibration of water distribution networks. 16th Conference on Water Distribution System Analysis.," *Procedia Engineering, 16th Conference on Water Distribution System Analysis, WDSA*, vol. 89, Israel, pp. 664–671, 2014.

[110] S. Sophocleous, D. A. Savić, Z. Kapelan, and O. Giustolisi, "A Two-stage Calibration for Detection of Leakage Hotspots in a Real Water Distribution Network," *Procedia Eng.*, vol. 186, no. 0, pp. 168–176, 2017, doi: 10.1016/j.proeng.2017.03.223.

[111] A. Di Nardo, M. Di Natale, C. Gisonni, and M. Iervolino, "A genetic algorithm for demand pattern and leakage estimation in a water distribution network," *J. Water Supply Res. Technol. - AQUA*, vol. 64, no. 1, pp. 35–46, 2015, doi: 10.2166/aqua.2014.004.

[112] S. Adachi, S. Takahashi, H. Kurisu, and H. Tadokoro, "Estimating area leakage in water networks based on hydraulic model and asset information,"

Procedia Eng., vol. 89, pp. 278–285, 2014, doi: 10.1016/j.proeng.2014.11.188.

[113] M. Powell, "The BOBYQA algorithm for bound constrained optimization without derivatives," *Dep. Appl. Math. Theor. Phys.,* p. 39, 2009, [Online]. Available: http://www6.cityu.edu.hk/rcms/publications/preprint26.pdf.

[114] L. S. Araujo, H. M. Ramos, and S. T. Coelho, "Pressure Control for Leakage Minimisation in Water Distribution Systems Management," *Water Resour. Manag.,* vol. 18, 2006, doi: 10.1007/s11269-006-4635-3.

[115] H. Abdelmeguid and B. Ulanicki, "Pressure and leakage management in water distribution systems via flow modulation PRVs," *Water Distrib. Syst. Anal. 2010 - Proc. 12th Int. Conf. WDSA 2010. Leicester, UK.,* vol. 41203, no. January, pp. 1124–1139, 2012, doi: 10.1061/41203(425)102.

[116] I. T. Telci and M. M. Aral, "Optimal energy recovery fromwater distribution systems using smart operation scheduling," *Water (Switzerland),* vol. 10, no. 10, 2018, doi: 10.3390/w10101464.

[117] M. Soltanjalili, O. B. Haddad, S. S. Aghmiuni, and M. A. Mariño, "Water distribution network simulation by optimization approaches," *Water Sci. Technol. Water Supply,* vol. 13, no. 4, pp. 1063–1079, 2013, doi: 10.2166/ws.2013.086.

[118] M. Nicolini, C. Giacomello, M. Scarsini, and M. Mion, "Numerical modeling and leakage reduction in the water distribution system of Udine," *Procedia Eng.,* vol. 70, pp. 1241–1250, 2014, doi: 10.1016/j.proeng.2014.02.137.

[119] M. Quiñones-Grueiro, M. Ares Milián, M. Sánchez Rivero, A. J. Silva Neto, and O. Llanes-Santiago, "Robust leak localization in water distribution networks using computational intelligence," *Neurocomputing,* vol. 438, pp. 195–208, 2021, doi: 10.1016/j.neucom.2020.04.159.

[120] Grupo Especialista en Benchmarking y Evaluación del Desempeño de la IWA, *Manual de Buenas Prácticas. Indicadores de Desempeño para Servicios de Abastecimiento de Agua - Tercera Edición.* 2018.

[121] M. Patelis, V. Kanakoudis, and K. Gonelas, "Combining pressure management and energy recovery benefits in a water distribution system installing PATs," *J. Water Supply Res. Technol. - AQUA,* vol. 66, no. 7, pp. 520–527, 2017, doi: 10.2166/aqua.2017.018.

[122] W. Winarni, "Infrastructure Leakage Index (ILI) as Water Losses Indicator," *Civ. Eng. Dimens.,* vol. 11, no. 2, pp. 126–134, 2009, [Online]. Available: http://www.freepatentsonline.com/article/Civil-Engineering-Dimension/212851407.html.

[123] D. Radivojevic, D. Milicevic, and B. Blagojevic, "IWA best practice and performance indicators for water utilities in Serbia: Case study Pirot," *Facta Univ. - Ser. Archit. Civ. Eng.,* vol. 6, no. 1, pp. 37–50, 2008, doi: 10.2298/fuace0801037r.

[124] A. O. Lambert, "International report: Water losses management and

techniques," *Water Sci. Technol. Water Supply*, vol. 2, no. 4, pp. 1–20, 2002, doi: 10.2166/ws.2002.0115.

[125]   L. E. C. Rosado, P. A. López-Jiménez, F. J. Sánchez-Romero, P. C. Fuertes, and M. Pérez-Sánchez, "Applied strategy to characterize the energy improvement using PATs in a water supply system," in *Water (,* vol. 12, no. 6, Switzerland, 2020, pp. 1–22.

[126]   L. E. C. Rosado, P. A. López–Jiménez, F. J. Sánchez–Romero, P. C. Fuertes, and M. Pérez–Sánchez, *Applied strategy to characterize the energy improvement using PATs in a water supply system,* vol. 12, no. 6. p. 1–22.

[127]   N. Fontana, M. Giugni, and G. Marini, "Experimental assessment of pressure-leakage relationship in a water distribution network," *Water Sci. Technol. Water Supply*, vol. 17, no. 3, pp. 726–732, 2017, doi: 10.2166/ws.2016.171.

[128]   B. Ristovski, "Pressure management and active leakage control in particular DMA (Lisiche) in the city of Skopje , FYROM," *Water Util. J. 2,* no. Figure 1, pp. 45–49, 2011.

[129]   E. Cabrera, E. Cabrera, R. Cobacho, and J. Soriano, "Towards an energy labelling of pressurized water networks," *Procedia Eng.,* vol. 70, no. December, pp. 209–217, 2014, doi: 10.1016/j.proeng.2014.02.024.

[130]   B. Levine, J. Lucas, P. Cynar, T. Hildebrand, and W. Morgan, "Pressure Management in the Pittsburgh Area : A Working and Economical Solution," *Conf. Proc.,* pp. 1–9, 2005.

[131]   M. Girard and R. A. Stewart, "Implementation of Pressure and Leakage Management Strategies on the Gold Coast, Australia: Case Study," *J. Water Resour. Plan. Manag.,* vol. 133, no. 3, pp. 210–217, 2007, doi: 10.1061/(asce)0733-9496(2007)133:3(210).

[132]   J. Koelbl, "SUSTAINABLE NETWORK MANAGEMENT PRACTISES," in *Water Service Group. IWA Efficient 2011 Conference, Jordan,* 2011.

[133]   R. Gupta, A. G. R. Nair, and L. Ormsbee, "Leakage as Pressure-Driven Demand in Design of Water Distribution Networks," *J. Water Resour. Plan. Manag.,* vol. 142, no. 6, p. 04016005, 2016, doi: 10.1061/(asce)wr.1943-5452.0000629.

[134]   European Commission, *EU Reference document Good Practices on Leakage Management WFD CIS WG PoM.* Luxembourg, 2015.

[135]   O. Giustolisi, L. Berardi, D. Laucelli, D. Savic, and Z. Kapelan, "Operational and Tactical Management of Water and Energy Resources in Pressurized Systems: Competition at WDSA 2014," *J. Water Resour. Plan. Manag.,* vol. 142, no. 5, 2016, doi: 10.1061/(asce)wr.1943-5452.0000583.

[136]   G. Cavazzini, G. Pavesi, and G. Ardizzon, "Optimal assets management of a water distribution network for leakage minimization based on an innovative index," *Sustain. Cities Soc.,* vol. 54, no. September 2019, p. 101890, 2020, doi: 10.1016/j.scs.2019.101890.

[137]   I. Karathanasi and C. Papageorgakopoulos, "Development of a Leakage

Control System at the Water Supply Network of the City of Patras," *Procedia Eng.*, vol. 162, pp. 553–558, 2016, doi: 10.1016/j.proeng.2016.11.100.

[138] L. E. C. Rosado, P. L. Amparo, and S. Francisco-javier, "Applied Strategy to Characterize the Energy," 2020.

[139] T. AL-Washali, S. Sharma, R. Lupoja, F. AL-Nozaily, M. Haidera, and M. Kennedy, "Assessment of water losses in distribution networks: Methods, applications, uncertainties, and implications in intermittent supply," *Resour. Conserv. Recycl.*, vol. 152, no. October 2019, p. 104515, 2020, doi: 10.1016/j.resconrec.2019.104515.

[140] S. M. Negharchi and R. Shafaghat, "Leakage estimation in water networks based on the BABE and MNF analyses: A case study in Gavankola village, Iran," *Water Sci. Technol. Water Supply*, vol. 20, no. 6, pp. 2296–2310, 2020, doi: 10.2166/ws.2020.137.

[141] M. Giugni, N. Fontana, and A. Ranucci, "Optimal Location of PRVs and Turbines in Water Distribution Systems," *J. Water Resour. Plan. Manag.*, vol. 140, no. 9, p. 06014004, 2014, doi: 10.1061/(asce)wr.1943-5452.0000418.

[142] M. Rossi, A. Nigro, G. R. Pisaturo, and M. Renzi, "Technical and economic analysis of Pumps-as-Turbines (PaTs) used in an Italian Water Distribution Network (WDN) for electrical energy production," *Energy Procedia*, vol. 158, pp. 117–122, 2019, doi: 10.1016/j.egypro.2019.01.055.

[143] J. C. Alberizzi, M. Renzi, A. Nigro, and M. Rossi, "Study of a Pump-as-Turbine (PaT) speed control for a Water Distribution Network (WDN) in South-Tyrol subjected to high variable water flow rates," *Energy Procedia*, vol. 148, no. October, pp. 226–233, 2018, doi: 10.1016/j.egypro.2018.08.072.

[144] C. Tricarico *et al.*, "Optimal water supply system management by leakage reduction and energy recovery," *Procedia Eng.*, vol. 89, pp. 573–580, 2014, doi: 10.1016/j.proeng.2014.11.480.

[145] S. Parra and S. Krause, "Pressure management by combining pressure reducing valves and pumps as turbines for water loss reduction and energy recovery," *Int. J. Sustain. Dev. Plan.*, vol. 12, no. 1, pp. 89–97, 2017, doi: 10.2495/SDP-V12-N1-89-97.

[146] L. Cimorelli, A. D'Aniello, L. Cozzolino, and D. Pianese, "Leakage reduction in WDNs through optimal setting of PATs with a derivative-free optimizer," *J. Hydroinformatics*, vol. 22, no. 4, pp. 713–724, 2020, doi: 10.2166/hydro.2020.142.

[147] K. D. Nguyen, P. D. Dai, D. Q. Vu, B. M. Cuong, V. P. Tuyen, and P. Li, "A MINLP model for optimal localization of pumps as turbines in water distribution systems considering power generation constraints," *Water (Switzerland)*, vol. 12, no. 7, 2020, doi: 10.3390/w12071979.

[148] G. M. Lima, E. Luvizotto, B. M. Brentan, and H. M. Ramos, "Leakage Control and Energy Recovery Using Variable Speed Pumps as Turbines," *J. Water*

Resour. Plan. Manag., vol. 144, no. 1, p. 04017077, 2018, doi: 10.1061/(asce)wr.1943-5452.0000852.

[149] M. Postacchini, G. Darvini, F. Finizio, L. Pelagalli, L. Soldini, and E. Di Giuseppe, "Hydropower generation through pump as turbine: Experimental study and potential application to small-scale WDN," *Water (Switzerland)*, vol. 12, no. 4, pp. 1–19, 2020, doi: 10.3390/W12040958.

[150] F. Pugliese, F. De Paola, N. Fontana, M. Giugni, and G. Marini, "Experimental characterization of two Pumps As Turbines for hydropower generation," *Renew. Energy*, vol. 99, pp. 180–187, Dec. 2016, doi: 10.1016/j.renene.2016.06.051.

[151] R. Ortiz Florez, "Reversibles Hydromaquines Aplicated to Microhydropower," *IEEE Latin America Transactions*, vol. 6, no. 2, Universidad del Valle, Cali, pp. 170–175, 2008.

[152] K. R. Sharma, "Small hydroelectric project-use of centrifugal pumps as turbines," *Tech. report. Bangalore, India Kirloskar Electr. Co.*, 1985.

[153] S. Derakhshan and A. Nourbakhsh, "Experimental study of characteristic curves of centrifugal pumps working as turbines in different specific speeds," *Exp. Therm. Fluid Sci.*, vol. 32, no. 3, pp. 800–807, 2008, doi: 10.1016/j.expthermflusci.2007.10.004.

[154] M. Pérez-Sánchez, F. J. Sánchez-Romero, H. M. Ramos, and P. A. López-Jiménez, "Improved planning of energy recovery in water systems using a new analytic approach to PAT performance curves," *Water (Switzerland)*, vol. 12, no. 2, 2020, doi: 10.3390/w12020468.

[155] F. A. Plua, F. J. Sánchez-Romero, V. Hidalgo, P. A. López-Jiménez, and M. Pérez-Sánchez, "New expressions to apply the variation operation strategy in engineering tools using pumps working as turbines," *Mathematics*, vol. 9, no. 8, p. 860, Apr. 2021, doi: 10.3390/math9080860.

[156] M. Tahani, A. Kandi, M. Moghimi, and S. D. Houreh, "Rotational speed variation assessment of centrifugal pump-as-turbine as an energy utilization device under water distribution network condition," *Energy*, vol. 213, p. 118502, 2020, doi: https://doi.org/10.1016/j.energy.2020.118502.

[157] S. Chen and B. Chen, "Urban energy–water nexus: A network perspective," *Appl. Energy*, vol. 184, pp. 905–914, 2016, doi: 10.1016/j.apenergy.2016.03.042.

[158] T. Niet, N. Arianpoo, K. Kuling, and A. S. Wright, "Embedding the United Nations sustainable development goals into energy systems analysis: expanding the food–energy–water nexus," *Energy. Sustain. Soc.*, vol. 11, no. 1, pp. 1–12, 2021, doi: 10.1186/s13705-020-00275-0.

[159] M. Pérez-Sánchez, P. A. López-Jiménez, and H. M. Ramos, "Modified Affinity Laws in Hydraulic Machines towards the Best Efficiency Line," *Water Resour. Manag.*, vol. 32, no. 3, pp. 829–844, Feb. 2018, doi: 10.1007/s11269-017-1841-

0.

[160]   C. Mataix, *Turbomáquinas Hidráulicas.* Madrid: Universidad Pontificia Comillas, 2009.

[161]   J. Hyypiä, "Hydraulic energy recovery by replacing a control valve with a centrifugal pump used as a turbine," LAPPEENRANTA UNIVERSITY OF TECHNOLOGY, LUT School of Energy Systems, 2016.

[162]   L. Nygren, "Hydraulic energy harvesting with variable-speed-driven centrifugal pump as turbine," Lappeenranta University of Technology, 2017.

[163]   A. Carravetta, M. C. Conte, O. Fecarotta, and H. M. Ramos, "Evaluation of PAT performances by modified affinity law," *Procedia Eng,* vol. 89, pp. 581–587, 2014.

[164]   KSB, "PATs curves," *Catalogue,* 2019. .

[165]   S. V Jain, A. Swarnkar, K. H. Motwani, and R. N. Patel, "Effects of impeller diameter and rotational speed on performance of pump running in turbine mode," *Energy Convers. Manag.,* vol. 89, pp. 808–824, 2015, doi: https://doi.org/10.1016/j.enconman.2014.10.036.

[166]   S. Abazariyan, R. Rafee, and S. Derakhshan, "Experimental study of viscosity effects on a pump as turbine performance," *Renew. Energy,* vol. 127, pp. 539–547, 2018, doi: https://doi.org/10.1016/j.renene.2018.04.084.

[167]   M. Kramer, K. Terheiden, and S. Wieprecht, "Pumps as turbines for efficient energy recovery in water supply networks," *Renew. Energy,* vol. 122, pp. 17–25, 2018, doi: https://doi.org/10.1016/j.renene.2018.01.053.

[168]   J. Delgado, J. P. Ferreira, D. I. C. Covas, and F. Avellan, "Variable speed operation of centrifugal pumps running as turbines. Experimental investigation," *Renew. Energy,* vol. 142, pp. 437–450, Nov. 2019, doi: 10.1016/j.renene.2019.04.067.

[169]   M. Stefanizzi, M. Torresi, B. Fortunato, and S. M. Camporeale, "Experimental investigation and performance prediction modeling of a single stage centrifugal pump operating as turbine," *Energy Procedia,* vol. 126, pp. 589–596, 2017, doi: https://doi.org/10.1016/j.egypro.2017.08.218.

[170]   M. Postacchini, G. Darvini, F. Finizio, L. Pelagalli, L. Soldini, and E. Di Giuseppe, "Hydropower Generation Through Pump as Turbine: Experimental Study and Potential Application to Small-Scale WDN," *Water ,* vol. 12, no. 4. 2020, doi: 10.3390/w12040958.

[171]   O. Fecarotta, A. Carravetta, H. M. Ramos, and R. Martino, "An improved affinity model to enhance variable operating strategy for pumps used as turbines," *J. Hydraul. Res.,* vol. 54, no. 3, pp. 332–341, 2016, doi: 10.1080/00221686.2016.1141804.

[172]   M. C. Morani, A. Carravetta, C. D'Ambrosio, and O. Fecarotta, "A New Preliminary Model to Optimize PATs Location in a Water Distribution Network," *Environ. Sci. Proc.,* vol. 2, no. 1, p. 57, 2020, doi:

10.3390/environsciproc2020002057.

[173] F. Manzano-Agugliaro, M. Taher, A. Zapata-Sierra, A. Juaidi, and F. G. Montoya, "An overview of research and energy evolution for small hydropower in Europe," *Renew. Sustain. Energy Rev.*, vol. 75, no. May 2015, pp. 476–489, 2017, doi: 10.1016/j.rser.2016.11.013.

[174] J. Gallagher, I. M. Harris, A. J. Packwood, A. McNabola, and A. P. Williams, "A strategic assessment of micro-hydropower in the UK and Irish water industry: Identifying technical and economic constraints," *Renew. Energy*, vol. 81, pp. 808–815, 2015, doi: 10.1016/j.renene.2015.03.078.

[175] S. Childs, "Convert pumps to turbines and recover HP," *Hydrocarb. Process. Pet. Refin. 41(10)*, pp. 173–174, 1962.

[176] K. M. Grover, "Conversion of pumps to turbines.," *GSA Inter Corp.*, Katonah, New York, 1980.

[177] A. Williams, "The turbine performance of centrifugal pumps : a comparison of prediction methods," *Jounal of Power and Energ ProcInstnEngs*, vol. 208, pp. 59–66, 1994, doi: 10.1243/PIME.

[178] C. Alatorre-Frenk, K. MI, and A. Karin, "Cost Minimisation in Micro-Hydro Systems Using Pumps-as-Turbines.," *Ph.D. Thesis, Univ. Warwick, Coventry, UK*, 1994.

[179] S. Derakhshan and A. Nourbakhsh, "Theoretical, numerical and experimental investigation of centrifugal pumps in reverse operation," *Exp. Therm. Fluid Sci.*, vol. 32, no. 8, pp. 1620–1627, Sep. 2008, doi: 10.1016/j.expthermflusci.2008.05.004.

[180] J. C. Páscoa, F. J. Silva, J. S. Pinheiro, and D. J. Martins, "A new approach for predicting PAT-pumps operating point from direct pumping mode characteristics," 2012.

[181] M. Rossi and M. Renzi, "A general methodology for performance prediction of pumps-as-turbines using Artificial Neural Networks," *Renew. Energy*, vol. 128, pp. 265–274, Dec. 2018, doi: 10.1016/J.RENENE.2018.05.060.

[182] M. Pérez-Sánchez, F. J. Sánchez-Romero, H. M. Ramos, and P. A. López-Jiménez, "Improved Planning of Energy Recovery in Water Systems Using a New Analytic Approach to PAT Performance Curves," *Water 2020, Vol. 12, Page 468*, vol. 12, no. 2, p. 468, Feb. 2020, doi: 10.3390/W12020468.

[183] C. A. M. Ávila, F.-J. Sánchez-Romero, P. A. López-Jiménez, and M. Pérez-Sánchez, "Definition of the Operational Curves by Modification of the Affinity Laws to Improve the Simulation of PATs," *Water 2021, Vol. 13, Page 1880*, vol. 13, no. 14, p. 1880, Jul. 2021, doi: 10.3390/W13141880.

[184] D. Novara and A. McNabola, "A model for the extrapolation of the characteristic curves of Pumps as Turbines from a datum Best Efficiency Point," *Energy Convers. Manag.*, vol. 174, pp. 1–7, Oct. 2018, doi: 10.1016/j.enconman.2018.07.091.

[185] F. Moazeni and J. Khazaei, "Optimal energy management of water-energy networks via optimal placement of pumps-as-turbines and demand response through water storage tanks," *Appl. Energy*, vol. 283, no. November 2020, p. 116335, 2021, doi: 10.1016/j.apenergy.2020.116335.

[186] T. Lydon, P. Coughlan, and A. McNabola, "Pressure management and energy recovery in water distribution networks: Development of design and selection methodologies using three pump-as-turbine case studies," *Renew. Energy*, vol. 114, pp. 1038–1050, 2017, doi: 10.1016/j.renene.2017.07.120.

[187] M. Rossi, M. Righetti, and M. Renzi, "Pump-as-turbine for Energy Recovery Applications: The Case Study of An Aqueduct," *Energy Procedia*, vol. 101, no. September, pp. 1207–1214, 2016, doi: 10.1016/j.egypro.2016.11.163.

[188] M. ciudad de K. (Grec Patelis, V. Kanakoudis, and K. Gonelas, "Combining pressure management and energy recovery benefits in a water distribution system installing PATs," *J. Water Supply Res. Technol. - AQUA*, vol. 66, no. 7, pp. 520–527, 2017, doi: 10.2166/aqua.2017.018.

[189] A. Mejía, M. N. Hubner, E. R. Sánchez, and M. Doria, "Water and Sustainability. A Review of Targets, Tools and Regional Cases," 2012.

[190] C. Macias Ávila, S. Francisco-javier, P. L. Amparo, and M. Pérez–Sánchez, "Leakage Management and Pipe System Efficiency . Its Influence in the Improvement of the Efficiency Indexes," *Integr. Manag. Water Syst. Energy Recover. Press. Control. Smart Solut.*, 2021.

[191] P. Kynčlová, S. Upadhyaya, and T. Nice, "Composite index as a measure on achieving Sustainable Development Goal 9 (SDG-9) industry-related targets: The SDG-9 index," *Appl. Energy*, vol. 265, no. February, 2020, doi: 10.1016/j.apenergy.2020.114755.

[192] G. Nhamo, C. Nhemachena, and S. Nhamo, "Is 2030 too soon for Africa to achieve the water and sanitation sustainable development goal?," *Sci. Total Environ.*, vol. 669, pp. 129–139, 2019, doi: 10.1016/j.scitotenv.2019.03.109.

[193] J. M. Diaz-Sarachaga and D. Jato-Espino, "Development and application of a new Resilient, Sustainable, Safe and Inclusive Community Rating System (RESSICOM)," *J. Clean. Prod.*, vol. 207, pp. 971–979, 2019, doi: 10.1016/j.jclepro.2018.10.061.

[194] C. Bruce M, H. James, R. Janie, S. Clare M, T. Stephen, and (Lini) Wollenberg Eva, "Urgent action to combat climate change and its impacts (SDG 13): transforming agriculture and food systems," *Curr. Opin. Environ. Sustain.*, vol. 34, no. Sdg 13, pp. 13–20, 2018, doi: 10.1016/j.cosust.2018.06.005.

[195] M. Pérez-Sánchez, F. Sánchez-Romero, H. Ramos, and P. López-Jiménez, "Modeling Irrigation Networks for the Quantification of Potential Energy Recovering: A Case Study," *Water*, vol. 8, no. 6, pp. 1–26, Jun. 2016, doi: 10.3390/w8060234.

[196] J. Almandoz, E. Cabrera, F. Arregui, E. CabreraJr., and R. Cobacho, "Leakage

Assessment through Water Distribution Network Simulation," in *Journal of Water Resources Planning and Management,* vol. 131, no. 6, American Society of Civil Engineers, 2005, pp. 458–466.

[197] J. Almandoz, E. Cabrera, F. Arregui, E. Cabrera, and R. Cobacho, "Leakage Assessment through Water Distribution Network Simulation," *J. Water Resour. Plan. Manag.,* vol. 131, no. 6, pp. 458–466, 2005, doi: 10.1061/(asce)0733-9496(2005)131:6(458).

[198] G. Germanopoulos, "A technical note on the inclusion of pressure dependent demand and leakage terms in water supply network models," *Civ. Eng. Syst.,* vol. 2, no. 3, pp. 171–179, Sep. 1985, doi: 10.1080/02630258508970401.

[199] M. Pérez-Sánchez, F. J. Sánchez-Romero, P. A. López-Jiménez, and H. M. Ramos, "PATs selection towards sustainability in irrigation networks: Simulated annealing as a water management tool," *Renew. Energy,* vol. 116, pp. 234–249, Feb. 2018, doi: 10.1016/J.RENENE.2017.09.060.

[200] a Marryott, "Optimal Groundwater Management Annealing Because the do The majority pr ..'•," *Water Resour. Res.,* vol. 27, no. 10, 1991.

[201] M. Pérez-Sánchez, F. J. Sánchez-Romero, H. M. Ramos, and P. A. López-Jiménez, "Improved Planning of Energy Recovery in Water Systems Using a New Analytic Approach to PAT Performance Curves," *Water,* vol. 12, no. 2, p. 468, Feb. 2020, doi: 10.3390/w12020468.

[202] I. F. García, D. Novara, and A. M. Nabola, "A Model for Selecting the Most Cost-Effective Pressure Control Device for More Sustainable Water Supply Networks," *Water 2019, Vol. 11, Page 1297,* vol. 11, no. 6, p. 1297, Jun. 2019, doi: 10.3390/W11061297.

[203] A. Carravetta, O. Fecarotta, M. Sinagra, and T. Tucciarelli, "Cost-Benefit Analysis for Hydropower Production in Water Distribution Networks by a Pump as Turbine," *J. Water Resour. Plan. Manag.,* vol. 140, no. 6, p. 04014002, Jun. 2013, doi: 10.1061/(ASCE)WR.1943-5452.0000384.

[204] L. A. Rossman, *EPANET 2: User's manual,* U.S. EPA. Cincinnati, 2000.

[205] W. jing Niu and Z. kai Feng, "Evaluating the performances of several artificial intelligence methods in forecasting daily streamflow time series for sustainable water resources management," *Sustain. Cities Soc.,* vol. 64, p. 102562, Jan. 2021, doi: 10.1016/J.SCS.2020.102562.

[206] M. S. Islam and M. S. Babel, "Economic Analysis of Leakage in the Bangkok Water Distribution System," *J. Water Resour. Plan. Manag.,* vol. 139, no. 2, pp. 209–216, 2013, doi: 10.1061/(asce)wr.1943-5452.0000235.

[207] S. E. Bibri and J. Krogstie, "Smart sustainable cities of the future: An extensive interdisciplinary literature review," *Sustain. Cities Soc.,* vol. 31, pp. 183–212, May 2017, doi: 10.1016/J.SCS.2017.02.016.

[208] R. H. S. Beuken, C. S. W. Lavooij, A. Bosch, and P. G. Schaap, "Low leakage in the Netherlands confirmed," *8th Annu. Water Distrib. Syst. Anal. Symp. 2006,*

p. 174, 2007, doi: 10.1061/40941(247)174.

[209]   Lambert A.O., "International Report: Water losses management and techniques," *Water Sci. Technol. Water Supply*, vol. 2, no. 4, pp. 1–20, 2002, [Online]. Available: http://www.iwaponline.com/ws/00204/ws002040001.htm.

[210]   R. Liemberger and A. Wyatt, "Quantifying the global non-revenue water problem," *Water Sci. Technol. Water Supply*, vol. 19, no. 3, pp. 831–837, 2019, doi: 10.2166/ws.2018.129.

[211]   R. Li, H. Huang, K. Xin, and T. Tao, "A review of methods for burst/leakage detection and location in water distribution systems," *Water Supply*, vol. 15, no. 3, pp. 429–441, Jun. 2015, doi: 10.2166/WS.2014.131.

[212]   A. V. Serafeim, G. Kokosalakis, R. Deidda, I. Karathanasi, and A. Langousis, "Probabilistic Minimum Night Flow Estimation in Water Distribution Networks and Comparison with the Water Balance Approach: Large-Scale Application to the City Center of Patras in Western Greece," *Water (Switzerland)*, vol. 14, no. 1, 2022, doi: 10.3390/w14010098.

[213]   A. O. Lambert, T. G. Brown, M. Takizawa, and D. Weimer, "A review of performance indicators for real losses from water supply systems," *J. Water Supply Res. Technol. - AQUA*, vol. 48, no. 6, pp. 227–237, 1999, doi: 10.2166/aqua.1999.0025.

[214]   K. B. Adedeji, Y. Hamam, B. T. Abe, and A. M. Abu-Mahfouz, "Burst leakage-pressure dependency in water piping networks: Its impact on leak openings," *2017 IEEE AFRICON Sci. Technol. Innov. Africa, AFRICON 2017*, no. September, pp. 1502–1507, 2017, doi: 10.1109/AFRCON.2017.8095704.

[215]   J. Schwaller and J. E. van Zyl, "Modeling the Pressure-Leakage Response of Water Distribution Systems Based on Individual Leak Behavior," *J. Hydraul. Eng.*, vol. 141, no. 5, p. 04014089, 2015, doi: 10.1061/(asce)hy.1943-7900.0000984.

[216]   S. Wu, L. Yang, C. Zhou, and J. Zhang, "Leakage modeling and leakage control analysis by pressure management in water supply system of DMA," *ICPTT 2013 Trenchless Technol. - Best Choice Undergr. Pipeline Constr. Renewal, Proc. Int. Conf. Pipelines Trenchless Technol.*, pp. 141–150, 2013, doi: 10.1061/9780784413142.015.

[217]   A. Gupta, N. Bokde, D. Marathe, and K. Kulat, "Leakage Reduction in Water Distribution Systems with Efficient Placement and Control of Pressure Reducing Valves Using Soft Computing Techniques," *Eng. Technol. Appl. Sci. Res.*, vol. 7, no. 2, pp. 1528–1534, Apr. 2017, doi: 10.48084/ETASR.1032.

[218]   G. Ferrarese, S. Benzi, M. M. A. Rossi, and S. Malavasi, "Experimental characterization of a self-powered control system for a real-time management of water distribution networks," *https://doi.org/10.1080/1573062X.2021.1992453*, vol. 19, no. 2, pp. 208–219,

2021, doi: 10.1080/1573062X.2021.1992453.

[219] N. Fontana, M. Asce, ; G Marini, and E. Creaco, "Comparison of PAT Installation Layouts for Energy Recovery from Water Distribution Networks," *J. Water Resour. Plan. Manag.*, vol. 147, no. 12, p. 04021083, Sep. 2021, doi: 10.1061/(ASCE)WR.1943-5452.0001480.

[220] M. Latifi *et al.*, "Pressure and Energy Management in Water Distribution Networks through Optimal Use of Pump-As-Turbines along with Pressure-Reducing Valves," *J. Water Resour. Plan. Manag.*, vol. 147, no. 7, p. 04021039, May 2021, doi: 10.1061/(ASCE)WR.1943-5452.0001392.

[221] J. Almandoz, E. Cabrera, F. Arregui, E. CabreraJr., and R. Cobacho, "Leakage Assessment through Water Distribution Network Simulation," *J. Water Resour. Plan. Manag.*, vol. 131, no. 6, pp. 458–466, Nov. 2005, doi: 10.1061/(ASCE)0733-9496(2005)131:6(458).

[222] D. N. Moriasi, J. G. Arnold, M. W. Van Liew, R. L. Binger, R. D. Harmel, and T. L. Veith, "Model evaluation guidelines for systematic quantification of accuracy in watershed simulations," *Trans. ASABE*, vol. 50, no. 3, pp. 885–900, 2007, doi: 10.13031/2013.23153.

[223] R. del Teso, E. Gómez, E. Estruch-Juan, and E. Cabrera, "Topographic Energy Management in Water Distribution Systems," *Water Resour. Manag.*, vol. 33, no. 12, pp. 4385–4400, 2019, doi: 10.1007/s11269-019-02375-9.

[224] M. Pérez-Sánchez, F. J. Sánchez-Romero, H. M. Ramos, and P. A. López-Jiménez, "Optimization strategy for improving the energy efficiency of irrigation systems by micro hydropower: Practical application," *Water (Switzerland)*, vol. 9, no. 10, 2017, doi: 10.3390/w9100799.

[225] M. Pérez-Sánchez, F. J. Sánchez-Romero, P. A. López-Jiménez, and H. M. Ramos, "PATs selection towards sustainability in irrigation networks: Simulated annealing as a water management tool," *Renew. Energy*, vol. 116, pp. 234–249, 2018, doi: 10.1016/j.renene.2017.09.060.

[226] E. Renaud, M. T. Sissoko, M. Clauzier, D. Gilbert, and D. Khedhaouiria, "Comparative study of different methods to assess average pressures in water distribution zones - Archive ouverte HAL," *waterloss*, 2012.

[227] F. J. Lugauer, J. Kainz, and M. Gaderer, "Techno-Economic Efficiency Analysis of Various Operating Strategies for Micro-Hydro Storage Using a Pump as a Turbine," *Energies 2021, Vol. 14, Page 425*, vol. 14, no. 2, p. 425, Jan. 2021, doi: 10.3390/EN14020425.

[228] M. De Marchis, B. Milici, R. Volpe, and A. Messineo, "Energy Saving in Water Distribution Network through Pump as Turbine Generators: Economic and Environmental Analysis," *Energies 2016, Vol. 9, Page 877*, vol. 9, no. 11, p. 877, Oct. 2016, doi: 10.3390/EN9110877.